Short title:

One-Center Calculations of HCl

Ph.D. thesis

J.E. Grabenstetter
Chemistry Department

ONE-CENTER CALCULATIONS OF HCl: THE ELECTRIC FIELD GRADIENT

by

James E. Grabenstetter

A thesis submitted to the Faculty of Graduate Studies and Research in partial fulfilment of the requirements for the degree of Doctor of Philosophy

Department of Chemistry,
McGill University,
Montreal, Quebec,
Canada.

February 1974

ABSTRACT

Ph.D. James E. Grabenstetter Chemistry

ONE-CENTER CALCULATIONS OF HCl: THE ELECTRIC FIELD GRADIENT

A 29-orbital basis set has been developed for ab-initio One Center Expansion-Self Consistent Field (OCE-SCF) calculations of HCl. The calculated energy and several one-electron properties (including the electric field gradient (EFG) at the Cl nucleus) agreed better with experiment than results in a 71-orbital OCE basis published previously. The calculated EFG was compared with results from two-center calculations, and analysed as a function of distance from the Cl nucleus. The first and second derivatives of the EFG with respect to internuclear distance were calculated in the 29- and 71-orbital OCE bases and compared with experiment; results in the 71-orbital basis were better than those in the 29-orbital basis, but for the second derivative both agreed poorly with experiment. The 1σ molecular orbital EFG was studied, including polarization both by the quadrupolar nucleus and by the proton and valence electrons.

RESUME

Ph.D. James E. Grabenstetter Département de Chimie

CALCULS CENTRE-UNIQUE DE HCl:

LE GRADIENT DU CHAMP ELECTRIQUE

Une base de 29 orbitales a été developpée pour des calculs Centre Unique-Champ Auto-Cohérent de HCl. L'énergie et le gradient du champ électrique au noyau Cl calculés dans cette base sont en meilleur accord avec les résultats expérimentaux que ceux dans une base de 71 orbitales antérieurement publiée. Le gradient du champ électrique calculé dans la base de 29 orbitales a été comparé aux résultats dans des bases comprenant des orbitales sur les deux noyaux, et a été analysé comme fonction de la distance du noyau Cl. La première et deuxième derivées du gradient du champ électrique par rapport à la distance internucléaire ont été calculées dans les bases de 29 et de 71 orbitales; les résultats dans la base de 71 orbitales sont meilleurs que ceux dans la base de 29 orbitales, mais pour la deuxième derivée les deux bases ne s'accordent pas avec l'expérience. Le gradient du champ électrique de l'orbitale moléculaire 1σ a été étudié, comprenant la polarisation due d'une part au noyau quadripolaire et d'autre part au proton et aux couches électroniques de valence.

Acknowledgments

The author wishes to express his gratitude to the following:

his wife Christine for patience during the long haul;

Renée Charron for an excellent job typing some very difficult copy;

the National Research Council for supporting this research;

his fellow graduate students over the years, in particular Donald Lo, Russell Boyd, Geoffrey Zeiss, Warren Kramberg, Jim Pulfer, Marcel Gilbert, and Radovan Bogdanovic, for asking penetrating questions and answering stupid ones;

Dr. J.M. Sichel, for reading the first draft with a sharp eye for inaccuracy, omission, and vagueness; the final thesis owes much to his criticism;

and

to Dr. M.A. Whitehead who, despite a long, unfortunate, and unavoidable absence, directed this research with undiminished effectiveness.

Table of Contents

	Page
Chapter I: Introduction	1
1. Electronic wavefunctions and their calculation	2
2. Experimental measurement of eQq	17
3. Determination of the nuclear quadrupole moment	27
4. Previous investigations of a similar nature	30
5. Computational facilities	31
References	32
Chapter II: One Center Expansion-Self Consistent Field calculations of HCl	36
1. Types of OCE wavefunctions	38
2. Characteristics of the OCE-SCF method and wavefunctions	38
3. Choice of basis	43
4. Evaluation of electronic integrals	53
5. Organization of the SCF calculation	56
6. OCE-SCF calculations of HCl	61
7. Comparison with extensive two-center ab-initio calculations of HCl	89
References	92
Chapter III: Electric Field Gradient at the Cl nucleus from OCE-SCF wavefunctions ...	95
1. Operator for the integral over basis orbitals	97
2. Evaluation of q_{zz} from an OCE-SCF wavefunction	101
3. Analysis by MO's of the EFG; comparison with the Cl^- ion	104

Page

4. The 4σ and 5σ MO's: basis set effects 117
5. Analysis of q_{elec} by orbital-pair type 122
6. Contributions to q_{elec} of inner shells 126
References 131

Chapter IV: Comparison of the EFG from two-center and one-center calculations of HCl 133
1. Evaluation of q in a two-center basis of STO's 134
2. MO q's from the TCE-SCF wavefunctions for HCl 138
3. Convergence of OCE-SCF properties with basis enlargement 145
4. Overlap of OCE-SCF MO's with TCE-SCF MO's 151
References 156

Chapter V: Radial analysis of the EFG 158
1. Qualitative considerations 160
2. Spatial and radial weighting 163
3. Radial analysis of the EFG 167
4. Results of radial analysis of EFG for OCE-SCF wavefunctions 171
5. Radial analysis of the EFG in terms of electron shells 186
References 194

Chapter VI: R-dependence of q: vibrational averaging of eQq 196

Page

1. The general problem 196
2. Polynomial fit of q 199
3. Calculation of the $\langle\xi\rangle^i$ 209
4. Calculation of q_{vJ} 214
5. Error introduced by Born-Oppenheimer failure 217
6. Analysis of the R-dependence of q 218

References 224

Chapter VII: EFG of the 1σ MO 227

1. The Sternheimer Effect 227
2. Inclusion of the nuclear quadrupole interaction in the SCF Hamiltonian 235
3. Polarization of the 1σ MO by the proton 254

References 261

Appendix I: Integral evaluation 264

1. Definitions 264
2. One-center integrals 265
   Flowchart for program WINZ 288
   Subroutine calling diagram for program WINZ 289
   Subroutine descriptions, program WINZ .. 290
   FORTRAN listing, program WINZ 291
3. Two-center EFG integrals 299
   Flowchart for program TOOCE 316
   Subroutine calling diagram for program TOOCE 317
   Subroutine descriptions, program TOOCE 318
   FORTRAN listing, program TOOCE 320

Page

References 342

Appendix II: Program for OCE-SCF calculations 345

Flowchart for program WUNIT 351

Subroutine calling diagram for program WUNIT 352

Subroutine descriptions, program WUNIT 353

FORTRAN listing, program WUNIT 356

References 381

Claims to Original Research 382

List of Figures

Page

Chapter I

Figure 1. Schematic diagram of an atomic beam magnetic resonance apparatus 23

Chapter V

Figure 1. Regions of positive and negative contributions to q at the Cl nucleus from the electron density 161

Figure 2. Graph of typical $r^m \exp(-tr)$ to illustrate numerical problems in integrations over intervals in r 170

Figure 3a. Charge density weighted by q; values integrated over angular variables for range of values of r 181

Figure 3b. Detail of 3a for r= .45 to 1 au 182

Figure 4. Density differences between z-axis and x-axis for HCl in the GW+9 basis 183

Figure 5. Density difference along z-axis between HCl in the GW+9 basis and Cl^- in the GW basis 185

Chapter VII

Figure 1. Possible orientations of the Cl nucleus 253

List of Tables

Page

Chapter II

Table I. Radial peaking of STO's 46

Table II. The Moccia OCE basis for HCl 48

Table III. GW+9 OCE basis for HCl 54

Table IV. Moccia's OCE-SCF MO's for HCl, R = 2.424 au 62

Table V. 71-STO OCE-SCF MO's for HCl, R = 2.424 au, this work 65

Table VI. 71-STO OCE-SCF MO's for HCl, R = 2.4087 au (equilibrium distance), this work 69

Table VII. OCE-SCF MO's for HCl, R = 2.4087 au (equilibrium distance), in the GW+9 basis of Table III 72

Table VIII. OCE-SCF energy partitioning, 71-STO and GW+9 bases, R = 2.4087 au (equilibrium distance), this work 75

Table IX. Test of cusp condition, OCE-SCF MO's for HCl, R = 2.4087 au (equilibrium distance), GW+9 and 71-STO bases, this work 79

Table X. OCE-SCF dipole moments, 71-STO and GW+9 wavefunctions for HCl, R = 2.4087 au (equilibrium distance), this work 82

Table XI. Molecular quadrupole moment and related quantities, 71-STO and GW+9 OCE-SCF wavefunctions, R = 2.4087 au (equilibrium distance), this work .. 84

Page

Table XII. Hellman-Feynman force on the Cl nucleus, 71-STO and GW+9 OCE-SCF wavefunctions, R = 2.4087 au (equilibrium distance), this work 87

Table XIII. $\langle r^{-1} \rangle$ and $\langle r^{-2} \rangle$, 71-STO and GW+9 OCE-SCF wavefunctions, R = 2.4087 au (equilibrium distance), this work 88

Table XIV. Comparison of properties calculated from the 71-STO and GW+9 OCE-SCF wavefunctions for HCl with the two-center results of McLean and Yoshimine and Cade and Huo 90

Chapter III

Table I. q for MO's from OCE-SCF calculations of HCl, Moccia and modified GW bases, for comparison of 3σ and 1π q 103

Table II. Electron shell analysis of q_{elec} for HCl and Cl^- in several OCE basis sets 106

Table III. Coefficients of SCF orbitals of Cl^- ion, 71-orbital basis 107

Table IV. q_{elec} by orbitals for Cl^-, several basis sets 111

Table V. Bagus and Clementi bases for Cl^- 112

Table VI. Gilbert-Wahl basis for Cl_2 115

Table VII. Coefficients of the $2p_z$ (3σ) orbital of Cl^- in several bases 116

Table VIII. HCl MO q for OCE-SCF wavefunctions in the basis series formed by successively adding to the GW basis of

Page

Table VI 9s, 9p, etc. orbitals with ζ = 3.32129 119

Table IX. Orbital pair analysis, GW basis extended with n = 9 orbitals, r_{max} = 2.4087 au 124

Table X. Coefficients of 5σ MO of HCl, GW series of bases with n = 9, r_{max} = 2.4087 au orbitals added 127

Table XI. Shell analysis of q_{elec}, HCl, GW basis series 130

Chapter IV

Table I. MO q expectation values for SCF calculations of HCl in several bases 140

Table II. Convergence of $\langle \hat{z} \rangle_{elec}$, $\langle \hat{q} \rangle_{elec}$, and $\langle \hat{r}^{-1} \rangle_{elec}$ with basis enlargement; also individual MO values for one basis 147

Table III. Convergence of total energy of HCl with enlargement of OCE basis 150

Table IV. Overlaps of OCE-SCF MO's of 10-basis series with corresponding MO's of McLean-Yoshimine wavefunction 152

Chapter V

Table I. Integrals over intervals in r of charge density weighted by $\hat{q}$ 173

Table II. Partitioning of the q_n of Table I into contributions from the three electron shells, for n = 1 to 5 187

Page

Table III. Integrals over intervals in r of unweighted electron density 189

Table IV. Partitioning of the p_n of Table III into contributions from the three electron shells, for n = 1 to 5 191

Table V. Electron densities of the GW Cl^- wavefunction and the GW+9 HCl wavefunction along the z-axis 193

Chapter VI

Table I. q and total energy from OCE-SCF wavefunctions 205

Table II. EFG fitting coefficients and variances for fitting polynomials of degrees 1, 2, and 3 206

Table III. Coefficients and expected errors for degree 2 polynomial fitting of q from OCE-SCF wavefunctions 208

Table IV. Spectroscopic constants and dimensionless potential coefficients a_i for $H^{35}Cl$, $D^{35}Cl$, and $T^{35}Cl$ 212

Table V. $\langle\xi\rangle_{01}$ and $\langle\xi^2\rangle_{01}$ for $H^{35}Cl$, $D^{35}Cl$, and $T^{35}Cl$ from Schlier and Zeiger-Bolef formulas 215

Table VI. Calculated and experimental vibrationally averaged q for HCl in the v = 0, J = 1 state 216

Table VII. Analysis by electron shell of the OCE-SCF calculated q_{elec} for a series of internuclear distances 220

Table VIII. Difference table constructed from Table VII 221

Chapter VII

Table I. Analysis by electron shells of

Page

HCl q_{elec} from the McLean-Yoshimine and Cade-Huo two-center and GW+9 one-center bases 228

Table II. Effect of including ^{35}Cl quadrupole interaction in Hamiltonian upon calculated q_{elec} in HCl in two OCE bases .. 246

Table III. Orbital pair type analysis of total q_{elec} and q of the 1σ MO for OCE-SCF calculations of HCl in 22-orbital basis including nuclear quadrupole interaction 251

Table IV. Electron shell analysis of q_{elec}, and energies, for HCl in 22-orbital bases, GW+2pσ+3dσ, r_{max} = .01, .025, .05 au 257

Table V. Orbital pair type analysis of q_{elec} for HCl OCE-SCF wavefunctions in 22-orbital bases, GW+2pσ+3dσ, r_{max} = .01, .025, .05 au 259

Appendix I

Table I. Integrals over three complex spherical harmonics; comparison between subroutine DGAUNT and tables of Rotenberg et al. 270

Table II. Pearson's incomplete Γ-function as calculated using ATTSER and as tabulated 276

Table III. Comparison of one-center electron repulsion integrals routine REP1C with published values 282

Table IV. Nuclear attraction integral with off-center nucleus 286

Table V. Comparison of our two-center EFG

Page

integral routines with values published by Flygare et al. for H_2CO 311

Table VI. Comparison of our routines for two-center EFG integrals with values published by Scrocco 313

Appendix II

Table I. OCE-SCF calculation of HCl at R_e = 2.4087 au with electron repulsion integrals rounded to 6 significant figures 347

CHAPTER I: Introduction

The nuclear quadrupole coupling constant is of interest to spectroscopists because it can be determined rather accurately for atoms and molecules by a variety of methods[1]. This coupling constant, denoted eQq, is the product of a nuclear property Q, the electric quadrupole moment, and an electronic property q, the electric field gradient (EFG) at the quadrupolar nucleus. For most common quadrupolar nuclei (^{14}N excepted[2]) Q is known to about 3 significant figures[3]; measurement of eQq allows determination of q to the same accuracy. Predictions of q can be made from approximate electronic wavefunctions; comparison with the experimental value allows one to decide whether the approximate wavefunction reproduces acceptably well those details of the electronic structure which determine q.

In particular, q is highly dependent upon the electron distribution close to the quadrupolar nucleus (Chapter V); in calculating an electronic wavefunction for prediction of q one seeks to allow as much flexibility as possible in this region. A technique which accomplishes this is the One-Center Expansion-Self Consistent Field (OCE-SCF) method[4,5], which yields a Hartree-Fock-Roothaan[6] wavefunction in a basis set whose members are all centered (in this case) on the quadrupolar nucleus. A molecule which suggests itself for study of q by this method is HCl, since for both ^{35}Cl and ^{37}Cl Q is rather accurately

known[3] and since the electronic structure of HCl is well suited for calculation by the OCE-SCF technique (Chapter II). In addition a very precise measurement of eQq for HCl has been made[7]. This thesis reports calculations of OCE-SCF wavefunctions for HCl and the q calculated from them. Before reporting the calculations we give a survey of the theory of electronic wavefunction calculations, and brief descriptions of the techniques for determination of Q and eQq.

1. Electronic wavefunctions and their calculation

a) Schroedinger equation for a many-particle system

The Hamiltonian operator for an N-particle system (n electrons, N-n nuclei) will be taken as

$$H = \sum_{i=1}^{N} -\frac{1}{2m_i}\nabla_i^2 + \frac{1}{2}\sum_{i=1}^{N}\sum_{j\neq i}\frac{q_i q_j}{r_{ij}}, \qquad (1)$$

with m_i the mass and q_i the charge of the ith particle. (1) is written in atomic units[8]; the units of mass and charge are the electronic mass m_e and the proton charge e. The Bohr radius a_0 of the hydrogen 1s orbital is the unit of length (the bohr); the unit of energy (the hartree) is e^2/a_0, which is minus the potential energy of the H atom. The unit of angular momentum is $\hbar$. ∇_i^2 is the Laplacian in the coordinates of particle i, which in Cartesian coordinates is

$$\nabla_i^2 = \partial^2/\partial x_i^2 + \partial^2/\partial y_i^2 + \partial^2/\partial z_i^2 . \qquad (2)$$

The Hamiltonian (1) considers only the non-relativistic kinetic energy and that part of the potential energy due to electrostatic interactions between point charges; relativistic effects and those due to the finite size of the particles are neglected. (1) is called the non-relativistic or spin-free Hamiltonian. The exact Hamiltonian involves addition of several terms (usually small in magnitude and difficult to calculate) to (1)[9]. One such term, due to the nuclear quadrupole moment, is considered in Chapter VII.

The wavefunction Φ for the system satisfies the Schroedinger equation

$$H\Phi = E\Phi . \tag{3}$$

In most cases infinitely many pairs (E,Φ) satisfy (3); the Φ corresponding to the lowest E (lowest total energy) is the ground state wavefunction for the system. The variable dependence of Φ is

$$\Phi \equiv \Phi\ (\bar{x}_1,\ldots,\bar{x}_N); \tag{4}$$

The $\bar{x}_i$ are 4-coordinate vectors consisting of the three spatial coordinates of particle i and a spin coordinate. The spatial coordinates take a continuous range of values; the spin coordinate takes 2s +1 discrete values, with s the spin number of the particle (section 2). Even for the spin-free Hamiltonian the spin coordinate enters the wavefunction because of symmetry

requirements[10]. Φ is assumed normalized,

$$\int \Phi^*(\bar{x}_i,\ldots,\bar{x}_N)\Phi(\bar{x}_1,\ldots,\bar{x}_N)d\tau_1\ldots d\tau_N = 1, \qquad (5)$$

with Φ^* the complex conjugate and $d\tau_i$ an infinitesimal space and spin volume element centered at $\bar{x}_i$. The probability that particle 1 is in $d\tau_1$, particle 2 in $d\tau_2$, etc., is[11]

$$\Phi^*(\bar{x}_1,\ldots,\bar{x}_N)\Phi(\bar{x}_1,\ldots,\bar{x}_N)d\tau_1\ldots d\tau_N. \qquad (6)$$

b) Separation of electronic and nuclear coordinates

Solution of (3) is considerably simpler if the electronic and nuclear coordinates can be separated. Born and Oppenheimer[12] partitioned the Hamiltonian (1) into two parts: (i) the electronic kinetic energy and total potential energy of the system, and (ii) the nuclear kinetic energy. The nuclear kinetic energy was treated as a perturbation,

$$H_N = \sum_\alpha -\frac{1}{2m_\alpha}\nabla_\alpha^2,$$

with α ranging over all nuclei, but H_N was written

$$H_N = -\frac{\kappa^4}{2m_e}\sum_\alpha \mu_\alpha \nabla_\alpha^2, \qquad (7)$$

with m_e the electron mass,

$$\kappa = (m_e/M)^{\frac{1}{2}},$$

with the constant M an average nuclear mass (M can be defined in several ways) and

$$\mu_\alpha = M/m_\alpha;$$

M must be defined so that all the μ_α are roughly of the order of 1. A common choice is the average of the nuclear masses. (7) expresses the perturbing Hamiltonian as a small constant (κ^4) times a term the same order of magnitude as the electronic kinetic energy. Born and Oppenheimer showed that Φ could be written as a sum of products of three functions,

$$\Phi = \sum_{i=0}^{\infty} \sum_{j=0}^{\infty} \sum_{k=0}^{\infty} \phi_i(\bar{x}_1,\ldots,\bar{x}_n)\chi_j(X_1,\ldots,X_P)\zeta_k(\bar{\theta}), \qquad (8)$$

where the $\bar{x}_i$ are electronic and the X_i nuclear coordinates. P is the number of independent nuclear coordinates; P=3(N-n)-5 for a linear molecule and 3(N-n)-6 otherwise. $\bar{\theta}$ denotes a set of angular coordinates which measure molecular rotation. The three functions correspond to electronic motion, nuclear vibration, and molecular rotation respectively. In particular, Born and Oppenheimer showed that, except in cases of ground state electronic degeneracy such as give rise to the Renner and Jahn-Teller effects[13], the first term of (8),

$$\Phi_0 \equiv \phi_0(\bar{x}_1,\ldots,\bar{x}_n)\chi_0(X_1,\ldots,X_P)\zeta_0(\bar{\theta}) \qquad (9)$$

gives the energy E of (3) through fourth order in κ, with the first and third orders vanishing,

$$E = E_0 + \kappa^2 E_2 + \kappa^4 E_4 + \ldots,$$

with E_0 corresponding to the electronic, $\kappa^2 E_2$ the vibrational, and $\kappa^4 E_4$ the rotational energy. The first neglected non-vanishing term is of order κ^6. Since $\kappa^4 < m_e/m_p \approx .0005$, with m_p the proton mass, the neglected term is $<.00001$ times the electronic, .0005 times the vibrational, and .02 times the rotational energy. The effect of the neglected terms is observable spectroscopically[14,15]; however it is difficult to calculate (8) beyond the first term, though attempts have been made for small systems[16]. The wavefunctions reported in this thesis are the electronic functions ϕ_0 of (9); the nuclear coordinates enter only as fixed parameters. Some effects of breakdown of the Born-Oppenheimer approximation are examined in Chapter VI.

c) <u>The electronic wavefunction</u>

In what follows attention is confined to the electronic Schroedinger equation

$$H_e \phi_e = E_e \phi_e, \tag{10}$$

with

$$H_e = -\tfrac{1}{2} \sum_{i=1}^{n} \nabla_i^2 + \tfrac{1}{2} \sum_{i=1}^{n} \sum_{j \neq i} \frac{1}{r_{ij}} - \sum_{i=1}^{n} \sum_{\alpha} \frac{Z_\alpha}{r_{i\alpha}}, \tag{11}$$

where i and j range over electrons and α over nuclei. Z_α is the atomic number of nucleus α; the variables in ϕ_e are the n 4-coordinate electron position and spin vectors, with the 3-coordinate nuclear position vectors entering only as parameters. ϕ_e is assumed normalized. E_e is the electronic energy of the system; it includes the electronic kinetic energy, the electron repulsion energy, and the energy of attraction between the electrons and nuclei. The "total" molecular energy as calculated from ϕ_e is

$$E_{tot} = E_e + E_{nuc}, \tag{12}$$

with E_{nuc} the point-charge repulsion energy of the nuclei. E_{tot} does not include the nuclear kinetic energy, and is thus not the total energy of any real molecular state; it is rather the potential energy for motion of the nuclei.

d) <u>One-electron properties</u>

Many molecular properties, such as the electric dipole moment and the EFG, are expectation values of one-electron operators, which depend upon averages over the positions of the electrons but not their distances from each other. The expectation value of a one-electron operator $\hat{\delta}$ over the electronic wavefunction is

$$\langle\delta_e\rangle = \sum_{i=1}^{n} \int d\tau\, \phi_e^* \,\delta_i\, \phi_e \equiv \langle\phi_e|\sum_{i=1}^{n} \delta_i|\phi_e\rangle,$$

where $\hat{o}_i$ is in the coordinates of electron i; since the n electrons are indistinguishable,

$$\langle\delta\rangle_e = n\langle\phi_e|\delta_1|\phi_e\rangle. \tag{13}$$

Analogously to (12), the total expectation value of δ over ϕ_e is

$$\langle\delta\rangle_{tot} = \langle\delta\rangle_e + \langle\delta\rangle_{nuc}$$

with $\langle\delta\rangle_{nuc}$ calculated considering the nuclei as fixed point charges. Specific forms for $\langle\delta\rangle_e$ are given below as forms for ϕ_e are developed.

e) Orbitals; the Hartree-Fock equations

An orbital is a normalized function of the coordinates of a single electron. The square of the absolute value of an orbital at any point gives the relative probability of finding the electron at that point. An orbital can be a function either of the 3-coordinate position vector or the 4-coordinate space-spin vector. An orbital in the 3-dimensional space (a spatial orbital) is denoted:

$$\psi = \psi(x_i, y_i, z_i); \tag{14}$$

the arguments denote any spatial coordinates, not necessarily Cartesian. An orbital in the 4-dimensional position-spin

space (a spinorbital[17]) is normally the product of a spatial orbital and a spin function,

$$\chi = \psi(x_i, y_i, z_i)\eta(s_i), \tag{15}$$

with η the spin function and s_i the spin coordinate. η is unity for one of the two (for the electron) allowed values of s_i and zero for the other[10]; the two electronic spin functions are α(=1 for $s_i=\frac{1}{2}$, 0 for $s_i=-\frac{1}{2}$) and β(=1 for $s_i=-\frac{1}{2}$, 0 for $s_i=+\frac{1}{2}$). α and β are orthonormal.

A useful approximate form for ϕ_e is an antisymmetrized (since ϕ_e changes sign upon exchange of two electron coordinates[18]) product of n spinorbitals,

$$\phi_e = \frac{1}{n!}\,\mathrm{Det}(\chi_1(\bar{x}_1)\ldots\chi_n(\bar{x}_n)), \tag{16}$$

with

$$\mathrm{Det}(\chi_1(\bar{x}_1)\ldots\chi_n(\bar{x}_n)) \equiv \begin{vmatrix} \chi_1(\bar{x}_1)\ldots\chi_n(\bar{x}_1) \\ \chi_1(\bar{x}_2)\ldots\chi_n(\bar{x}_2) \\ \ldots \\ \chi_1(\bar{x}_n)\ldots\chi_n(\bar{x}_n) \end{vmatrix}.$$

(16) is called a determinantal wavefunction, and the determinant a Slater determinant[19]. The $\bar{x}_i$ above are 4-dimensional

coordinate vectors including spin. A determinantal wavefunction is closed shell if the n χ_i can be grouped into n/2 pairs, both members of a pair having the same spatial factor, but one with α and one with β spin. Determinantal wavefunctions not satisfying this condition are called open shell. Except in a few cases a single open-shell determinant is not a good approximation to any real molecular state[20]; in what follows we concentrate on the closed-shell case. HCl can be fairly well approximated by a single closed-shell determinant.

The Hartree-Fock (H-F) wavefunction for a system is the wavefunction of the form (16) with the lowest possible expectation value for the electronic energy[6],

$$E_e = \langle \Phi_e | H_e | \Phi_e \rangle \ .$$

Since the wavefunction is now approximate the energy is not an eigenvalue as in (10).

Since only closed-shell systems are treated, it is convenient to make a notational change. We now denote by 2n the number of electrons (necessarily even); n is the number of doubly occupied spatial orbitals. The closed shell wavefunction is then

$$\Phi_e = \frac{1}{(2n)!} \mathrm{Det}(\phi_1(1)\alpha(1)\phi_1(2)\beta(2)\ldots\phi_n(2n)\beta(2n)). \qquad (17)$$

The spatial orbitals ϕ_i are called molecular orbitals (MO's)

or atomic orbitals (AO's) depending on the system. Fock[21] showed that the n spatial orbitals satisfy the system of n one-electron equations (pseudoeigenvalue equations)

$$F(1)\psi_i(1) = \epsilon_i\psi_i(1), \tag{18}$$

with the Fock operator in the coordinates of electron 1 given by

$$F(1) = -\tfrac{1}{2}\nabla_1^2 - \sum_\alpha \frac{Z_\alpha}{r_{1\alpha}} + \sum_{j=1}^{n} (2J_j(1,2)-K_j(1,2)), \tag{19}$$

with the coulomb operator J and exchange operator K given by

$$J_j(1,2)\psi_i(1) = [\int \psi_j^*(2)\psi_j(2)\frac{1}{r_{12}}\, d\tau_2]\psi_i(1) \tag{20}$$

$$K_j(1,2)\psi_i(1) = [\int \psi_j^*(2)\psi_i(2)\frac{1}{r_{12}}\, d\tau_2]\psi_j(1). \tag{21}$$

The system (18) is coupled, all ψ_j appearing in the equation for ψ_i. It is because of this coupling that the system is termed pseudoeigenvalue instead of eigenvalue, since the operator F(1) is not defined until all the ψ_i are known. The system can be solved by initially guessing all the ψ_i, constructing the Fock operator, solving for a new set of ψ_i, and repeating until the ψ_i remain essentially unchanged between successive iterations. When this occurs the electron distribution is said to generate a self-consistent field (SCF). The electronic energy

from the closed-shell single determinant wavefunction is

$$E_e = 2\sum_{i=1}^{n} H_{ii} + \sum_{i=1}^{n}\sum_{j=1}^{n} (2J_{ij}-K_{ij}), \qquad (22)$$

where the summations are over spatial orbitals and

$$H_{ii} = \langle\psi_i(1)| -\tfrac{1}{2}\nabla_1^2-\sum_{\alpha}\frac{Z_\alpha}{r_{1\alpha}} |\psi_i(1)\rangle$$

$$J_{ij} = \int d\tau_1\int d\tau_2\psi_i^*(1)\psi_i(1)\frac{1}{r_{12}}\psi_j^*(2)\psi_j(2)$$

$$K_{ij} = \int d\tau_1\int d\tau_2\psi_i^*(1)\psi_j(1)\frac{1}{r_{12}}\psi_j^*(2)\psi_i(2),$$

with the volume elements and integrations for spatial coordinates only. The one-electron property (13) becomes, for the wavefunction (18),

$$\langle\delta\rangle_e = 2\sum_{j=1}^{n}\langle\psi_j|\delta_1|\psi_j\rangle. \qquad (23)$$

The ψ_i form an orthonormal set with respect to integration over the spatial coordinates.

The system (18) can be solved numerically[22], however Roothaan[6] obtained a solution by expanding the ψ_i as linear combinations of basis functions. The ψ_i are expanded in terms of k basis functions ϕ_j:

$$\psi_i = \sum_{j=1}^{k} C_{ji}\phi_j, \quad k \geq n. \qquad (24)$$

The equations which arise from substituting (24) into (18) (Roothaan's equations) are, in matrix form,

$$FC = SCE, \tag{25}$$

with F a kxk hermitian matrix (the Fock matrix), C a kxn eigenvector matrix, S a kxk hermitian matrix (the overlap matrix), and E an nxn diagonal matrix of the eigenvalues (the ε_i of (18)). The elements of F and S are

$$F_{ij} = H_{ij} + \sum_{\ell=1}^{k} \sum_{m=1}^{k} P_{\ell m}([ij|\ell m] - \tfrac{1}{2}[i\ell|jm]) \tag{26}$$

$$S_{ij} = \langle\phi_i|\phi_j\rangle, \tag{27}$$

with

$$H_{ij} = \langle\phi_i(1)|-\tfrac{1}{2}\nabla_1^2 - \sum_{\alpha}\frac{Z_\alpha}{r_{1\alpha}}|\phi_j(1)\rangle \tag{28}$$

and

$$[ij|\ell m] \equiv \int d\tau_1 d\tau_2 \phi_i^*(1)\phi_j(1) r_{12}^{-1} \phi_\ell^*(2)\phi_m(2)$$

The elements $P_{\ell m}$ of the one-electron density matrix are, for the single-determinant closed-shell case,

$$P_{\ell m} = \sum_j N_j \, C_{j\ell} C_{jm}, \tag{29}$$

with j ranging over the MO's and N_j the number of electrons

occupying ψ_j (for this case all N_j are either two or zero). If all integrals in (26) and (27) are rigorously calculated, the resulting wavefunction is referred to as ab-initio; if the integrals are approximated or some are neglected the wavefunction is called an approximate MO wavefunction; if the approximations use experimental data other than the fundamental constants, the wavefunction is called semiempirical[23]. It should be emphasized, however, that all MO wavefunctions, whether ab-initio or semi-empirical, are approximate since the form (16) cannot be the exact wavefunction for a system with more than one electron, because of electron correlation (section 1g). Only the ab-initio wavefunction satisfies the variation theorem; i.e. for an ab-initio ϕ_e the expectation value $\langle\phi_e|H_e|\phi_e\rangle$ of the electronic energy is certain to lie above the true electronic energy of the system[58]. The wavefunctions calculated in this work are ab-initio.

A common form for the basis functions ϕ_j is

$$\phi_j(n,\ell,m,\zeta,\bar{r}) = Nr^{n-1}\exp(-\zeta r)S_{\ell m}(\theta,\phi),$$

with N a normalization constant and $S_{\ell m}$ a spherical harmonic (Appendix I). $\bar{r}$ is measured in a spherical system centered on one of the nuclei. This type of basis function is called a Slater-type orbital (STO)[24]. The basis functions used in this work are STO's.

The wavefunction (17) with the spatial factors

constrained to be identical for the α and β spin pairs is known as the Restricted Hartree-Fock (RHF) function. The calculations reported here are of this type. This constraint can be relaxed (yielding the Unrestricted Hartree-Fock (UHF) wavefunction), but for closed shell systems the UHF wavefunction is identical to the RHF[25].

f) <u>One-electron properties from RHF MO wavefunctions</u>

From (24) it follows that the expression (23) for the expectation value of a one-electron operator becomes

$$\langle \delta \rangle_e = \sum_{\ell=1}^{n} N_\ell \sum_{i=1}^{k} \sum_{j=1}^{k} C_{ik} C_{jk} o_{ij} \equiv \sum_i \sum_j P_{ij} o_{ij}, \qquad (30)$$

with

$$o_{ij} = \langle \phi_i(1) | \delta_1 | \phi_j(1) \rangle,$$

and the P_{ij} of (29). It is often convenient to analyse a one-electron property in terms of contributions from the individual MO's; the first expression in (30) gives this partitioning.

g) <u>Configuration interaction</u>

(16) cannot be the exact wavefunction for a system of more than one electron, since the instantaneous (as opposed to average) electron repulsions cannot be accounted for. However a linear combination of Slater determinants,

$$\Phi_{CI} = \sum_k C_k \Phi_k, \tag{31}$$

with each Φ_k of the form (16), can approach the exact wavefunction in the limit of an infinite sum. Φ_{CI} is a configuration interaction (CI) wavefunction. Φ_{CI} can account for the effects of instantaneous electron interactions (electron correlation) because an arbitrary function of n variables (e.g. the exact electronic wavefunction) can be expanded as a sum of products of n functions, each of a single variable[26]. If Φ_{CI} represents the ground state and one of the Φ_k in (31) is the H-F determinant, it usually has the largest coefficient. A natural question is how much electronic properties are affected as (31) is extended beyond the H-F determinant. Moller and Plesset[27] treated the difference between the H-F Hamiltonian and the true Hamiltonian as a perturbation; they showed that to first order the one-electron density matrix (given for the H-F wavefunction by (29), but this form must be extended for Φ_{CI}) is unchanged. Thus to first-order the expectation value of a one-electron operator (30) is unchanged by inclusion of CI. Thus if one is interested in one-electron properties it is reasonable to perform an H-F calculation without CI (single determinant ab-initio wavefunctions constructed by the Roothaan procedure approach the H-F wavefunction as the basis approaches completeness). This is an important simplification since the number of possible determinants rises rapidly with basis size and it is difficult to predict which determinants

(after the H-F) contribute heavily to the CI wavefunction. Non-negligible changes in one-electron properties upon inclusion of CI have been observed[28], but the EFG of HCl at the Cl nucleus is not such a case; therefore CI was not done in the calculations reported in this thesis.

2. Experimental measurement of eQq

Electronic wavefunctions are usually calculated for isolated molecules; results of such calculations are directly comparable only with molecular properties in the gas phase. We therefore confine discussion to measurement of eQq in the gas phase, although a large body of eQq data has been accumulated for solid compounds by pure nuclear quadrupole resonance[1]. For atoms in the gas phase there are two common techniques[1]: measurement of hyperfine splitting in atomic emission spectra[29], and atomic beam magnetic resonance spectroscopy[30]. For molecules there are three common techniques: microwave rotational spectroscopy[31], and molecular beam electric and magnetic resonance spectroscopy[30]. Atomic emission spectroscopy was the method by which the nuclear quadrupole moment was first experimentally detected[32], but it has not been used in the determination of Q for ^{35}Cl or ^{37}Cl and is not discussed here. Molecular beam magnetic resonance is important only for homonuclear diatomic molecules[1], so it too will not be discussed. Atomic and molecular measurements are both of interest since atomic measurements

provide the Q values for ^{35}Cl and ^{37}Cl.

a) Definitions (conventions of Bardeen and Townes[33])

(i) $$Q = \frac{1}{e}\int \rho(\bar{r}) r^2 (3\cos^2\theta - 1) d\tau, \qquad (32)$$

with $\rho(\bar{r})$ the nuclear charge density in the state $m_I = I$ (see below). θ is the angle between $\bar{r}$ and the nuclear spin quantization axis. Q has dimensions L^2 (with M mass, L length, and C charge).

(ii) $$q = \partial^2 V/\partial z^2, \qquad (33)$$

with V the electrostatic potential at the nuclear center of mass due to all particles in the system except those within a small sphere surrounding the nucleus (Chapter III). V has dimensions C/L; hence q has dimensions C/L^3. Some authors take V as 1/L, q as $1/L^3$, and the nuclear quadrupole coupling constant as e^2Qq[34]. q is a component of a tensor; analogously to (33) the others are $\partial^2 V/\partial x \partial y$, etc. The z-axis in (33) is the principal axis of this tensor, the direction of the largest component of the tensor in the axis system in which it is diagonal (Chapter III).

(iii) eQq: from (i) and (ii) the dimensions of eQq are C^2/L, which is energy.

(iv) Quantum numbers characterizing the systems:

I: nuclear spin quantum number. The nuclear angular

momentum vector $\bar{I}$ has magnitude $I(I+1)\hbar^2$ and is allowed projections on the spin quantization axis of $m_I\hbar$, m_I taking values $I, I-1, \ldots, -I$. I can be integral (nuclei with even mass numbers) or half-integral (odd mass numbers)[35].

J: total angular momentum quantum number excluding nuclear spin. For atoms the angular momentum vector $\bar{J}=\bar{L}+\bar{S}$ with $\bar{L}$ and $\bar{S}$ the electronic orbital and spin angular momentum vectors. For $^1\Sigma$ molecules, with $\bar{L}$ and $\bar{S}$ vanishing (e.g. HCl in the ground state), $\bar{J}$ is due to rotation of the whole molecule. The projections on the quantization axis $m_J\hbar$ take values analogously to $m_I\hbar$. J can be integral or half-integral.

F: quantum number for total angular momentum vector $\bar{F}=\bar{I}+\bar{J}$. m_F is allowed values analogously to m_I and m_J. F takes values $I+J, \ldots, |J-I|$.

b) <u>Interaction of nucleus with external potential</u>

The energy of a nuclear charge distribution $\rho^{(m)}(\bar{r})$ in nuclear state $m_I=m$ in a potential field $V(\bar{r})$ due to charges external to $\rho^{(m)}$ is[36]

$$E = \int \rho^{(m)}(\bar{r})V(\bar{r})d\tau; \qquad (34)$$

here we take $\bar{r}=(x,y,z)$. $V(\bar{r})$ can be expanded as a Taylor series in x,y, and z about the nuclear center of mass $\bar{r}_0$:

$$V(x,y,z)=V(\bar{r}_0)+\sum_{i=1}^{3} x_i\left(\frac{\partial V}{\partial x_i}\right)_{\bar{r}=\bar{r}_0}+\tfrac{1}{2}\sum_{i=1}^{3}\sum_{j=1}^{3} x_i x_j\left(\frac{\partial^2 V}{\partial x_i \partial x_j}\right)_{\bar{r}=\bar{r}_0}+\ldots,$$

with $x_1=x$, $x_2=y$, $x_3=z$. Substituting in (34),

$$E=V(\bar{r}_0)\int\rho^{(m)}(\bar{r})d\tau+\sum_{i=1}^{3}\left(\frac{\partial V}{\partial x_i}\right)_{\bar{r}=\bar{r}_0}\int\rho^{(m)}(\bar{r})x_i d\tau$$

$$+\tfrac{1}{2}\sum_{i=1}^{3}\sum_{j=1}^{3}\left(\frac{\partial^2 V}{\partial x_i\partial x_j}\right)_{\bar{r}=\bar{r}_0}\int\rho^{(m)}(\bar{r})x_i x_j d\tau+\ldots \qquad (35)$$

the integral in the first term is the nuclear charge Ze; its product with $V(\bar{r}_0)$ is the point charge interaction energy, which is independent of m. The integral in the second term is the x_i- component of the nuclear electric dipole moment in the state $m_I=m$. Because of symmetry requirements these and all similar integrals containing the product of an odd number of the x_i vanish for all nuclei[34]. For the third term, we switch to a more standard form. The tensor $\bar{Q}^{(m)}$ with components

$$\bar{Q}_{ij}^{(m)}=\frac{1}{e}\int\rho^{(m)}(\bar{r})x_i x_j d\tau$$

is not traceless since $\bar{Q}_{11}^{(m)}+\bar{Q}_{22}^{(m)}+\bar{Q}_{33}^{(m)}=\frac{1}{e}\int\rho^{(m)}(\bar{r})r^2 d\tau\neq 0$. A traceless tensor is desirable since it has one less independent component. A standard way to construct a traceless tensor $Q^{(m)}$ from $\bar{Q}^{(m)}$ is[37]

$$Q_{ij}^{(m)}=3\bar{Q}_{ij}^{(m)}-\delta_{ij}\sum_{k=1}^{3}\bar{Q}_{kk}^{(m)}.$$

The third term in (35) becomes

$$\frac{e}{2}\sum_i\sum_j\left(\frac{\partial^2 V}{\partial x_i \partial x_j}\right)_{\bar{r}=\bar{r}_0}\bar{Q}_{ij}^{(m)} = \frac{e}{6}\sum_i\sum_j\left(\frac{\partial^2 V}{\partial x_i \partial x_j}\right)_{\bar{r}=\bar{r}_0}\left(Q_{ij}^{(m)} + \delta_{ij}\sum_k \bar{Q}_{kk}^{(m)}\right)$$

$$= \frac{e}{6}\sum_i\sum_j\left(\frac{\partial^2 V}{\partial x_i \partial x_j}\right)_{r=r_0} Q_{ij}^{(m)} + \frac{e}{6}\left[\sum_i\left(\frac{\partial^2 V}{\partial x_i^2}\right)\right]_{\bar{r}=\bar{r}_0}\left(\sum_k \bar{Q}_{kk}^{(m)}\right).$$

Since V is due to charges outside the nucleus, Laplace's equation holds,

$$\left(\frac{\partial^2 V}{\partial x^2}\right)_{\bar{r}=\bar{r}_0} + \left(\frac{\partial^2 V}{\partial y^2}\right)_{\bar{r}=\bar{r}_0} + \left(\frac{\partial^2 V}{\partial z^2}\right)_{\bar{r}=\bar{r}_0} = 0,$$

which gives, defining $(\partial^2 V/\partial x_i \partial x_j)_{\bar{r}=\bar{r}_0} \equiv q_{ij}$,

$$\frac{e}{2}\sum_i\sum_j \bar{Q}_{ij}^{(m)} q_{ij} = \frac{e}{6}\sum_i\sum_j Q_{ij}^{(m)} q_{ij}, \tag{36}$$

a convenient form for the third term of (35). The fourth term of (35) (electric octupole term) involves the product of an odd number of the x_i and vanishes by the same arguments as for the second term. For a nucleus with $I=\frac{3}{2}$ (e.g. ^{35}Cl and ^{37}Cl), the order 3(=2I) moment (octupole moment) is the highest possible non-zero moment[34]; thus for $I=\frac{3}{2}$ (35) becomes

$$E = e\left(ZV(\bar{r}_0) + \frac{1}{6}\sum_i\sum_j Q_{ij}^{(m)} q_{ij}\right),$$

with the $Q_{ij}^{(m)}$ given explicitly by

$$Q_{ij}^{(m)} = \frac{1}{e}\int \rho^{(m)}(\bar{r})(3x_i x_j - \delta_{ij} r^2)d\tau;$$

the z-axis coincides with the nuclear spin quantization axis (Chapter VII).

c) eQq from atomic beam magnetic resonance spectra

The apparatus for this method (Figure 1) consists of an atomic source and two separated inhomogeneous magnetic fields directed opposite to each other and perpendicular to the beam. Between them the beam passes simultaneously through a homogeneous magnetic field and an electromagnetic field[30]. The first inhomogeneous magnetic field deflects the beam (if the atoms have a non-zero magnetic moment); the homogeneous magnetic field causes a splitting of energy levels by interaction with the nuclear and electronic magnetic moments, but produces no further deflection. The levels are further split by the magnetic and nuclear quadrupole hyperfine interactions. The electromagnetic field may produce transitions between levels if it is at a resonant frequency. The second inhomogeneous field then redeflects the beam. If the electromagnetic field has induced a transition, the interaction with the second inhomogeneous field is different from that with the first; the second field is adjusted to redeflect onto a detector either those atoms which have not undergone transition or those which have undergone a particular transition. Correlation of detector current with electromagnetic field frequency yields the energies of the allowed transitions. These combined with the dependence of the nuclear quadrupole interaction on I,J, and F[34] yield eQq.

FIGURE 1: Schematic diagram of an atomic beam magnetic resonance apparatus.

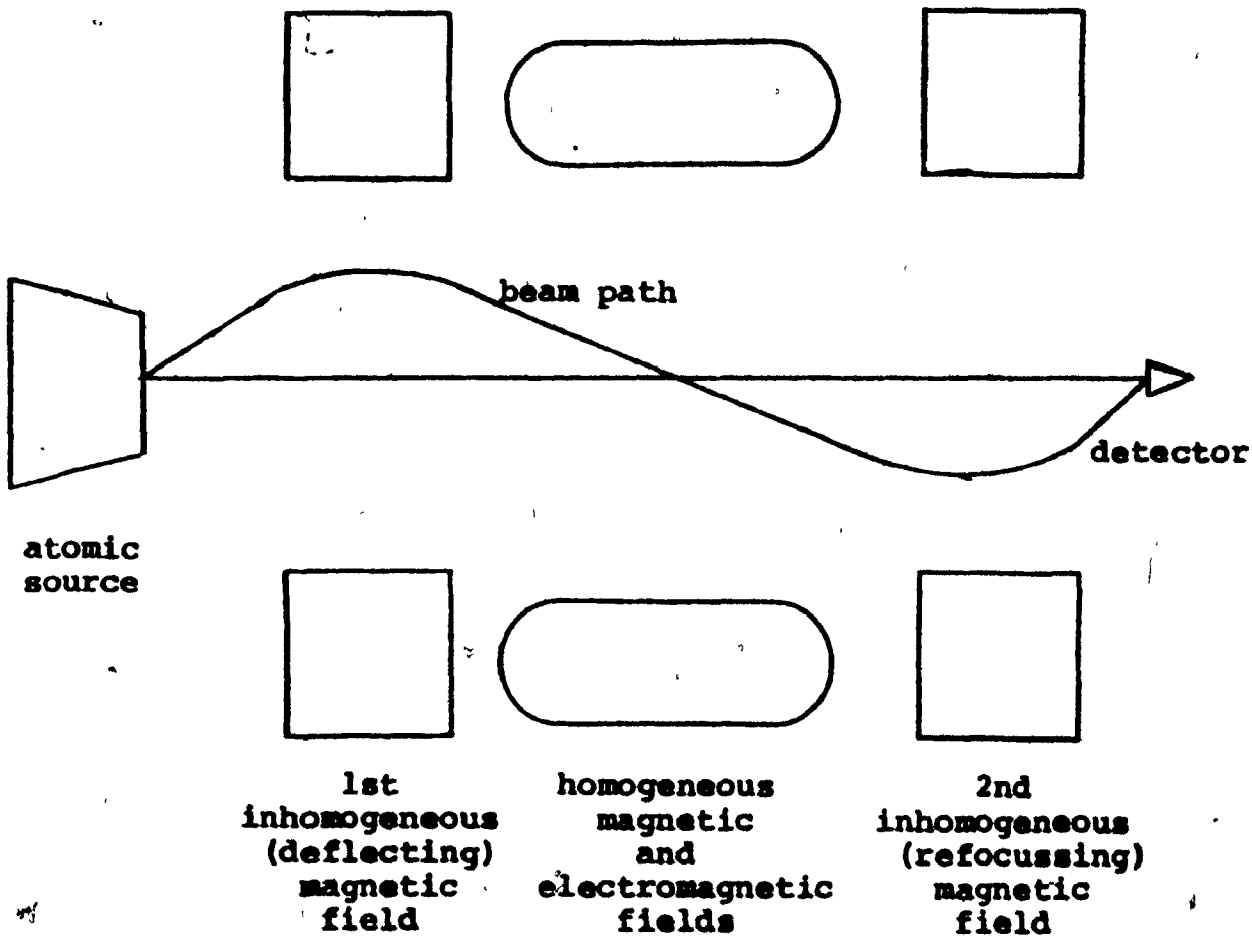

The allowed transitions are ($\Delta F=0$, $\Delta m_F=0,\pm1$) for a weak homogeneous field and ($\Delta m_J=\pm1$, $\Delta m_I=0$) or ($\Delta m_J=0$, $\Delta m_I=\pm1$) for a strong field[1]; these transitions are in the radio-frequency region.

The measurement by Jaccarino and King[38] of eQq for the Cl atom in the $^2P_{\frac{3}{2}}$ state (109.746±.010 MHz), which is the basis of all subsequent estimates of Q for ^{35}Cl and ^{37}Cl[39,40], used this method with a weak homogeneous field. The weak-field case allows determination of the sign of eQq while the high-field case does not[1].

d) <u>eQq from molecular beam electric resonance spectra</u>

This method is similar to the above except that the applied fields are electric rather than magnetic. Electric resonance cannot be used for atoms or homonuclear diatomic molecules since they have no permanent electric dipole moment and are not deflected by an inhomogeneous electric field. Molecular electric dipole moments are much larger than atomic magnetic moments; greater deflections are produced and more precise measurements of the resonance frequency can be made. Transitions are observed between levels with different angular momentum orientations (($\Delta F,\Delta m_F$) or ($\Delta m_I,\Delta m_J$) depending on the homogeneous field strength). These occur at radio frequencies. Because the interaction with the electric field becomes complicated for non-linear molecules with permanent dipole moments[1], this method is largely limited to diatomics. Besides eQq, for

which this method yields sign and magnitude, the equilibrium internuclear distance R_e and the permanent electric dipole moment μ can be measured. Kaiser[7] has determined eQq, R_e, and μ for $H^{35}Cl$ and $D^{35}Cl$ by this method; eQq and μ were determined to five significant figures, R_e to six. Kaiser's measurements are those with which the quantities calculated in this thesis are compared. Kaiser reported an eQq of -67.61893±.00047 MHz for $H^{35}Cl$ and -67.39338±.00009 MHz for $D^{35}Cl$ in the v=0, J=1 state with v the vibrational quantum number. The J=0 states cannot be measured because q averages to zero over random molecular motion in the absence of rotation (eq. (37)). Kaiser also did a vibrational-rotational analysis to obtain eQq for $H^{35}Cl$ in the hypothetical $v=-\frac{1}{2}$, J=0 state (stationary nuclei); this value should be independent of the H-isotope (and was so found by Kaiser to within the experimental uncertainty). The value obtained was -66.7751±.0030 MHz; using $Q(^{35}Cl)=-.0782\times10^{-24}$ cm^2 (see below) this corresponds to q=3.6339±.0003 atomic units (au); subtracting the q due to the proton at R_e=2.4087 au[41], this corresponds to an electronic q of 3.4908±.0003 au.

e) <u>eQq from microwave rotation spectra</u>

The nuclear quadrupole interaction energy for a diatomic molecule is[34]

$$E_Q = -\frac{eQq}{2I(2I-1)(2J-1)(2J+3)}[\tfrac{3}{2}C(C+1)-I(I+1)J(J+1)], \qquad (37)$$

with

$$C = F(F+1)-I(I+1)-J(J+1).$$

This equation includes the averaging of q (measured in a fixed molecular axis system) over the rotational motion of the molecule; note that for J=0, C=0 since F=I (section 2a(iv)), and thus $E_Q=0$ from (37). In microwave spectroscopy the transitions observed, because of the frequency used, are $\Delta J=\pm 1$, $\Delta F=0,\pm 1$. (37) gives the dependence of the splittings of the $\Delta J=\pm 1$ lines on J, F, and I; the intensities also depend on these numbers[42]. From the frequency and intensity data eQq can be deduced. Microwave measurements of eQq are inherently less precise than molecular beam electric resonance measurements since in microwave spectroscopy one measures the relatively small differences in $\Delta J=\pm 1$ transitions for different ΔF values; in molecular beam electric resonance the ΔF transitions are measured directly. However microwave spectroscopy is the most accurate available method for determining eQq in polyatomic molecules[1]. A molecule must have a permanent dipole moment to absorb microwaves. Both sign and magnitude of eQq are determined by this method. Gordy and coworkers have made two microwave studies of HCl and DCl: an early series (including TCl)[43-45], and a recent study[46]; the early work gave eQq to about two significant figures (-68.0±2.8 MHz for $H^{35}Cl$, -67.3±.7 MHz for $D^{35}Cl$, -67.0±.6 MHz for $T^{35}Cl$), the later to about three (-67.800±.095 MHz for $H^{35}Cl$, -67.417±.098 MHz for $D^{35}Cl$).

3. Determination of the nuclear quadrupole moment

Koster[47] has discussed several methods for obtaining Q from experimental data or combinations of experimental data and theoretically calculated quantities, three of which have been applied to HCl:

(i) Ratio of magnetic and quadrupole hyperfine constants

The atomic magnetic hyperfine interaction energy is

$$\Delta E = aC/2,$$

with C as in (37) and[47]

$$a = (\mu\mu_0/I)[2L(L+1)/J(J+1)]\langle r^{-3}\rangle F_r, \qquad (38)$$

with μ_0 the Bohr magneton, L the total electronic orbital angular momentum, μ the nuclear magnetic moment, $\langle r^{-3}\rangle$ the expectation value of r^{-3} for the unpaired electron giving rise to q, and F_r a relativistic correction factor given by Casimir[48]. a can be measured by atomic beam magnetic resonance. The nuclear quadrupole hyperfine interaction energy is (for atoms)[34]

$$E_Q = \frac{eQq}{2I(2I-1)J(2J-1)}[C(C+1)-I(I+1)J(J+1)]$$

$$\equiv \frac{b}{I(2I-1)J(2J-1)}[C(C+1)-I(I+1)J(J+1)]$$

with[47]

$$b \equiv \frac{eQq}{2} = e^2Q(2L/2L+3)\langle r^{-3}\rangle R_r, \qquad (39)$$

where R_r is another relativistic correction given by Casimir[48]. It is then possible to calculate Q without a value for $\langle r^{-3}\rangle$, which would have to be calculated from an atomic wavefunction, by the following formula[49]

$$Q = \frac{2(\mu\mu_0/e^2 I)(L+1)(2L+3)}{J(J+1)} \left(\frac{F_r}{R_r}\right) \left(\frac{b}{a}\right); \qquad (40)$$

b and a are both measurable by atomic beam magnetic resonance. Davis et al.[49] have questioned the reliability of the F_r factors for large nuclei, and Koster[47] has examined the possibility that more than one Slater determinant is necessary to give Q accurately; (38), and therefore (40), are altered upon inclusion of CI (section 1g). Thus although (40) is attractive because it circumvents calculation of $\langle r^{-3}\rangle$, it is of doubtful reliability. Jaccarino and King[38] used (40) and their eQq value for ^{35}Cl in the $^2P\frac{3}{2}$ state to calculate $Q(^{35}Cl) = (-.07894 \pm .00002) \times 10^{-24}$ cm^2.

(ii) Ratio of fine structure splitting to quadrupole hyperfine interaction.

The fine structure splitting δ (energy separation between the two allowed J values for an atom with $S=\frac{1}{2}$) can be expressed[47]

$$\delta = (3\mu_0^2/e) Z_i \langle r^{-3}\rangle H_r, \qquad (41)$$

with Z_i an effective nuclear charge defined by Casimir[50], and H_r a relativistic correction (≈ 1) given by Casimir[48]. (41) and (39) give

$$Q = (b/\delta)(3\mu_0^2/e^3)((2L+3)/2L)(H_r/R_r) Z_i. \qquad (42)$$

Again $\langle r^{-3}\rangle$ is not needed, but Z_i must be estimated. Koster[48] has given a method for estimating Z_i for Cl, and also shown that the cancellation of $\langle r^{-3}\rangle$ in (42) is to a first approximation unchanged by inclusion of CI, unlike (40). Using the data of Jaccarino and King[38], Koster recalculated $Q(^{35}Cl)$ by (42) and obtained $-.0782\times10^{-24}$ cm^2 (no uncertainty given, but Ramsey[3] gives $\pm.0002\times10^{-24}$ cm^2).

(iii) Direct calculation of $\langle r^{-3}\rangle$.

If one can calculate $\langle r^{-3}\rangle$ for the unpaired electron in Cl, it can be used in (39) with the experimental value of b to give Q directly. Korolkov and Makhanek[51] have calculated $\langle r^{-3}\rangle$ for p-electrons in several atoms by a modified Thomas-Fermi method[52]; their $\langle r^{-3}\rangle$ and the b of Jaccarino and King give $Q(^{35}Cl)=-.0793\times10^{-24}$ cm^2.

Note that methods (ii) and (iii), which should be more accurate than (i), give $Q(^{35}Cl)$ lower and higher in absolute value, respectively, than (i); thus the exact value of $Q(^{35}Cl)$ is still an open question. However methods (i)-(iii) all assume that q is due only to a single electron or hole outside spherical closed shells, these shells not contributing to q (Chapters III and VII). However Sternheimer[53] pointed out that the aspherical electron distribution outside the closed shells distorts them so that they too contribute to q (Chapter VII). Sternheimer[40,55,56] has calculated factors by which values of Q calculated neglecting this effect should be mul-

tiplied; the most recently calculated value for this factor for Cl is 1.045[40]. Using this factor Sternheimer[40] obtained a corrected $Q(^{35}Cl)$ of $(-.08249\pm.00002)\times10^{-24}$ cm^2; Sternheimer used the Jaccarino and King value of $(-.07894\pm.00002)\times10^{-24}$ cm^2 (method (i)) as the uncorrected Q. The uncorrected Q's of Koster and of Korolkov and Makhanek (methods (ii) and (iii)) give corrected values of $-.0817\times10^{-24}$ cm^2 and $-.0829\times10^{-24}$ cm^2 respectively.

It is not the place here to propose values for $Q(^{35}Cl)$; for comparison with experimental Koster's method (ii) value of $-.0782\times10^{-24}$ cm^2 is used without the Sternheimer correction throughout this thesis. This value was recommended by Ramsey[3] and used in the major experimental[7] and theoretical[54] studies of HCl. However the 4.5% change in Q induced by the Sternheimer effect should be kept in mind as another uncertainty added to the published uncertainties in q as calculated from eQq measurements by Kaiser[7], who purposely did not include the uncertainty in Q in his uncertainty estimates.

4. Previous investigations of a similar nature

Only one previous detailed ab-initio study of the EFG at the Cl nucleus in HCl has appeared, a two-center double-zeta STO (two STO's of different ζ for each (n,ℓ,m) combination) study by Scrocco and Tomasi[57]. Their analysis was in terms of bonding between H and Cl atoms and studied the degree of par-

ticipation in the MO's of basis orbitals centered on H; in the calculations of this thesis all basis orbitals are centered on Cl and the HCl molecule is viewed more nearly as a Cl^- ion perturbed by the proton. Thus this work does not seek to revise the previous work, but studies the same problem by different techniques.

5. Computational facilities

All calculations reported in this thesis were done in double precision (~16 significant figures) on the IBM 360/75 computer at the McGill University Computing Centre.

REFERENCES

1. E.A.C. Lucken, Nuclear Quadrupole Coupling Constants, Academic, N.Y., 1969. Chapter 3.
2. C.T. O'Konski and Tae-Kyu Ha, J. Chem. Phys. 49, 5354 (1968).
3. N.F. Ramsey, Molecular Beams, Oxford, 1956. p. 172.
4. R. Moccia, J. Chem. Phys. 40, 2164 (1964).
5. D.M. Bishop, Adv. Quant. Chem. 3, 25 (1967).
6. C.C.J. Roothaan, Revs. Mod. Phys. 23, 69 (1951).
7. E.W. Kaiser, J. Chem. Phys. 53, 1686 (1970).
8. R. McWeeny, Nature 243, 196 (1973).
9. S. Fraga and G. Malli, Many-Electron Systems: Properties and Interactions, Saunders, Philadelphia, 1968. p. 6.
10. R. McWeeny and B.T. Sutcliffe, Methods of Molecular Quantum Mechanics, Academic, London, 1969. Chapter 3.
11. Ref. 10, Chapter 4.
12. M. Born and R. Oppenheimer, Ann, der Physik 84, 457 (1927).
13. G. Herzberg, Electronic Spectra of Polyatomic Molecules, Van Nostrand, Princeton, 1967. Chapter 1.
14. J.K.G. Watson, J. Mol. Spec. 45, 99 (1973).
15. P.R. Bunker, J. Mol. Spec. 45, 151 (1973).
16. W. Kolos, Adv. Quant. Chem. 5, 99 (1970).
17. R.S. Mulliken, J. Chem. Phys. 23, 2005 (1955).
18. W. Pauli, Zeits. fur Physik 43, 601 (1927).
19. J.C. Slater, Phys. Rev. 34, 1293 (1929).

20. C.C.J. Roothaan, Revs. Mod. Phys. 32, 179 (1960).

21. V. Fock, Zeits. fur Physik 61, 126 (1930).

22. D.R. Hartree, The Calculation of Atomic Structures, Wiley, N.Y., 1957.

23. J.A. Pople and D.L. Beveridge, Approximate Molecular Orbital Theory, McGraw-Hill, N.Y., 1970.

24. J.C. Slater, Phys. Rev. 36, 57 (1930).

25. Ref. 10, p. 120.

26. Ref. 10, Chapter 2.

27. Chr. Moller and M.S. Plesset, Phys. Rev. 46, 618 (1934).

28. S.L. Kahalas and R.K. Nesbet, J. Chem. Phys. 39, 529 (1963).

29. H.B.G. Casimir, On the Interaction between Atomic Nuclei and Electrons, Freeman, S.F., 2nd edition, 1963. Section 8.

30. Ref. 3, Chapter VI.

31. C.H. Townes and A.L. Schawlow, Microwave Spectroscopy, McGraw-Hill, N.Y., 1955.

32. H. Schuler and Th. Schmidt, Zeits. fur Physik 94, 457 (1935).

33. J. Bardeen and C.H. Townes, Phys. Rev. 73, 97 (1948).

34. N.F. Ramsey, Nuclear Moments, Wiley, N.Y., 1953. Chapter 2.

35. Ref. 34, Chapter 1.

36. J.D. Jackson, Classical Electrodynamics, Wiley, N.Y., 1962. p. 100.

37. E.P. Wigner, Group Theory and its Application to the Quantum Mechanics of Atomic Spectra, Academic, N.Y., 1959. p. 169.

38. V. Jaccarino and J.G. King, Phys. Rev. 83, 471 (1951).

39. G.H. Fuller and V.W. Cohen, Nucl. Data A5, 433 (1969).

40. R.M. Sternheimer, Phys. Rev. A6, 1702 (1972).

41. P.R. Bunker, J. Mol. Spec. 39, 90 (1971).

42. Ref. 31, p. 152.

43. G. Jones and W. Gordy, Phys. Rev. 136, A1229 (1964).

44. M. Cowan and W. Gordy, Phys. Rev. 111, 209 (1958).

45. C.A. Burns, W. Gordy, B. Benjamin, and R. Livingston, Phys. Rev. 97, 1661 (1955).

46. F.C. DeLucia, P. Helminger, and W. Gordy, Phys. Rev. A3, 1849 (1971).

47. G.F. Koster, Phys. Rev. 86, 148 (1952).

48. Ref. 29, p. 54.

49. L. Davis, Jr., B.T. Feld, C.W. Zabel, and J.R. Zacharias, Phys. Rev. 76, 1076 (1949).

50. Ref. 29, p. 50.

51. V.S. Korolkov and A.G. Makhanek, Opt. and Spectry. (Eng. trans.) 12, 87 (1962).

52. J.C. Slater, Quantum Theory of Atomic Structure, v. 1, McGraw-Hill, N.Y., 1960. Appendix 17.

53. R.M. Sternheimer, Phys. Rev. 80, 102 (1950).

54. A.D. McLean and M. Yoshimine, J. Chem. Phys. 47, 3256 (1967).

55. R.M. Sternheimer, Phys. Rev. 84, 244 (1951).

56. R.M. Sternheimer, Phys. Rev. 86, 316 (1952).

57. E. Scrocco and J. Tomasi, Theor. Chim. Acta 2, 386 (1964).

58. For any wavefunction ϕ_a, $\langle\phi_a|H_e|\phi_a\rangle \geq E_e$, with E_e the true electronic energy, but if ϕ_a is an approximate wavefunction obtained from an approximate electronic Hamiltonian H_a (as is the case in most "approximate" MO methods), there is no guarantee that $\langle\phi_a|H_a|\phi_a\rangle$, which is usually taken as the expectation value of the electronic energy, lies above E_e.

CHAPTER II: One Center Expansion - Self Consistent Field Calculations of HCl

Solution of the Hartree-Fock-Roothaan (HFR) equations (Chapter I) is considerably simplified (cf. section 2) if the basis orbitals ϕ_i are centered on the same point. Wavefunctions in such bases are One Center Expansion (OCE) wavefunctions. An OCE basis is appropriate either when the molecule has high symmetry about a point and no inner-shell electrons except at that point (e.g. CH_4[1] or NH_3[2]), or when one is interested in a molecular property highly dependent on the electron distribution near one point. The calculations reported here fall into the latter class. As an OCE basis is increased, it can approach a complete set[3,4] (one able to approximate any spatial function arbitrarily closely); thus the OCE wavefunction can in principle approach the Hartree-Fock (H-F) wavefunction, although in practice OCE bases are of limited size and far from complete.

The property of interest here is the EFG at the Cl nucleus in HCl, the operator for which is $(3\cos^2\theta_\alpha-1)/r_\alpha^3$, with r_α the distance from the Cl nucleus and θ_α the angle from the principal axis of the EFG tensor (Chapter III). This operator is large for small values of r_α, so electron density near the Cl nucleus is expected to dominate the contributions to this property (Chapter V). Thus it is likely that an OCE basis for HCl centered on Cl could approximate this property well,

since a large OCE basis is very flexible near its center. An OCE calculation of HCl in a basis including 71 Slater-type orbitals (STO's) has been done by Moccia[5], and indeed the reported EFG agreed with the best experimental value available at that time[6] to within the experimental uncertainty. It was decided to repeat this calculation to study the relation of the electron distribution to the EFG.

However, because in the Moccia calculation the electron repulsion integrals were stored only to 6 significant figures[7], while in ours they were stored to 16, the occupied MO's with higher eigenvalues, which are the most sensitive to changes in the integrals (section 5c), differed enough in the two calculations to give a difference in the EFG of 6%. A 6% difference from the experimental value is less than that from the two-center double-ζ STO calculation of Scrocco (8% error)[8], but greater than that from the extensive two-center ab-initio STO calculations of HCl (1%-2% error)[9,10]. Thus the problem becomes one of determining why Moccia's basis gives a less accurate EFG than two-center bases which include fewer orbitals on Cl, and of constructing an OCE basis more accurate for this property. These questions are examined in later chapters; this chapter describes OCE wavefunctions and presents those calculated in this work.

1. Types of OCE wavefunctions

Most OCE wavefunctions fall into one of two classes: (i) configuration interaction wavefunctions (OCE-CI), which are linear combinations of Slater determinants formed from orthogonalized atomic basis orbitals, or (ii) molecular orbital self-consistent field (OCE-SCF) wavefunctions, which are HFR wavefunctions in an OCE basis. There is current work both with OCE-CI[11] and OCE-SCF[2] wavefunctions. Some calculations use both procedures[12], with a single determinant optimized by the HFR procedure and other determinants constructed with the unoccupied HFR orbitals. For reasons described in Chapter I, the OCE-SCF method was chosen over OCE-CI for this work.

2. Characteristics of the OCE-SCF method and wavefunctions

a) Computational advantages

Only if OCE-SCF calculations are simpler or quicker than many-center calculations of comparable accuracy is their use justified. However all electron repulsion integrals in an OCE-SCF calculation can be evaluated quickly compared to the multicenter integrals which arise otherwise. In a two-center STO basis for a diatomic molecule, for example, if the orbitals ϕ_p, ϕ_q, ϕ_r, and ϕ_s in the electron repulsion integral

$$[pq|rs] \equiv \int d\tau_1 d\tau_2 \phi_p(1)\phi_q(1)(r_{12}^{-1})\phi_r(2)\phi_s(2)$$

are not centered at the same point, the products of the orbitals and r_{12}^{-1} must be expanded either in an elliptical coordinate system[13,14] or a spherical system on one of the centers[15]. The expansion is integrated term-by-term; the process is lengthy because the series converges slowly.

In an OCE-SCF calculation, the orbital products and r_{12}^{-1} are expressed as finite combinations of products of spherical harmonics on the expansion center; because of the properties of integrals over products of spherical harmonics[16] many terms vanish upon integration over the angular coordinates; thus these integrals are evaluated much more rapidly in an OCE basis. The number of non-zero electron repulsion integrals is also substantially reduced: because of the symmetry of the spherical harmonics, about 85% of the possible integrals vanish; for typical many-center calculations this fraction is less than 50%[17].

Another advantage arises in calculating OCE-SCF wavefunctions at a series of internuclear distances. Since [pq|rs] is independent of internuclear distance if all orbitals are on the same center, a change in internuclear distance without a change of basis requires no recalculation of the [pq|rs]. Some nuclear attraction integrals must be recalculated, but these are few compared to the [pq|rs]. In a two-center basis all [pq|rs] involving both centers must be recalculated at each internuclear distance.

b) <u>Limitations of the OCE-SCF wavefunction</u>

The exact molecular electronic ψ satisfies the Schroedinger equation,

$$(-\tfrac{1}{2}\sum_i \nabla_i^2 + \tfrac{1}{2}\sum_{ij}\sum(r_{ij}^{-1}) - \sum_{i\alpha}\sum\frac{Z_\alpha}{r_{i\alpha}})\psi = E\psi, \qquad (1)$$

with i, j labeling electrons and α labeling nuclei (Chapter I). At nucleus α, where $r_{i\alpha}$ vanishes, ψ is multiplied by an infinite factor on the left of (1). It has been shown[18,19] that if the ratio $H\psi/\psi(=E)$ is to remain finite at $r_{i\alpha}=0$, ψ must satisfy

$$(\partial\hat{\psi}/\partial r_{i\alpha})_{r_{i\alpha}=0} = Z_\alpha\psi(r_{i\alpha}=0), \qquad (2)$$

with $\hat{\psi}$ the average of ψ over a sphere of radius $r_{i\alpha}$. (2) is called the cusp condition on ψ[20]; for non-zero $\psi(r_{i\alpha}=0)$, (2) implies a discontinuity in directional derivatives of ψ through the point $r_{i\alpha}=0$[21].

Consider an OCE basis composed of STO's

$$\phi_i(n,\ell,m,\zeta,r,\theta,\phi) = N(n,\zeta)r^{n-1}\exp(-\zeta r)S_{\ell m}(\theta,\phi), \qquad (3)$$

with $N(n,\zeta)$ a normalization factor and $S_{\ell m}(\theta,\phi)$ a spherical harmonic (see below). If the basis includes STO's with n=1, the OCE wavefunction can satisfy (2) if α is the expansion center, since for n=1, $(\partial\phi_i/\partial r)_{r=0} = -\zeta N(n,\zeta)S_{\ell m}(0,0)\neq 0$. If α is not the expansion center, (2) cannot be satisfied, since

directional derivatives of (3) are continuous everywhere but $r=0$. However if enough basis functions are included the OCE wavefunction can approximate a cusped function arbitrarily closely at an off-center α.

Another question is how well an OCE-SCF wavefunction accounts for the energy of attraction between the nuclei and electrons and the energy of repulsion between electrons. The potential at a point $\bar{r}=(r,\theta,\phi)$ due to a nucleus α is

$$V_\alpha(\bar{r}) = Z_\alpha/r_\alpha, \tag{4}$$

with Z_α the nuclear charge and r_α the distance of $\bar{r}$ from α. $V_\alpha(\bar{r})$ can be expanded (Appendix I),

$$V_\alpha(\bar{r}) = 4\pi Z_\alpha \sum_{\ell=0}^{\infty} \frac{1}{2\ell+1} \frac{r_<^\ell}{r_>^{\ell+1}} \sum_{m=-\ell}^{\ell} S_{\ell m}(\theta_\alpha,\phi_\alpha) S_{\ell m}(\theta,\phi), \tag{5}$$

with $(r_<,r_>)$ the (lesser, greater) of (r_α,r), and $\theta_\alpha,\phi_\alpha$ the angular coordinates of α. The attraction between the electrons and nucleus α in the H-F approximation is

$$E_{n\alpha} = -\sum_k N_k \langle\psi_k|V_\alpha|\psi_k\rangle, \tag{6}$$

by Chapter I, equation (23). Each ψ_k is expanded in terms of the basis orbitals,

$$\psi_k = \sum_i C_{ik}\phi_i,$$

with ϕ_i given by (3). Then (6) can be expressed in terms of integrals of the form

$$\int_0^\infty dr\, g(r) \int_0^\pi d\theta \sin\theta \int_0^{2\pi} d\phi\, S_{\ell_i m_i}(\theta,\phi) S_{\ell_j m_j}(\theta,\phi) S_{\ell m}(\theta,\phi), \qquad (7)$$

where $S_{\ell_i m_i}(\theta,\phi)$ and $S_{\ell_j m_j}(\theta,\phi)$ are from basis orbitals and $S_{\ell m}(\theta,\phi)$ from (5). The exact form of the radial integrands $g(r)$ is not important. The angular integral in (7) is zero unless[16]

$$\ell_i + \ell_j \geq \ell$$

and (8)

$$|\ell_i - \ell_j| \leq \ell.$$

Thus in an OCE basis terms in (7) with ℓ larger than twice the largest ℓ-value in the basis vanish. If orbitals are included on another center, their expansion in terms of spherical harmonics on the first center is infinite; there would then be no largest ℓ_i or ℓ_j in (7). Thus a two-center basis does not result in neglect of higher ℓ-terms in (5), so restricting the basis to a finite set on one center causes truncation of the off-center nuclear attraction energy. Bishop has discussed this[4].

Similarly, the electron repulsion operator r_{12}^{-1} can be expanded

$$r_{12}^{-1} = 4\pi \sum_{\ell=0}^{\infty} \frac{1}{2\ell+1} \frac{r_<^\ell}{r_>^{\ell+1}} \sum_{m=-\ell}^{\ell} S_{\ell m}(\theta_1,\phi_1) S_{\ell m}(\theta_2,\phi_2),$$

with $(r_<, r_>)$ now the (lesser, greater) of (r_1, r_2). In evaluating $[pq|rs]$ terms arise containing the factors

$$\int_0^{\pi} d\theta_1 \sin\theta_1 \int_0^{2\pi} d\phi_1 \, S_{\ell_p m_p}(\theta_1,\phi_1) S_{\ell_q m_q}(\theta_1,\phi_1) S_{\ell m}(\theta_1,\phi_1)$$

and

$$\int_0^{\pi} d\theta_2 \sin\theta_2 \int_0^{2\pi} d\phi_2 \, S_{\ell_r m_r}(\theta_2,\phi_2) S_{\ell_s m_s}(\theta_2,\phi_2) S_{\ell m}(\theta_2,\phi_2);$$

the product of these vanishes unless $\ell_p+\ell_q \geq \ell$ and $\ell_r+\ell_s \geq \ell$, so there is also truncation of the electron repulsion energy in a finite OCE basis. In a given basis these errors can be reduced by adding orbitals of higher ℓ.

Despite these limitations the OCE-SCF method was chosen for this work because of the computational advantages and because the OCE-SCF wavefunction has the proper behavior near the expansion center.

3. Choice of basis

The general form (3) of the STO contains the spherical harmonic $S_{\ell m}(\theta,\phi)$. A spherical harmonic is the product of a θ-dependent and a ϕ-dependent factor; normalized associated Legendre polynomials are chosen as the θ-dependent part[13]. For the ϕ-dependent factor there are two common choices: the complex functions $\exp(im\phi)$[22], or the real functions $\sin|m|\phi$ and $\cos|m|\phi$[13,23]. For this work the real functions were chosen because they lead to Fock matrices (Chap-

ter I) with real elements; with complex orbitals the Fock matrix is in general complex. Complex matrices have two disadvantages: they require twice as much computer memory as the corresponding real matrix, and many matrix diagonalization methods[24] are restricted to real matrices. Formulas for the real spherical harmonics are given in Appendix I.

Yet to be determined are the number of basis orbitals and their n, ℓ, m, and ζ parameters. For an SCF calculation of HCl the necessary m-values can be determined exactly. Consider HCl with Cl at the origin and the proton on the +z-axis. The MO structure of HCl is[25] $(1s\sigma)^2\ (2s\sigma)^2\ (2p\sigma)^2\ (2p\pi)^4\ (3s\sigma)^2\ (3p\sigma)^2\ (3p\pi)^4$. All MO's are either of the σ or π type. The σ MO's depend upon the angle ϕ about the z-axis in the same way as does the ϕ-factor of a spherical harmonic with $m=0$; the π MO's have the ϕ-dependence of a spherical harmonic with $m=\pm 1$. Thus the ϕ-dependence of all MO's of HCl is given correctly by a basis including STO's with only the three m-values $-1, 0$, and $+1$.

No limit can be placed on the n- or ℓ-values needed. The n-value determines the sharpness of the radial peaking and the ℓ-value the sharpness of the angular peaking, higher values implying sharper peaking for both. For $n > 1$, the radial factor of an STO,

$$R(n,\zeta,r) = r^{n-1}\exp(-\zeta r), \tag{9}$$

vanishes for $r=0$ and approaches 0 as $r \to \infty$, with a maximum at a point r_{max} in between. A measure of the sharpness of this maximum is the width at half-height of (9); i.e., the distance in au between the points less than and greater than r_{max} at which (9) has half its maximum value. Differentiation of (9) gives

$$r_{max} = (n-1)/\zeta, \tag{10}$$

with r_{max} given in au. Table I lists the widths at half height of the radial function (9) for values of n from 4 to 20 and $r_{max}=2.41$ au (to 2 decimal places the equilibrium internuclear distance R_e for HCl). These values are to be compared with a similar value for the 1s orbital of H, since one adds orbitals to an OCE basis for HCl to approximate electron density at the proton. The radial part of the H 1s orbital is

$$R_H(r) = \exp(-r),$$

which falls to half its maximum value ($r_{max}=0$) at $r=.69$ au, and the quantity corresponding to width at half height of the STO's on Cl is twice this, 1.38 au. Table I shows that this sharpness is attained only for $n \geqslant 18$. Even this peaking is illusory, for it occurs in all directions, though needed only at the proton[26].

TABLE I: Radial peaking of STO's. Widths at half height (au) for STO's with r_{max}=2.41 au.

n	width (au)
4	3.32
5	2.87
6	2.56
7	2.33
8	2.15
9	2.00
10	1.90
11	1.80
12	1.72
13	1.64
14	1.57
15	1.52
16	1.47
17	1.42
18	1.37
19	1.34
20	1.30

In practice orbitals with n=18 are not used in OCE bases; in one approach[3] n- and ℓ-values are selected by constructing normalized OCE-MO's to maximize overlap with MO's from existing two-center calculations, and determining the n- and ℓ-values necessary to give an overlap close to one; selection of the exponents ζ is then done by minimizing the molecular energy in a series of calculations.

Another approach (that of the present work) is to start (in the case of HCl) with an accurate published basis for Cl in a two-center calculation of Cl_2[27] and add orbitals to approximate the electron distribution near the proton. The basis enlargement process is reported in Chapter III, section 4. A rather small basis constructed in this way yielded a lower molecular energy and several molecular properties closer to the H-F limit for HCl than the 71-STO basis of Moccia[5]. Properties calculated in this basis are presented later in this chapter.

Moccia developed a very large OCE basis for HCl by the first approach over a number of years[3,5]; this basis is listed in Table II, with n,ℓ,m,ζ, and r_{max} values. The basis includes 71 orbitals, but only 51 are listed because for each orbital with m=1 there is another with identical n,ℓ, and ζ but with m=-1. A similar convention is followed later in listing π MO's.

Orbitals 1 through 9 are essentially a triple-ζ set of 1s, 2s, and 3s orbitals (3 ζ-values for every n,ℓ,m combi-

TABLE II: The Moccia[5] OCE basis for HCl. 71 STO's, 31 σ orbitals and 20 π pairs.

σ orbitals	n	ℓ	m	ζ	r_{max} (au)
1	1	0	0	23.980	0.000
2	1	0	0	15.305	0.000
3	1	0	0	10.000	0.000
4	2	0	0	8.502	0.118
5	2	0	0	6.297	0.159
6	2	0	0	4.000	0.250
7	3	0	0	1.767	1.132
8	3	0	0	1.104	1.812
9	3	0	0	0.805	2.484
10	9	0	0	3.419	2.340
11	2	1	0	8.885	0.113
12	2	1	0	5.725	0.175
13	3	1	0	4.361	0.459
14	3	1	0	2.004	0.998
15	3	1	0	1.222	1.637
16	3	1	0	0.862	2.320
17	9	1	0	3.419	2.340
18	3	2	0	2.224	0.899
19	3	2	0	1.492	1.340
20	6	2	0	2.137	2.340
21	9	2	0	3.419	2.340

continued

TABLE II: (cont'd.)

σ orbitals	n	ℓ	m	ζ	r_{max}(au)
22	4	3	0	1.675	1.791
23	4	3	0	2.125	1.412
24	9	3	0	3.419	2.340
25	5	4	0	2.000	2.000
26	9	4	0	3.419	2.340
27	6	5	0	2.136	2.341
28	9	5	0	3.419	2.340
29	7	6	0	2.564	2.340
30	9	6	0	3.419	2.340
31	9	7	0	3.419	2.340

π orbitals	n	ℓ	m	ζ	r_{max}(au)
32	2	1	1	8.990	0.111
33	2	1	1	5.720	0.175
34	3	1	1	4.330	0.462
35	3	1	1	2.340	0.855
36	3	1	1	1.270	1.575
37	6	1	1	2.137	2.340
38	9	1	1	3.419	2.340
39	3	2	1	1.700	1.176
40	3	2	1	1.100	1.818
41	4	2	1	1.200	1.667

continued

TABLE II: (cont'd.)

π orbitals	n	ℓ	m	ζ	r_{max} (au)
42	7	2	1	2.564	2.340
43	4	3	1	1.600	1.875
44	4	3	1	1.100	2.727
45	7	3	1	2.564	2.340
46	5	4	1	1.500	2.667
47	9	4	1	3.419	2.340
48	6	5	1	2.136	2.341
49	9	5	1	3.419	2.340
50	8	6	1	2.990	2.341
51	9	7	1	3.419	2.340

nation). A 9s orbital with r_{max}=2.34 au (orbital 10) is added for electron density near the proton. The pσ orbitals 11-17 follow a similar pattern, but with two 2pσ and four 3pσ orbitals included[28]. Beyond this point the σ-orbital pattern is less simple; for $1 \leqslant \ell \leqslant 3$ two orbitals of the minimum n(=ℓ+1) and at least one of a higher n for density at the proton are added. For $4 \leqslant \ell \leqslant 6$, there is one orbital with n=ℓ+1 and one with n=9; for ℓ=7, the highest included, there is only the n=9 orbital. The π orbitals follow a similar pattern (s orbitals are excluded from the π set by symmetry) with one less ℓ=6 orbital.

The π set is almost as radially flexible as the σ set; although there are 31 σ-orbitals and only 20 π-orbitals for each m-value, 10 of the σ-orbitals are s-orbitals (ℓ=0). For $\ell \geqslant 1$ there are 21 σ-orbitals and 20 π-orbitals, and the orbital of largest r_{max} (orbital 44, r_{max}=2.727 au) is a π-orbital.

Two major criticisms can be made of Moccia's basis. It was too costly to energy-optimize the ζ of the whole 71-STO set, so 43 orbitals were first selected and the energy minimized with respect to the ζ of these orbitals[5]; then several unimportant orbitals were discarded and orbitals with higher n and ℓ added with exponents chosen to put r_{max} near the proton. No reoptimization of exponents was done after addition of these orbitals. Since several of the MO's involve the high-n basis orbitals heavily (Table V), it is likely that the role of some

orbitals of the 43-orbital set with low exponents (i.e. higher r_{max}) is now taken by orbitals with higher n, and that the charge distribution would be better approximated if the exponents of some lower-n orbitals were increased to provide flexibility in the intermediate region of space. However, adjusting the orbital exponents would require much computer time, so the reoptimization of the 71-STO set was not undertaken in this work.

A second criticism of Moccia's basis is the large number of π orbitals. Since most of the bonding in HCl involves σ orbitals (in a minimal two-center basis for HCl, for example, no π orbitals are included on H), it seems more efficient to leave the π basis at roughly the size necessary for an accurate calculation of the Cl^- ion and make most of the orbital additions to the σ set. Also in order not to induce artificial deviations from spherical symmetry in MO's describing inner electron shells (Chapters III and VII) it is important to have the exponents of, for example, the $2p\pi$ basis orbitals equal or very nearly equal to those of the corresponding $2p\sigma$ set and allow the small polarization to be produced by differences in the MO coefficients, which is possible as long as there is more than one 2p orbital of each symmetry. The basis of Table II, however, has differences of up to .1 between corresponding $2p\sigma$ and $2p\pi$ exponents. A calculation of Cl^- in this basis (Chapter III) produced a charge distribution which deviated significantly from spherical symmetry.

The bases developed in this work (Chapter III, section 4) were constructed by adding orbitals with n=9 and r_{max}=2.4087 au to the Gilbert-Wahl (GW) basis for Cl_2[27], which was developed from the basis for Cl of Bagus[29]. The largest basis used (29 STO's) is given in Table III.

4. Evaluation of electronic integrals

In Chapter I the types of electronic integrals over the basis orbitals which arise in HFR calculations were defined. Techniques for evaluation of all the integrals which occur in an OCE-SCF calculation are well-known because they arise in atomic calculations[22] except for the off-center nuclear attraction integrals[30]. The integral routines used in this work were written independently and were designed to be completely general; there is no limit to the size of the n, ℓ, m, or ζ parameters which the routines can handle except the largest number which the computer can represent.

It is important that one who writes routines for the evaluation of electronic integrals prove the accuracy of these routines, since the molecular energy and MO's are seriously affected if there are errors in integral evaluation[31]. To this end derivations of the integral formulas are given in Appendix I with comparisons between integrals evaluated by these routines and published values.

TABLE III: GW+9 OCE basis for HCl. 29 STO's, 19 σ orbitals, 5 π pairs. Basis developed from Cl_2 basis of Gilbert and Wahl[27].

σ orbitals	n	ℓ	m	ζ	r_{max}(au)
1	1	0	0	18.424	0.000
2	2	0	0	16.187	0.062
3	2	0	0	6.092	0.164
4	3	0	0	2.608	0.767
5	3	0	0	1.597	1.252
6	2	1	0	10.267	0.097
7	2	1	0	5.608	0.178
8	3	1	0	2.608	0.767
9	3	1	0	1.463	1.367
10	3	2	0	1.943	1.029
11	9	0	0	3.32129	2.4087
12	9	1	0	3.32129	2.4087
13	9	2	0	3.32129	2.4087
14	9	3	0	3.32129	2.4087
15	9	4	0	3.32129	2.4087
16	9	5	0	3.32129	2.4087
17	9	6	0	3.32129	2.4087
18	9	7	0	3.32129	2.4087
19	9	8	0	3.32129	2.4087

continued

TABLE III: (cont'd.)

π orbitals	n	ℓ	m	ζ	r_{max}(au)
20	2	1	1	10.267	0.097
21	2	1	1	5.608	0.178
22	3	1	1	2.608	0.767
23	3	1	1	1.463	1.367
24	3	2	1	1.943	1.029

5. Organization of the SCF calculation

The computer programs used to perform the calculations are listed in Appendix II. In the present section some general problems which arise in performing closed-shell SCF calculations are discussed.

a) Orthonormalization of basis

Roothaan's[32] adaptation of the Hartree-Fock equations results in the matrix equation (Chapter I),

$$FC = SCE, \tag{11}$$

with F the Fock matrix, C the coefficient matrix of the MO's, S the overlap matrix of the basis set, and E the diagonal eigenvalue matrix (Chapter I).

Each iteration of the SCF process involves one solution of (11), finding C and E given F and S. (11) cannot be solved directly; however if the nxn matrix A has an inverse, (11) can be rewritten

$$FAA^{-1}C = SAA^{-1}CE;$$

multiplying both sides on the left by $A^{\dagger}$, the transpose or (if A is complex) conjugate transpose of A,

$$(A^{\dagger}FA)(A^{-1}C) = (A^{\dagger}SA)(A^{-1}C)E. \tag{12}$$

Suppose A has been chosen so that

$$A^{\dagger}SA = I, \tag{13}$$

with I the nxn identity matrix. Then, defining $F' = A^{\dagger}FA$ and

$C' = A^{-1}C$, (12) becomes

$$F'C' = C'E,$$

or

$$C'^{-1}FC' = E. \tag{14}$$

Since F is symmetric, C' can be found such that E is diagonal and real and C' is unitary (i.e. $C^{-1} = C^{\dagger}$)[33]. Efficient computer routines exist which find C' and E in (14)[24].

Thus the problem in solving (11) is finding A such that (13) is satisfied, which is equivalent to transforming the given basis to an orthonormal set (one whose overlap matrix is the identity matrix). There are several ways to do this[34]; the method used here is the Lowdin Orthogonalized Atomic Orbital (OAO) method[35], which consists in taking as A the matrix

$$S^{-\frac{1}{2}} = UD^{-\frac{1}{2}}U^{\dagger}, \tag{15}$$

with U a unitary matrix satisfying

$$U^{\dagger}SU = D, \tag{16}$$

with D diagonal. $D^{-\frac{1}{2}}$ is a diagonal matrix whose non-zero elements are the reciprocal square roots of the corresponding elements of D. Substituting on the left of (13),

$$(S^{-\frac{1}{2}})^{\dagger}SS^{-\frac{1}{2}} = UD^{-\frac{1}{2}}U^{\dagger}SUD^{-\frac{1}{2}}U^{\dagger} = UD^{-\frac{1}{2}}DD^{-\frac{1}{2}}U^{\dagger} = I,$$

so (13) is satisfied. The only possible problem with this method is that if the basis is or is nearly linearly dependent, the diagonalization (16) gives an inaccurate matrix U. Problems of this kind were not encountered in this work.

b) Initiation of the iterative process

Since the elements of the Fock matrix (Chapter I) depend upon the MO coefficients, these coefficients must be guessed to start the iterative process. In this work the published MO coefficients of Moccia[5] were used to initiate the 71-STO calculations; calculations in the GW basis[27] were initiated with the MO coefficients of the Cl^- ion in this basis, which itself was initiated by simple guesses of orbital occupancies in the ion. Calculations in the enlarged GW bases (Chapter III) were initiated with the coefficient matrices of the previous member of the series. Once an initial C is provided, the iterative process involves constructing F from C by the formulas of Chapter I, transforming to the orthonormal set to give F', diagonalizing to get C', transforming back to C, constructing a new F, and continuing the process until it converges.

c) Convergence criterion for the iterative process

In the iterative process one records changes in a relevant quantity from one iteration to the next, accepting the process as converged when the change falls below a chosen limit. For an SCF calculation one can check changes in the

electronic energy,

$$E_{elec} = \frac{1}{2} \sum_i \sum_j P_{ij}(H_{ij} + F_{ij}), \tag{17}$$

with P_{ij}, H_{ij}, and F_{ij} elements of the first-order density, one-electron Hamiltonian, and Fock matrices respectively (Chapter I). The sums range over basis orbitals. The first convergence criterion used in this work was that the relative change in E_{elec} between the i-th and the i+1-st iterations be less than $.5\times10^{-12}$, i.e. that

$$\Delta E_i/E_i \equiv |E_{i+1} - E_i|/E_i < .5\times10^{-12}.$$

This is equivalent to requiring 12 significant figures in the electronic energy.

It was found that even when this criterion was satisfied, the eigenvalue and coefficients of the highest occupied MO still changed in the fifth figure. Storing a whole coefficient matrix from iteration to iteration is costly of computer memory, so the following procedure was used. The energy criterion of $.5\times10^{-12}$ was checked until satisfied. Thereafter the relative change in the eigenvalue of the highest occupied MO was checked until it fell below $.5\times10^{-6}$. Experience has shown that the MO coefficients are accurate to the same number of decimal places as the corresponding eigenvalue. The coefficients of the highest occupied MO tend to be the most mobile from iteration to iteration for the following reason: the

successive iterated Fock matrices can be considered perturbations of the final Fock matrix; the n-th eigenvector at any iteration can then be estimated to first order from the corresponding converged eigenvector by Rayleigh-Schroedinger perturbation theory[36],

$$\psi_n' = \psi_n^\circ + \sum_{m \neq n} \frac{F_{mn}^{(1)}}{E_n^\circ - E_m^\circ} + \ldots, \tag{18}$$

with ψ_n° the converged n-th eigenvector of F and $F_{mn}^{(1)}$ the difference between F_{mn} at self-consistency and F_{mn} at a particular iteration. E_n° and E_m° are eigenvalues of the converged eigenvectors. For HCl the lowest eigenvalue is much lower than the next lowest, and successive eigenvalues of occupied orbitals occur increasingly densely[9,10]; thus the occupied eigenvector with the highest eigenvalue has many small denominators in the summation in (18) and hence relatively large corrections to ψ_n°; the eigenvector with the lowest eigenvalue, however, always has relatively large denominators, and relatively small corrections to its eigenvector.

The first-order density matrix P, with elements

$$P_{ij} = \sum_k N_k C_{ik} C_{jk}, \tag{19}$$

with the sum over the MO's ψ_k and N_k the occupation number of ψ_k, is intermediate in accuracy between the electronic energy and the coefficients. It was observed in comparing prelimi-

nary calculations using an energy convergence criterion of $.5\times10^{-9}$ with later ones using $.5\times10^{-12}$ that the $.5\times10^{-9}$ criterion gave about six significant figures in the density matrix. Roughly, one expects that if 9 figures in the energy give 6 in the density matrix, then 12 in the energy give 8 in the density matrix. This could be tested by using a still smaller energy criterion, but this was not done since it might exceed the accuracy limits of the integral routines. We estimate that the largest density matrix elements (≈ 1) have 8 significant figures, and the rest are accurate to the same number of decimal places.

6. OCE-SCF calculations of HCl

Moccia[5] published OCE-SCF MO's for HCl in the basis of Table II for R=2.424 au (R_e=2.4087 au[37]); these MO coefficients are listed in Table IV. This calculation was repeated with the program described above at the same internuclear distance; the MO's obtained are listed in Table V.

The eigenvalues differ by about .007 au, with Moccia's lower; the electronic energies differ by about the same amount. In the higher energy MO's, such as 5σ and 2π, there are rather large differences in the coefficients (e.g. basis orbital 15 in 5σ, orbital 36 in 2π). The integral routines described in Appendix I were thoroughly tested; the apparent source of the differences is the difference in integral storage length mentioned above. In order to test whether this suffices to explain the

TABLE IV: Moccia's OCE-SCF MO's for HCl[5], R=2.424 au. Basis orbital numbers refer to Table II.

E_{elec} = -467.07130 au, E_{tot} = -460.05810 au

	σ MO coefficients				
basis orb.	1σ	2σ	3σ	4σ	5σ
1	.09166	.00189	-.00003	-.02578	.00897
2	1.07967	-.20587	.00098	.27135	-.09095
3	-.22474	-.22100	.00074	-.24859	.09151
4	.11990	.11237	.00017	.56940	-.19886
5	-.06529	.93843	-.00566	-1.18487	.38862
6	.01557	.11949	.00130	.57420	-.19952
7	-.02284	-.00770	.00050	1.02584	-.24753
8	-.00159	-.00508	-.00005	.17500	-.09601
9	.00073	.00233	.00000	-.10227	.06199
10	.00264	.00803	-.00012	-.32499	.20646
11	.00021	.00059	.31653	-.01056	-.04967
12	-.00022	.00249	.63172	-.01773	-.19011
13	.00011	.00082	.11804	-.00486	.08679
14	-.00004	.00017	-.02183	.12564	.54599
15	.00001	-.00024	-.02286	-.00885	.61500
16	.00004	.00007	.00622	.00370	-.17441
17	.00001	.00022	.02737	.05752	-.08456
18	.00004	.00423	.00371	-.00019	.06836
19	.00001	-.00717	-.00580	.07935	.05115

continued

TABLE IV: (cont'd.)

	σ MO coefficients (cont'd.)				
basis orb.	1σ	2σ	3σ	4σ	5σ
20	-.00002	.00332	.00260	-.05934	.02405
21	.00001	.00081	.00076	.07764	.13177
22	.00000	-.00006	.00018	-.04105	-.01571
23	.00000	.00024	.00070	.03780	.03370
24	.00000	.00001	-.00059	.06759	.11942
25	.00000	.00020	.00023	-.00107	-.01311
26	.00000	-.00011	-.00008	.04053	.09389
27	.00000	-.00004	-.00006	-.02374	-.03729
28	.00000	.00010	.00015	.04760	.08541
29	.00000	-.00004	-.00002	-.03322	-.05715
30	.00000	.00007	.00008	.04877	.08771
31	.00000	.00002	.00004	.01113	.02175
Eigen-value (au)	-104.85153	-10.57766	-8.03915	-1.12047	-.62171

	π MO coefficients	
basis orb.	1π	2π
32	.30703	-.07154
33	.64523	-.19524
34	.12233	.01423
35	-.05300	.67714

continued

TABLE IV: (cont'd.)

	π MO coefficients (cont'd.)	
basis orb.	1π	2π
36	.06102	.43384
37	-.07671	.03839
38	.04082	-.06366
39	-.02731	.02735
40	.09636	-.01801
41	-.06315	.01925
42	-.01247	.01127
43	.00112	.02340
44	-.00010	-.00454
45	-.00099	.00311
46	-.00003	.00062
47	.00006	.00989
48	.00000	-.00070
49	.00003	.00694
50	.00001	.00382
51	.00001	.00234
Eigenvalue (au)	-8.03815	-.48078

TABLE V: 71-STO OCE-SCF MO's for HCl, R=2.424 au, this work. Basis orbital numbers refer to Table II.

E_{elec} = -.467.06581 au, E_{tot} = -460.05261 au

	σ MO coefficients				
basis orb.	1σ	2σ	3σ	4σ	5σ
1	.091670	.001782	-.000030	-.030236	.010533
2	1.079626	-.205252	.000910	.305130	-.103061
3	-.224687	-.221808	.000722	-.296716	.108246
4	.119841	.113155	.000170	.636724	-.223144
5	-.065240	.937814	-.005461	-1.258011	.417160
6	.015554	.119670	.001370	.608137	-.212826
7	-.002838	-.007751	.000493	1.054873	-.263498
8	-.001574	-.004874	-.000072	-.017368	-.023937
9	.000721	.002220	.000014	-.008657	.026224
10	.002628	.007966	-.000107	-.238332	.178162
11	.000204	.000537	.316378	-.010524	-.050023
12	-.000214	.002290	.631979	-.017689	-.187287
13	.000105	.000832	.117847	-.005791	.073906
14	-.000035	.000151	-.022316	.137986	.685915
15	-.000036	-.000226	-.020702	-.046728	.189244
16	.000011	.000066	.005376	.019222	.008768
17	.000039	.000219	.026378	.073757	.074352
18	.000015	.004340	.003376	-.007574	.062203
19	-.000019	-.007351	-.005226	.094545	.065198

continued

TABLE V: (cont'd.)

basis orb.	σ MO coefficients (cont'd.)				
	1σ	2σ	3σ	4σ	5σ
20	.000013	.003489	.002400	-.076911	.005896
21	-.000005	.000734	.000637	.086517	.141916
22	.000000	-.000086	.000146	-.042512	-.018089
23	-.000004	.000238	.000727	.038534	.034955
24	.000002	.000037	-.000575	.069297	.121588
25	-.000002	.000206	.000275	.000138	-.008866
26	.000001	-.000112	-.000116	.040025	.090390
27	.000001	-.000042	-.000058	-.025685	-.040732
28	-.000001	.000097	.000153	.049849	.089026
29	.000001	-.000057	-.000081	-.037179	-.064425
30	-.000001	.000092	.000142	.052879	.094983
31	.000000	.000019	.000039	.011335	.021975
Eigen-value (au)	-104.845293	-10.571650	-8.033174	-1.109645	-.614132

basis orb.	π MO coefficients	
	1π	2π
32	.307736	-.073836
33	.643627	-.190227
34	.125505	-.005041
35	-.062738	.771225
36	.085110	.186711

continued

TABLE V: (cont'd.)

basis orb.	π MO coefficients (cont'd.) 1π	2π
37	-.103622	.171809
38	.049498	-.010326
39	.019308	.059578
40	-.065216	-.131750
41	.043036	.092976
42	.007474	.026113
43	.001155	.023257
44	-.000103	-.005019
45	-.001021	.003552
46	-.000026	.000685
47	.000060	.009799
48	-.000006	-.000930
49	.000029	.007160
50	.000015	.003831
51	.000010	.002349
Eigenvalue (au)	-8.032160	-.474829

discrepancy a test calculation was done truncating our integrals to 6 significant figures (Appendix II)[38]; this calculation agreed well with results published by Moccia. Since the differences in these calculations produce important differences in the calculated EFG, all discussion below of results in the 71-STO basis refers to calculations performed in this laboratory with integrals stored to 16 figures. The basis was taken unchanged from Moccia[5]. Calculations in the basis series constructed from the GW Cl_2 basis[27] (section 3 and Chapter III) are also presented.

a) Calculations of HCl at equilibrium separation

Since the EFG at the Cl nucleus contains a nuclear contribution dependent on the internuclear distance, for comparison with experiment the OCE-SCF wavefunction must be calculated at the experimental equilibrium internuclear distance, 2.4087 au (corrections for vibrational motion are discussed in Chapter VI). The OCE-SCF wavefunction in the 71-STO basis for R=2.4087 au is presented in Table VI; that in the GW+9 basis (largest of the GW series) of Table III is presented in Table VII.

b) Partitioning of the electronic energy

The electronic energy (17) can be partitioned

$$E_{elec} = E_k + E_n + E_r , \qquad (20)$$

TABLE VI: 71-STO OCE-SCF MO's for HCl, R=2.4087 au (equilibrium distance), this work. Basis orbital numbers refer to Table II.

E_{elec} = -467.110343555 au, E_{tot} = -460.052594562 au

	σ MO coefficients				
basis orb.	1σ	2σ	3σ	4σ	5σ
1	.091670	.001781	-.000032	-.030112	.010761
2	1.079625	-.205248	.000924	.304084	-.105032
3	-.224686	-.221809	.000701	-.295327	.110723
4	.119841	.113158	.000199	.634410	-.227399
5	-.065240	.937791	-.005490	-1.254730	.423567
6	.015554	.119689	.001382	.606324	-.216195
7	-.002838	-.007743	.000509	1.055546	-.263282
8	-.001574	-.004874	-.000068	-.019138	-.028528
9	.000721	.002220	.000012	-.008023	.027585
10	.002628	.007961	-.000118	-.238212	.178306
11	.000203	.000537	.316378	-.010921	-.050463
12	-.000214	.002284	.631975	-.017860	-.186765
13	.000105	.000831	.117845	-.006335	.072664
14	-.000035	.000161	-.022299	.142439	.691212
15	-.000036	-.000221	-.020691	-.048699	.182983
16	.000011	.000064	.005373	.019741	.009618
17	.000039	.000211	.026363	.073848	.074437
18	.000015	.004311	.003356	-.009365	.058740

continued

TABLE VI: (cont'd.)

	σ MO coefficients (cont'd.)				
basis orb.	1σ	2σ	3σ	4σ	5σ
19	-.000019	-.007286	-.005162	.100752	.075486
20	.000013	.003459	.002374	-.081324	-.003198
21	-.000005	.000723	.000620	.087095	.142830
22	.000000	-.000084	.000149	-.044176	-.022354
23	-.000004	.000244	.000739	.040367	.038526
24	.000002	.000031	-.000585	.069757	.122019
25	-.000002	.000215	.000296	.001294	-.006872
26	.000001	-.000121	-.000135	.039217	.088204
27	.000001	-.000042	-.000056	-.026198	-.041544
28	-.000001	.000097	.000152	.050529	.089604
29	.000001	-.000057	-.000080	-.037890	-.065301
30	-.000001	.000092	.000141	.053697	.095705
31	.000000	.000020	.000039	.011423	.021891
Eigen-value (au)	-104.845043	-10.571612	-8.033157	-1.111257	-.615937

	π MO coefficients	
basis orb.	1π	2π
32	.307732	-.073810
33	.643622	-.190175
34	.125519	-.005163
35	-.062740	.771408

continued

TABLE VI: (cont'd.)

basis orb.	π MO coefficients (cont'd.) 1π	2π
36	.085112	.186757
37	-.103625	.171217
38	.049499	-.009963
39	.019249	.059531
40	-.065004	-.130000
41	.042897	.091644
42	.007447	.025875
43	.001160	.023808
44	-.000104	-.005289
45	-.001024	.003289
46	-.000027	.000534
47	.000061	.009963
48	-.000006	-.001024
49	.000028	.007277
50	.000015	.003848
51	.000010	.002359
Eigenvalue (au)	-8.032113	-.475190

TABLE VII: OCE-SCF MO's for HCl, R=2.4087 au (the equilibrium distance), in the GW+9 basis of Table III.

E_{elec} = -467.126687373 au, E_{tot} = -460.068938380 au

	σ MO coefficients				
basis orb.	1σ	2σ	3σ	4σ	5σ
1	-.862215	.241176	.001031	-.068740	-.020113
2	-.164576	.140574	.000582	-.050338	-.015187
3	-.001581	-1.079872	-.004792	.376436	.112567
4	.000243	-.031849	.002367	-.771859	-.274708
5	-.000171	.025517	-.002162	-.285324	.018969
6	-.000117	-.000328	.205165	.005950	-.041974
7	.000070	-.003269	.821186	.028664	-.189712
8	-.000055	-.000961	.023040	-.050990	.423846
9	.000081	.000752	-.010228	-.105968	.521532
10	-.000007	-.000878	.000864	-.052502	.120225
11	.000069	-.011499	.001186	-.026842	.057587
12	-.000049	-.000511	.003157	-.025759	.084182
13	.000005	.000394	-.000322	-.057651	.160545
14	.000002	-.000159	.000209	-.062789	.138888
15	.000001	-.000098	.000167	-.040680	.084296
16	.000001	-.000063	.000114	-.026350	.053252
17	.000000	-.000042	.000078	-.017425	.034550
18	.000000	-.000028	.000054	-.011753	.022946

continued

TABLE VIII (cont'd.)

	σ MO coefficients				
basis orb.	1σ	2σ	3σ	4σ	5σ
19	.000000	-.000017	.000037	-.008023	.015628
Eigen-value (au)	-104.846577	-10.571981	-8.041414	-1.115449	-.621367

	π MO coefficients	
basis orb.	1π	2π
20	.206048	-.051177
21	.821462	-.228703
22	.018728	.540581
23	-.005187	.564570
24	.000235	.027335
Eigenvalue (au)	-8.037564	-.476228

with E_k, E_n, and E_r representing kinetic, nuclear attraction, and electron repulsion energy respectively. The first two terms can be directly partitioned into MO contributions,

$$E_k = \sum_j E_k^j, \quad E_k^j = -\tfrac{1}{2}N_j \langle \psi_j | \nabla^2 | \psi_j \rangle \tag{21}$$

and

$$E_n = \sum_j E_n^j, \quad E_n^j = -N_j \langle \psi_j | \sum_\alpha \frac{Z_\alpha}{r_\alpha} | \psi_j \rangle, \tag{22}$$

α ranging over nuclei and j over MO's. For closed-shell molecules, the electron repulsion energy can be written[32],

$$E_r = \sum_\ell^{occ} \sum_m^{occ} (2J_{\ell m} - K_{\ell m}), \tag{23}$$

with $J_{\ell m}$ and $K_{\ell m}$ defined in Chapter I. (23) can be partitioned,

$$E_r = \sum_\ell^{occ} E_r^\ell, \quad E_r^\ell = \sum_m^{occ} (2J_{\ell m} - K_{\ell m}). \tag{24}$$

Table VIII gives the partitioning of E_k, E_n, and E_r into MO contributions for the wavefunctions of Tables VI and VII. E_n is resolved into contributions from the proton and the Cl nucleus.

c) Virial theorem; calculated R_e

The exact wavefunction for HCl at R_e satisfies the virial theorem[39,40]

$$E_{pot}/E_k = -2, \tag{25}$$

TABLE VIII: OCE-SCF energy partitioning, 71-STO and GW+9 bases, R=2.4087 au (equilibrium distance), this work. E_k, E_n, and E_r defined below equation (20).

A. 71-STO (wavefunction of Table VI). Energies in au.

MO	E_k	$E_{n,tot}$	$E_{n,Cl}$	$E_{n,H}$	E_r
1σ	274.285943	-563.872979	-563.042652	-.830326	39.948475
2σ	43.560534	-113.479046	-112.648083	-.830963	24.387644
3σ	41.136374	-109.549221	-108.707555	-.841666	26.173266
4σ	5.599702	-29.245521	-28.218354	-1.027167	10.711652
5σ	3.876404	-23.827384	-22.577841	-1.249543	9.359553
1π	41.248925	-109.682513	-108.857984	-.824529	26.184681
2π	4.426839	-25.154384	-24.419729	-.734655	9.888583
Totals	459.810485	-1109.647945	-1101.749911	-7.898033	182.727118

continued

TABLE VIII: (cont'd.)

B. GW+9 (wavefunction of Table VII). Energies in au.

MO	E_k	$E_{n,tot}$	$E_{n,Cl}$	$E_{n,H}$	E_r
1σ	274.261578	-563.848572	-563.018246	-.830326	39.946920
2σ	43.421407	-113.311710	-112.480691	-.831018	24.373170
3σ	41.219572	-109.635223	-108.793710	-.841513	26.166412
4σ	5.712308	-29.392261	-28.375288	-1.016973	10.724528
5σ	3.856888	-23.663926	-22.418303	-1.245623	9.282152
1π	41.327918	-109.766012	-108.941503	-.824509	26.181483
2π	4.441651	-25.215903	-24.488405	-.727498	9.910898
Totals	460.010891	-1109.815522	-1101.946054	-7.869467	182.677944

with E_{pot} the total potential energy and E_k the kinetic energy of the electrons, which is the total kinetic energy assuming stationery nuclei. At R=2.4087 au, the 71-STO basis gave -2.000526 for the ratio (25); the GW+9 basis gave -2.000126. (25) holds for the exact and H-F wavefunctions if the nuclei are at the calculated equilibrium position. Although R_e=2.4087 au for HCl experimentally, it is not the R_e calculated in the OCE bases, so the virial theorem is not expected to hold in these bases for R=2.4087 au. In order to locate the OCE-SCF R_e values, a series of calculations was done at R=2.3887, 2.3987, 2.4087, 2.4187, and 2.4287 au for the 71-STO basis and at the additional points R=2.3787 and 2.4387 au for the GW+9 basis (see Chapter VI for selection of these points); a polynomial was fitted[41] to the total energies and the OCE-SCF R_e calculated by differentiating and setting to zero. This gave R_e=2.4181 au for the 71-STO basis and 2.5098 au for the GW+9 basis, which indicates the more accurate R-dependence of the 71-STO wavefunction (Chapter VI). Polynomial interpolation of virial ratios in the 71-STO basis gave a ratio of -2.00054 at R=2.4181 au; no similar calculation was done for the GW+9 basis since the calculated R_e lay outside the range of calculations. The deviation of these ratios from -2 measures the limitations of the OCE bases; a near H-F two-center calculation of HCl at R=2.4087 au gives the ratio -2.00003[10].

d) Cusp conditions

In section 2 the cusp condition (2) was introduced. Since the H-F equation for each orbital has the same nuclear singularities as the total Hamiltonian (Chapter I), each H-F orbital ψ_i must (if $\psi_i(r_{i\alpha}=0)\neq 0$) satisfy (2). The case $\psi_i(r_{i\alpha}=0)=0$, which arises for π MO's, was treated by Pack and Brown[42]. Any MO can be expanded about nucleus α,

$$\psi = \sum_{\ell=0}^{\infty} \sum_{m=-\ell}^{\ell} r^{\ell} f_{\ell m}(r_\alpha) S_{\ell m}(\theta_\alpha, \phi_\alpha); \tag{26}$$

the exact form of the $f_{\ell m}(r_\alpha)$ is not important. Pack and Brown showed that for $H\psi$ to remain finite at $r_\alpha=0$, the relation

$$(\bar{\ell}+1)(df_{\bar{\ell}m}(r_\alpha)/dr_\alpha)_{r_\alpha=0} = -Z_\alpha f_{\bar{\ell}m}(0) \tag{27}$$

must hold, where $\bar{\ell}$ is the lowest ℓ in (26) for which $f_{\ell m}(0)\neq 0$. The ratio of the left side to $f_{\bar{\ell}m}(0)$ is called the cusp ratio here, although the term is strictly correct only if $\psi(r_\alpha=0)\neq 0$. For OCE-SCF MO's if α is the expansion center the $f_{\ell m}(r)$ are linear combinations of radial portions (9) of STO's. Cusp ratios for the occupied MO's of HCl in the 71-STO and GW+9 bases at R=2.4087 au are presented in Table IX. Note that the cusp ratios of higher energy MO's (all cusp ratios = -17 for the H-F orbitals) deteriorate in the 71-STO basis, but that fair accuracy is retained in the GW+9 basis.

TABLE IX: Test of cusp condition, OCE-SCF MO's for HCl, R=2.4087 au (equilibrium distance), GW+9 and 71-STO bases, this work.

A. 71-STO (wavefunction of Table VI)

MO	$f_{\bar{\ell}m}(0)^a$	$df_{\bar{\ell}m}(r)/dr)^a_{r=0}$	cusp ratio[b]
1σ	-38.53566	657.46495	-17.06121
2σ	10.77286	-182.27271	-16.91962
3σ	-.04162	.70227	-16.87197
4σ	-3.00834	47.48094	-15.78311
5σ	.85974	-13.31622	-15.48871
1π	144.26299	-2196.50257	-15.22568
2π	-37.83658	580.29930	-15.33699

B. GW+9 (wavefunction of Table VII)

MO	$f_{\bar{\ell}m}(0)^a$	$df_{\bar{\ell}m}(r)/dr)^a_{r=0}$	cusp ratio[b]
1σ	-38.46951	652.20231	-16.95375
2σ	10.76057	-182.20243	-16.93242
3σ	.04598	-.79021	-17.18585
4σ	-3.06696	50.45245	-16.45030
5σ	-.89737	14.67686	-16.35545

continued

TABLE IX: (cont'd.)

MO	$f_{\bar{\ell}m}(0)$[a]	$(df_{\bar{\ell}m}(r)/dr)^{a}_{r=0}$	cusp ratio[b]
1π	151.00611	-2442.06206	-16.17194
2π	-39.62862	645.33162	-16.28448

[a]Defined in equation (27) of text. For σ MO's, $\bar{\ell} = 0$; for π MO's, $\bar{\ell} = 1$.

[b]For exact Hartree-Fock orbitals, the cusp ratio = -17.

e) Dipole moment

For HCl with the proton on the +z-axis, the electronic contribution to the dipole moment μ is

$$\mu_{elec} = -\sum_k N_k \langle \psi_k | z | \psi_k \rangle ,$$

with the sum over MO's. Table X gives the MO analysis of μ_{elec} for the GW+9 and 71-STO OCE-SCF calculations at R_e=2.4087 au, as well as μ_{elec} in debyes (D) and au. The total dipole moment is also listed,

$$\mu = \mu_{elec} + \mu_{nuc}.$$

The nuclear contribution is the proton charge times its distance from the Cl nucleus. The conversion factor 1 au = 2.54158D[10] was used. The 71-STO and GW+9 MO contributions to μ_{elec} are similar, the result in the 71-STO basis being slightly closer to the experimental value (1.1085D[43]). Both OCE bases underestimate the magnitude of μ_{elec}, because they place too little electron density near the proton. This is expected, since STO's centered on Cl are unable to produce a sharp peak in the electron density at the proton. The OCE calculated μ's differ from experiment by about 20%.

f) Molecular quadrupole moment

The molecular quadrupole moment in au is defined by

$$\theta = \sum_\alpha Z_\alpha r_\alpha^2 - \frac{3}{2} \langle z^2 \rangle + \frac{1}{2} \langle r^2 \rangle ; \qquad (28)$$

TABLE X: OCE-SCF dipole moments, 71-STO and GW+9 wavefunctions for HCl, R=2.4087 au (equilibrium distance), this work.

	μ_{elec} (au)	
MO	71-STO (Table VI)	GW+9 (Table VII)
1σ	-.000016	-.000017
2σ	-.003564	-.003956
3σ	.002420	.002988
4σ	-.772231	-.784781
5σ	-.838568	-.910279
1π	-.000335	-.000076
2π	.135995	-.088381
Total (au)	-1.884619	-1.872958
Total (D)	-4.789910	-4.760273
μ_{nuc} (au)	2.408700	2.408700
μ_{nuc} (D)	6.121904	6.121904
μ_{tot} (au)	.524081	.535742
μ_{tot} (D)	1.331994	1.361631

Experimental[43] μ_{tot} = 1.1085 D.

$\langle z^2 \rangle$ and $\langle r^2 \rangle$ are expectation values of the indicated one-electron operators (Chapter I). (28) transforms under a change of origin,

$$\theta' = \theta - 2\mu\Delta,$$

with μ defined above and Δ the distance of the origin shift along the molecular axis[10]. For comparison with experiment, the origin must coincide with the molecular center of mass, which lies .06753 au from the Cl nucleus[10]. On the basis of several experimental measurements, the recommended experimental value[44] for θ of HCl is 3.8×10^{-26} esu-cm^2. At R=2.4087 au the 71-STO basis gives 3.95×10^{-26} esu-cm^2, the GW+9 3.80×10^{-26} esu-cm^2. Both agree well with experiment, the GW+9 particularly well, even though $\langle z^2 \rangle$ and $\langle r^2 \rangle$ depend strongly on regions of space far from the Cl nucleus. However θ is a measure of the deviation of the charge distribution from spherical symmetry; it is seen in later chapters that the GW+9 basis reproduces these deviations extremely well. Calculations of θ in the two bases are summarized in Table XI.

g) <u>Electrostatic force on the Cl nucleus</u>

At the equilibrium internuclear distance there is no net force on either nucleus in HCl. Since the experimental R_e does not coincide with the OCE-SCF calculated R_e, the OCE-SCF wavefunctions at the experimental R_e give a non-zero

TABLE XI: Molecular quadrupole moment and related quantities, 71-STO and GW+9 OCE-SCF wavefunctions, R=2.4087 au (equilibrium distance), this work.

	$\langle z^2 \rangle$ (au)		$\langle r^2 \rangle$ (au)	
MO	71-STO[a]	GW+9[b]	71-STO[a]	GW+9[b]
1σ	.007467	.007468	.022400	.022405
2σ	.154533	.154452	.462924	.462971
3σ	.246423	.245301	.410569	.408828
4σ	2.744387	2.831999	6.253550	6.348369
5σ	6.361377	6.695791	9.378785	9.754053
1π	.081895	.081425	.409296	.407124
2π	1.798804	1.663878	8.425603	8.313055
Total	13.275585	13.425616	34.198027	34.436985

$\frac{1}{2}(3\langle z^2 \rangle - \langle r^2 \rangle)_{elec}$ = 2.814364 au (71-STO)

= 2.919932 au (GW+9)

$\frac{1}{2}(3\langle z^2 \rangle - \langle r^2 \rangle)^{c}_{nuc}$ = 5.801836 au

Molecular quadrupole moment (esu-cm^2)[d] = 3.9471×10^{-26} (71-STO)

= 3.7966×10^{-26} (GW+9)

Recommended experimental value[44]: 3.8×10^{-26} esu-cm^2

continued

TABLE XI: (cont'd.)

[a]Table VI.

[b]Table VII.

[c]Contribution from a proton 2.4087 au from the coordinate center on the +z-axis.

[d]In molecular center-of-mass coordinates. Conversion factor is 1 au = 1.3449×10^{-26} esu-cm^2. Experimental dipole moment[43] used in conversion.

force on both nuclei. The difference of this quantity from zero gives an indication of the deviation of the approximate wavefunction from the exact wavefunction. For the exact wavefunction, forces on the nuclei are equal to the average electrostatic forces (Hellman-Feynman theorem[45]); the operator for the electrostatic force in the z-direction on nucleus α is $Z_\alpha(z_\alpha/r_\alpha^3)$, with Z_α the atomic number and z_α the distance along the z-axis from nucleus α. Calculations of this quantity with α the Cl nucleus for the OCE-SCF wavefunctions in the 71-STO and GW+9 bases are summarized in Table XII. The GW+9 basis gives a smaller force than the 71-STO basis although the 71-STO calculated R_e is much closer to the experimental value than that in the GW+9 basis (section c). This illustrates the approximate nature of the Hellman-Feynman theorem when applied to approximate wavefunctions[45].

h) Expectation values of r^{-1} and r^{-2}

Expectation values of these operators are given in Table XIII. $\langle r^{-1}\rangle$ is compared with values from near H-F two-center calculations in the next section. No comparison is available for $\langle r^{-2}\rangle$. Note that for $\langle r^{-1}\rangle$ the 71-STO and GW+9 values are identical through the third figure, and for $\langle r^{-2}\rangle$ through the fourth.

TABLE XII: Hellman-Feynman force on the Cl nucleus, 71-STO and GW+9 OCE-SCF wavefunctions, R=2.4087 au (equilibrium distance), this work.

MO	$\langle z/r^3 \rangle$ (au) 71-STO[a]	GW+9[b]
1σ	.014937	.015939
2σ	.024491	.027064
3σ	-.018271	-.020608
4σ	.152157	.151849
5σ	-.063156	-.054857
1π	.002362	.000280
2π	.017936	.018085
Total	.150754	.156117

$\langle z/r^3 \rangle_{nuc}^{c} = .172359$

Hellman-Feynman force on Cl[d] = -.367289 au (71-STO)

= -.276114 au (GW+9)

[a]Table VI.

[b]Table VII.

[c]Due to proton 2.4087 au from coordinate center on +z-axis.

[d]Equal to -17 ($\langle z/r^3 \rangle_{nuc} - \langle z/r^3 \rangle_{elec}$). The Hellmann-Feynman force for the exact wavefunction is zero.

TABLE XIII: $\langle r^{-1} \rangle$ and $\langle r^{-2} \rangle$, 71-STO and GW+9 OCE-SCF wavefunctions, R=2.4087 au (equilibrium distance), this work. No experimental values available.

	$\langle r^{-1} \rangle$ (au)		$\langle r^{-2} \rangle$ (au)	
MO	71-STO[a]	GW+9[b]	71-STO[a]	GW+9[b]
1σ	33.120156	33.118720	1106.373872	1105.520522
2σ	6.626358	6.616511	90.299100	90.060466
3σ	6.394562	6.399630	28.327213	28.508806
4σ	1.659903	1.669135	7.850022	8.050258
5σ	1.328108	1.318724	2.323223	2.354455
1π	6.403411	6.408324	28.414347	28.577817
2π	1.436455	1.440494	2.286048	2.300540
Total	64.808818	64.820356	1296.574218	1296.251221

[a]Table VI.

[b]Table VII.

7. Comparison with extensive two-center ab-initio calculations of HCl

There are two near-H-F two-center SCF (TCE-SCF) calculations of HCl at R=2.4087 au: one by Cade and Huo[9] in a 32-STO basis, and one by McLean and Yoshimine[46] in a 49-STO basis. McLean and Yoshimine[10] have published a number of one-electron properties calculated from both these wavefunctions; a number are compared with the corresponding quantities in the 71-STO and GW+9 bases in Table XIV. It is with these TCE-SCF properties that the OCE-SCF values should be compared for judging the suitability of the basis, since these TCE-SCF wavefunctions approximate closely the best possible single-determinant molecular wavefunction (Chapter I). Note that for expectation values of properties depending on regions far from the Cl nucleus (e.g. $\langle z^2 \rangle$, $\langle r^2 \rangle$), the 71-STO basis is closer to the TCE-SCF results; for those dependent on regions closer to the Cl nucleus (e.g. $\langle r^{-1} \rangle$, $\langle z/r^3 \rangle$), the GW+9 basis gives better agreement. Reasons for this are examined in the next chapter.

TABLE XIV: Comparison of properties calculated from the 71-STO and GW+9 OCE-SCF wavefunctions for HCl with the two-center results of McLean and Yoshimine[10] and Cade and Huo[9]. All wavefunctions for R=2.4087 au (equilibrium distance). Except as noted, all two-center properties from the compilation of McLean and Yoshimine[10].

Property	McL-Yosh[10]	Cade-Huo	GW+9[b]	71-STO[a]
Electronic energy (au)	-467.1696	-467.1680	-467.1267	-467.1103
Total energy (au)	-460.1119	-460.1103	-460.0689	-460.0526
Potential energy (au)	-920.2110	-920.2049	-920.0798	-919.8631
Kinetic energy (au)	460.0991	460.0946	460.0109	459.8105
Virial ratio (E_{pot}/E_{kin})	-2.00003	-2.00003	-2.00013	-2.00053
Orbital eigenvalues (au)				
1σ	-104.8479	-104.8485	-104.8466	-104.8450
2σ	-10.5732	-10.5741	-10.5720	-10.5716
3σ	- 8.0405	-8.0420	-8.0414	-8.0332
4σ	-1.1164	-1.1168	-1.1154	-1.1113
5σ	-.6254	-.6262	-.6214	-.6159

continued

TABLE XIV: (cont'd.)

Property	McL-Yosh[10]	Cade-Huo	GW+9[b]	71-STO[a]
Orbital eigenvalues (au) (cont'd.)				
1π	-8.0387	-8.0394	-8.0376	-8.0321
2π	-.4763	-.4762	-.4762	-.4752
$\langle r^{-1}\rangle^c$ (au)	64.8218	64.8209	64.8204	64.8088
$\langle r^2\rangle^c$ (au)	34.2597	34.2639	34.4370	34.1980
$\langle z\rangle^c$ (au)	1.9307	1.9379[47]	1.8730	1.8846
$\langle z^2\rangle^c$ (au)	13.3887	13.3622	13.4256	13.2756
Dipole moment (D)	1.215	1.197[47]	1.362	1.332
Molecular quadrupole moment ($\times 10^{-26}$ esu-cm^2)	3.74	3.80	3.80	3.95
Force on Cl nucleus (Hellman-Feynman) (au)	-.0682	-.1821	-.2761	-.3673

[a]Table VI.

[b]Table VII.

[c]Measured from Cl nucleus.

REFERENCES

1. D.M. Bishop, Mol. Phys. 6, 305 (1963).
2. P. Grigolini and R. Moccia, J. Chem. Phys. 57, 1369 (1972).
3. R. Moccia, J. Chem. Phys. 40, 2164, 2186 (1964).
4. D.M. Bishop, Adv. Quant. Chem. 3, 25 (1967).
5. R. Moccia, Theoret. Chim. Acta 8, 8 (1967).
6. M. Cowan and W. Gordy, Phys. Rev. 111, 209 (1958).
7. R. Moccia, private communication, January, 1973.
8. E. Scrocco and J. Tomasi, Theoret. Chim. Acta 2, 386 (1964).
9. P.E. Cade and W.M. Huo, J. Chem. Phys. 47, 649 (1967).
10. A.D. McLean and M. Yoshimine, J. Chem. Phys. 47, 3256 (1967).
11. R.F. Borkman, J. Chem. Phys. 53, 3153 (1970).
12. A.L.H. Chung, J. Chem. Phys. 46, 3144 (1967).
13. C.C.J. Roothaan, J. Chem. Phys. 19, 1445 (1951).
14. I.I. Guseinov, J. Phys. B, 3, 1399 (1970).
15. M.P. Barnett and C.A. Coulson, Phil. Trans. Roy. Soc. A243, 221 (1951).
16. E.U. Condon and G.H. Shortley, The Theory of Atomic Spectra, Cambridge, 1935. p. 176.
17. N.W. Winter, W.C. Ermler, and R.M. Pitzer, Chem. Phys. Lett. 19, 179 (1973).
18. T. Kato, Comm. Pure Appl. Math. 10, 151 (1957).

19. E. Steiner, J. Chem. Phys. 39, 2365 (1963).

20. C.C.J. Roothaan and A.W. Weiss, Revs. Mod. Phys. 32, 194 (1960).

21. W.A. Bingel, Theoret. Chim. Acta 8, 54 (1967).

22. C.C.J. Roothaan and P.S. Bagus, Meth. Comp. Phys. 2, 47 (1967).

23. R.M. Pitzer, C.W. Kern, and W.N. Lipscomb, J. Chem. Phys. 37, 267 (1962).

24. G.W. Stewart, Comm. Assoc. Comp. Mach. 13, 369 (1970).

25. G. Herzberg, Molecular Spectra and Molecular Structure: I. Spectra of Diatomic Molecules, 2nd edition, Van Nostrand, N.Y., 1950. p. 341.

26. P.E. Cade, R.F.W. Bader, W.H. Henneker, and I. Keaveny, J. Chem. Phys. 50, 5313 (1969).

27. T.L. Gilbert and A.C. Wahl, J. Chem. Phys. 55, 5247 (1971).

28. R.S. Mulliken, J. Chem. Phys. 36, 3428 (1962).

29. P.S. Bagus, Phys. Rev. 139, A619 (1965).

30. B.D. Joshi, J. Chem. Phys. 43, S40 (1965).

31. C.F. Bender and S. Rothenberg, J. Chem. Phys. 55, 2000 (1971).

32. C.C.J. Roothaan, Revs. Mod. Phys. 23, 69 (1951).

33. H. Margenau and G.M. Murphy, The Mathematics of Chemistry and Physics, v. I, 2nd edition, Van Nostrand, N.Y. 1956. p. 331.

34. P.O. Lowdin, Adv. Quant. Chem. 5, 185 (1970).

35. P.O. Lowdin, J. Chem. Phys. 18, 365 (1950).

36. H. Eyring, J. Walter, and G.E. Kimball, Quantum Chemistry, Wiley, N.Y., 1944. p. 94.

37. P.R. Bunker, J. Mol. Spec. 39, 90 (1971).

38. This calculation was suggested by Dr. J.M. Sichel.

39. J.C. Slater, J. Chem. Phys. 1, 687 (1933).

40. P.O. Lowdin, J. Mol. Spec. 3, 46 (1959).

41. Subroutine CURVFT, McGill University Computing Centre.

42. R.T. Pack and W.B. Brown, J. Chem. Phys. 45, 556 (1966).

43. E.W. Kaiser, J. Chem. Phys. 53, 1686 (1970).

44. D.E. Stogryn and A.P. Stogryn, Mol. Phys. 11, 371 (1966).

45. F.L. Pilar, Elementary Quantum Chemistry, McGraw-Hill, N.Y., 1968. p. 475.

46. A.D. McLean and M. Yoshimine, Tables of Linear Molecule Wave Functions, supplement to IBM Journal of Research and Development, 1967.

47. P.E. Cade and W.M. Huo, J. Chem. Phys. 45, 1063 (1966).

CHAPTER III: Electric Field Gradient at the Cl nucleus from OCE-SCF wavefunctions

The operator in atomic units for the electrostatic potential V at a point due to a unit positive charge is $\hat{V}=1/r$, where r measures the distance from the point. The circumflex on $\hat{V}$ identifies it as an operator. The partial derivatives of $\hat{V}$ with respect to the three cartesian variables form the negatives of the operators for the components of the electric field vector. The explicit forms for these operators are:

$$
\begin{aligned}
-\hat{E}_x &= \partial\hat{V}/\partial x = -x/r^3 \\
-\hat{E}_y &= \partial\hat{V}/\partial y = -y/r^3 \qquad (1) \\
-\hat{E}_z &= \partial\hat{V}/\partial z = -z/r^3
\end{aligned}
$$

Each component may in turn be differentiated with respect to the three cartesian variables. Taking the three partial derivatives of a component is equivalent to applying the gradient operator[1]

$$\nabla = \left(\frac{\partial}{\partial x}, \frac{\partial}{\partial y}, \frac{\partial}{\partial z}\right) = \hat{i}\frac{\partial}{\partial x} + \hat{j}\frac{\partial}{\partial y} + \hat{k}\frac{\partial}{\partial z}$$

to that component. The $\hat{i}$, $\hat{j}$, and $\hat{k}$ here are unit vectors, not operators. As the term is usually used, the gradient operator is applied to a scalar-valued function and yields a vector-valued function, the gradient[2]. However, there is an alternate

usage[3,4] in which the gradient operates in the form of a tensor product upon a vector,

$$\begin{pmatrix} \partial/\partial x \\ \partial/\partial y \\ \partial/\partial z \end{pmatrix} (\partial V/\partial x, \frac{\partial V}{\partial y}, \partial V/\partial z) = \begin{pmatrix} \partial^2 V/\partial x^2 & \partial^2 V/\partial x \partial y & \partial^2 V/\partial x \partial z \\ \partial^2 V/\partial y \partial x & \partial^2 V/\partial y^2 & \partial^2 V/\partial y \partial z \\ \partial^2 V/\partial z \partial x & \partial^2 V/\partial z \partial y & \partial^2 V/\partial z^2 \end{pmatrix}; \quad (2)$$

$\partial^2 V/\partial x^2$ is the expectation value of $\partial^2 \hat{V}/\partial x^2$. The tensor on the right of (2) is called the electric field gradient (EFG) tensor and will be so referred to here, although with the components of the electric field as defined in (1) it is strictly speaking the negative of the EFG tensor. This reversal of sign is firmly established in the literature[5]. The EFG tensor as defined in (2) is not necessarily traceless: by Poisson's equation[6],

$$\frac{\partial^2 V}{\partial x^2} + \frac{\partial^2 V}{\partial y^2} + \frac{\partial^2 V}{\partial z^2} = - \frac{\partial E_x}{\partial x} - \frac{\partial E_y}{\partial y} - \frac{\partial E_z}{\partial z} = -4\pi\rho,$$

where ρ is the charge density at the point from which r is measured in (1). However it can be shown that the part of V which is due to the electron density at r=0 does not affect spacing of energy levels in interaction with a nucleus[7]; it is more convenient to consider the gradient of the field produced by the electron density excluding that at r=0. The trace of this tensor is zero; it is formed from the original EFG tensor by adding $4\pi\rho/3$ to each diagonal element. A traceless tensor is desirable because there is one less independent element in a trace-

less tensor than in one of arbitrary trace. It is this traceless tensor that will from now on be referred to as the EFG tensor, i.e. that of (2) with $4\pi\rho/3$ added to each of the diagonal elements. Alternatively, (2) may be taken to define the EFG tensor directly if V is defined as the electrostatic potential from the charge distribution with the density at r=0 deleted. The standard notation[8]

$$\begin{pmatrix} \frac{\partial^2 V}{\partial x^2} & \frac{\partial^2 V}{\partial x \partial y} & \frac{\partial^2 V}{\partial x \partial z} \\ \partial^2 V/\partial y \partial x & \partial^2 V/\partial y^2 & \partial^2 V/\partial y \partial z \\ \partial^2 V/\partial z \partial x & \partial^2 V/\partial z \partial y & \partial^2 V/\partial z^2 \end{pmatrix} = \begin{pmatrix} q_{xx} & q_{xy} & q_{xz} \\ q_{yx} & q_{yy} & q_{yz} \\ q_{zx} & q_{zy} & q_{zz} \end{pmatrix} \qquad (3)$$

will be used for convenience. The dimensions of the EFG are charge/(length)^3.

Thus the definition of the EFG runs counter to normal terminology in three ways: the gradient is a tensor rather than a vector, it refers to the negative of the electric field rather than the electric field itself, and its trace is zero and not $-4\pi\rho$ as expected from Poisson's equation.

1. Operator for the integral over basis orbitals

Only a single element of the EFG tensor will be treated here. This suffices because the tensor is symmetric (since $\partial(\partial V/\partial x)/\partial y = \partial(\partial V/\partial y)/\partial x$); thus the axis system can be rotated so that the tensor is diagonal in the new axis system[9].

The axis system in which the tensor is diagonal is known as the principal axis system of the tensor. This rotation does not change the trace of the tensor (since it undergoes a unitary transformation), so the sum of the three non-zero elements of the tensor is zero,

$$q_{xx} + q_{yy} = -q_{zz},$$

so that any one and the difference of the other two determine all three elements. By convention the diagonal element of largest absolute value is labeled q_{zz} and is chosen as the single element; the absolute value of the difference of the other two elements, $|q_{xx} - q_{yy}|$, is chosen as the other quantity, with $|q_{xx}| < |q_{yy}|$. This absolute value, when divided by $|q_{zz}|$, is known as the asymmetry parameter η. All physical information contained in the EFG tensor is known if q_{zz} and η are known. In the case of HCl, which possesses cylindrical symmetry, q_{zz} lies along the internuclear axis; q_{xx} and q_{yy} are equal because of the cylindrical symmetry, and η is zero. For this molecule, then, attention may be confined to q_{zz}.

Then the only operator which need be evaluated over the basis orbitals is

$$\hat{q}_{zz} = \frac{\partial^2}{\partial z^2}\left(\frac{1}{r}\right) = (3z^2 - r^2)/r^5 = (3\cos^2\theta - 1)/r^3, \qquad (4)$$

provided that the proton is placed on the +z axis in the MO

calculation of HCl. For the moment the $4\pi\rho/3$ correction is ignored; it will be treated later.

The matrix element of $\hat{q}_{zz}$ between basis orbitals ϕ_i and ϕ_j is

$$\langle\phi_i|\frac{\partial^2}{\partial z^2}\left(\frac{1}{r}\right)|\phi_j\rangle = \int d\tau_1 \phi_i(\bar{r}_1)[(3\cos^2\theta-1)/r^3]\phi_j(\bar{r}_1), \qquad (5)$$

with $\bar{r}_1 \equiv (x_1, y_1, z_1)$ the position vector of an electron in an arbitrary coordinate system; r measures the distance of the electron from the point at which the EFG is calculated and θ measures the angle between the line from the EFG center to the electron and the principal axis of the EFG tensor. (5) is a special case of

$$\langle\phi_i|\frac{\partial^a}{\partial z^a}\left(\frac{1}{r}\right)|\phi_j\rangle;$$

for $a = 0,1$ the integral converges to a unique value; for $a = 2$ (assuming r cannot be factored from ϕ_i or ϕ_j) the integral converges to different values depending on the limiting process used to exclude the singular point (conditional convergence); for $a > 2$ the integral diverges[10]. Thus in (5) one must choose the limiting process which gives the most convenient result. In the last section it was mentioned that electron density within a small sphere surrounding the EFG center can be deleted without affecting the spacing of energy levels in interaction with a nucleus; the correct limiting process for this is, in a

spherical system on the EFG center,

$$\lim_{\varepsilon\to 0} \int_{\varepsilon}^{\infty} dr\, r^2 \int_{0}^{\pi} d\theta \sin\theta \int_{0}^{2\pi} d\phi\, \phi_i(\bar{r}_1)[(3\cos^2\theta-1)/r^3]\phi_j(\bar{r}_1).$$

Since[11] $3\cos^2\theta-1 = (4\sqrt{\pi}/\sqrt{5})S_{20}(\theta,\phi)$, and since in the OCE-SCF calculations the ϕ are STO's on the EFG center (Chapter II, equation (3)), (5) becomes

$$\lim_{\varepsilon\to 0} K \int_{\varepsilon}^{\infty} dr\, r^{n_i+n_j-3} \exp(-(\zeta_i+\zeta_j)r)$$

$$\int_{0}^{\pi} d\theta \sin\theta \int_{0}^{2\pi} d\phi\, S_{\ell_i m_i}(\theta,\phi) S_{\ell_j m_j}(\theta,\phi) S_{20}(\theta,\phi), \qquad (6)$$

with K the product of the orbital normalization constants and $4\sqrt{\pi}/\sqrt{5}$. For $n_i+n_j \geqslant 3$, which is the case unless $n_i=n_j=1$, the radial integral becomes, as $\varepsilon \to 0$, an integral of the type of Appendix I, equation (8), which is finite and easily evaluated. (6) is the product of this quantity and the angular integral, given by Appendix I, equation (7). If $n_i=n_j=1$, the radial integral diverges for $\varepsilon = 0$; however for any $\varepsilon > 0$, the radial integral is finite; the angular integral is zero since $\ell_i+\ell_j = 0+0 < 2$ (Chapter II, equation (8)). Thus the limit as $\varepsilon \to 0$ in (6) is zero for this case. It has been shown[12-15] that if (5) is evaluated in coordinate systems in which the convenient limiting process is other than exclusion of a sphere, the value of (5) is that obtained by the process (6) minus $(4\pi/3)\phi_i(r=0)\phi_j(r=0)$. Thus the integral as evaluated in (6) already has $(4\pi/3)\phi_i(r=0)\phi_j(r=0)$ added to it, relative to a

general coordinate system. Summed over the MO's and multiplied by the occupation numbers this added term is the correction $(4\pi/3)\rho(r=0)$ necessary to make the EFG tensor traceless. Thus evaluation of the $\hat{q}_{zz}$ integrals in the OCE basis by (6) gives the traceless EFG tensor automatically.

Thus the integrals (5) can be easily evaluated if ϕ_i and ϕ_j are centered on the point at which the EFG is being evaluated; if $n_i=n_j=1$ the integral is zero; otherwise it can be evaluated as a product of integrals of types (7) and (8), Appendix I. The tensor evaluated from these matrix elements and a molecular wavefunction will be traceless.

2. Evaluation of q_{zz} from an OCE-SCF wavefunction

For convenience in subscripting, $\hat{q}_{zz}$ will from now on be referred to simply as $\hat{q}$. The expectation value of this operator, including electronic and nuclear contributions, is denoted q. That part of q due to the electrons is denoted q_{elec}. No confusion can result since q_{zz} is the only necessary element of the EFG tensor. As developed in Chapter I,

$$q_{elec} = -\sum_k N_k \langle\psi_k|\partial^2\hat{V}/\partial z^2|\psi_k\rangle$$

$$= -\sum_k N_k \sum_i \sum_j C_{ik}C_{jk}\langle\phi_i|\partial^2\hat{V}/\partial z^2|\phi_j\rangle, \qquad (7)$$

with N_k the occupation number of the MO ψ_k and C_{ik} the coefficient of basis orbital ϕ_i in ψ_k. Index k ranges through the

MO's while i and j range through the basis orbitals. The minus sign is due to the negative charge on the electron. For the OCE-SCF calculation of HCl at r=2.4087 au in the 71-orbital Moccia basis reported in Chapter II, the q_{elec} from the individual MO's and the total q_{elec} by (7) are given in Table I. Comparison with the experimental value[16], also listed in Table I, shows that the total q,

$$q = q_{elec} + q_{nuc},$$

is about 6.5% too high. The nuclear contribution q_{nuc} is also listed there; this is simply

$$q_{nuc} = Z_\alpha(3\cos^2\theta_\alpha - 1)/r^3_\alpha = 2/(2.4087)^3,$$

since the proton (Z_α=1) lies on the z-axis ($\cos\theta_\alpha$=1) a distance 2.4087 au from the Cl nucleus.

The convergence criterion used in this work guarantees six significant figures in the coefficients of the occupied MO of highest energy (Chapter II); all other MO coefficients are expected to have this many or more significant figures. Thus a conservative estimate is that each MO q has five significant figures. However the HCl MO with the q of largest magnitude, the 3σ MO with q = -160 au (Table I), has only two decimal places accuracy with five significant figures; our experience in changing convergence criteria (Chapter II, section 5c) indicates, however, that q_{elec}, the sum of the MO

TABLE I: q for MO's from OCE-SCF calculations of HCl, Moccia and modified GW bases, for comparison of 3σ and 1π q. Agreement is not expected for 4σ, 5σ, and 2π since only the 3d orbital of the modified GW basis has r_{max} near the proton.

MO	Moccia basis[b]	Modified GW basis[a]
1σ	-.00010	-.00001
2σ	-.01230	-.01752
3σ	-156.23061	-159.73185
4σ	-.21302	-.34254
5σ	-6.92658	-7.89900
1π	78.56465	80.10303
2π	4.99300	4.99912
Total q_{elec}	3.73268	2.21339
q_{tot}	3.87579	2.35650

experimental q_{elec} = 3.4908 au[16]; experimental q_{tot} = 3.6339 au[16].

$$q_{nuc} = 2/(2.4087)^3 = .14311 \text{ au.}$$

[a]Basis of Table VI but with ζ of orbitals 10 and 15 decreased to .83032 (page 118).

[b]Chapter II, Table II.

q's, is accurate to four decimal places and the individual MO q's to five places. This implies that the 3σ MO q is accurate to 8 significant figures, which is reasonable since it is expected to be accurate to more figures than the q of the highest MO (Chapter II). In the tables both the MO q and q_{elec} are given to five places, so q_{elec} is quoted to one more place than is significant.

3. Analysis by MO's of the EFG; comparisons with the Cl^- ion

Roughly, the 1σ, 2σ, 3σ, 1π, 4σ, 5σ, and 2π orbitals of HCl correspond to the 1s, 2s, $2p_z$, $2p_x$ and $2p_y$, 3s, $3p_z$, and $3p_x$ and $3p_y$ orbitals of the Cl^- ion respectively. Roughly, again, the 1s, 2s, and three 2p orbitals are not involved in the bonding of the proton in HCl, being too low in energy and too close to the Cl nucleus, so as a first approximation the 1σ, 2σ, 3σ, and 1π MO's of HCl are unchanged from the 1s, 2s, and 2p orbitals of Cl^-. The EFG can indicate how close to true this is for a given wavefunction for HCl. Since q for a spherical charge distribution is zero (because then the angular part of the charge distribution is $S_{00}(\theta,\phi)$, which is orthogonal to $3\cos^2\theta-1$ in (4)), and since a closed (fully occupied) shell or subshell of electrons is a spherically symmetric distribution of charge, the q of the 1σ and 2σ orbitals and the sum of the q's of the 3σ and two 1π orbitals should be zero if these orbitals correspond exactly to the ionic orbitals. The total q of the 1σ MO of the 71-orbital wavefunction for

HCl (corresponding to the first electron shell of the Cl^- ion), the sum of the q's of the 2σ, 3σ, and the two 1π MO's (corresponding to the second electron shell of Cl^-), and the sum of the q's of the 4σ, 5σ, and two 2π MO's (corresponding only loosely to the third shell of Cl^- because of the bonding of the proton) are listed in Table II, column 1. The q from the second shell of the 71-orbital wavefunction for HCl is quite large, nearly 25% of the total q_{elec}. This could mean either of two things: the inner electrons of HCl are indeed quite distorted in the Hartree-Fock approximation from their spherical distribution in the ion, or else the Moccia 71-orbital basis (Chapter II, Table II) is poorly chosen in the region of space occupied by the second shell electrons and gives an electron distribution far different from that which a good basis would give.

If the latter is true, it should appear in a calculation of the Cl^- ion as well as the HCl molecule, because if the basis set is deficient in an inner shell region the Cl^- wavefunction will necessarily be of poor quality. To this end a calculation of the Cl^- ion was performed with the same 71-orbital basis set. The OCE-SCF orbitals for Cl^- are given in Table III, with the correct designations of the Cl^- orbitals (1s, 2s, 2p, 3s, and 3p) and also the designations corresponding to the HCl MO's (1σ, etc.). Because the 71-orbital basis does not include σ and π basis orbitals in equal numbers or with equal exponents, it is not possible in this basis to

TABLE II: Electron shell analysis of q_{elec} for HCl and Cl^- in several OCE basis sets.

shell	shell contribution to q_{elec} (au)	
	HCl, 7l-orbital (Moccia)[c]	HCl, Modified GW[a]
1	-.00010	-.00001
2	.88639	.45669
3	2.84640	1.75670

shell	Cl^-, 7l-orbital (Moccia)[c]	Cl^-, Bagus[18] and Clementi[17]	Cl^-, GW[b]
1	.00000	.00000	.00000
2	.46814	.00000	.00000
3	.27836	.00000	.00000

[a]Basis of Table VI but with ζ of orbitals 10 and 15 decreased to .83032 (page 118).

[b]Table VI. d-orbitals are excluded from occupied orbitals of Cl^- by symmetry.

[c]Chapter II, Table II.

TABLE III: Coefficients of SCF orbitals of Cl^- ion, 71-orbital basis[a].

	σ-orbitals - coefficients				
basis orb.	1s(1σ)	2s(2σ)	$2p_z$(3σ)	3s(4σ)	$3p_z$(5σ)
1	.091667	-.001801	.000000	.032553	.000000
2	1.079649	.205396	.000000	-.326118	.000000
3	-.224714	.221636	.000000	.322189	.000000
4	.119858	-.112909	.000000	-.684036	.000001
5	-.065253	-.938178	.000000	1.335364	-.000001
6	.015558	-.119491	.000000	-.651123	.000001
7	-.002837	.007888	.000000	-1.042062	.000000
8	-.001578	.004804	.000000	-.085866	.000005
9	.000722	-.002218	.000000	.038972	-.000007
10	.002629	-.008009	.000000	.291567	-.000001
11	.000000	.000000	.316789	.000000	.051868
12	.000000	.000000	.632752	.000000	.223082
13	.000000	.000000	.116331	.000000	-.107332
14	.000000	.000000	-.022586	.000001	-.705221
15	.000000	.000000	-.020570	.000000	-.279968
16	.000000	.000000	.005324	.000000	-.141212
17	.000000	.000000	.026339	.000000	.091027
18	.000000	-.000246	.000000	.000704	-.000002
19	.000002	.000427	.000000	-.001108	.000001
20	.000000	-.000220	.000000	-.000081	-.000003

continued

TABLE III: (cont'd.)

basis orb.	σ-orbitals - coefficients				
	1s(1σ)	2s(2σ)	$2p_z$(3σ)	3s(4σ)	$3p_z$(5σ)
21	-.000001	-.000021	.000000	.000723	.000001
22	.000000	.000000	.000015	-.000001	-.000288
23	.000000	.000000	.000020	.000000	-.000064
24	.000000	.000000	-.000032	.000000	.000230
25	.000000	.000000	.000000	.000001	.000000
26	.000000	.000000	.000000	-.000001	.000000
27	.000000	.000000	.000000	.000000	.000001
28	.000000	.000000	.000000	.000000	-.000001
29	.000000	.000000	.000000	.000000	.000000
30	.000000	.000000	.000000	.000000	.000000
31	.000000	.000000	.000000	.000000	.000000
Eigen-value(au)	-104.503665	-10.227805	-7.688527	-.726876	-.144297

basis orb.	π-orbitals - coefficients	
	$2p_x, 2p_y$(1π)	$3p_x, 3p_y$(2π)
32	.307611	.063095
33	.643273	.197590
34	.126312	-.036933
35	-.063391	-.583277
36	.086453	-.514115

continued

TABLE III: (cont'd.)

basis orb.	π-orbitals - coefficients	
	$2p_x, 2p_y (1\pi)$	$3p_x, 3p_y (2\pi)$
37	-.105056	-.064939
38	.049995	.083743
39	.000001	.000005
40	-.000003	-.000014
41	.000002	.000011
42	.000000	.000001
43	.000058	-.000455
44	-.000003	-.000109
45	-.000054	.000438
46	.000000	.000000
47	.000000	.000000
48	.000000	.000001
49	.000000	-.000001
50	.000000	.000000
51	.000000	.000000
Eigenvalue (au)	-7.689198	-.147681

[a]Chapter II, Table II.

construct a σ ionic orbital which is exactly degenerate with a π orbital pair; thus the 2p and 3p orbitals are not triply degenerate as they would be in a calculation with a symmetric basis; they are instead an exactly degenerate pair (corresponding to an HCl π pair) and another orbital (corresponding to an HCl σ orbital) with nearly, but not exactly, the same eigenvalue . The q's for these Cl^- orbitals are given in Table IV.

There are in the literature two accurate (near Hartree-Fock) wavefunctions for the Cl^- ion in bases of STO's: one by Clementi[17] using a 25-orbital basis and one by Bagus[18] using a 28-orbital basis. The Bagus set gives a slightly lower energy and is thus closer to the Hartree-Fock limit. These basis sets are given in Table V. The q's for the orbitals of Cl^- calculated from the published coefficients (the Clementi calculation was repeated in this laboratory; the coefficients agreed exactly with the published values) using the integrals described in section 1 are listed in Table IV, and the analysis by electron shells is given in Table II. The only serious disagreement between the 71-orbital Cl^- and the near Hartree-Fock Cl^- wavefunctions is in the 2p orbitals. The 71-orbital basis gives q of −156.5 au for the $2p_z$ and 78.5 au for the $2p_x$ and $2p_y$ orbitals, while the near Hartree-Fock functions both give q's of −160.7 au for $2p_z$ and 80.4 au for $2p_x$ and $2p_y$. Thus it appears that the Moccia basis is poorly chosen for the second electron shell, since it gives orbital

TABLE IV: q_{elec} by orbitals for Cl^-, several basis sets. All values in au.

orbital (corresp. to HCl)	71-orbital[a]	Clementi[17]	Bagus[18]	GW[b]	GW-Bagus[c]
1s (1σ)	.00000	0.	0.	0.	0.
2s (2σ)	-.00061	0.	0	0	0.
$2p_z$ (3σ)	-156.54762	-160.71315	-160.72161	-160.19510	-155.41731
3s (4σ)	-.00008	0.	0.	0.	-.00005
$3p_z$ (5σ)	-8.70673	-9.19287	-9.17898	-9.14711	-9.36622
$2p_x, 2p_y$ (1π)	78.50819	80.35[illegible]58	80.36081	80.09755	80.09464
$3p_x, 3p_y$ (2π)	4.49258	4.59643	4.58949	4.57355	4.58016
Total	.74650	0.	0.	0.	4.56602

[a]Chapter II, Table II.

[b]Table VI.

[c]Basis of Table VI with orbitals 6 and 7 deleted and the following orbitals added: $2p_z$, ζ=7.535; $2p_z$, ζ=4.385; $4p_z$, ζ=7.200.

TABLE V: Bagus[18] and Clementi[17] bases for Cl^-.

	Bagus			Clementi		
	orb.	ζ	r_{max}	orb.	ζ	r_{max}
σ				σ		
	1s	19.955	.000	1s	17.2875	.000
	2s	14.545	.069	1s	28.4472	.000
	3s	16.000	.125	2s	6.8172	.147
	3s	9.951	.201	2s	15.3682	.065
	2s	5.748	.174	3s	2.8669	.698
	3s	2.823	.708	3s	1.6723	1.196
	3s	1.651	1.211	3s	5.9503	.336
	$2p_z$	15.380	.065	$2p_z$	7.6419	.131
	$2p_z$	7.535	.133	$2p_z$	13.9763	.072
	$2p_z$	4.385	.228	$3p_z$	2.8985	.690
	$4p_z$	7.200	.417	$3p_z$	1.0374	1.928
	$3p_z$	2.612	.766	$3p_z$	5.9321	.337
	$4p_z$	1.826	1.643	$3p_z$	1.8615	1.074
	$3p_z$	.920	2.174			
π				π		
	$2p_x,2p_y$	15.380	.065	$2p_x,2p_y$	7.6419	.131
	$2p_x,2p_y$	7.535	.133	$2p_x,2p_y$	13.9763	.072
	$2p_x,2p_y$	4.385	.228	$3p_x,3p_y$	2.8985	.690
	$4p_x,4p_y$	7.200	.417	$3p_x,3p_y$	1.0374	1.928
	$3p_x,3p_y$	2.612	.766	$3p_x,3p_y$	5.9321	.337
	$4p_x,4p_y$	1.826	1.643	$3p_x,3p_y$	1.8615	1.074
	$3p_x,3p_y$	.920	2.174			

q's for the shell in Cl^- very different from those of the near Hartree-Fock wavefunctions. However before this can be concluded one further point must be checked: it is possible that while the Moccia basis is poorly suited to describe the second shell in Cl^-, it is well suited to describe this shell in HCl. This is unlikely, since this implies a large difference in the structure of the non-valence shells of Cl^- and HCl; indeed, comparison with two-center calculations in Chapter VII shows that the 71-STO basis is also poor for the q of the 3σ and 1π MO's of HCl.

It appears fairly certain, then, that the Moccia basis could be improved upon by starting with the Bagus[18] basis for Cl^- and adding orbitals to minimize the HCl energy; it is tempting to think that the Moccia basis might be substantially improved by simple replacement of the orbitals which contribute heavily to the 3σ and 1π MO's by the corresponding orbitals of the Bagus basis. Recalculation of the electron repulsion integrals in the 71-STO basis resulting from this replacement would be costly of computer time and was not done in this work. However a test was made of such a replacement in a smaller basis. The basis set was taken from a calculation of Cl_2 by Gilbert and Wahl[19] (GW). This basis was chosen because of its small size; however it was carefully optimized by Gilbert and Wahl and experience in this laboratory has shown that for investigating the effects of basis set change in OCE-SCF wavefunctions of HCl it is as effective as the

Clementi Cl^- basis and 5 orbitals smaller, giving a large saving in computer time. The GW 20 orbital basis (10σ orbitals, 5π pairs) is listed in Table VI. If it were true that mere inclusion of the three appropriate σ orbitals from the Bagus basis ($2p_z$ with exponent 7.535, $2p_z$ with exponent 4.385, and $4p_z$ with exponent 7.200) guaranteed an accurate 3σ MO, then a calculation of Cl^- with the GW $2p_z$ orbitals replaced by these three should give a $2p_z$ Cl^- orbital with q close to the Hartree-Fock value; this was tried (Table IV) with the result that the q from $2p_z$ orbital was even lower than that from the Moccia basis and far from the Hartree-Fock value. Thus while the Bagus basis produces a q of -160.7 au for the $2p_z$ orbital of Cl^-, and while only three orbitals of the basis contribute heavily to this ionic orbital (Table VII), the insertion of these orbitals in the GW basis results in a q of -155.4 au for the $2p_z$ orbital, even though again only these three orbitals contribute heavily (Table VII). Thus it is not likely that merely replacing the orbitals of the Moccia basis which contribute to the 3σ and 1π MOs by the corresponding orbitals in the Bagus basis would improve the quality of these orbitals. The conclusion, then, is that the Moccia 71-orbital basis is not sufficiently flexible in the second shell region, but that there is no simple way to improve this by changing a few orbital exponents. A complete rebuilding of the basis would be necessary, preferably using the Bagus Cl^- basis as a starting point.

TABLE VI: Gilbert-Wahl[19] basis for Cl_2

	orb.	ζ	r_{max}
σ			
1	1s	18.424	.000
2	2s	16.187	.062
3	2s	6.092	.164
4	3s	2.608	.767
5	3s	1.597	1.252
6	$2p_z$	10.267	.097
7	$2p_z$	5.608	.178
8	$3p_z$	2.608	.767
9	$3p_z$	1.463	1.367
10	$3d_{z^2-r^2}$	1.943	1.029
π			
11	$2p_x, 2p_y$	10.267	.097
12	$2p_x, 2p_y$	5.608	.178
13	$3p_x, 3p_y$	2.608	.767
14	$3p_x, 3p_y$	1.463	1.367
15	$3d_{xz}, 3d_{yz}$	1.943	1.029

TABLE VII: Coefficients of the $2p_z$ (3σ) orbital of Cl^- in several bases

Bagus[18] basis			GW[19] basis			GW-Bagus[a]		
orb.	ζ	coeff.	orb.	ζ	coeff.	orb.	ζ	coeff.
$2p_z$	15.380	.01990	$2p_z$	10.267	.205835	$2p_z$	7.535	-.842174
$2p_z$	7.535	.68564	$2p_z$	5.608	.821569	$2p_z$	4.385	.167440
$2p_z$	4.385	.19201	$3p_z$	2.608	.018959	$4p_z$	7.200	-.370138
$4p_z$	7.200	.16481	$3p_z$	1.463	-.005252	$3p_z$	2.608	-.075149
$3p_z$	2.612	.00296				$3p_z$	1.463	.027146
$4p_z$	1.826	-.00058						
$3p_z$	.920	.00024						

[a]See note C, Table IV.

This was not undertaken in the present work because of the prohibitive expense; instead further investigations of basis set effects were made using the GW basis. Even with this rather limited starting point a basis was obtained which yielded an energy lower than that from the Moccia 71-orbital basis and which in addition yielded a q much closer to the experimental value. These investigations are reported in the next section.

4. The 4σ and 5σ MO's:basis set effects

Table II, column 1 indicates that the most important MO's in determining q_{elec} are those of the third electron shell of HCl, i.e. the 4σ, 5σ, and 2π orbitals. Since the $3p_x$ and $3p_y$ orbitals are, in the simple bonding picture, unchanged from their form in Cl^- (since there are in this picture no π orbitals on H), we here make the assumption that the important effects to be observed upon increasing the basic Cl^- basis will be in the 4σ and 5σ orbitals, which means that the effects can be observed by adding only σ orbitals to the basis. Tables I and IV support this assumption, since they show that for HCl and Cl^- there is little difference in the q of the 2π MO in very different bases.

A series of calculations was done starting with the GW basis and successively adding 9s, 9p, 9d, etc. orbitals with m=0 and r_{max}=2.4087 au, i.e. with the radial maxima at the proton. The exponent for these orbitals is 3.32129.

In calculating Tables I & II the GW basis was modified so that the 3d orbitals had their radial maxima at the proton, in the calculations of this section the 3d exponent is that of the Gilbert-Wahl calculation of Cl_2[19] as it appears in Table VI. This is because the calculations of Tables I and II involved inner shell orbitals and it was necessary to have some density near the proton for a generally correct description of the electron distribution; in this section the density near the proton is described by the n=9 orbitals; the 3d exponent is returned to its molecular calculation value to give more flexibility in intermediate regions between the Cl nucleus and the proton. The basis series is labeled in this way: GW+1 denotes the 21 orbital basis consisting of the GW basis plus a 9s orbital with ζ=3.32129, GW+2 denotes the 22 orbital basis consisting of GW plus 9s and 9p with ζ=3.32129, and so on with GW+9 the 29 orbital basis including a 9k orbital. The GW+9 basis is listed in Chapter II, Table III.

The q_{elec} and individual MO q values for this series of basis sets is given in Table VIII. The process was halted with the addition of the 9k (ℓ=8) orbital since this value of ℓ is the largest allowed value for n=9. The basis set enlargement could have been continued with higher n and higher ℓ, but it was decided that the trends were clear with the additions through 9k. Comparison of the value of q_{elec} for the basis including through the 9k orbital (3.49418 au) with Kaiser's[16] experimental value (3.4908 au) shows very close

TABLE VIII: HCl MO q for OCE-SCF wavefunctions in the basis series formed by successively adding to the GW basis of Table VI 9s, 9p, etc. orbitals with ζ=3.32129.

		q (au)			
MO	GW	GW+1	GW+2	GW+3	GW+4
1σ	-.00002	-.00002	-.00002	-.00003	-.00004
2σ	-.00214	-.00211	-.00213	-.00479	-.00455
3σ	-159.81711	-159.83041	-159.82821	-159.78359	-159.77342
4σ	-.27932	-.27894	-.27928	-.25108	-.23098
5σ	-8.21412	-8.20252	-8.23275	-7.86197	-7.48301
1π	80.09098	80.09895	80.09529	80.11365	80.12693
2π	4.94887	4.95051	4.95234	5.01231	5.06159
Total	1.76700	1.78493	1.75288	2.35045	2.88505

		q (au)		
MO	GW+5	GW+6	GW+7	GW+8
1σ	-.00004	-.00005	-.00005	-.00005
2σ	-.00455	-.00458	-.00460	-.00462
3σ	-159.76293	-159.75641	-159.75235	-159.74981
4σ	-.22292	-.21955	-.21795	-.21713
5σ	-7.28938	-7.18000	-7.11492	-7.07493
1π	80.13523	80.14004	80.14292	80.14469
2π	5.08426	5.09654	5.10373	5.10812
Total	3.15916	3.31257	3.40343	3.45908

continued

TABLE VIII: (cont'd.)

	q (au)
MO	GW+9
1σ	-.00005
2σ	-.00463
3σ	-159.74818
4σ	-.21670
5σ	-7.04966
1π	80.14581
2π	5.11089
Total	3.49418

agreement; the agreement is illusory however because the whole series of calculations indicates that addition of higher ℓ-values would raise q_{elec} above 3.5 au; the series of q_{elec} values appears to be converging to roughly 3.6 au.

The greatest changes in MO q upon addition of higher ℓ orbitals with r_{max}=2.4087 au occurs in the 4σ (-.28 au to -.22 au) and 5σ (-8.20 au to -7.05 au) MO's. The 3σ MO experiences a change of about the same size as the change in q of the 4σ (-159.83 au to -159.75 au) but this change is much smaller relative to the q of the MO. In both the 4σ and 5σ MO's the change, to a lower absolute value of q, corresponds to transfer of electron density from closer to the Cl nucleus (where $1/r^3$ is larger) to farther from the Cl nucleus (where $1/r^3$ is smaller). This is as expected for addition of basis orbitals with r_{max} far from the Cl nucleus.

Addition of the orbitals of higher angular momentum quantum number allows a greater angular concentration of charge because the interval between nodes of the θ-dependent factor of the m=0 spherical harmonic decreases with increasing ℓ[20]. Since the proton is placed at θ=0 and the angular part of the q operator is $3\cos^2\theta-1$, which attains its highest absolute value at cosθ=1, allowing greater concentration of charge close to θ=0 allows an increase in the magnitude of q_{elec}. Thus the radial and angular effects work in opposite directions; from Table VIII the radial effect dominates strongly after the first few additions. A qualitative description of this balance

is that the higher angular momentum numbers allow a build-up of charge near the proton to be produced by orbitals with the appropriate r_{max}; this produces a substantial energy lowering which ensures that these orbitals contribute to the 4σ and 5σ MO's; the radial effect dominates in determining the change in q as the orbitals are added.

5. Analysis of q_{elec} by orbital-pair type

By equation (7), the total q_{elec}, and the q of each of the individual MO's, is a sum of terms which contain an integral of the form $\langle\phi_i|\partial^2V/\partial z^2|\phi_j\rangle$. One possible way of classifying the terms is by the pair of angular momentum quantum numbers ℓ_i and ℓ_j belonging to ϕ_i and ϕ_j. Since the integral is symmetric in ϕ_i and ϕ_j the order of ϕ_i and ϕ_j is not important in the classification. By (5), the integral $\langle\phi_i|\partial^2V/\partial z^2|\phi_j\rangle$ has as a factor the angular integral

$$\int_0^{\pi}d\theta\sin\theta\int_0^{2\pi}d\phi S_{\ell_i m_i}(\theta,\phi)S_{\ell_j m_j}(\theta,\phi)S_{20}(\theta,\phi); \qquad (9)$$

from conditions introduced earlier (Chapter II, equation (8)) this integral vanishes unless

$$\ell_i + \ell_j \geq 2 \qquad (10)$$

and

$$|\ell_i - \ell_j| \leq 2. \qquad (11)$$

An additional identity for these integrals[21] implies that (9) vanishes unless $\ell_i - \ell_j$ is even. Using this condition and (10) and (11), it is easy to see that the only possible orbital pairs that can make non-zero contributions to q_{elec} when the highest ℓ-value in the basis is 8 (a k-orbital) are (orbital types to left, ℓ-values in parentheses):

s-d	(0-2)	
p-p	(1-1)	
p-f	(1-3)	
d-d	(2-2)	
d-g	(2-4)	
f-f	(3-3)	
f-h	(3-5)	(12)
g-g	(4-4)	
g-i	(4-6)	
h-h	(5-5)	
h-j	(5-7)	
i-i	(6-6)	
i-k	(6-8)	
j-j	(7-7)	
k-k	(8-8)	

In Table IX the total q_{elec}'s of (7) for the 10 basis sets of Table VIII are broken down into contributions from the orbital pairs of (12). The conclusion to be drawn from Table IX is that while addition of orbitals with higher ℓ greatly affects q_{elec}, it does this indirectly by allowing a more important contribution from the 9p orbital to the 5σ MO rather than directly through orbital pair contributions to

TABLE IX: Orbital pair analysis, GW basis extended with n=9 orbitals, r_{max}=2.4087 au.

	q (au)			
pair type	GW	GW+1	GW+2	GW+3
sd	-.03514	-.03498	-.03496	-.03329
pp	1.82154	1.83932	1.80727	2.39721
pf				
dd	-.01940	-.01942	-.01943	-.01347

pair type	GW+4	GW+5	GW+6
sd	-.02992	-.02883	-.02827
pp	2.95952	3.24075	3.39730
pf	-.02883	-.03093	-.03211
dd	-.01465	-.01524	-.01556
dg		-.00492	-.00534
ff	-.00107	-.00126	-.00137
fh			-.00143
gg		-.00042	-.00048
hh			-.00018

continued

TABLE IX: (cont'd.)

pair type	q (au) GW+7	GW+8	GW+9
sd	-.02797	-.02780	-.02770
pp	3.48981	3.54642	3.58210
pf	-.03271	-.03307	-.03330
dd	-.01577	-.01590	-.01599
dg	-.00560	-.00574	-.00584
ff	-.00142	-.00146	-.00148
fh	-.00154	-.00161	-.00165
gg	-.00051	-.00053	-.00055
gi	-.00059	-.00063	-.00066
hh	-.00020	-.00021	-.00022
hj		-.00026	-.00028
ii	-.00008	-.00009	-.00009
ik			-.00012
jj		-.00004	-.00004
kk			-.00002

q_{elec} involving the higher ℓ quantum numbers. The coefficients of the 9p basis orbital to the 5σ MO for the various basis sets are given in Table X to illustrate this. Note that the magnitude of the 9p coefficient steadily increases as the higher-ℓ n=9 orbitals are added.

6. Contribution to q_{elec} of inner shells

Although this effect will be examined in more detail in Chapter VII, attention should be called at this point to the non-zero contributions of the 1σ, 2σ, and 1π MO's, which correspond to the inner shells of the Cl^- ion. This effect is usually referred to as the Sternheimer effect[22,23]. Table XI gives the shell contributions to the total q_{elec} for the series of calculations described in section 4, analogously to Table II. For the 29-orbital set including ℓ=8, the contributions from shells 1 and 2 total .53876 au compared to a total q_{elec} of 3.49418 au, or 15%. This is considerably less than the 25% which was predicted by Moccia's 71-orbital basis (section 3), and is in qualitative agreement with the result of the early calculation by Scrocco and Tomasi[24]. It will be compared with the accurate two-center calculations of Cade and Huo[25] and of McLean and Yoshimine[26] in Chapter VII.

TABLE X: Coefficients of 5σ MO of HCl, GW series of bases with n=9, r_{max}=2.4087 orbitals added.

		coefficient			
orb.	ζ	GW	GW+1	GW+2	GW+3
1s	18.424	-.018548	.018241	.018248	.018620
2s	16.187	-.014398	.013830	.013831	.014080
2s	6.092	.105325	-.102304	-.102324	-.104287
3s	2.608	-.276551	.252747	.252516	.255651
3s	1.597	.071784	-.026342	-.025579	-.021046
2pσ	10.267	-.046900	.046899	.045809	.044693
2pσ	5.608	-.201134	.200903	.204820	.200323
3pσ	2.608	.434062	-.433388	-.457893	-.447645
3pσ	1.463	.625434	-.625729	-.571120	-.556738
3dσ	1.943	.161126	-.161214	-.161281	-.108753
9s	3.32129		-.032493	-.033424	-.043202
9pσ	3.32129			-.041130	-.055217
9dσ	3.32129				-.125341

continued

TABLE X: (cont'd.)

orb.	ζ	coefficient GW+4	GW+5	GW+6
1s	18.424	.019194	-.019555	-.019794
2s	16.187	.014503	-.014771	-.014950
2s	6.092	-.107464	.109468	.110798
3s	2.608	.262879	-.267513	-.270596
3s	1.597	-.019942	.019500	.019252
2pσ	10.267	.043436	-.042789	-.042419
2pσ	5.608	.195268	-.192780	-.191380
3pσ	2.608	-.436142	.430615	.427518
3pσ	1.463	-.540786	.532298	.527426
3dσ	1.943	-.115371	.117557	.118700
9s	3.32129	-.050240	.053561	.055396
9pσ	3.32129	-.069481	.075991	.079674
9dσ	3.32129	-.142362	.151168	.155433
9fσ	3.32129	-.117973	.127592	.133176
9gσ	3.32129		.073848	.078735
9hσ	3.32129			.048203

continued

TABLE X: (cont'd.)

orb.	ζ	coefficient GW+7	GW+8	GW+9
1s	18.424	-.019948	.020048	-.020113
2s	16.187	-.015064	.015138	-.015187
2s	6.092	.111653	-.112205	.112567
3s	2.608	-.272581	.273866	-.274708
3s	1.597	.019110	-.019024	.018969
2pσ	10.267	-.042197	.042061	-.041974
2pσ	5.608	-.190547	.190036	-.189712
3pσ	2.608	.425682	-.424557	.423846
3pσ	1.463	.524498	-.522684	.521532
3dσ	1.943	.119450	-.119922	.120225
9s	3.32129	.056485	-.057158	.057587
9pσ	3.32129	.081897	-.083288	.084182
9dσ	3.32129	.157972	-.159543	.160545
9fσ	3.32129	.136021	-.137776	.138888
9gσ	3.32129	.081741	-.083309	.084296
9hσ	3.32129	.050764	-.052389	.053252
9iσ	3.32129	.032270	-.033651	.034550
9jσ	3.32129		-.022175	.022946
9kσ	3.32129			.015628

TABLE XI: Shell analysis of q_{elec}, HCl, GW basis series. All quantities in au.

shell	GW	GW+1	GW+2	GW+3
1	-.00002	-.00002	-.00002	-.00003
2	.36271	.36538	.36024	.43892
3	1.40430	1.41956	1.39265	1.91157

shell	GW+4	GW+5	GW+6
1	-.00004	-.00004	-.00005
2	.47589	.50298	.51909
3	2.40919	2.65622	2.79353

shell	GW+7	GW+8	GW+9
1	-.00005	-.00005	-.00005
2	.52889	.53495	.53881
3	2.87459	2.92418	2.95542

REFERENCES

1. R.B. McQuistan, Scalar and Vector Fields: A Physical Interpretation, Wiley, N.Y., 1965. p. 135.
2. N. Coburn, Vector and Tensor Analysis; Dover, N.Y., 1970. p. 43.
3. E. Hylleraas, Mathematical and Theoretical Physics, vol. 1, Wiley-Interscience, N.Y., 1970. p. 49.
4. L. Brand, Vector Analysis, Wiley, N.Y., 1957. pp. 94, 99.
5. M.H. Cohen and F. Reif, in Solid State Physics, v. 5, Academic, N.Y., 1957. p. 321.
6. L.D. Landau and E.M. Lifschitz, Classical Theory of Fields, Addison-Wesley, Reading, Mass., Revised 2nd edition, 1962. p. 100.
7. N.F. Ramsey, Nuclear Moments, Wiley, N.Y., 1953. p. 20.
8. J. Bardeen and C.H. Townes, Phys. Rev. 73, 97 (1948).
9. Reference 2, page 175.
10. A.N. Tychonov and A.A. Samarski, Partial Differential Equations of Mathematical Physics, vol. I, Holden-Day, San Francisco, 1964. Section 4-5.
11. H. Eyring, J. Walter, and G.E. Kimball, Quantum Chemistry, Wiley, N.Y., 1944. p. 59.
12. H.J. Kolker and M. Karplus, J. Chem. Phys. 36, 960 (1962).
13. R.M. Pitzer, C.W. Kern, and W.N. Lipscomb, J. Chem. Phys. 37, 267 (1962).
14. M.J. Stephen and J.P. Auffray, J. Chem. Phys. 31, 1329 (1959).

15. R.M. Pitzer, J. Chem. Phys. 51, 3191 (1969).

16. E.W. Kaiser, J. Chem. Phys. 53, 1686 (1970).

17. E. Clementi, Tables of Atomic Wavefunctions, supplement to IBM Journal of Res. and Dev. 9, 2 (1965).

18. P.S. Bagus, Phys. Rev. 139, A619 (1965).

19. T.L. Gilbert and A.C. Wahl, J. Chem. Phys. 55, 5247 (1971).

20. G. Birkhoff and G.C. Rota, Ordinary Differential Equations, Blaisdell, Waltham, Mass., 2nd edition, 1969. p.60.

21. E.U. Condon and G.H. Shortley, The Theory of Atomic Spectra, Cambridge, 1935. p. 176.

22. R. Sternheimer, Phys. Rev. 80, 102 (1950).

23. R. Sternheimer, Phys. Rev. 84, 244 (1951).

24. E. Scrocco and J. Tomasi, Theoret. Chim. Acta, 2, 386 (1964).

25. P.E. Cade and W.M. Huo, J. Chem. Phys. 47, 649 (1967).

26. A.D. McLean and M. Yoshimine, J. Chem. Phys. 47, 3256 (1967).

CHAPTER IV: Comparison of the EFG from two-center and one-center calculations of HCl

An ab-initio OCE-SCF calculation on a diatomic molecule is of interest only if it can economically approach the result which a more time-consuming two-center calculation would yield. As either a one-center or two-center basis is increased toward completeness, the molecular wavefunction calculated in this basis approaches the Hartree-Fock (H-F) wavefunction, which is that single determinant wavefunction which gives the lowest possible energy (Chapter I). The physical properties calculated from the wavefunction also approach the H-F limit, although this convergence is not necessarily monotonic; that is, while addition of an orbital to the basis always lowers the energy and brings it closer to the H-F value, for a property like the dipole moment addition of an orbital may take the expectation value of that property farther from the H-F value[1]. Goodisman[2] has shown that one-electron properties are expected to converge to the H-F limit upon addition of basis orbitals much more slowly than the energy. In assessing the utility of an OCE-SCF prediction of a particular property, then, there are two points to be investigated: a) whether the property converges with addition of basis orbitals to a limit in a small enough basis that the OCE-SCF calculation is still economical, and b) whether this limit is the H-F limit or an artificial one caused by the limitations of the finite

one-center basis. In this chapter the series of OCE-SCF calculations starting with the GW basis[3] and adding successively 9s, 9p, etc. orbitals with r_{max}=2.4087 au (Chapter III, section 4) is examined for convergence of the q values of the individual MO's and compared with the results of accurate two-center (TCE-SCF) calculations by Cade and Huo[4] and by McLean and Yoshimine[5,6], which are close to the H-F limit[7].

1. Evaluation of q in a two-center basis of STO's

The wavefunctions[4,5] and the total q_{elec} values[6] for the Cade-Huo and McLean-Yoshimine calculations of HCl have been published; the individual MO q expectation values have not. In order to make the comparison with the OCE-SCF MO's, the MO q expectation values for the TCE-SCF wavefunctions had to be computed in this laboratory. Calculations of the expectation value of this operator over wavefunctions in two-center bases of STO's were first published by Richardson[8]; however this early treatment employed some approximations of uncertain accuracy. Later Kolker and Karplus[9] gave some formulas useful for evaluation of certain of the necessary integrals and Stephen and Auffray[10] outlined a method, used by Kahalas and Nesbet for LiH[11], for evaluating the integrals by numerical integration; McLean and Yoshimine[12] have also given a method involving numerical integration. More recently interest in formulas for these integrals over STO's has waned with the development of Gaussian transform techniques[13-15], in which the STO is ap-

proximated as an integral transform of a Gaussian function; the integrals over the q operator are then done over the Gaussian functions, which is a relatively simple problem[15-16], and the result for the STO's found by inverse transformation. This method has the great advantage over a direct formula for STO's that the Gaussian transform technique can handle three-center integrals, which arise in evaluation of q for polyatomic molecules[15a]. The disadvantage of the Gaussian transform technique, if one is interested only in diatomic molecules, is that the accuracy is limited because of the integral transform approximation of the STO[14], and the initial programming is complex compared to that involved for a direct formula. Thus a general formula for the integrals of the q operator (Chapter III, equation (4)) over STO's with no restriction on the n, ℓ, or m quantum numbers is desirable; however none exists in the literature.

The form of an STO on a given center a is

$$\phi_i(n_i,\ell_i,m_i,\zeta_i,r_a,\theta_a,\phi_a) =$$

$$N_i(n_i,\zeta_i)r_a^{n_i-1}\exp(-\zeta_i r_a)S_{\ell_i m_i}(\theta_a,\phi_a) \qquad (1)$$

where $(N_i(n_i,\zeta_i)$ is a normalization constant and $S_{\ell_i m_i}(\theta_a,\phi_a)$ is a real spherical harmonic (Appendix I). The coordinates r_a,θ_a, and ϕ_a are measured in a spherical system centered at a. An expression similar to (1) applies for an STO

$\phi_j(n_j, \ell_j, m_j, \zeta_j, r_b, \theta_b, \phi_b)$ centered on b with the coordinates measured in a spherical system centered at b. In a diatomic molecule the spherical systems on a and b can be chosen so that they have a common z-axis (the axis about which ϕ_a and ϕ_b are measured); this choice is made here. We further assume that b lies upon the positive z-axis as measured from a and that a lies on the negative z-axis measured from b. This differs from the convention of many authors[9,17,18], who pick the z-axis so that b lies on the positive z-axis of a right-handed system centered on a and a lies on the positive z-axis of a left-handed system centered on b; it was decided for this work to keep a fixed positive direction and handedness for both centers. This is purely a matter of taste and the results are the same either way; it must however be clear which convention is used. A common way to handle problems involving two centers is to introduce elliptical coordinates[17,19],

$$\begin{aligned} \mu &= (r_a + r_b)/R \\ \nu &= (r_a - r_b)/R \\ \phi &= \phi_a = \phi_b \\ d\tau &= (R^3/8)\ (\mu^2-\nu^2)d\mu d\nu d\phi, \end{aligned} \tag{2}$$

with $d\tau$ the volume element for integrations over all space and ϕ measured from the xz plane. R is the distance between a and b. Using a form of $\hat{q}$ introduced in Chapter III,

$$\hat{q} \equiv \partial^2\hat{V}/\partial z^2 = \frac{1}{r_a^3}(4\sqrt{\pi}/\sqrt{5})S_{20}(\theta_a,\phi_a), \qquad (3)$$

where the EFG is calculated at a, the integral of $\hat{q}$ between orbitals ϕ_i and ϕ_j becomes

$$\langle\phi_i|\hat{q}|\phi_j\rangle = \int N_i N_j R_i(r_a) R_j(r_b) r_a^{-3}(4\sqrt{\pi}/\sqrt{5})S_{20}(\theta_a,\phi_a)$$

$$S_{\ell_i m_i}(\theta_a,\phi_a) S_{\ell_j m_j}(\theta_b,\phi_b)d\tau \qquad (4)$$

where $R_i(r_a)$ stands for the radial part of ϕ_i in (1). Before the integration can be performed it is necessary to express all functions of r_a, r_b, θ_a, and θ_b in terms of μ, ν, and R. The ϕ_a- and ϕ_b- dependent parts are unchanged. This fact effects a significant simplification. Since $S_{\ell m}(\theta,\phi)$ is a product of normalized θ- and ϕ- dependent parts (Chapter II and Appendix I),

$$S_{\ell m}(\theta,\phi) = \Theta_{\ell m}(\theta)\Phi_m(\phi), \qquad (5)$$

with the $\Phi_m(\phi)$ orthogonal for different m, the integration over ϕ in (4) becomes (since $S_{20}(\theta,\phi)$ is independent of ϕ[20]),

$$\int d\phi \Phi_{m_i}(\phi)\Phi_{m_j}(\phi) = \delta_{m_i m_j}.$$

Thus the integral $\langle\phi_i|\hat{q}|\phi_j\rangle$ vanishes unless $m_i = m_j$, and then equals the integral over μ and ν alone. Full details are given in Appendix I; the crucial point in obtaining a general expression for (4) is obtaining a general expansion in the elliptical

coordinates (2) for the product

$$\Theta_{\ell_i m_i}(\theta_a)\Theta_{\ell_j m_j}(\theta_b)$$

of the θ-dependent parts of the spherical harmonics on the different centers. Guseinov[18] has published a general formula for this expansion; this, coupled with certain techniques of manipulation due to Kolker and Karplus[9] and some integral formulas due to Ruedenberg et al.[21] enabled the author to construct a computer program to evaluate $\langle\phi_i|\hat{q}|\phi_j\rangle$ for any STO's ϕ_i and ϕ_j centered on a and b respectively. An extension of Guseinov's formula to the case where ϕ_i and ϕ_j are both on b enabled the calculation of $\langle\phi_i|\hat{q}|\phi_j\rangle$ with ϕ_i and ϕ_j on b. The mathematical details and the computer program, along with documentation against integral values in the literature, is given in Appendix I.

2. MO q's from the TCE-SCF wavefunctions for HCl

The total q_{elec} and the contributions of individual MO's for the Cade-Huo and McLean-Yoshimine TCE-SCF wavefunctions for HCl are given in Table I. It should be noted that the values for the total q_{elec} are in the case of the McLean-Yoshimine wavefunction slightly, and in the case of the Cade-Huo wavefunction rather greatly, different from those calculated by McLean and Yoshimine[6] for the same wavefunctions, which are also given in Table I. The q integral routines written by the author were carefully checked against values in the literature to insure

that this was not the source of the discrepancy. The disagreement with the McLean-Yoshimine value is easily explained. This wavefunction was published[5] with coefficients to five decimal places; in most cases this is also five significant figures. The individual MO q expectation values calculated from these published coefficients should then also have about five significant figures; in the case of the MO with the largest q value (3σ) this means an accuracy of two decimal places or an absolute uncertainty of ±.005 au. The two 1π orbitals have q values with about half the magnitude of that of the 3σ MO, so the absolute error of this MO q is about half that of the 3σ MO q. These are the largest MO q's and thus contribute the largest part of the absolute uncertainty of the sum over the 9 MO's. The absolute uncertainty from these MO's is about 2(±.005)=±.01 au; the disagreement between q_{elec} calculated in this laboratory from the published wavefunction and that calculated by McLean and Yoshimine is .007 au, which is within the above estimate. The McLean-Yoshimine q_{elec} is more accurate than ours since it was calculated with coefficients to the full computer word-length.

The disagreement between q_{elec} calculated by the author from the published Cade-Huo wavefunction and that calculated for this function by McLean and Yoshimine[6] is .06 au and cannot be explained by the above reasoning. However McLean and Yoshimine did not use the coefficients published by Cade and Huo; they independently calculated an SCF wavefunction for

TABLE I: MO q expectation values for SCF calculations of HCl in several bases. Limit of the GW basis enlargement series is also given.

MO	q (au) McL-Yosh[5]	C-H[4]	wavefunction 71-orb.[a]	GW+9[b]	GW limit[c]	
1σ	-.00214	-.00013	-.00010	-.00005	-.00005	(1)
2σ	-.01200	-.00615	-.01230	-.00463	-.00465	(2)
3σ	-160.37392	-160.30674	-156.23061	-159.74818	-159.743	(2)
4σ	-.20523	-.19098	-.21302	-.21670	-.215	(1)
5σ	-7.05643	-7.02929	-6.92658	-7.04966	-7.02	(2)
1π	80.41931	80.41716	78.56465	80.14581	80.150	(3)
2π	5.11146	5.11595	4.99300	5.11089	5.112	(1)
total[d]	3.41182	3.53293	3.73268	3.49418	3.58	(5)
total (calc. by McLean-Yoshimine[6])	3.4192	3.4694	EXPERIMENTAL[31]: 3.4908 a.u.			

continued

TABLE I: (cont'd.)

[a]Chapter II, Table V. Basis from reference 32.

[b]Chapter III, Table VIII.

[c]Estimated from Chapter III, Table VIII. Uncertainty in last place in parentheses.

[d]Calculated in this laboratory.

HCl with the same basis and internuclear distance used by Cade and Huo. They report[6] "complete agreement" with the Cade-Huo wavefunction, however the fact that distinct computer programs were used to generate the two wavefunctions means that there must be some limit to the number of decimal places to which the MO coefficients agree. There is no way to obtain this information from the coefficients themselves, since they were not published by McLean and Yoshimine; however it is possible to estimate these differences from differences in one-electron properties. Cade and Huo[22] published the dipole moment expectation value from their HCl wavefunction; they report $\langle\psi|\sum_k \hat{z}_k|\psi\rangle = -19.7404$ au. The summation is over all electrons. Cade and Huo did not report what coordinate system this refers to; however comparison with values published for HF by Bender and Davidson[23] indicates that Cade and Huo used the same convention as Bender and Davidson, which was that the origin was the midpoint of the internuclear line, with the proton on the positive and the heavy atom on the negative z-axis. McLean and Yoshimine[6] take the origin at the heavy atom and the proton on the positive z-axis; thus

$$z(M-Y) = z(C-H) + R/2$$

and

$$\langle\psi|\sum_k \hat{z}_k|\psi\rangle\ (M-Y) = \langle\psi|\sum_k \hat{z}_k|\psi\rangle\ (C-H) + n_{elec} \times R/2,$$

where n_{elec} is the number of electrons in the system. Then,

using the published Cade-Huo value[22],

$$\langle\psi|\sum_k \hat{z}_k|\psi\rangle \cdot (M-Y) = -19.7404 + \frac{18\times 2.4087}{2} = 1.9379 \text{ au.}$$

McLean and Yoshimine report 1.9381 au. The difference of .0002 au is small and subject to a 50% probable error; however the difference is significant since the R value of 2.4087 au was used by both sets of authors as an exact number subject only to the word-length errors of the computer and not to the full experimental uncertainty. To estimate the number of significant figures agreement for the individual MO q which this implies, some knowledge of the individual MO $\langle\hat{z}\rangle$ is necessary. Those calculated for the OCE-SCF wavefunction in Chapter II, Table VIII give this information, since they should be roughly the same as for the TCE-SCF calculations. This table indicates that the net $\langle\hat{z}\rangle_{elec}$ is principally due to four MO's (4σ, 5σ, and the 2π pair) each of which has $\langle\hat{z}\rangle$ of roughly .5 au; all are of the same sign. Then the absolute uncertainty in $\langle\hat{z}\rangle_{elec}$ is about four times the uncertainty in any one of these orbital $\langle z\rangle$; if the discrepancy between the McLean-Yoshimine and Cade-Huo $\langle\hat{z}\rangle_{elec}$ (.0002 au) is taken as the absolute uncertainty in $\langle\hat{z}\rangle_{elec}$, this implies an uncertainty of .00005 au in each of the dominant MO $\langle\hat{z}\rangle$, or four significant figures. If each MO q is then also assumed to agree with the corresponding quantity calculated by McLean and Yoshimine to four significant figures, an argument similar to that used above

to estimate the uncertainty in q_{elec} from the McLean-Yoshimine wavefunction gives an expected disagreement between the calculation of q_{elec} from the published Cade-Huo coefficients[4] and that calculated by McLean and Yoshimine[6] for the Cade-Huo wavefunction of 2 x.05 = .1 au. The discrepancy observed (.06 au) is within this range. Thus the q_{elec} values calculated by the author from the published MO coefficients of Cade and Huo agree with that calculated in the same basis by McLean and Yoshimine as well as can be expected; there is no strong reason to suspect either a q integral error or a misprint in the Cade-Huo MO coefficients. Given the rather large difference between q_{elec} in the Cade-Huo and McLean-Yoshimine bases (Table I), the H-F limit for this property can be placed no more accurately than 3.5 ± .1 au.

The MO q values from the 71-orbital Moccia basis (Chapter II) and the 29-orbital GW+9 basis (Chapter II, Table III) OCE-SCF calculations of HCl are also given in Table I for comparison with the TCE-SCF values. Also listed are estimated limits for the MO q values for continued addition of orbitals with higher ℓ values and r_{max}=2.4087 au. These estimates were made by inspection from Chapter III, Table VIII. Since the GW+9 basis includes an ℓ=8 orbital, and since this is the maximum allowed ℓ for n=9, further additions of n=9 orbitals cannot be made; however the radial functions for n=10, 11 etc. do not differ importantly from that for n=9 (cf. Chapter II, Table I), so the series formed by adding 10ℓ, 11m, etc. or-

bitals with r_{max}=2.4087 au should converge to roughly the limit indicated by the series ending with the GW+9 basis.

The table shows that the GW+9 wavefunction agrees approximately with all the MO q of the TCE-SCF wavefunctions except for the 1σ and 2σ MO's, whose q values are very small. The 3σ and 1π MO's show a slight disagreement; this is probably due to differences in the basis set choice for the second electron shell (Chapter III, Table IV). However the differences are balanced so that the sum of the q of the 3σ and 1π pair from the GW+9 wavefunction is about the same as the corresponding sum for the TCE-SCF wavefunctions. The Moccia basis gives large disagreements in the 3σ and 1π orbitals. The q of the 4σ MO of the GW+9 basis also disagrees slightly with the TCE-SCF wavefunctions; this could only be improved by increasing the flexibility of the OCE basis in the intermediate region between the proton and the Cl nucleus.

3. Convergence of OCE-SCF properties with basis enlargement

Chapter III, Table IV shows that the OCE-SCF q_{elec} has not completely converged upon addition of basis orbitals through 9k with r_{max}=2.4087 au; addition of the last basis orbital induced a change of .045 au or 1.3% of the total value. Table I of the present chapter shows that the value to which q_{elec} converges is within the rather broad uncertainty bounds upon the H-F limit. Since the basis orbitals added in this series were chosen to describe the electron density near the

proton, one expects that the density far from the Cl nucleus changes more with basis enlargement than the density near the Cl nucleus, and that therefore a property such as $\langle\hat{z}\rangle_{elec}$ which depends heavily on density far from the Cl nucleus would converge with basis enlargement more slowly than q, which is weighted near the Cl nucleus. This is not true, however, as is shown in Table II. The change in $\langle\hat{z}\rangle_{elec}$ upon addition of the last (9k) orbital is only .64% of the total value, or about half the change observed in q.

The reason for this unexpectedly slow convergence of q lies in the large cancellation of the individual MO q values in the summation for the total q_{elec}. The individual MO $\langle\hat{z}\rangle$ values are all (save one unimportant exception) of the same sign; $\langle\hat{z}\rangle_{elec}$ is then larger in magnitude than the largest MO contribution rather than smaller, as is the case for q. Thus convergence of the individual MO expectation values to a given number of significant figures yields convergence to a smaller number of figures in the case of q_{elec}, but the same number of figures in the case of $\langle\hat{z}\rangle_{elec}$. A property which has spatial weighting similar to that of q but no cancellation is $\langle\hat{r}^{-1}\rangle$, with r measured from the Cl nucleus; Table II shows that this converges quickly and to a value in excellent agreement with the near H-F values. The individual MO expectation values for these three properties are also given in Table II for the GW+9 basis. Note that little change in the electronic properties takes place until addition of the 9d orbital (GW+3 basis); this

TABLE II: Convergence of $\langle\hat{z}\rangle_{elec}$, $\langle\hat{q}\rangle_{elec}$, and $\langle\hat{r}^{-1}\rangle_{elec}$ with basis enlargement; also individual MO values for one basis. Atomic units.

	GW[a]	GW+1	GW+2
$\langle\hat{z}\rangle_{elec}$	1.13458	1.14532	1.14765
$\langle\hat{q}\rangle_{elec}$	1.76700	1.78493	1.75288
$\langle\hat{r}^{-1}\rangle_{elec}$	64.86707	64.86346	64.86428

	GW+3	GW+4	GW+5
$\langle\hat{z}\rangle_{elec}$	1.44161	1.64673	1.75489
$\langle\hat{q}\rangle_{elec}$	2.35045	2.88505	3.15916
$\langle\hat{r}^{-1}\rangle_{elec}$	64.84972	64.83614	64.82900

	GW+6	GW+7	GW+8
$\langle\hat{z}\rangle_{elec}$	1.81104	1.84274	1.86146
$\langle\hat{q}\rangle_{elec}$	3.31257	3.40343	3.45908
$\langle\hat{r}^{-1}\rangle_{elec}$	64.82500	64.82266	64.82124

	GW+9	limit[b]	McL-Yosh[5]	Cade-Huo[4]
$\langle\hat{z}\rangle_{elec}$	1.87296	1.91±.02	1.9307[c]	1.9381[d]
$\langle\hat{q}\rangle_{elec}$	3.49418	3.58±.05	3.4192[c]	3.53293[e]
$\langle\hat{r}^{-1}\rangle_{elec}$	64.82036	64.816±.005	64.8218[c]	64.8209[d]

continued

TABLE II: (cont'd.)

	Individual MO values, GW+9		
	$\langle\hat{z}\rangle$	$\langle\hat{q}\rangle$	$\langle\hat{r}^{-1}\rangle$
1σ	.00002	-.00005	33.11872
2σ	.00396	-.00463	6.61651
3σ	-.00299	-159.74818	6.39963
4σ	.78478	-.21670	1.66913
5σ	.91028	-7.04966	1.31872
1π	.00008	80.14581	6.40832
2π	.08838	5.11089	1.44049

[a]Basis series defined Chapter III, section 4.

[b]Estimated from preceding values.

[c]Property reported in reference 6.

[d]Property reported in reference 6 for wavefunction computed by McLean and Yoshimine[6] using Cade-Huo basis[4].

[e]Property calculated in this laboratory from coefficients of reference 4.

is apparently because with only s and p orbitals of r_{max}=2.4087 au sufficiently sharp angular peaking of the electron density cannot be achieved to produce significant energy lowering and allow large contributions of the n=9 basis orbitals to the MO's (cf. Chapter III, section 4).

Another quantity of interest is the value to which the total molecular energy of HCl converges as the basis is enlarged. Table III shows the sequence of total energy values and an estimate of the limit to which the sequence converges, -460.075±.005 au. This is to be compared with the McLean-Yoshimine result of -460.1119 au. Part of the difference between these two values, .037±.005 au, is due to the inadequacy of the GW basis for the Cl^- ion. The Bagus[24] near H-F value for the energy of Cl^- is -459.5768 au, while the calculation of Cl^- done in this laboratory with the GW basis (Chapter III) gave -459.5546 au. The difference between these two, .0222 au, leaves .015±.005 au in the HCl energy difference unaccounted for. This is not the error due to finite maximum ℓ value discussed in Chapter II, section 2b, since the above limit is as ℓ_{max} approaches infinity. Thus this difference of .015±.005 au represents the energy that could be gained by carefully choosing the exponents of the orbitals to be added to the GW set instead of always choosing r_{max}=2.4087 au as was done in this series.

TABLE III: Convergence of total energy of HCl with enlargement of OCE basis. Atomic units.

	GW[a]	GW+1	GW+2
E_{total}	-459.942154	-459.942574	-459.942847

	GW+3	GW+4	GW+5
E_{total}	-459.966638	-460.010621	-460.035942

	GW+6	GW+7	GW+8
E_{total}	-460.050933	-460.059942	-460.065467

	GW+9	limit[b]	McL-Yosh[6]	Cade-Huo[4]
E_{total}	-460.068938	-460.075±.005	-460.1119	-460.1103

[a]Basis series defined Chapter III, section 4.

[b]Estimated from preceding values.

4. Overlap of OCE-SCF MO's with TCE-SCF MO's

The overlap of a normalized approximate wavefunction ϕ with a known normalized exact wavefunction ψ,

$$\langle\phi|\psi\rangle = \int\phi^{*}\psi d\tau \qquad (6)$$

is often used as a measure of how well ϕ approximates ψ[25-28]. Closeness of $\langle\phi|\psi\rangle$ to unity implies closeness of ϕ to ψ. The overlap is directly related to the integral over all space of the squared difference of the two functions, since

$$\int|\phi-\psi|^{2}d\tau = \langle\phi|\phi\rangle - 2\langle\phi|\psi\rangle + \langle\psi|\psi\rangle = 2(1-\langle\phi|\psi\rangle),$$

with an overlap of unity implying identity of the wavefunctions over all space.

In order to determine how accurately the OCE-SCF MO's for HCl calculated in the enlarged GW bases approximate the near H-F MO's calculated by McLean and Yoshimine[5], the overlap integrals (6) were calculated between corresponding MO's for the series of 10 bases introduced in Chapter III, section 4, and are listed in Table IV, along with the overlaps between the OCE-SCF MO's in the 71-orbital Moccia basis and the McLean-Yoshimine MO's. Since the McLean-Yoshimine MO coefficients were published only to five decimal places, the fifth decimal place in the table is uncertain by about two units, as evidenced by the impossible values of 1.00001 which appear in

TABLE IV: Overlaps of OCE-SCF MO's of 10-basis series with corresponding MO's of McLean-Yoshimine wavefunction[5].

MO	GW[a]	GW+1	GW+2	GW+3
1σ	1.00000	1.00000	1.00000	1.00000
2σ	.99998	.99998	.99998	.99998
3σ	1.00000	1.00000	1.00000	1.00001
4σ	.99470	.99472	.99472	.99560
5σ	.97191	.97207	.97221	.98040
1π	.99999	.99999	.99999	.99999
2π	.99937	.99937	.99937	.99947

MO	GW+4	GW+5	GW+6	GW+7
1σ	1.00000	1.00000	1.00000	1.00000
2σ	.99998	.99998	.99998	.99998
3σ	1.00001	1.00001	1.00001	1.00001
4σ	.99766	.99850	.99888	.99906
5σ	.99153	.99566	.99734	.99805
1π	.99999	.99999	.99999	.99999
2π	.99953	.99953	.99952	.99952

continued

TABLE IV: (cont'd.)

MO	GW+8	GW+9	71-orbital[b]
1σ	1.00000	1.00000	1.00000
2σ	.99998	.99998	.99999
3σ	1.00001	1.00001	.99997
4σ	.99914	.99918	.99955
5σ	.99837	.99852	.99898
1π	.99999	.99999	.99996
2π	.99952	.99952	.99995

[a]Basis series defined Chapter III, section 4.

[b]Calculation in this laboratory, basis of reference 32.

the table. Two-center overlap integrals between STO's were needed to calculate the MO overlaps because of the orbitals on the proton in the McLean-Yoshimine basis; because of the high ℓ-values occurring in the Moccia and enlarged GW bases the usual tables of overlap formulas were not sufficient[17,29,30]; instead a general overlap routine able to handle STO's of arbitrary n, ℓ, and m values was written using Guseinov's[18] formula for the expansion of associated Legendre polynomials on different centers in elliptical coordinates.

Table IV shows that only the 4σ and 5σ MO's are significantly affected by the enlargement of the GW basis, as is expected since the added basis orbitals have radial maxima at the proton and contribute heavily only to the valence-shell MO's. The lower σ MO's and all π MO's in the GW series have overlaps with the corresponding McLean-Yoshimine MO close to unity for all bases in the series. The 71-orbital basis OCE-SCF MO's all have equal or higher overlaps with the McLean-Yoshimine MO's than do the GW+9 MO's except for the 3σ and 1π MO's; these MO's are poor for q in this wavefunction because of poor basis choice (Chapter III). The fact that the 3σ and 1π overlaps are so close to unity, while the q's differ greatly from the McLean-Yoshimine values, illustrates the insensitivity of overlap compared to q.

Convergence of the 4σ and 5σ MO's to the H-F MO's with basis enlargement is slow; from the table it is apparent that many additional orbitals would have to be added to bring the 5σ

overlap above .999 or the 4σ overlap above .9999. Overlaps with the Cade-Huo[4] MO's for HCl were also calculated, with essentially the same results.

REFERENCES

1. H.F. Schaefer III, The Electronic Structure of Atoms and Molecules, Addison-Wesley, Reading, Mass., 1972. p. 81.
2. J. Goodisman, J. Chem. Phys. 38, 304 (1963).
3. T.L. Gilbert and A.C. Wahl, J. Chem. Phys. 55, 5247 (1971).
4. P.E. Cade and W.M. Huo, J. Chem. Phys. 47, 649 (1967).
5. A.D. McLean and M. Yoshimine, Tables of Linear Molecule Wave Functions, Supplement to IBM Journal of Research and Development, 1967.
6. A.D. McLean and M. Yoshimine, J. Chem. Phys. 47, 3256 (1967).
7. W.G. Richards, T.E.H. Walker and R.K. Hinkley, A Bibliography of ab initio Molecular Wave Functions, Oxford, 1971. p. 25.
8. J.W. Richardson, Rev. Mod. Phys. 32, 461 (1960).
9. H.J. Kolker and M. Karplus, J. Chem. Phys. 36, 960 (1962).
10. M.J. Stephen and J.P. Auffray, J. Chem. Phys. 31, 1329 (1959).
11. S.L. Kahalas and R.K. Nesbet, J. Chem. Phys. 39, 529 (1963).
12. A.D. McLean and M. Yoshimine, J. Chem. Phys. 46, 1812 (1967).
13. I. Shavitt and M. Karplus, J. Chem. Phys. 36, 550 (1962).

14. I. Shavitt, Meth. Comp. Phys. 2, 1 (1963).

15. a. C.W. Kern and M. Karplus, J. Chem. Phys. 42, 1062 (1965).

b. O. Matsuoka, Int. J. Quant. Chem. 5, 1 (1971).

16. S.F. Boys, Proc. Roy. Soc. A200, 542 (1950).

17. R.S. Mulliken, C.A. Rieke, O. Orloff, and H. Orloff, J. Chem. Phys. 17, 1248 (1949).

18. I.I. Guseinov, J. Phys. B.: Atom. Molec. Phys. 3, 1399 (1970).

19. H. Eyring, J. Walter, and G.E. Kimball, Quantum Chemistry, Wiley, N.Y., 1944. p. 367.

20. Reference 19, p. 58.

21. K.Ruedenberg, C.C.J. Roothaan, and W. Jaunzemis, J. Chem. Phys. 24, 201 (1956).

22. P.E. Cade and W.M. Huo, J. Chem. Phys. 45, 1063 (1966).

23. C.F. Bender and E.R. Davidson, Phys. Rev. 183, 21 (1969).

24. P.S. Bagus, Phys. Rev. 139, A619 (1965).

25. C. Eckart, Phys. Rev. 36, 878 (1930).

26. F. Weinhold, J. Math. Phys. 11, 2127 (1970).

27. R.G. Gordon, J. Chem. Phys. 48, 4984 (1968).

28. H. Weinstein and R. Pauncz, Chem. Phys. Lett. 14, 161 (1972).

29. H.H. Jaffé, J. Chem. Phys. 21, 258 (1953).

30. A. Lofthus, Mol. Phys. 5, 105 (1962).

31. E.W. Kaiser, J. Chem. Phys. 53, 1686 (1970).

32. R. Moccia, Theoret. Chim. Acta 8, 8 (1967).

CHAPTER V: Radial analysis of the EFG

The preceding chapters have rested heavily on the assumption that q_{elec} is due principally to electron density close to the Cl nucleus. In the present chapter this assumption is tested by integrating over nested spherical shells the product of charge density and the $\hat{q}$ operator, which gives q_{elec} when integrated over all space. The method used involves separating the integral over all space into the product of a radial and an angular integral, performing the full angular integration, and then performing the radial integration over a number of finite intervals; hence the term radial analysis of the EFG.

An OCE-SCF wavefunction is expected to give the expectation value of a one-electron property close to the Hartree-Fock value only if the operator corresponding to that property is heavily weighted in regions of space close to the expansion center, where the OCE basis is sufficiently flexible to yield an electron density close to that of the H-F wavefunction. The operator for the EFG at the expansion center,

$$\hat{q} = (3\cos^2\theta-1)/r^3 = (4\sqrt{\pi}/\sqrt{5})S_{20}(\theta,\phi)/r^3, \qquad (1)$$

where all coordinates are in a spherical system on the expansion center and θ is measured from the principal field gradient axis (Chapter III), appears to fulfill this condition, since

$1/r^3$ is very large near the expansion center and very small far from it.

However if $\rho(\bar{r})$ is a spherically symmetric charge distribution due to an electronic wavefunction Φ, then[1]

$$\rho(\bar{r}) = f(r)\ S_{00}(\theta,\phi)$$

with f an arbitrary function of r only. Then the expectation value of $\hat{q}$ over Φ is

$$q_{elec} = -\int \rho(\bar{r})\hat{q}(r)d\tau = \int f(r) S_{00}(\theta,\phi)(4\sqrt{\pi}/\sqrt{5}) S_{20}(\theta,\phi)/r^3 d\tau$$

$$= 0, \qquad (2)$$

by the orthogonality of the spherical harmonics. Thus no matter how heavily f(r) is concentrated at low values of r, q_{elec} vanishes if the distribution is spherically symmetric.

Thus for HCl there are two opposite tendencies: the radial factor of $\hat{q}$ tends to make the property principally dependent on density close to the Cl nucleus, but the angular factor tends to make small the sum of the contributions of the 1σ, 2σ, 3σ, and 1π MO's (Chapter III, Table XI), which correspond closely to the spherically symmetric inner shells of the Cl^- ion, although it is to precisely these MO's that most of the electron density close to the Cl nucleus is due. In this chapter the balance between these two tendencies is examined

by integration over small ranges of r.

1. Qualitative considerations

The sign of $(3\cos^2\theta-1)/r^3$ is determined completely by the angular factor; it is positive for $0 < \theta < 54°44'$, negative for $54°44 < \theta < 125°16'$, and positive for $125°16' < \theta < 180°$. Because of the negative charge of the electron, the sign of the contribution to q_{elec} from the electron density at a point with a given θ is opposite to the above pattern; these regions of space are labelled with the sign of the contribution to q_{elec} in Figure 1. The four regions of the plane in Figure 1 are only two distinct regions in three-dimensional space because regions 1 and 3 form a single cone, and regions 2 and 4 the complement to this cone. Since the π MO's of HCl (essentially p_x and p_y atomic orbitals) are contained mostly in regions 2 and 4 of Figure 1, where the contribution to q_{elec} is positive, the q values of these MO's are expected to be rather large and positive, as confirmed by Chapter III, Table VIII. Similarly the 3σ and 5σ MO's of HCl correspond to p_z atomic orbitals which are contained mostly in regions 1 and 3 of Figure 1, where the contributions to q_{elec} are negative; these MO's are then expected to make rather large negative contributions to q_{elec}, which is again confirmed by Chapter III, Table VIII.

The 1σ and 2σ MO's have high density in all four regions, since they correspond closely to 1s and 2s AO's; however in the molecule s AO's are of the same symmetry (σ)

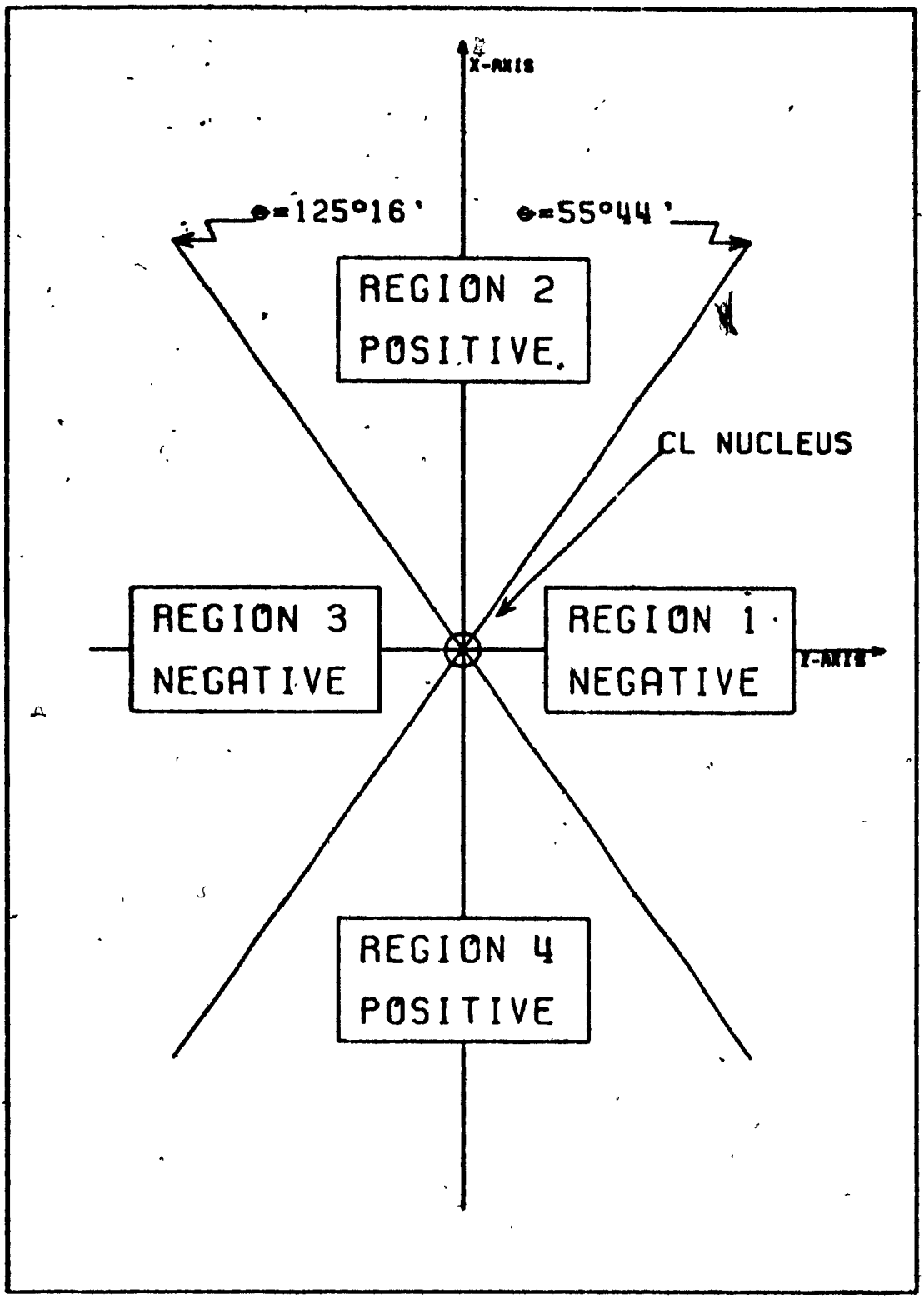

Figure 1. Regions of positive and negative contributions to q at the Cl nucleus from the electron density.

as the p_z AO's; the admixture of p_z AO's and other σ AO's of higher ℓ to the s AO's in the 1σ and 2σ MO's gives them a small negative q. The 4σ MO, which is similar to the 1σ and 2σ but with greater admixture of higher ℓ AO's, gives a negative contribution to q intermediate between those of 1σ or 2σ and the 3σ or 5σ MO's.

In analysing the changes in q_{elec} upon enlargement of the OCE basis one must examine how q_{elec} is affected by shifts in the electron density. Since the shapes of the MO's do not change greatly as the basis is enlarged, the important changes are the radial density shifts (cf. Chapter III, section 4). Shifting electron density from a region near the Cl nucleus to a region far from the nucleus decreases the value of $1/r^3$; thus for a given θ such a shift in electron density results in a decrease of the absolute value of the contribution to q_{elec}. In regions 1 and 3 of Figure 1 a decrease in the absolute value of the contribution is an increase in the numerical value; in regions 2 and 4 a decrease in the absolute value is also a decrease in the numerical value. Thus as σ AO's with r_{max} near the proton are added to the GW basis[2] (Chapter III, Table IV) for OCE-SCF calculations of HCl, electron density in the σ MO's, and particularly the valence MO's 4σ and 5σ, is shifted farther from the Cl nucleus; since these MO's make negative contributions to q_{elec}, the decrease in absolute value of these contributions results in a rise in the numerical value of q_{elec}. However, q_{elec} is

positive, since the negative contributions of the σ MO's are more than cancelled by the positive contributions of the π MO's; thus the absolute value of q_{elec} rises as the basis is enlarged in the manner of Chapter III, section 4. This result taken alone may seem paradoxical, since shifts in electron distribution in a direction which makes the contributions to the property decrease in absolute value result in an expectation value for the property of greater absolute value; however when q_{elec} is analysed as a sum of MO contributions there is no paradox. Chapter III, Table VIII illustrates these points.

2. Spatial and radial weighting

Weighting is defined here with reference to integration of a function over an interval. If f(r) is an arbitrary function of r, then

$$\int_a^b f(r)w(r)dr \qquad (3)$$

is the integral of f over r on the interval (a,b) with the weight function w[3,4]. It is usual in rigorous definitions of weighting to require that w be positive in the interval under consideration; it is also usual to consider only weight functions of a single variable[3,4]. Kern and Karplus[5] have introduced a broader concept of weighting. If $\rho(\bar{r})$ is the charge density from an electron distribution at point $\bar{r}$ and $\delta(\bar{r})$ a one-electron multiplicative operator evaluated at point $\bar{r}$, then the expec-

tation value

$$\langle\hat{o}\rangle = \int\rho(\bar{r})\hat{o}(\bar{r})d\tau \qquad (4)$$

may be considered the integral over all space of a weighted charge density $\rho(\bar{r})\hat{o}(\bar{r})$. The form (4) differs from (3) in that ρ and $\hat{o}$ are now functions of three spatial variables, and it may not be possible to decompose ρ or $\hat{o}$ into a product of three factors each dependent on a single variable. Also $\hat{o}(\bar{r})$ may be negative in some regions of space, as is the case if $\hat{o}$ is taken to be $\hat{q}$.

The weighted charge density arising from an operator and a given electron distribution is useful in weighted density maps, which give a visual indication of what regions of space are important in determining the expectation value (4) of the operator[5]. Chen and coworkers[6,7,8] have developed techniques for judging the suitability of approximate wavefunctions using the spatial weighting of operators corresponding to one-electron properties.

A concept related to spatial weighting is that of radial weighting. Expanding $\rho(\bar{r})\hat{o}(\bar{r})$ as a sum over contributions from real MO's ψ_k,

$$\rho(\bar{r})\hat{o}(\bar{r}) = -\sum_k N_k(\psi_k(\bar{r}))^2\hat{o}(\bar{r}),$$

with N_k the occupation number of ψ_k. The negative sign enters

because of the charge of the electron. Expanding the MO's as linear combinations of real AO's ϕ_i,

$$\rho(\bar{r})\delta(\bar{r}) = -\sum_k N_k \sum_i \sum_j C_{ik}C_{jk}\phi_i(\bar{r})\phi_j(\bar{r})\delta(\bar{r}), \tag{5}$$

where i and j range over the basis orbitals. Taking each AO to be the product of a radial and an angular factor,

$$\phi_i = f_i(r)\ S_{\ell_i m_i}(\theta,\phi),$$

(5) becomes

$$\rho(\bar{r})\delta(\bar{r}) = -\sum_k N_k \sum_i \sum_j C_{ik}C_{jk}f_i(r)f_j(r)\cdot$$

$$\cdot S_{\ell_i m_i}(\theta,\phi)S_{\ell_j m_j}(\theta,\phi)\delta(\bar{r}) \tag{6}$$

Finally, it is assumed that $\delta(\bar{r})$ is the product of a radial and an angular factor,

$$\delta(\bar{r}) = R_o(r)A_o(\theta,\phi), \tag{7}$$

as is the case for most one-electron properties of interest. Then (6) becomes

$$\rho(\bar{r})\delta(\bar{r}) = -\sum_k N_k \sum_i \sum_j C_{ik}C_{jk}f_i(r)f_j(r)R_o(r)\cdot$$

$$\cdot S_{\ell_i m_i}(\theta,\phi)S_{\ell_j m_j}(\theta,\phi)A_o(\theta,\phi) \quad . \tag{8}$$

Integrating (8) over all space as in (4), and using $d\tau = r^2 \sin\theta dr d\theta d\phi$,

$$\langle\delta\rangle = -\sum_k N_k \sum_i \sum_j C_{ik} C_{jk} \int_0^\infty f_i(r) f_j(r) R_o(r) r^2 dr \cdot$$

$$\cdot \int_0^\pi \int_0^{2\pi} S_{\ell_i m_i}(\theta,\phi) S_{\ell_j m_j}(\theta,\phi) A_o(\theta,\phi) \sin\theta d\theta d\phi. \qquad (9)$$

Inspection of the radial integrals in (9),

$$\int_0^\infty f_i(r) f_j(r) R_o(r) r^2 dr,$$

shows that by (3) this is the integral of the product $f_i(r) f_j(r)$ over r with weight function $R_o(r) r^2$, if $R_o(r)$ is positive for all values of r. Note that even if δ is the identity operator (in which case $\langle\delta\rangle$ is the overlap) the radial integrals in (9) still have the weight factor r^2, arising from the volume element. By (9), if $R_o(r)$ is positive, the expectation value of a one-electron operator is a sum of weighted radial integrals in the rigorous sense of (3).

Ehrenson and coworkers[9,10] have discussed use of radial weight factors in determining least-squares fitting of GTO's to STO's in order to improve the property corresponding to the weight factor calculated in a basis of GTO's contracted to approximate STO's.

3. Radial analysis of the EFG

For the EFG operator $\hat{q}$ of (1), the radial and angular factors of (7) are

$$R_q(r) = 1/r^3$$
$$A_q(r) = (4\sqrt{\pi}/\sqrt{5})S_{20}(\theta,\phi). \tag{10}$$

In this case (9) becomes

$$q_{elec} = -\sum_k N_k \sum_i \sum_j C_{ik}C_{jk}\left(\int_0^\infty f_i(r)f_j(r)r^{-1}dr\right)(4\sqrt{\pi}/\sqrt{5})\cdot$$
$$\cdot\int_0^\pi\int_0^{2\pi} S_{\ell_i m_i}(\theta,\phi)S_{\ell_j m_j}(\theta,\phi)S_{20}(\theta,\phi)\sin\theta d\theta d\phi. \tag{11}$$

Evaluation of the radial and angular integrals in (11) was discussed in Chapter III, section 1. However (11) can be rewritten in the form

$$q_{elec} = -\int_0^\infty dr\Big[\sum_k N_k \sum_i \sum_j C_{ik}C_{jk}f_i(r)f_j(r)r^{-1}(4\sqrt{\pi}/\sqrt{5})\cdot$$
$$\cdot\int_0^\pi\int_0^{2\pi} S_{\ell_i m_i}(\theta,\phi)S_{\ell_j m_j}(\theta,\phi)S_{20}(\theta,\phi)\sin\theta d\theta d\phi\Big]$$
$$\equiv -\int_0^\infty dr C_\Delta(r), \tag{12}$$

with $C_\Delta(r)$ introduced as a notational convenience. Then an interval size h may be chosen for r and (12) written as an

infinite sum of integrals over an interval in r of length h:

$$q_{elec} = -\sum_{n=1}^{\infty} \int_{(n-1)h}^{nh} C_{\Delta}(r)dr. \tag{13}$$

Thus q_{elec} can be expressed as a convergent series the nth term of which is associated with a spherical shell $(n-1)h<r<nh$. Explicitly the nth term of (13) is

$$-\int_{(n-1)h}^{nh} C_{\Delta}(r)dr = -\sum_k N_k \sum_i \sum_j C_{ik}C_{jk}\left(\int_{(n-1)h}^{nh} f_i(r)f_j(r)r^{-1}dr\right)\cdot$$

$$\cdot(4\sqrt{\pi}/\sqrt{5})\int_0^{\pi}\int_0^{2\pi} S_{\ell_i m_i}(\theta,\phi)S_{\ell_j m_j}(\theta,\phi)\cdot$$

$$\cdot S_{20}(\theta,\phi)\sin\theta d\theta d\phi. \tag{14}$$

The angular integral in (14) is that of Appendix I, equation (7). However because of the non-zero lower limit, the radial integral is not that of Appendix I, equation (8). Since for STO's (Chapter I),

$$f_i(r) = r^{n_i-1}\exp(-\zeta_i r),$$

the integral to be evaluated has the form

$$\int_a^b r^m \exp(-tr), \tag{15}$$

with $m = n_i + n_j - 3$ and $t = \zeta_i + \zeta_j$. The only case for which m is

negative, $n_i = n_j = 1$, need not be considered because the angular integral vanishes (Chapter III, section 1). Then (15) can be rewritten

$$\int_a^b r^m \exp(-tr)dr = \int_a^\infty r^m \exp(-tr)dr - \int_b^\infty r^m \exp(-tr)dr \qquad (16)$$

or

$$\int_a^b r^m \exp(-tr)dr = \int_0^b r^m \exp(-tr)dr - \int_0^a r^m \exp(-tr). \qquad (17)$$

Since subtraction is involved in (16) and (17), for a and b sufficiently close, and for certain values of m and t, these formulas are subject to large numerical errors. The graph of $r^m \exp(-tr)$ is qualitatively (for $m > 0$) a curve which is 0 at $r = 0$, rises to a maximum at $r = m/t$, and then falls back toward zero as r increases (Figure 2). Consider the pair of points A, B to the left of the maximum in the figure. If the integral (15) between these points is evaluated by (16), both integrals on the right-hand side include the large area under the maximum, and their difference may be very small, giving numerical error in the subtraction. Evaluation of the same integral by (17) has a less serious numerical error, since the difference between the integrals is the same as in (16) but both integrals are much smaller. Similarly, the integral (15) between the points E and F in Figure 2 is more accurately evaluated by (16). For a pair of points such as C, D which straddle the maximum either (16) or (17) is appropriate; (16)

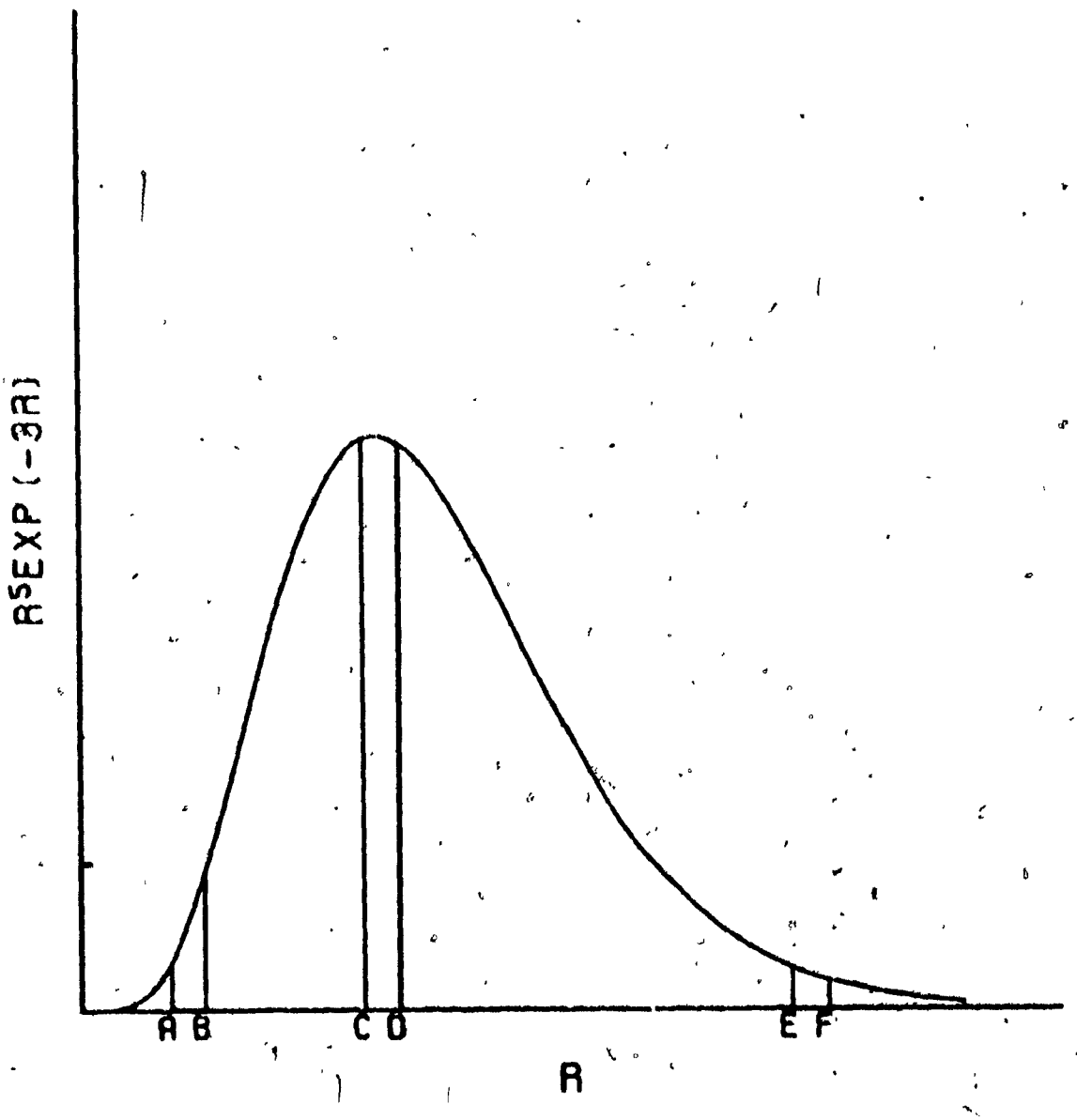

Figure 2. Graph of typical $r^m \exp(-tr)$ to illustrate numerical problems in integrations over intervals in r.

was used in this work because it is computationally quicker. While this is not a rigorous analysis of numerical error in the evaluation of (15), it gives a prescription which can be tested for accuracy; the above method proved accurate to at least eight significant figures for a range of m, t, and (b-a) values such as occurred in evaluation of (13). The integrals on the right-hand sides of (16) and (17) can be reduced to integrals of the type of Appendix I, equations (9) and (10). For m = 0, (15) can be integrated directly. For a = 0, (15) can be reduced directly to the form of Appendix I, equation (10).

Thus all integrals in (13) for an OCE basis can be evaluated relatively simply. For a two-center basis the basis orbitals on the non-EFG center nucleus would have to be expanded about the EFG center by, for example, the Barnett-Coulson method[11,12], which is complicated and time-consuming, or the radial integration in (4) could be done numerically over a number of sub-intervals, but this would be time-consuming and of questionable accuracy. Thus quick and simple radial analysis of one-electron properties by (13) seems limited to OCE-SCF wavefunctions. To our knowledge this method of analysis has not previously been applied.

4. Results of radial analysis of EFG for OCE-SCF wavefunctions

A convenient stepsize h of (13) for analysis of the EFG in HCl was found to be .1 au, since this breaks the inter-

nuclear distance (2.4087 au) into a rather large number of intervals. In the cases tested this stepsize caused no numerical difficulties. For presentation of this analysis, the following quantities are defined:

$$C_n = -\int_{.1\times(n-1)}^{.1\times n} C_\Delta(r)dr$$

$$q_n = \sum_{i=1}^{n} C_i, \tag{18}$$

with $C_\Delta(r)$ as in (12). Table I presents the C_n and q_n values for the series of ten GW+N basis OCE-SCF calculations of HCl (Chapter III, section 4) for n = I to 50. Note that for all bases q_{50} differs by no more than .00002 au from the limit as $n \to \infty$ (Chapter III, Table VIII); this confirms the accuracy of the method of evaluation of (15) outlined above, and shows that essentially all of q_{elec} is due to electron density within 5 au of the Cl nucleus.

There are several general features of Table I to be noted:

(a) The largest C_n is for n = 1, the interval closest to the Cl nucleus.

(b) The greatest changes upon basis enlargement take place for low n.

(c) In all bases q_n has converged to within .02 au of its limiting value with r smaller than the internuclear distance (2.4087 au).

TABLE I: Integrals over intervals in r of charge density weighted by q. Quantities defined in (18).

GW				GW+1			
n	r (au)	C_n (au)	q_n (au)	n	r (au)	C_n (au)	q_n (au)
1	0.0-0.1	0.33851	0.45851	1	0.0-0.1	0.86642	0.86642
2	0.1-0.2	0.63793	1.49644	2	0.1-0.2	0.64429	1.51070
3	0.2-0.3	0.22232	1.71876	3	0.2-0.3	0.22489	1.73560
4	0.3-0.4	0.05749	1.77626	4	0.3-0.4	0.05830	1.79390
5	0.4-0.5	0.00880	1.78506	5	0.4-0.5	0.00891	1.80281
6	0.5-0.6	-0.00116	1.78390	6	0.5-0.6	-0.00129	1.80151
7	0.6-0.7	-0.00100	1.78290	7	0.6-0.7	-0.00118	1.80033
8	0.7-0.8	0.00044	1.78334	8	0.7-0.8	0.00030	1.80063
9	0.8-0.9	0.00112	1.78446	9	0.8-0.9	0.00105	1.80168
10	0.9-1.0	0.00099	1.78545	10	0.9-1.0	0.00099	1.80266
11	1.0-1.1	0.00043	1.78587	11	1.0-1.1	0.00048	1.80314
12	1.1-1.2	-0.00025	1.78563	12	1.1-1.2	-0.00016	1.80298
13	1.2-1.3	-0.00085	1.78478	13	1.2-1.3	-0.00074	1.80224
14	1.3-1.4	-0.00129	1.78348	14	1.3-1.4	-0.00118	1.80106
15	1.4-1.5	-0.00157	1.78192	15	1.4-1.5	-0.00146	1.79960
16	1.5-1.6	-0.00169	1.78023	16	1.5-1.6	-0.00160	1.79801
17	1.6-1.7	-0.00169	1.77854	17	1.6-1.7	-0.00162	1.79639
18	1.7-1.8	-0.00162	1.77691	18	1.7-1.8	-0.00156	1.79483
19	1.8-1.9	-0.00149	1.77542	19	1.8-1.9	-0.00145	1.79337
20	1.9-2.0	-0.00134	1.77408	20	1.9-2.0	-0.00132	1.79206
21	2.0-2.1	-0.00119	1.77290	21	2.0-2.1	-0.00116	1.79089
22	2.1-2.2	-0.00102	1.77188	22	2.1-2.2	-0.00101	1.78988
23	2.2-2.3	-0.00087	1.77101	23	2.2-2.3	-0.00087	1.78901
24	2.3-2.4	-0.00073	1.77028	24	2.3-2.4	-0.00074	1.78827
25	2.4-2.5	-0.00061	1.76967	25	2.4-2.5	-0.00062	1.78765
26	2.5-2.6	-0.00051	1.76916	26	2.5-2.6	-0.00051	1.78714
27	2.6-2.7	-0.00042	1.76873	27	2.6-2.7	-0.00042	1.78671
28	2.7-2.8	-0.00034	1.76840	28	2.7-2.8	-0.00035	1.78636
29	2.8-2.9	-0.00028	1.76813	29	2.8-2.9	-0.00028	1.78608
30	2.9-3.0	-0.00023	1.76790	30	2.9-3.0	-0.00023	1.78585
31	3.0-3.1	-0.00019	1.76772	31	3.0-3.1	-0.00019	1.78566
32	3.1-3.2	-0.00015	1.76757	32	3.1-3.2	-0.00015	1.78551
33	3.2-3.3	-0.00012	1.76746	33	3.2-3.3	-0.00012	1.78539
34	3.3-3.4	-0.00009	1.76736	34	3.3-3.4	-0.00010	1.78529
35	3.4-3.5	-0.00007	1.76729	35	3.4-3.5	-0.00008	1.78522
36	3.5-3.6	-0.00006	1.76723	36	3.5-3.6	-0.00006	1.78516
37	3.6-3.7	-0.00005	1.76718	37	3.6-3.7	-0.00005	1.78511
38	3.7-3.8	-0.00004	1.76714	38	3.7-3.8	-0.00004	1.78507
39	3.8-3.9	-0.00003	1.76711	39	3.8-3.9	-0.00003	1.78504
40	3.9-4.0	-0.00002	1.76709	40	3.9-4.0	-0.00002	1.78501
41	4.0-4.1	-0.00002	1.76707	41	4.0-4.1	-0.00002	1.78500
42	4.1-4.2	-0.00001	1.76706	42	4.1-4.2	-0.00001	1.78498
43	4.2-4.3	-0.00001	1.76705	43	4.2-4.3	-0.00001	1.78497
44	4.3-4.4	-0.00001	1.76704	44	4.3-4.4	-0.00001	1.78496
45	4.4-4.5	-0.00001	1.76703	45	4.4-4.5	-0.00001	1.78495
46	4.5-4.6	-0.00001	1.76702	46	4.5-4.6	-0.00001	1.78495
47	4.6-4.7	-0.00000	1.76702	47	4.6-4.7	-0.00000	1.78494
48	4.7-4.8	-0.00000	1.76701	48	4.7-4.8	-0.00000	1.78494
49	4.8-4.9	-0.00000	1.76701	49	4.8-4.9	-0.00000	1.78494
50	4.9-5.0	-0.00000	1.76701	50	4.9-5.0	-0.00000	1.78493

#2 - TABLE I

GW+2

n	r(au)	C_n(au)	q_n(au)
1	0.0-0.1	0.85842	0.85842
2	0.1-0.2	0.62950	1.48791
3	0.2-0.3	0.21802	1.70594
4	0.3-0.4	0.05694	1.76288
5	0.4-0.5	0.00901	1.77189
6	0.5-0.6	-0.00143	1.77046
7	0.6-0.7	-0.00176	1.76870
8	0.7-0.8	-0.00045	1.76825
9	0.8-0.9	0.00040	1.76865
10	0.9-1.0	0.00058	1.76923
11	1.0-1.1	0.00033	1.76956
12	1.1-1.2	-0.00010	1.76946
13	1.2-1.3	-0.00053	1.76893
14	1.3-1.4	-0.00089	1.76804
15	1.4-1.5	-0.00116	1.76688
16	1.5-1.6	-0.00131	1.76557
17	1.6-1.7	-0.00138	1.76419
18	1.7-1.8	-0.00138	1.76281
19	1.8-1.9	-0.00132	1.76149
20	1.9-2.0	-0.00123	1.76025
21	2.0-2.1	-0.00112	1.75913
22	2.1-2.2	-0.00100	1.75813
23	2.2-2.3	-0.00088	1.75725
24	2.3-2.4	-0.00076	1.75648
25	2.4-2.5	-0.00065	1.75583
26	2.5-2.6	-0.00055	1.75528
27	2.6-2.7	-0.00046	1.75482
28	2.7-2.8	-0.00038	1.75444
29	2.8-2.9	-0.00032	1.75412
30	2.9-3.0	-0.00026	1.75386
31	3.0-3.1	-0.00021	1.75366
32	3.1-3.2	-0.00017	1.75349
33	3.2-3.3	-0.00013	1.75335
34	3.3-3.4	-0.00011	1.75325
35	3.4-3.5	-0.00008	1.75316
36	3.5-3.6	-0.00007	1.75310
37	3.6-3.7	-0.00005	1.75305
38	3.7-3.8	-0.00004	1.75301
39	3.8-3.9	-0.00003	1.75298
40	3.9-4.0	-0.00002	1.75295
41	4.0-4.1	-0.00002	1.75293
42	4.1-4.2	-0.00001	1.75292
43	4.2-4.3	-0.00001	1.75291
44	4.3-4.4	-0.00001	1.75290
45	4.4-4.5	-0.00001	1.75290
46	4.5-4.6	-0.00000	1.75289
47	4.6-4.7	-0.00000	1.75289
48	4.7-4.8	-0.00000	1.75289
49	4.8-4.9	-0.00000	1.75288
50	4.9-5.0	-0.00000	1.75288

GW+3

n	r(au)	C_n(au)	q_n(au)
1	0.0-0.1	1.14027	1.14027
2	0.1-0.2	0.83128	1.97154
3	0.2-0.3	0.28194	2.25349
4	0.3-0.4	0.06959	2.32308
5	0.4-0.5	0.00932	2.33239
6	0.5-0.6	-0.00122	2.33116
7	0.6-0.7	0.00079	2.33195
8	0.7-0.8	0.00399	2.33594
9	0.8-0.9	0.00576	2.34170
10	0.9-1.0	0.00606	2.34776
11	1.0-1.1	0.00543	2.35319
12	1.1-1.2	0.00434	2.35753
13	1.2-1.3	0.00314	2.36067
14	1.3-1.4	0.00202	2.36269
15	1.4-1.5	0.00106	2.36376
16	1.5-1.6	0.00030	2.36405
17	1.6-1.7	-0.00028	2.36377
18	1.7-1.8	-0.00069	2.36308
19	1.8-1.9	-0.00096	2.36212
20	1.9-2.0	-0.00111	2.36101
21	2.0-2.1	-0.00118	2.35984
22	2.1-2.2	-0.00118	2.35866
23	2.2-2.3	-0.00113	2.35753
24	2.3-2.4	-0.00105	2.35648
25	2.4-2.5	-0.00096	2.35552
26	2.5-2.6	-0.00085	2.35467
27	2.6-2.7	-0.00074	2.35393
28	2.7-2.8	-0.00064	2.35329
29	2.8-2.9	-0.00054	2.35274
30	2.9-3.0	-0.00046	2.35229
31	3.0-3.1	-0.00033	2.35191
32	3.1-3.2	-0.00031	2.35160
33	3.2-3.3	-0.00025	2.35135
34	3.3-3.4	-0.00020	2.35115
35	3.4-3.5	-0.00016	2.35099
36	3.5-3.6	-0.00013	2.35086
37	3.6-3.7	-0.00010	2.35077
38	3.7-3.8	-0.00009	2.35069
39	3.8-3.9	-0.00006	2.35063
40	3.9-4.0	-0.00005	2.35059
41	4.0-4.1	-0.00003	2.35055
42	4.1-4.2	-0.00003	2.35052
43	4.2-4.3	-0.00002	2.35051
44	4.3-4.4	-0.00001	2.35049
45	4.4-4.5	-0.00001	2.35048
46	4.5-4.6	-0.00001	2.35047
47	4.6-4.7	-0.00001	2.35047
48	4.7-4.8	-0.00000	2.35046
49	4.8-4.9	-0.00000	2.35046
50	4.9-5.0	-0.00000	2.35046

#3 - TABLE I

GW+4

n	r (au)	C_n (au)	q_n (au)
1	0.0-0.1	1.40390	1.40390
2	0.1-0.2	1.02380	2.42770
3	0.2-0.3	0.34515	2.77285
4	0.3-0.4	0.08324	2.85609
5	0.4-0.5	0.01024	2.86633
6	0.5-0.6	-0.00119	2.86514
7	0.6-0.7	0.00251	2.86766
8	0.7-0.8	0.00716	2.87481
9	0.8-0.9	0.00955	2.88436
10	0.9-1.0	0.00976	2.89413
11	1.0-1.1	0.00858	2.90271
12	1.1-1.2	0.00673	2.90944
13	1.2-1.3	0.00470	2.91414
14	1.3-1.4	0.00278	2.91692
15	1.4-1.5	0.00112	2.91803
16	1.5-1.6	-0.00022	2.91782
17	1.6-1.7	-0.00124	2.91658
18	1.7-1.8	-0.00196	2.91462
19	1.8-1.9	-0.00243	2.91220
20	1.9-2.0	-0.00268	2.90952
21	2.0-2.1	-0.00277	2.90675
22	2.1-2.2	-0.00273	2.90401
23	2.2-2.3	-0.00261	2.90141
24	2.3-2.4	-0.00242	2.89899
25	2.4-2.5	-0.00220	2.89679
26	2.5-2.6	-0.00196	2.89483
27	2.6-2.7	-0.00171	2.89312
28	2.7-2.8	-0.00148	2.89165
29	2.8-2.9	-0.00125	2.89039
30	2.9-3.0	-0.00105	2.88934
31	3.0-3.1	-0.00087	2.88847
32	3.1-3.2	-0.00072	2.88775
33	3.2-3.3	-0.00059	2.88717
34	3.3-3.4	-0.00047	2.88670
35	3.4-3.5	-0.00037	2.88632
36	3.5-3.6	-0.00030	2.88603
37	3.6-3.7	-0.00023	2.88580
38	3.7-3.8	-0.00018	2.88562
39	3.8-3.9	-0.00014	2.88548
40	3.9-4.0	-0.00011	2.88537
41	4.0-4.1	-0.00008	2.88529
42	4.1-4.2	-0.00006	2.88523
43	4.2-4.3	-0.00005	2.88519
44	4.3-4.4	-0.00003	2.88515
45	4.4-4.5	-0.00003	2.88512
46	4.5-4.6	-0.00002	2.88510
47	4.6-4.7	-0.00001	2.88509
48	4.7-4.8	-0.00001	2.88508
49	4.8-4.9	-0.00001	2.88507
50	4.9-5.0	-0.00001	2.88506

GW+5

n	r (au)	C_n (au)	q_n (au)
1	0.0-0.1	1.53640	1.53640
2	0.1-0.2	1.12004	2.65644
3	0.2-0.3	0.37678	3.03322
4	0.3-0.4	0.09021	3.12343
5	0.4-0.5	0.01078	3.13422
6	0.5-0.6	-0.00121	3.13301
7	0.6-0.7	0.00324	3.13625
8	0.7-0.8	0.00858	3.14483
9	0.8-0.9	0.01131	3.15614
10	0.9-1.0	0.01156	3.16770
11	1.0-1.1	0.01022	3.17792
12	1.1-1.2	0.00810	3.18601
13	1.2-1.3	0.00576	3.19177
14	1.3-1.4	0.00354	3.19531
15	1.4-1.5	0.00160	3.19691
16	1.5-1.6	0.00002	3.19693
17	1.6-1.7	-0.00119	3.19574
18	1.7-1.8	-0.00207	3.19367
19	1.8-1.9	-0.00266	3.19100
20	1.9-2.0	-0.00301	3.18800
21	2.0-2.1	-0.00315	3.18484
22	2.1-2.2	-0.00315	3.18170
23	2.2-2.3	-0.00303	3.17867
24	2.3-2.4	-0.00284	3.17583
25	2.4-2.5	-0.00259	3.17324
26	2.5-2.6	-0.00232	3.17092
27	2.6-2.7	-0.00204	3.16888
28	2.7-2.8	-0.00177	3.16711
29	2.8-2.9	-0.00151	3.16561
30	2.9-3.0	-0.00127	3.16434
31	3.0-3.1	-0.00105	3.16328
32	3.1-3.2	-0.00087	3.16242
33	3.2-3.3	-0.00070	3.16171
34	3.3-3.4	-0.00057	3.16115
35	3.4-3.5	-0.00045	3.16069
36	3.5-3.6	-0.00036	3.16034
37	3.6-3.7	-0.00028	3.16006
38	3.7-3.8	-0.00022	3.15984
39	3.8-3.9	-0.00017	3.15967
40	3.9-4.0	-0.00013	3.15954
41	4.0-4.1	-0.00010	3.15945
42	4.1-4.2	-0.00007	3.15937
43	4.2-4.3	-0.00006	3.15932
44	4.3-4.4	-0.00004	3.15928
45	4.4-4.5	-0.00003	3.15924
46	4.5-4.6	-0.00002	3.15922
47	4.6-4.7	-0.00002	3.15921
48	4.7-4.8	-0.00001	3.15919
49	4.8-4.9	-0.00001	3.15918
50	4.9-5.0	-0.00001	3.15918

GW+6

n	r(au)	C_n(au)	q_n(au)
1	0.0-0.1	1.61029	1.61029
2	0.1-0.2	1.17351	2.73390
3	0.2-0.3	0.39433	3.12826
4	0.3-0.4	0.09409	3.22235
5	0.4-0.5	0.01109	3.23344
6	0.5-0.6	-0.00123	3.23221
7	0.6-0.7	0.00368	3.23589
8	0.7-0.8	0.00336	3.23921
9	0.8-0.9	0.01229	3.25149
10	0.9-1.0	0.01256	3.26405
11	1.0-1.1	0.01114	3.27519
12	1.1-1.2	0.00889	3.28408
13	1.2-1.3	0.00639	3.29047
14	1.3-1.4	0.00401	3.29448
15	1.4-1.5	0.00231	3.29681
16	1.5-1.6	0.00023	3.29704
17	1.6-1.7	-0.00119	3.29585
18	1.7-1.8	-0.00207	3.29378
19	1.8-1.9	-0.00273	3.29105
20	1.9-2.0	-0.00313	3.28792
21	2.0-2.1	-0.00332	3.28460
22	2.1-2.2	-0.00333	3.28127
23	2.2-2.3	-0.00323	3.27804
24	2.3-2.4	-0.00304	3.27500
25	2.4-2.5	-0.00279	3.27221
26	2.5-2.6	-0.00251	3.26970
27	2.6-2.7	-0.00221	3.26749
28	2.7-2.8	-0.00192	3.26557
29	2.8-2.9	-0.00164	3.26393
30	2.9-3.0	-0.00139	3.26254
31	3.0-3.1	-0.00115	3.26139
32	3.1-3.2	-0.00095	3.26044
33	3.2-3.3	-0.00077	3.25967
34	3.3-3.4	-0.00062	3.25905
35	3.4-3.5	-0.00050	3.25855
36	3.5-3.6	-0.00039	3.25816
37	3.6-3.7	-0.00031	3.25785
38	3.7-3.8	-0.00024	3.25761
39	3.8-3.9	-0.00019	3.25742
40	3.9-4.0	-0.00014	3.25728
41	4.0-4.1	-0.00011	3.25717
42	4.1-4.2	-0.00008	3.25709
43	4.2-4.3	-0.00006	3.25703
44	4.3-4.4	-0.00005	3.25698
45	4.4-4.5	-0.00003	3.25695
46	4.5-4.6	-0.00002	3.25693
47	4.6-4.7	-0.00002	3.25691
48	4.7-4.8	-0.00001	3.25690
49	4.8-4.9	-0.00001	3.25689
50	4.9-5.0	-0.00001	3.25688

GW+7

n	r(au)	C_n(au)	q_n(au)
1	0.0-0.1	1.65399	1.65399
2	0.1-0.2	1.20526	2.85926
3	0.2-0.3	0.43474	3.29399
4	0.3-0.4	0.09639	3.38038
5	0.4-0.5	0.00127	3.37165
6	0.5-0.6	-0.00124	3.37041
7	0.6-0.7	0.00387	3.37428
8	0.7-0.8	0.00981	3.38409
9	0.8-0.9	0.01295	3.39694
10	0.9-1.0	0.01315	3.41009
11	1.0-1.1	0.01168	3.42177
12	1.1-1.2	0.00935	3.43112
13	1.2-1.3	0.00675	3.43788
14	1.3-1.4	0.00430	3.44218
15	1.4-1.5	0.00213	3.44431
16	1.5-1.6	0.00035	3.44466
17	1.6-1.7	-0.00104	3.44362
18	1.7-1.8	-0.00206	3.44156
19	1.8-1.9	-0.00276	3.43880
20	1.9-2.0	-0.00319	3.43561
21	2.0-2.1	-0.00340	3.43221
22	2.1-2.2	-0.00343	3.42878
23	2.2-2.3	-0.00331	3.42545
24	2.3-2.4	-0.00314	3.42231
25	2.4-2.5	-0.00289	3.41941
26	2.5-2.6	-0.00260	3.41681
27	2.6-2.7	-0.00230	3.41451
28	2.7-2.8	-0.00200	3.41251
29	2.8-2.9	-0.00171	3.41080
30	2.9-3.0	-0.00145	3.40935
31	3.0-3.1	-0.00120	3.40815
32	3.1-3.2	-0.00099	3.40715
33	3.2-3.3	-0.00081	3.40635
34	3.3-3.4	-0.00065	3.40570
35	3.4-3.5	-0.00052	3.40518
36	3.5-3.6	-0.00041	3.40477
37	3.6-3.7	-0.00032	3.40445
38	3.7-3.8	-0.00025	3.40420
39	3.8-3.9	-0.00019	3.40401
40	3.9-4.0	-0.00015	3.40386
41	4.0-4.1	-0.00011	3.40375
42	4.1-4.2	-0.00008	3.40366
43	4.2-4.3	-0.00006	3.40360
44	4.3-4.4	-0.00005	3.40355
45	4.4-4.5	-0.00003	3.40352
46	4.5-4.6	-0.00003	3.40349
47	4.6-4.7	-0.00002	3.40347
48	4.7-4.8	-0.00001	3.40346
49	4.8-4.9	-0.00001	3.40345
50	4.9-5.0	-0.00001	3.40344

#5 - TABLE I

GW+8				GW+9			
n	r (au)	C_n (au)	q_n (au)	n	r (au)	C_n (au)	q_n (au)
1	0.0-0.1	1.68074	1.68074	1	0.0-0.1	1.69761	1.69761
2	0.1-0.2	1.22463	2.90538	2	0.1-0.2	1.23684	2.93446
3	0.2-0.3	0.41109	3.31647	3	0.2-0.3	0.41510	3.34955
4	0.3-0.4	0.09779	3.41426	4	0.3-0.4	0.09868	3.44823
5	0.4-0.5	0.01138	3.42564	5	0.4-0.5	0.01145	3.45968
6	0.5-0.6	-0.00124	3.42440	6	0.5-0.6	-0.00125	3.45843
7	0.6-0.7	0.00401	3.42841	7	0.6-0.7	0.00409	3.46253
8	0.7-0.8	0.01008	3.43849	8	0.7-0.8	0.01026	3.47278
9	0.8-0.9	0.01319	3.45169	9	0.8-0.9	0.01341	3.48619
10	0.9-1.0	0.01350	3.46519	10	0.9-1.0	0.01373	3.49992
11	1.0-1.1	0.01201	3.47720	11	1.0-1.1	0.01222	3.51214
12	1.1-1.2	0.00963	3.48683	12	1.1-1.2	0.00981	3.52194
13	1.2-1.3	0.00699	3.49382	13	1.2-1.3	0.00713	3.52908
14	1.3-1.4	0.00447	3.49829	14	1.3-1.4	0.00459	3.53365
15	1.4-1.5	0.00225	3.50054	15	1.4-1.5	0.00233	3.53598
16	1.5-1.6	0.00043	3.50097	16	1.5-1.6	0.00048	3.53646
17	1.6-1.7	-0.00100	3.49997	17	1.6-1.7	-0.00097	3.53549
18	1.7-1.8	-0.00205	3.49792	18	1.7-1.8	-0.00204	3.53345
19	1.8-1.9	-0.00278	3.49515	19	1.8-1.9	-0.00279	3.53066
20	1.9-2.0	-0.00322	3.49193	20	1.9-2.0	-0.00324	3.52742
21	2.0-2.1	-0.00344	3.48849	21	2.0-2.1	-0.00347	3.52395
22	2.1-2.2	-0.00349	3.48499	22	2.1-2.2	-0.00352	3.52043
23	2.2-2.3	-0.00339	3.48160	23	2.2-2.3	-0.00343	3.51700
24	2.3-2.4	-0.00320	3.47840	24	2.3-2.4	-0.00324	3.51376
25	2.4-2.5	-0.00295	3.47545	25	2.4-2.5	-0.00299	3.51077
26	2.5-2.6	-0.00266	3.47279	26	2.5-2.6	-0.00269	3.50808
27	2.6-2.7	-0.00235	3.47043	27	2.6-2.7	-0.00238	3.50570
28	2.7-2.8	-0.00205	3.46839	28	2.7-2.8	-0.00207	3.50362
29	2.8-2.9	-0.00175	3.46663	29	2.8-2.9	-0.00178	3.50184
30	2.9-3.0	-0.00148	3.46515	30	2.9-3.0	-0.00150	3.50034
31	3.0-3.1	-0.00123	3.46392	31	3.0-3.1	-0.00125	3.49909
32	3.1-3.2	-0.00102	3.46290	32	3.1-3.2	-0.00103	3.49806
33	3.2-3.3	-0.00083	3.46207	33	3.2-3.3	-0.00084	3.49722
34	3.3-3.4	-0.00067	3.46141	34	3.3-3.4	-0.00068	3.49654
35	3.4-3.5	-0.00053	3.46087	35	3.4-3.5	-0.00054	3.49600
36	3.5-3.6	-0.00042	3.46045	36	3.5-3.6	-0.00043	3.49557
37	3.6-3.7	-0.00033	3.46012	37	3.6-3.7	-0.00033	3.49524
38	3.7-3.8	-0.00026	3.45987	38	3.7-3.8	-0.00026	3.49498
39	3.8-3.9	-0.00020	3.45967	39	3.8-3.9	-0.00020	3.49478
40	3.9-4.0	-0.00015	3.45952	40	3.9-4.0	-0.00015	3.49463
41	4.0-4.1	-0.00011	3.45941	41	4.0-4.1	-0.00012	3.49451
42	4.1-4.2	-0.00009	3.45932	42	4.1-4.2	-0.00009	3.49443
43	4.2-4.3	-0.00006	3.45926	43	4.2-4.3	-0.00007	3.49436
44	4.3-4.4	-0.00005	3.45921	44	4.3-4.4	-0.00005	3.49431
45	4.4-4.5	-0.00004	3.45917	45	4.4-4.5	-0.00004	3.49428
46	4.5-4.6	-0.00003	3.45915	46	4.5-4.6	-0.00003	3.49425
47	4.6-4.7	-0.00002	3.45913	47	4.6-4.7	-0.00002	3.49423
48	4.7-4.8	-0.00001	3.45911	48	4.7-4.8	-0.00001	3.49422
49	4.8-4.9	-0.00001	3.45910	49	4.8-4.9	-0.00001	3.49420
50	4.9-5.0	-0.00001	3.45910	50	4.9-5.0	-0.00001	3.49420

NOTE TO TABLE I

[a]Basis sets defined Chapter III, section 4.

(d) C_n is large and positive for $n = 1$, drops quickly with increasing n, is small and negative for $r \approx .5$ au, increases and is positive but smaller than the first positive range until $r \approx 1.5$ au (for bases GW+3 and larger, cf. Chapter IV, section 3), and then becomes negative for the rest of the range (2 positive ranges, 2 negative ranges, 3 nodes).

Points (b) and (c) do not require further comment; attention will be turned to (a) and (d). The quantity $C_\Delta(r)$, defined in (12), is graphed for the GW+9 basis HCl OCE-SCF wavefunction in Figure 3 to illustrate these points. $C_\Delta(r)$ includes the radial volume factor r^2, so that q_{elec} is simply the integral over r of $C_\Delta(r)$. The graph makes clear the origins of the positive and negative regions of C_n. However the reasons for the r-dependent behavior of $C_\Delta(r)$ require some study. Roughly, by the arguments of section 1, $C_\Delta(r)$ is negative when the electron density along the z-axis for the given r (regions 1 and 3 of Figure 1) is greater than the corresponding density along the x-axis (regions 2 and 4 of Figure 1), and positive when the reverse is true. By elementary bonding theory, formation of the HCl molecule from the Cl^- ion with the proton on the +z-axis involves shifting electron density from regions close to the nucleus on the z-axis to regions farther from the nucleus along the z-axis, while leaving the

distribution along the x-axis largely unchanged. This makes the z-axis density smaller than the x-axis density near the nucleus and larger farther away. This simple picture predicts a $C_\Delta(r)$ which is positive for low values of r, decreases monotonically, becomes negative, and remains negative. Two characteristics of Figure 3 contradict this prediction: the vanishing $C_\Delta(r)$ for $r = 0$ and the small negative region between .5 and .6 au. The first effect is trivial: by (12) $C_\Delta(r)$ vanishes at $r = 0$ if the product $f_i(r)f_j(r)$ contains as a factor r^n with $n > 1$; in all cases when this is not true (ϕ_i and ϕ_j both 1s or one 1s and the other 2s or 2p) the angular factor is zero. Explanation of the second effect requires an examination of the electron density along the x- and z-axes. The electron density difference between the z- and x-axes,

$$\rho_{\Delta(z-x)} = \rho_z - \rho_x, \tag{20}$$

is graphed for $x = z = -2$ au to +2.5 au in Figure 4. The figure shows that $\rho_{\Delta(z-x)}$ is different in several respects from the qualitative description given above. Very close to the nucleus there is an increase on the +z-axis and a decrease on the -z-axis of the electron density relative to the x-axis, with the decrease larger than the increase. Thus z-axis depletion dominates, giving a positive $C_\Delta(r)$ in this region. From $r \approx .1$ au to $r \approx .35$ au both sides of the z-axis show a density decrease relative to the x-axis, and $C_\Delta(r)$ remains positive. At $r \approx .35$

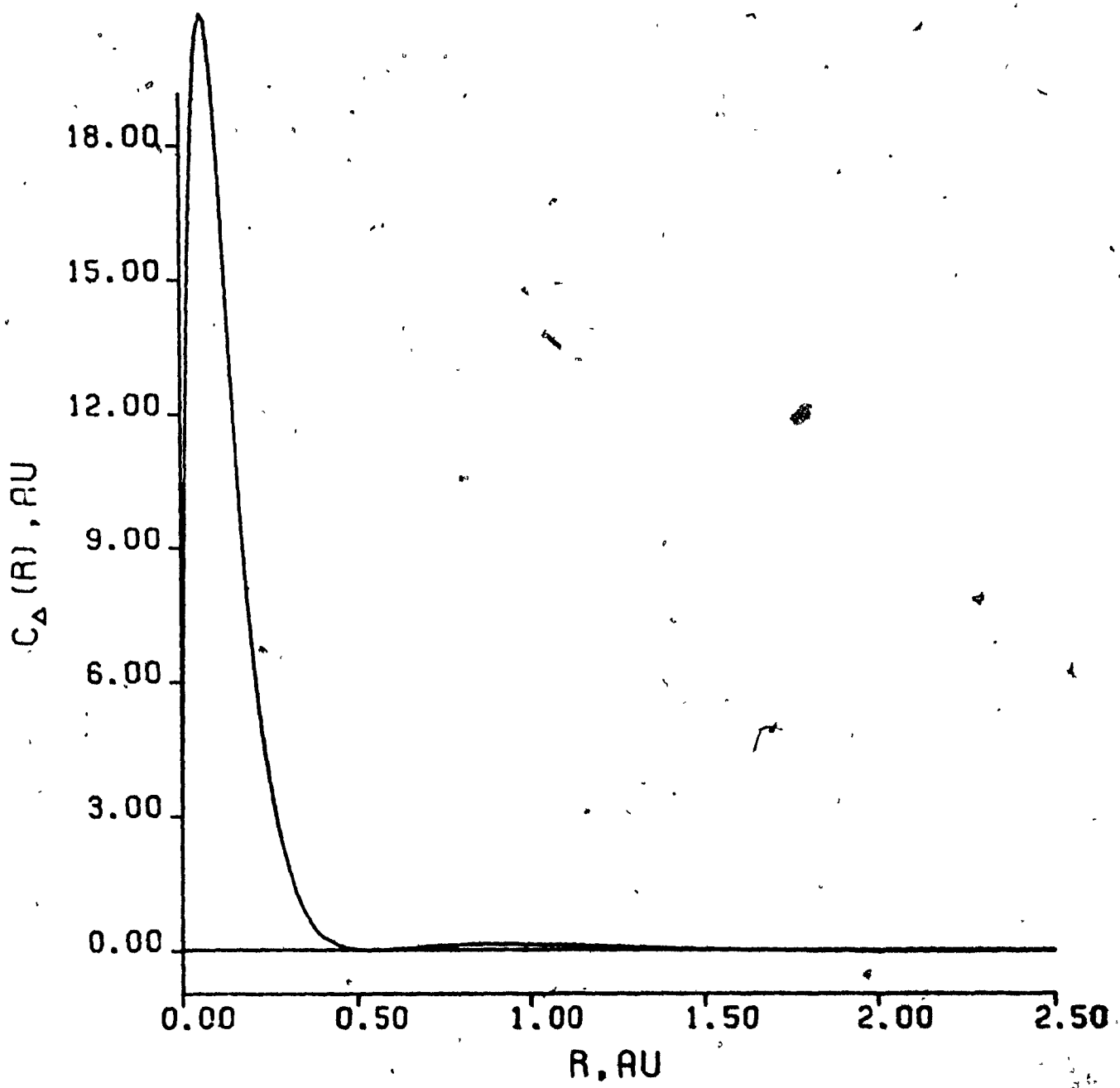

Figure 3a. Charge density weighted by q; values integrated over angular variables for range of values of r. $C_\Delta(r)$ defined in (12).

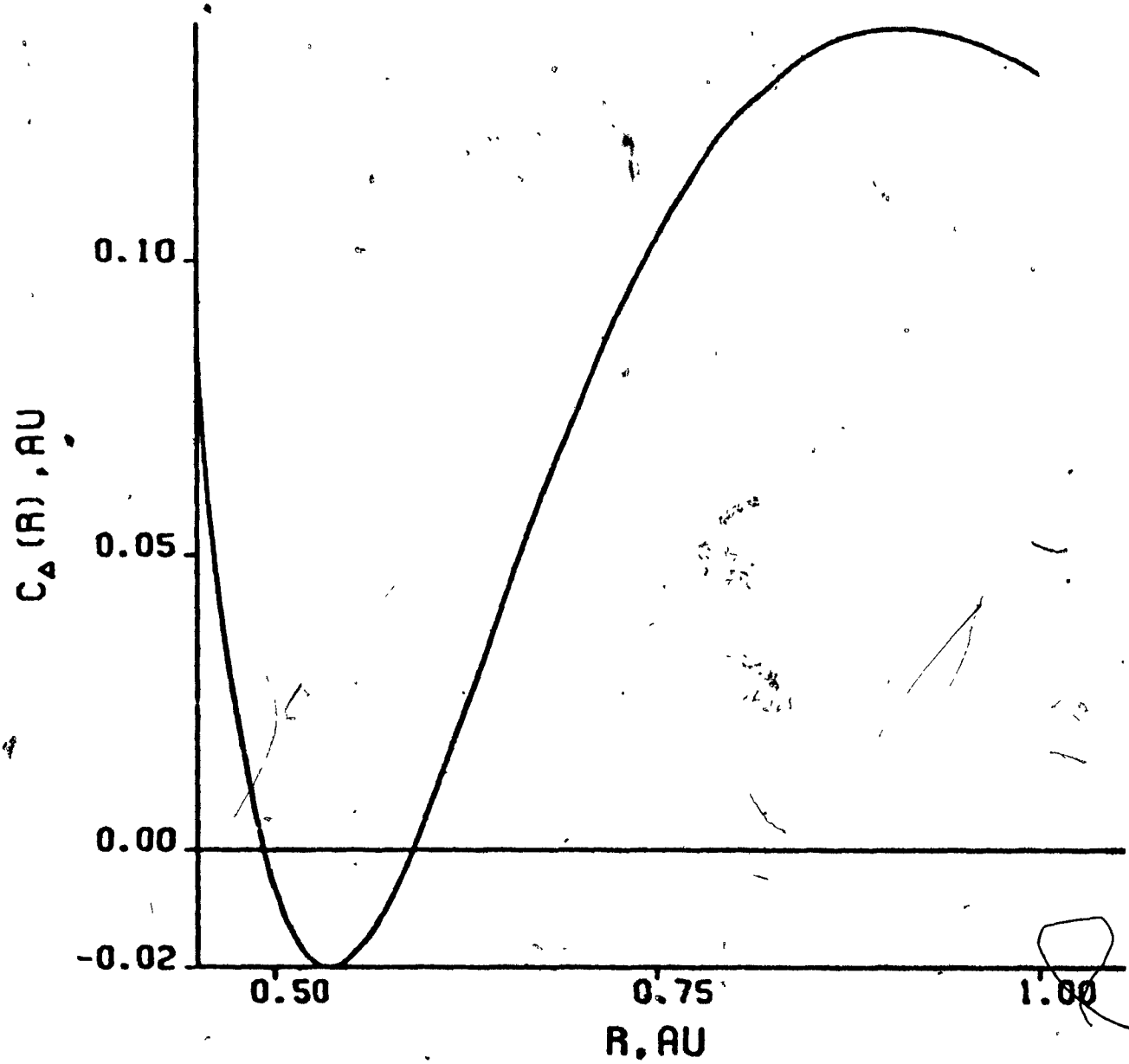

Figure 3b. Detail of 3a for r=.45 to 1 au.

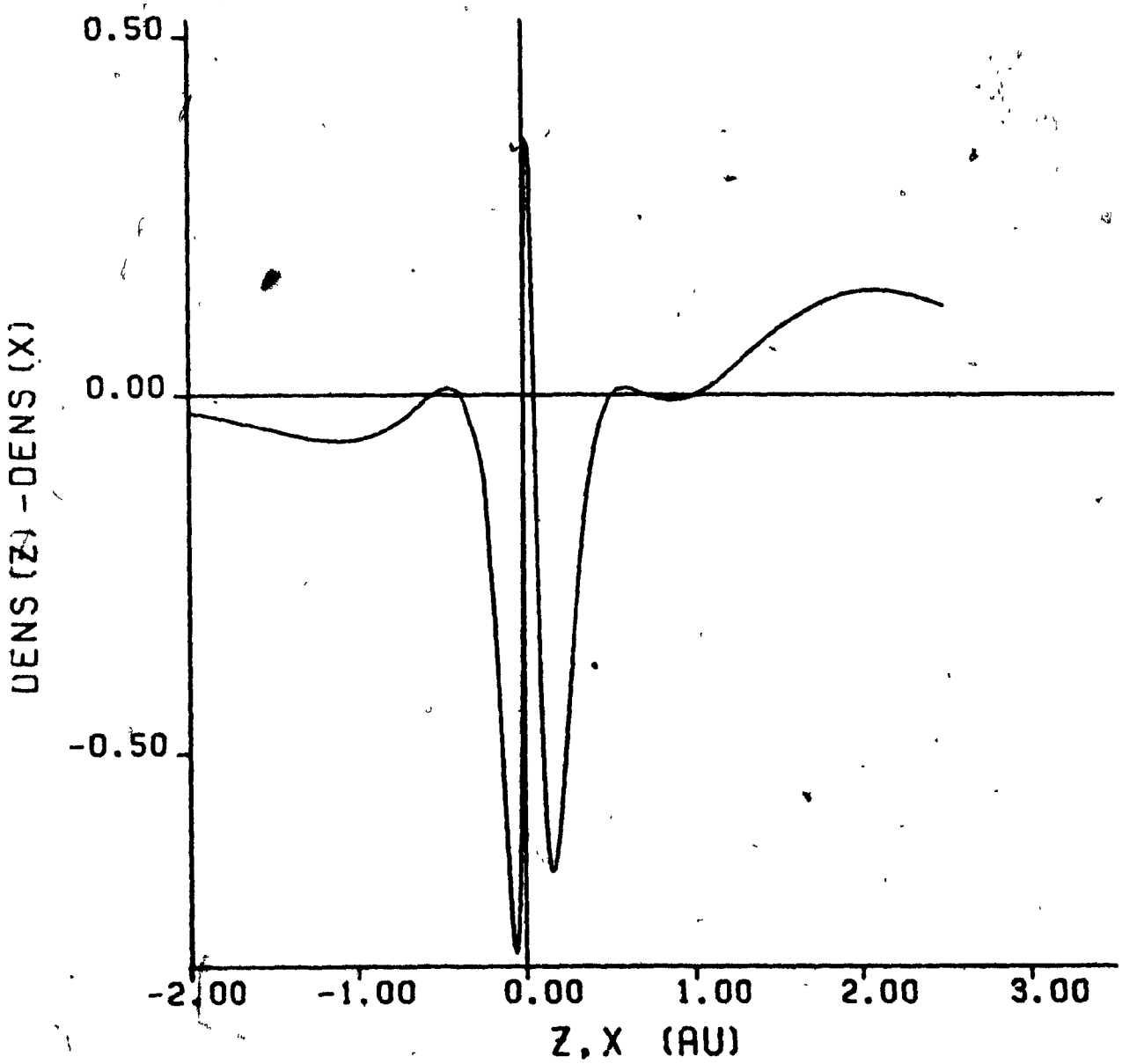

Figure 4. Density differences between z-axis and x-axis for HCl in the GW+9 basis. Densities in electrons/(au)^3. Basis defined Chapter III, section 4.

au the -z-axis shifts from decrease to increase relative to the x-axis density; this shift does not occur on the +z-axis until $r \approx .5$ au. For most of this region (.35 to .5 au) the decrease is larger than the increase, so $C_\Delta(r)$ remains positive. For a very short interval near $r = .5$ au both the +z and -z-axes show increased density relative to the x-axis, and $C_\Delta(r)$ becomes negative. The -z-axis very quickly shifts to decreased density, but for the interval $r \approx .5$ au to .6 au the increased density on the +z-axis dominates and $C_\Delta(r)$ is negative. The rest of the sign changes of $C_\Delta(r)$ in Figure 3 can similarly be related to Figure 4. The important point is that there is a region relatively close to the nucleus ($r \approx .5$ to .6 au) in which the z-axis density in HCl is larger than that along the x-axis, which is enclosed on both sides by regions where the x-axis density is higher. There is a similar region in the density difference along the z-axis between the GW+9 OCE-SCF wavefunction for HCl and the GW basis wavefunction for Cl^-,

$$\rho_\Delta(HCl-Cl^-) = \rho_{z,HCl} - \rho_{z,Cl^-} \tag{21}$$

which is graphed in Figure 5. Such regions have been observed and discussed before[13,14], and Feinberg and Ruedenberg[15,16] have examined the reasons for increases in electron density in regions relatively close to the nucleus during molecule formation in terms of balancing the decrease in potential energy resulting from the closer approach of the electrons

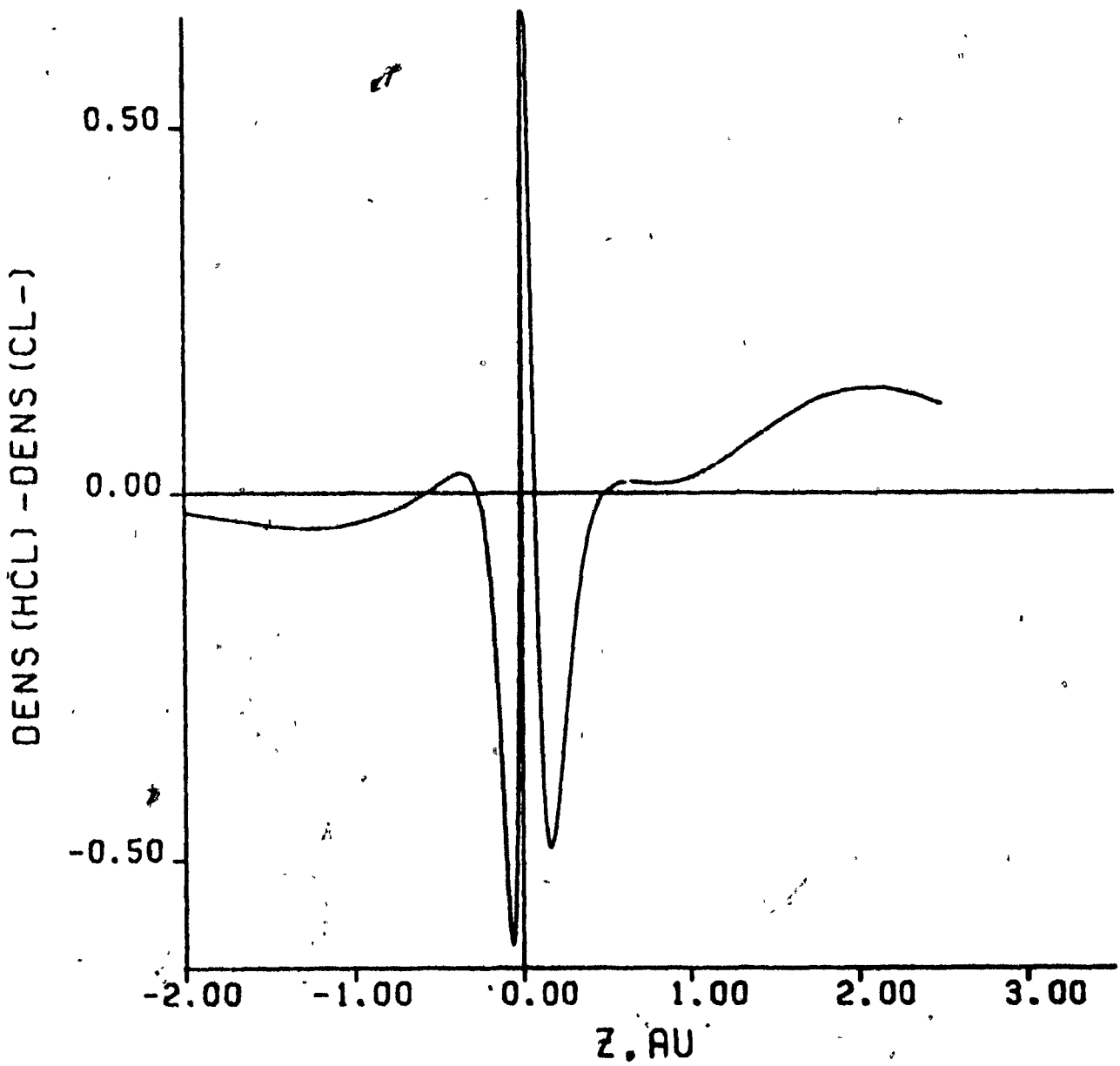

Figure 5. Density difference along z-axis between HCl in the GW+9 basis and Cl^- in the GW basis. Bases defined Chapter III, section 4. Densities in electron/$(au)^3$.

to the nuclei with the increased kinetic energy from the same effect in order to satisfy the virial theorem. However the existence of this region does not alter the observation that the major source of the EFG at the Cl nucleus in HCl is the sphere of radius $\approx .3$ au centered on the Cl nucleus, and that the contributions to q_{elec} within this sphere are due to a depletion of electron density along the z-axis relative to the x-axis (or equally the y-axis, because of the cylindrical symmetry of the molecule).

5. Radial analysis of the EFG in terms of electron shells

In Table II the q_n for $n = 1$ to 5 of Table I for the GW+9 basis OCE-SCF wavefunction for HCl are partitioned into contributions from the three electron shells (Chapter III, section 3). The table shows that the third shell dominates strongly in the sphere $r < .3$ au, as it must since this shell accounts for about 85% of q_{elec} (Chapter III, Table XI). However it is precisely this third shell which is expected to have the smallest electron density of the three shells within this sphere. In order to test this, the unweighted electron density

$$\rho(\bar{r}) = \sum_k N_k \psi_k^2(\bar{r}), \tag{22}$$

was integrated over intervals of r analogously to the inte-

TABLE II: Partitioning of the q_n of Table I into contributions from the three electron shells, for n=1 to 5. q_n is defined in (18). GW+9 basis.

n	r(au)	q_n (au)	1st shell	2nd shell	3rd shell
1	0.0-0.1	1.69761	-.00003	.29437	1.40326
2	0.1-0.2	2.93446	-.00004	.48155	2.45295
3	0.2-0.3	3.34955	-.00005	.53496	2.81464
4	0.3-0.4	3.44823	-.00005	.54499	2.90329
5	0.4-0.5	3.45968	-.00005	.54454	2.91519

gration of the charge density weighted by the $\hat{q}$ operator over intervals of r in (14). Note that the $\rho(\bar{r})$ of (22) is the electron density, while the $\rho(\bar{r})$ of (4)-(9), from which (14) was developed, was the charge density; the two differ in sign. Thus the formula of this section analogous to (14) would lack the leading minus sign. The angular integrals of (14) are replaced by the product of Kronecker deltas $\delta_{l_i l_j}$ $\delta_{m_i m_j}$ because of the orthonormality of the spherical harmonics. The radial integral for this calculation is of the same form as (15), but now $m = n_i + n_j$ instead of $n_i + n_j - 3$, as in (15). We define

$$B_n = \int_{.1\times(n-1)}^{.1\times n} dr \int_0^{\pi} \sin\theta d\theta \int_0^{2\pi} d\phi \; \rho(\bar{r})$$

$$p_n = \sum_{i=1}^{n} B_i \, . \tag{23}$$

In Table III B_n and p_n are presented for the GW+9 basis OCE-SCF wavefunction for HCl analogously to C_n and q_n in Table I. Note that p_n approaches the number of electrons in the molecule. The partitioning into shell contributions is given in Table IV. The table shows that indeed the third shell contributes the least density to the $r < .3$ au sphere of the three shells, accounting for about 3% of the density, although from Table II this shell accounts for 84% of the contribution to q_{elec} within this sphere.

The radial factor of the $\hat{q}$ operator, then, makes the

TABLE III: Integrals over intervals in r of unweighted electron density. Quantities defined in (23).

GW+9[a]

n	r(au)	B_n(au)	p_n(au)
1	0.0-0.1	1.43299	1.43299
2	0.1-0.2	1.40922	2.84220
3	0.2-0.3	1.75854	4.60074
4	0.3-0.4	1.87676	6.47750
5	0.4-0.5	1.48553	7.96303
6	0.5-0.6	0.99219	8.95522
7	0.6-0.7	0.62861	9.58383
8	0.7-0.8	0.43360	10.01743
9	0.8-0.9	0.36499	10.38240
10	0.9-1.0	0.35801	10.75042
11	1.0-1.1	0.40263	11.15104
12	1.1-1.2	0.43715	11.59821
13	1.2-1.3	0.46482	12.05303
14	1.3-1.4	0.47899	12.53203
15	1.4-1.5	0.47961	13.01164
16	1.5-1.6	0.46874	13.48038
17	1.6-1.7	0.44917	13.92955
18	1.7-1.8	0.42365	14.35320
19	1.8-1.9	0.39457	14.74776
20	1.9-2.0	0.36380	15.11156
21	2.0-2.1	0.33274	15.44430
22	2.1-2.2	0.30236	15.74666
23	2.2-2.3	0.27327	16.01993
24	2.3-2.4	0.24594	16.26578
25	2.4-2.5	0.22026	16.48604
26	2.5-2.6	0.19658	16.68262
27	2.6-2.7	0.17480	16.85742
28	2.7-2.8	0.15485	17.01226
29	2.8-2.9	0.13666	17.14892
30	2.9-3.0	0.12014	17.26906
31	3.0-3.1	0.10520	17.37425
32	3.1-3.2	0.09175	17.46600
33	3.2-3.3	0.07970	17.54570
34	3.3-3.4	0.06895	17.61464
35	3.4-3.5	0.05941	17.67406
36	3.5-3.6	0.05100	17.72506
37	3.6-3.7	0.04361	17.76867
38	3.7-3.8	0.03716	17.80584
39	3.8-3.9	0.03156	17.83740
40	3.9-4.0	0.02672	17.86412
41	4.0-4.1	0.02255	17.88667
42	4.1-4.2	0.01898	17.90565
43	4.2-4.3	0.01594	17.92158
44	4.3-4.4	0.01335	17.93493
45	4.4-4.5	0.01115	17.94609
46	4.5-4.6	0.00930	17.95539
47	4.6-4.7	0.00775	17.96314
48	4.7-4.8	0.00644	17.96958
49	4.8-4.9	0.00534	17.97492
50	4.9-5.0	0.00443	17.97935

continued

TABLE III: (cont'd.)

Note to TABLE III:

[a]B asis set defined in Chapter III, section 4.

TABLE IV: Partitioning of the p_n of Table III into contributions from the three electron shells, for n=1 to 5. p_n is defined in (23). GW+9 basis.

n	r(au)	p_n(au)	1st shell[a]	2nd shell[b]	3rd shell[b]
1	0.0-0.1	1.43298	1.27911	.14333	.01054
2	0.1-0.2	2.84220	1.91446	.87400	.05374
3	0.2-0.3	4.60074	1.99260	2.46777	.14038
4	0.3-0.4	6.47750	1.99942	4.26940	.20868
5	0.4-0.5	7.96303	1.99995	5.73280	.23028

[a]1st shell is occupied by two electrons.

[b]2nd and 3rd shells are occupied by eight electrons each.

largest contributions to this property come from very close to the nucleus[17]; the angular factor makes small the contributions from the nearly spherically symmetric inner shells. The rather small density of the 4σ, 5σ, and 2π MO's for $r < .3$ au accounts largely for q_{elec}. This explains why an OCE basis considerably larger than that necessary for a good calculation of the Cl^- ion is needed to give a wavefunction for HCl which yields a q_{elec} close to the H-F limit (Chapter III, Table VIII), even though the total electron density of HCl in the $r < .3$ au region is not greatly different from that in Cl^-. This last assertion may seem surprising in view of Figure 5; however the densities along the z-axis for HCl in the GW+9 basis and Cl^- in the GW basis, Table V, show that the differences are small for small r compared to the magnitude of the density itself.

TABLE V: Electron densities of the GW Cl^- wavefunction and the GW+9 HCl wavefunction along the z-axis. Basis sets defined in Chapter III, section 4.

z(au)	$\rho(Cl^-)$[a]	$\rho(HCl)$[a]
-.5	3.90846	3.91649
-.4	8.60379	8.62675
-.3	17.06658	17.08819
-.2	29.79914	29.71456
-.1	130.10196	129.61647
0.0	3211.25841	3211.81322
.1	130.10196	129.85713
.2	29.79914	29.34254
.3	17.06658	16.83383
.4	8.60379	8.53347
.5	3.90846	3.90557

[a]In electrons/$(au)^3$.

REFERENCES

1. P.M. Morse and H. Feshbach, Methods of Theoretical Physics, McGraw-Hill, N.Y., 1953. p. 1276.
2. T.L. Gilbert and A.C. Wahl, J. Chem. Phys. 55, 5247 (1971).
3. A. Ralston, A First Course in Numerical Analysis, McGraw-Hill, N.Y., 1965. p. 91.
4. G. Birkhoff and G.-C. Rota, Ordinary Differential Equations, 2nd edition, Blaisdell, Waltham, Mass., 1969. p. 279.
5. C.W. Kern and M. Karplus, J. Chem. Phys. 40, 1374 (1964).
6. J.C.Y. Chen, Phys. Lett. 16, 269 (1965).
7. J.C.Y. Chen, J. Chem. Phys. 43, 3673 (1965).
8. J.C.Y. Chen and S. Ehrenson, J. Chem. Phys. 44, 1020 (1966).
9. S. Ehrenson, Chem. Phys. Lett. 9, 521 (1971).
10. S. Ehrenson and M. Wong, Theor. Chim. Acta, 28, 283 (1973).
11. M.P. Barnett and C.A. Coulson, Phil. Trans. Roy. Soc. A243, 221 (1951).
12. W.H. Flygare, J.M. Pochan, G.I. Kerley, T. Caves, M. Karplus, S. Aung, R.M. Pitzer, and S.I. Chan, J. Chem. Phys. 45, 2793 (1966).
13. R.F.W. Bader, I. Keaveny, and P.E. Cade, J. Chem. Phys. 47, 3381 (1967).
14. P.E. Cade, R.F.W. Bader, W.H. Henneker, and I. Keaveny, J. Chem. Phys. 50, 5313 (1969).

15. M.J. Feinberg and K. Ruedenberg, J. Chem. Phys. 54, 1495 (1971). Especially p. 1508.

16. M.J. Feinberg, K. Ruedenberg, and E.L. Mehler, Adv. Quant. Chem. 5, 27 (1970).

17. Several authors (P. Pyykko, Proc. Phys. Soc. 92, 841 (1967); R.C. Henderson and D.D. Ebbing, J. Chem. Phys. 47, 69 (1967); D.M. Bishop, J. Chem. Phys. 49, 3718 (1968)) have pointed out that q_{elec} at a proton or deuteron depends heavily on electron density in the bonding region; Henderson and Ebbing have illustrated this with a function similar to our $C_{\Delta}(r)$; however, q_{elec} at a proton is likely to be determined by different factors than q_{elec} at a Cl nucleus because of the lack of inner electron shells about a proton.

Chapter VI: R-dependence of q: Vibrational Averaging of eQq

Conventional MO wavefunctions are completely determined by the atomic numbers and molecular geometry, and thus do not distinguish between isotopically substituted molecules, such as HCl and DCl. However MO wavefunctions can be used to estimate the differences in electronic properties in an isotopically substituted series (due to different vibrational and rotational wavefunctions, and hence different average molecular geometry) in two ways: (i) MO wavefunctions may be calculated for a small range of values of the internuclear distance about R_e, and spectroscopic constants used to take the vibrational-rotational average of the electronic property[1,2]; or (ii) the variation of calculated molecular energy with internuclear distance can be used to construct an approximate vibrational-rotational wavefunction, and this used to average the electronic property[3-5].

The first method is used here for vibrational averaging of q, since in this method errors in the vibrationally averaged quantity are due solely to errors in the R-dependence of q; in method (ii) errors are due to errors in R-dependence of both q and E.

1. The general problem

Following Dunham's treatment of the rotating vibrator[6], the vibrational-rotational wavefunction is denoted

$\psi_{vJ}(\xi)$, with

$$\xi = (R-R_e)/R_e, \tag{1}$$

with R the internuclear distance and R_e the internuclear distance at the minimum of the potential energy. The integers v and J are the vibrational and rotational quantum numbers, respectively. $\psi_{vJ}(\xi)$ is assumed real-valued and normalized,

$$\int_{-\infty}^{\infty}\psi_{vJ}^2(\xi)d\xi = 1. \tag{2}$$

An approximation has been introduced in setting the lower limit of integration at $-\infty$ rather than -1, since $R \geq 0$ implies $\xi \geq -1$, and R is inherently positive. However the extended integration interval introduces negligible error since ψ_{vJ} calculated for the extended range is small for arguments <-1[7]. If the system (which here is a diatomic molecule) has vibrational quantum number v and rotational quantum number J, then $\psi_{vJ}^2(\xi)d\xi$ is the probability that ξ is in the range $(\xi-\frac{d\xi}{2}, \xi+\frac{d\xi}{2})$, in the limit as $d\xi$ approaches zero.

Let $q(\xi)$ be the expectation value of q (including both electronic and nuclear contributions) over an electronic wavefunction calculated for $R=R_e\xi+R_e$. This definition of $q(\xi)$ is based on the assumption that the total wavefunction for the molecule can be approximated well by a product of one function in the electronic coordinates with R entering only as a parameter,

and one function in the nuclear coordinates only. This is the Born-Oppenheimer approximation[8] (Chapter I), which involves neglecting terms of order 6 and higher in the parameter $(m_e/M)^{\frac{1}{2}}$ in a power series expansion of the energy, with m_e the electronic mass and M the average nuclear mass. The vibrational energy is of order $(m_e/M)^{\frac{1}{2}}$, so the ratio of the first neglected term ($\approx (m_e/M)^{3/2}$) to the vibrational energy is (for HCl) $\approx 2.5\times10^{-5}$, which is within the range of experimental detectability[9,10]. However there is no practical way to circumvent the Born-Oppenheimer approximation; it is used in the calculations reported here and an estimate made in section 5 of the error introduced.

We assume that $q(\xi)$ is analytic in a region about $\xi=0$ (i.e. about $R=R_e$). Then $q(\xi)$ can be expanded as a power series in ξ in this region,

$$q(\xi) = q_0 + q_1\xi + q_2\xi^2 + \dots , \tag{3}$$

where the q_i are related to the i-th order derivatives at $\xi=0$ by the usual Taylor series formula. The vibrational average of q, which is the expectation value of $q(\xi)$ over ψ_{vJ}, is

$$q_{vJ} = \int_{-\infty}^{\infty}\psi_{vJ}^2(\xi)q(\xi)d\xi. \tag{4}$$

Substituting (3) into (4) and integrating term by term,

$$q_{vJ} = q_0 + q_1\langle\xi\rangle_{vJ} + q_2\langle\xi^2\rangle_{vJ} + \ldots, \tag{5}$$

with $\langle\xi^i\rangle_{vJ}$ the expectation values of ξ^i defined analogously to (4). Thus q_{vJ} can be calculated if enough of the q_i and $\langle\xi^i\rangle_{vJ}$ can be calculated that neglect of higher terms in (5) gives an acceptably small truncation error.

2. Polynomial fit of q

To determine the OCE-SCF q_i in (3) two series of calculations of HCl at different R were done: one in the 71-STO basis of Moccia[11], and one in the 29-STO GW+9 basis (Chapter III). The q_i were obtained for each series by a least-squares polynomial fit of the expectation values of q (including nuclear contributions).

The abscissas (ξ values at which the OCE-SCF calculations are done) had to be chosen carefully. We restrict the abscissa set to an odd number of points evenly placed about $\xi=0$; i.e., the 2n+1 points

$$-nh,\ (-n+1)h,\ \ldots,\ 0,\ h,\ \ldots,\ nh, \tag{6}$$

with n integral and h the increment in ξ. This restriction is imposed because the calculation of expected errors in the q_i[12] is simple only for abscissa sets of this type. This restriction poses no practical problem, since we are inter-

ested in the region about $\xi=0$.

In choosing the number of points economy is an important factor, especially for the 71-STO basis, since the iterative SCF procedure with a large basis is costly of computer time. It is seen below that q_i through $i=2$ are necessary for acceptable accuracy in (5), so the fitting polynomial must be at least of degree 2, which requires at least 3 points in the abscissa set.

However a polynomial fitted to the minimum number of points is not reliable[12], because the ordinates, in this case the calculated q, are not exact numbers; in Chapter III they were estimated to have 5 significant figures, or a relative error of about 1×10^{-5}. If the minimum number of abscissas is chosen, this noise in the q is reproduced by the fitted polynomial since it passes through all the ordinates. If a larger number is chosen, the fitted polynomial tends to average the errors in the data and approximate the ideal noise-free ordinates better than the data points themselves do[12]. Thus in order to obtain this smoothing effect with an odd number of abscissas for a second degree polynomial at least five abscissas are needed. For the 71-STO basis five calculations were done; expected errors in the q_i were calculated and were sufficiently small that an increase to seven or more points was not needed. For the less costly GW+9 basis a seven-point abscissa set was used in order to determine how much accuracy in the q_i is gained by the increase from 5 to 7 points.

The range of the abscissas (determined by h in (8)) must also be chosen. Two effects argue for a small range:

(i) The q_i in (3) are related to the i-th derivatives of q at $\xi=0$ by the Taylor series formula. Since we seek these coefficients, rather than approximate values of q for given values of ξ, it is important that the polynomial reproduce q and as many of its derivatives as possible at the single point $\xi=0$. Values of q and its derivatives for large $|\xi|$ do not enter (3), and for a fitting polynomial of low degree inclusion of such points may worsen the values of the derivatives at $\xi=0$.

(ii) Closed-shell SCF wavefunctions behave badly at large internuclear distances; e.g., they dissociate to ions instead of atoms for diatomic molecules[13,14], so values of q for large ξ are not reliable.

We illustrate (i) with an example. The Taylor series for exp(x) is

$$\exp(x) = 1 + x + \frac{x^2}{2} + \frac{x^3}{6} + \ldots \tag{7}$$

A fitting polynomial

$$p(x) = p_0 + p_1(x) + p_2(x) + \ldots$$

which reproduces well the derivatives of exp(x) at x=0 should then have

$$p_0 \approx 1,\ p_1 \approx 1,\ p_2 \approx \tfrac{1}{2},\ \text{etc.}$$

The function was fitted for two five-point abscissa sets:

$$\text{Set I:} \quad x = -2, -1, 0, 1, 2$$

$$\text{Set II:} \quad x = -.2, -.1, 0, .1, .2.$$

The coefficients for least-squares fitting of a second-degree polynomial to these sets are[15]

$$\text{Set I:} \quad p_0 = .89888, \quad p_1 = 1.68578, \quad p_2 = .71162 \tag{8}$$

$$\text{Set II:} \quad p_0 = .99999, \quad p_1 = 1.00568, \quad p_2 = .50184. \tag{9}$$

Thus although Set I should fit the curve better for larger x, Set II gives the derivatives at x=0 more accurately.

Thus a small range of ξ values about 0 should be chosen for the OCE-SCF calculations. However one effect argues against choosing too small a range. As recalled above, the q have a limited accuracy, so if the ξ are chosen so close together that the differences in q are less than or barely greater than the accuracy of the q, the fitting coefficients are meaningless.

The question arises of how one can estimate errors in the q_i induced by noise in the q. Ralston[12] has given a method using the variance of the ordinates,

$$\sigma^2 = \frac{1}{n-1} \sum_{m=1}^{n} [\bar{y}_m - y_m]^2,$$

with $\bar{y}_m$ the ordinate calculated from the fitting polynomial and y_m the true ordinate at x_m. As a test of this method, the fitting of exp(x) with the Set II abscissas was repeated, adding or subtracting small amounts randomly from the ordinates to produce changes in the second decimal place and simulate noise in the data. The fitting coefficients this yields are

$$p_0 = .99668$$
$$p_1 = 1.02000$$
$$p_2 = .68571,$$

with $\sigma^2=3.25\times10^{-5}$. Ralston's formula gives expected errors of

$$p_0 = .9967 \pm .0040$$
$$p_1 = 1.020 \pm .018$$
$$p_2 = .69 \pm .15.$$

Comparison with (9) shows that the actual errors for p_1 and p_2 are somewhat greater than the expected errors given by Ralston's formula; however in all cases the expected errors are of the right order of magnitude, and this suffices to indicate how many figures of the coefficients are significant.

From the above considerations it was decided to choose for the 71-STO basis a set of 5 R values about R_e with a step length of .01 au. Bunker's value of R_e=2.4087 au for HeI^{16} was used to calculate ξ by (1). The seven-point set for

the GW+9 basis was formed from the five-point set by addition of a higher and a lower point with the same increment. The R, ξ, q, and total energies for these two sets are presented in Table I. The increment .01 au was chosen because .001 au would have produced too little change in q and .1 au would have emphasized regions away from ξ=0. Had the expected errors been too large, the stepsize could have been changed or the number of points increased; this proved unnecessary. No claim is made that .01 au is a superior stepsize to, say, .005 au or .02 au.

Polynomials in ξ were fitted to the q of Table I by the least-squares method[15]. The fitting was started with degree 1 and continued until no significant decrease in σ^2 was observed. Table II presents the coefficients and variances for polynomials of degrees 1 through 3 fitting q in au to the dimensionless parameter ξ. The coefficients q_i are thus in atomic units of EFG.

The polynomials of degree 3 produce a much smaller relative decrease in σ^2 compared to degree 2 than degree 2 produces compared to degree 1, the drop in σ^2 between degrees 2 and 3 being less than a factor of 10, while the drop between degrees 1 and 2 is several orders of magnitude. This near independence of σ^2 upon degree is characteristic of fitting polynomials when increase in degree begins to reproduce noise in the data[12]; thus further analysis is confined to the fitting polynomial of degree 2.

TABLE I: q and total energy from OCE-SCF wavefunctions. Experimental R_e=2.4087 au[16,17].

A. 71-STO basis[11].

R(au)	ξ	q(au)	E(au)
2.3887	-.00830323	3.83206	-460.052370
2.3987	-.00415162	3.85416	-460.052512
2.4087	0.0	3.87579	-460.052595
2.4187	.00415162	3.89695	-460.052620
2.4287	.00830323	3.91772	-460.052588

B. GW+9 basis (Chapter III).

R(au)	ξ	q(au)	E(au)
2.3787	-.01245485	3.57755	-460.066456
2.3887	-.00830323	3.59812	-460.067355
2.3987	-.00415162	3.61805	-460.068183
2.4087	0.0	3.63729	-460.068938
2.4187	.00415162	3.65589	-460.069623
2.4287	.00830323	3.67380	-460.070237
2.4387	.01245485	3.69102	-460.070780

TABLE II: EFG fitting coefficients and variances for fitting polynomials of degrees 1, 2, and 3. Coefficients are defined in equation (3). Coefficients in au of EFG.

A. 71-STO basis[11].

coefficient	degree 1	degree 2	degree 3
q_0	3.875336	3.875782	3.875782
q_1	5.157278	5.157278	5.151868
q_2		-12.96715	-12.96715
q_3			92.31618
variance	$.233 \times 10^{-6}$	$.361 \times 10^{-9}$	$.939 \times 10^{-10}$

B. GW+9 basis (Chapter III).

coefficient	degree 1	degree 2	degree 3
q_0	3.635960	3.637299	3.637299
q_1	4.556008	4.556007	4.557928
q_2		-19.42955	-19.42955
q_3			-15.92623
variance	$.188 \times 10^{-5}$	$.814 \times 10^{-10}$	$.150 \times 10^{-10}$

Expected errors for the degree 2 polynomial were calculated by the Ralston formula and are presented in Table III. In order to decide if these expected errors are acceptably small, one must compare the accuracy of the corresponding experimental determinations. Kaiser[17] performed a vibrational-rotational analysis of his molecular beam electric resonance eQq measurements for HCl and DCl and obtained H-isotope independent values for q and its first and second derivatives with respect to ξ at $\xi=0$. The q_i deduced from these values are presented in Table III for comparison with the OCE-SCF q_i. For both the five-point fitting of the 71-STO q and the seven-point fitting of the GW+9 q the expected errors in the q_i are much smaller than the experimental uncertainties reported by Kaiser; increasing the abscissa set from 5 for the 71-STO basis to 7 for the GW+9 basis reduced the expected errors by a factor of between .15 and .3.

The calculated q_0 from the GW+9 basis differs from the experimental value by about 1%, which is outside the experimental error but still very good agreement; q_0 from the 71-STO basis differs from the experimental value by about 7%, and is in only fair agreement with the experimental value. The reasons for this were discussed in Chapters III and IV. However the calculated q_1 value for the GW+9 basis differs from the experimental value by about 12% and is outside the experimental error, while the 71-STO q_1 agrees with the experimental

TABLE III: Coefficients and expected errors for degree 2 polynomial fitting of q from OCE-SCF wavefunctions. Kaiser's experimental values[17] are listed for comparison. All values in au.

coefficient	OCE basis		
	71-STO	GW+9	exptl.
q_0	3.875782±.000013	3.637299±.000005	3.6339±.0001
q_1	5.1573±.0014	4.55601±.00041	5.32±.22
q_2	-12.97±.30	-19.430±.057	-6.00±.85

value to within the experimental error. The q_2 values from both bases are of the correct (negative) sign, but quite poor in magnitude, the 71-BTO value being 100% too large in magnitude, the GW+9 value 200%. Reasons for this behavior are examined in section 6.

3. Calculation of the $\langle\xi^i\rangle$

In Dunham's notation[6] the Schroedinger equation for ψ_{vJ} for a diatomic molecule is

$$\frac{d^2\psi_{vJ}(\xi)}{d\xi^2} + \frac{1}{hcB_e}\left[E_{vJ} - V(\xi) - hcB_e\frac{J(J+1)}{(1+\xi)^2}\right]\psi_{vJ}(\xi) = 0, \qquad (10)$$

with B_e the rotational constant[18] in cm^{-1} and

$$V(\xi) = hca_0\xi^2(1 + a_1\xi + a_2\xi^2 + \ldots), \qquad (11)$$

convergent for $|\xi| < 1$[40], and thus accurate only for low v[41]. The vibrational constant ω_e in cm^{-1} is simply related to a_0[6],

$$a_0 = \omega_e^2/4B_e.$$

The most accurate method currently available for calculating the $\langle\xi^i\rangle_{vJ}$ for a diatomic molecule is to construct a Rydberg-Klein-Rees (RKR) potential from the spectroscopic constants[19-22] and integrate the Schroedinger equation numerically[23]. Kaiser[17] modified this method and applied it for the v=0, J=0 state to

the infrared data for HCl[24] and DCl[25] of Rank et al. However q cannot be measured in the gas phase in a state with J=0[26]; no RKR $\langle\xi^i\rangle_{vJ}$ values have been published for J≠0. Schlier[27] derived expressions for $\langle\xi^i\rangle_{vJ}$ by treating the rotational and anharmonic vibrational terms of (10) as perturbations to the harmonic term of the vibrational potential; altering his notation somewhat,

$$\langle\xi\rangle_{vJ} = (B_e/\omega_e)[-3a_1(v+\tfrac{1}{2})] + (B_e/\omega_e)^2[4J(J+1)$$

$$+ (-\tfrac{15}{4}a_3 + \tfrac{23}{4}a_1a_2 - \tfrac{21}{8}a_1^3) + (v+\tfrac{1}{2})^2(-15a_3+39a_1a_2-\tfrac{45}{2}a_1^3)]$$

$$+ \text{terms in } (B_e/\omega_e)^3 \text{ and higher} \tag{12}$$

$$\langle\xi^2\rangle_{vJ} = 2(B_e/\omega_e)(v+\tfrac{1}{2}) + (B_e/\omega_e)^2[(-\tfrac{3}{2}a_2 + \tfrac{7}{4}a_1^2)$$

$$+ (v+\tfrac{1}{2})^2(-6a_2+15a_1^2)].$$

$$+ \text{terms in } (B_e/\omega_e)^3 \text{ and higher} \tag{13}$$

$$\langle\xi^3\rangle_{vJ} = (B_e/\omega_e)^2[-\tfrac{7}{4}a_1 - 15a_1(v+\tfrac{1}{2})^2]$$

$$+ \text{terms in } (B_e/\omega_e)^3 \text{ and higher} \tag{14}$$

$$\langle\xi^4\rangle_{vJ} = (B_e/\omega_e)^2[\tfrac{3}{2} + 6(v+\tfrac{1}{2})^2]$$

$$+ \text{terms in } (B_e/\omega_e)^3 \text{ and higher} \tag{15}$$

All higher $\langle\xi^i\rangle_{vJ}$ contain no terms lower than third order in (B_e/ω_e). For HCl, $(B_e/\omega_e)\approx 3.6\times10^{-3}$, so the magnitude of the first neglected term is roughly 1×10^{-5} times the magnitude of $\langle\xi\rangle_{vJ}$ and $\langle\xi^2\rangle_{vJ}$, so these quantities are given to about 5 significant figures. $\langle\xi^3\rangle_{vJ}$ and $\langle\xi^4\rangle_{vJ}$ are given only to 3 figures since the leading terms are second order in (B_e/ω_e). Higher order terms in (B_e/ω_e) could not be included because of lack of some necessary spectroscopic constants.

Rank et al[25] have determined a_1, a_2, a_3, and a_4 and the constants ω_e and B_e for $H^{35}Cl$ and $D^{35}Cl$ from infrared data[24]. These, along with ω_e and B_e for $T^{35}Cl$[28], are presented in Table IV. In the Born-Oppenheimer approximation the a_i are the same for HCl, DCl, and TCl. $\langle\xi\rangle_{01}$ and $\langle\xi^2\rangle_{01}$ for $H^{35}Cl$, $D^{35}Cl$, and $T^{35}Cl$ calculated by (12) and (13) with the constants of Table IV are given in Table V. $\langle\xi^3\rangle_{01}$ and $\langle\xi^4\rangle_{01}$ were not calculated, since the corresponding q_i in (5) are not given by the second degree fitting polynomial, which is the highest degree that does not begin to reproduce noise in the data.

The error introduced in (5) by neglecting terms in $\langle\xi^3\rangle_{vJ}$ and higher can be estimated by comparing the expressions for $\langle\xi^3\rangle_{vJ}$ and $\langle\xi^4\rangle_{vJ}$ with those for $\langle\xi\rangle_{vJ}$ and $\langle\xi^2\rangle_{vJ}$. We assume that all of the q_i are of the same order of magnitude; from Table II this is true through i=3 for the GW+9 basis and probably would be true for the 71-STO basis if more

TABLE IV: Spectroscopic constants and dimensionless potential coefficients a_i for $H^{35}Cl$, $D^{35}Cl$, and $T^{35}Cl$. In the Born-Oppenheimer approximation the a_i are the same for all three molecules.

A. Spectroscopic constants (cm^{-1})

	$H^{35}Cl$ (Ref. 24)	$D^{35}Cl$ (Ref. 24)	$T^{35}Cl$ (Ref. 28)
ω_e	2991.0904	2145.1973	1775.86
B_e	10.593553	5.4488411	3.7368

B. Potential coefficients (equation (11))[25]

a_1	-2.364519
a_2	3.66470
a_3	-4.6783
a_4	4.944

abscissas were used. q_{vJ} is of the order of 1 (see below), and since $q_3\langle\xi^3\rangle_{vJ}$ and $q_4\langle\xi^4\rangle_{vJ}$ are on the order of $10(B_e/\omega_e)^2=10^{-4}$, truncating (5) after $q_2\langle\xi^2\rangle_{vJ}$ limits the accuracy of q_{vJ} to four significant figures. The OCE-SCF q_0 have six significant figures, so truncation after $q_2\langle\xi^2\rangle_{vJ}$ causes loss of two significant figures; however the experimental q_0 has only five significant figures, so only one figure comparable with experiment is lost by truncation.

Zeiger and Bolef[29] have given an expression for q_{vJ} in an investigation of isotope effects upon eQq:

$$q_{vJ}(Z-B) = q_0 + (2B_e/\omega_e)^2 q_1 J(J+1)$$

$$+ [3q_1(B_e/\omega_e)(1+\frac{\alpha_e\omega_e}{6B_e^2}) + 2q_2(B_e/\omega_e)](v+\tfrac{1}{2}) \qquad (16)$$

α_e is a standard spectroscopic constant[18]. The coefficients of q_1 and q_2 must be $\langle\xi\rangle_{vJ}$ and $\langle\xi^2\rangle_{vJ}$, respectively, by comparison with (5), which implies from (16),

$$\langle\xi\rangle_{vJ}(Z-B) = 4(B_e/\omega_e)^2 J(J+1) + 3(B_e/\omega_e)(1+\frac{\alpha_e\omega_e}{6B_e^2})(v+\tfrac{1}{2})$$

$$\langle\xi^2\rangle_{vJ}(Z-B) = 2(B_e/\omega_e)(v+\tfrac{1}{2}). \qquad (17)$$

Dunham[6] gives $\alpha_e=-6(B_e^2/\omega_e)(1+a_1)$, so $\langle\xi\rangle_{vJ}(Z-B)$ reduces to

$$\langle\xi\rangle_{vJ}(Z-B) = -3a_1(B_e/\omega_e)(v+\tfrac{1}{2}) + 4(B_e/\omega_e)^2 J(J+1). \qquad (18)$$

Comparison of (18) with (12) and (17) with (13) shows that $\langle\xi^2\rangle_{vJ}(Z-B)$ neglects terms of order $(B_e/\omega_e) \simeq .5\times10^{-2}$, so only two-figure accuracy can be expected. $\langle\xi\rangle_{vJ}(Z-B)$ does not truncate consistently in (B_e/ω_e), only one of the four members of the Schlier $(B_e/\omega_e)^2$ term being retained in $\langle\xi\rangle_{vJ}(Z-B)$.

The case for the use of the Schlier expressions over those of Zeiger and Bolef is not as clear as it seems from the above, since the a_i are not tabulated for many molecules, although approximate expressions for them have been given in terms of the traditional spectroscopic constants[6,30]. But for molecules such as HCl for which the a_i are available, the Schlier expressions are clearly more accurate and consistent. $\langle\xi\rangle_{01}(Z-B)$ in $\langle\xi^2\rangle_{01}(Z-B)$ are listed in Table V for comparison with the values from the Schlier expressions.

4. Calculation of q_{vJ}

Using

$$q_{vJ} \simeq q_0 + q_1\langle\xi\rangle_{vJ} + q_2\langle\xi^2\rangle_{vJ}, \tag{19}$$

with the q_i of Table III and Schlier's $\langle\xi^i\rangle_{01}$ from Table V, q_{01} was calculated in au for $H^{35}Cl$, $D^{35}Cl$, and $T^{35}Cl$, for the q_i of both the 71-STO and GW+9 bases. The q_{01} are given in Table VI. Also given are the changes from q_0 caused by the vibrational averaging,

$$\Delta q_{vJ} = q_1\langle\xi\rangle_{vJ} + q_2\langle\xi^2\rangle_{vJ}.$$

TABLE V: $\langle\xi\rangle_{01}$ and $\langle\xi^2\rangle_{01}$ for $H^{35}Cl$, $D^{35}Cl$, and $T^{35}Cl$ from Schlier[27] and Zeiger-Bolef[29] formulas.

	$H^{35}Cl$		$D^{35}Cl$		$T^{35}Cl$	
	Schlier	Z-B	Schlier	Z-B	Schlier	Z-B
$\langle\xi\rangle_{01}$	.0127854	.0126620	.0091240	.0090605	.0075422	.0074986
$\langle\xi^2\rangle_{01}$	.0037895	.0035417	.0026675	.0025400	.0021917	.0021042

TABLE VI: Calculated and experimental vibrationally averaged q for HCl in the v=0, J=1 state. All quantities in au.

$H^{35}Cl$

	71-STO[a]	GW+9[b]	exptl.[17]
q_{01}	3.8926±.0015[c]	3.6185±.0006	3.679847±.000025
Δq_{01}	.0168±.0012	-.01538±.00024	.0459±.0003

$D^{35}Cl$

	71-STO[a]	GW+9[b]	exptl.[17]
q_{01}	3.8883±.0012	3.6236±.0005	3.667572±.000005
Δq_{01}	.0125±.0009	-.01026±.00018	.0337±.0003

$T^{35}Cl$

	71-STO[a]	GW+9[b]	exptl.[39]
q_{01}	3.8863±.0009	3.6257±.0004	3.65±.03
Δq_{01}	.0105±.0006	-.00822±.00012	.02±.03

[a]OCE basis of ref. 11.

[b]OCE basis described in Chapter III.

[c]All uncertainties estimated from uncertainties in the q_i, Table III.

The experimental q_{01} were obtained directly from Kaiser's observations of eQq (using the conversion factors $Q(^{35}Cl) = -.0782\times10^{-24}$ cm^2[31] and 1 hartree = 4.35942×10^{-11} erg, 1 bohr = 5.29167×10^{-9} cm, h = 6.62559×10^{-27} erg-sec[32]). The experimental Δq_{01} were obtained by subtracting Kaiser's experimental q_0 from the experimental q_{01}. The table shows that the 71-STO Δq_{01} are correctly ordered and of the right sign but too small by a factor of about 3. The GW+9 Δq are of the wrong sign and in reverse order to the observed quantities, the magnitudes being smaller than the observed magnitudes by a factor of about 3.

Table III shows that the OCE-SCF q_1 values are in fair (in the 71-STO case, good) agreement with experiment; the q_2 values are of correct (negative) sign but twice (in the GW+9 case, three times) the observed magnitude. Thus the OCE-SCF $q_2\langle\xi^2\rangle_{01}$ term is more negative than the corresponding experimental term and more nearly cancels (in the 71-STO case) or more than cancels (in the GW+9 case) the positive $q_1\langle\xi\rangle_{01}$ term, which is nearly the same for both the OCE-SCF and experimental q_1, and results in a lower Δq_{01}. The incorrect ordering of the GW+9 Δq_{01} is also a consequence of the large negative q_2.

5. Error introduced by Born-Oppenheimer failure

Schlier[27] has estimated (and it has been confirmed by more exact studies[9,10]) that an expectation value such as

q_{01} calculated by (5) with the hypothetical exact values of q_i and $\langle\xi^i\rangle_{01}$ for the $^1\Sigma$ electronic ground state of a diatomic molecule has a relative error with respect to the observed value of the order of $(B_e/\Delta E_e)$, where ΔE_e is an average electronic excitation energy. This error is due to terms in the exact wavefunction neglected in the Born-Oppenheimer approximation which involve an electronic term other than the ground state. For HCl $B_e \approx 10\ cm^{-1}$ from Table IV and $\Delta E_e \approx 100{,}000\ cm^{-1}$[18], so $(B_e/\Delta E_e) \approx 10^{-4}$. Thus q_{01} of (5) is limited to 5 significant figures by the Born-Oppenheimer approximation; since the OCE-SCF calculated q_{01} of Table VI agree with the experimental values to at most two significant figures, Born-Oppenheimer failure cannot be an important source of the discrepancy.

6. Analysis of the R-dependence of q

In this section some questions which arose in section 3 are examined. From Table III the 71-STO calculated q_0, q_1, and q_2 are 6% too high, nearly right, and 100% low, respectively, compared to the experimental value; in the GW+9 basis q_0, q_1, and q_2 are nearly right, 10% low, and 200% low respectively. The explanation of the differences in q_0 (which except for small changes due to the polynomial fitting is identical to the q of earlier chapters) was given in Chapter III: a poor basis choice for the 71-STO set caused the contribution to q_{elec} from the second electron shell to be con-

siderably larger than that of the GW+9 basis or the extensive TCE-SCF calculations[33,34].

In order to explain the better quality of the 71-STO q_1 than the GW+9 q_1 we advance the following hypothesis: the changes in q upon change of R (which determine q_1 since it is the first derivative of q with respect to ξ at ξ=0) are due mainly to changes in the contribution to q_{elec} of the third (outer) electron shell, for which the 71-STO basis is well chosen (cf. Chapter IV); since the 71-STO basis is larger and more flexible than the GW+9 set for the third shell it can reproduce these changes upon small changes in R better than can the GW+9 set, and thus gives a more accurate q_1.

In Table VII the partitioning of the total q at the various R from Table II into q_{elec} and q_{nuc} is given, with q_{elec} further partitioned into contributions from the three electron shells (Chapter III). In Table VIII a first difference table is constructed from Table VII (e.g. row 1, column 2 of the upper half of Table VIII is q_{elec} (R=2.3987 au) - q_{elec} (R=2.3887 au)). From Table VIII it is clear that changes in q_{elec} dominate the total changes in q, and that changes in the third shell dominate the changes in q_{elec}. Thus the above hypothesis is supported, since the poor behavior of the 71-STO basis in reproducing the second shell electron distribution introduces negligible error into the changes in q_{elec}, although it introduces considerable error into the value of q_{elec} itself. It is also to be expected that the GW+9 basis would not give

TABLE VII: Analysis by electron shell of the OCE-SCF calculated q_{elec} for a series of internuclear distances. All quantities in au. R_e=2.4087 au[16].

A. 71-STO basis[11]

R	q_{elec}	q_{nuc}	shell contributions to q_{elec} 1st shell	2nd shell	3rd shell
2.3887	3.68532	.14674	-.00010	.88319	2.80223
2.3987	3.70924	.14491	-.00010	.88480	2.82453
2.4087	3.73268	.14311	-.00010	.88639	2.84640
2.4187	3.75561	.14135	-.00010	.88792	2.86779
2.4287	3.77812	.13961	-.00010	.88945	2.88878

B. GW+9 basis (Chapter III)

R	q_{elec}	q_{nuc}	shell contributions to q_{elec} 1st shell	2nd shell	3rd shell
2.3787	3.42895	.14860	-.00005	.53710	2.89189
2.3887	3.45139	.14674	-.00005	.53772	2.91372
2.3987	3.47314	.14491	-.00005	.53828	2.93491
2.4087	3.49418	.14311	-.00005	.53881	2.95542
2.4187	3.51454	.14135	-.00005	.53930	2.97529
2.4287	3.53419	.13961	-.00005	.53975	2.99450
2.4387	3.55312	.13790	-.00005	.54011	3.01305

TABLE VIII: Difference table constructed from TABLE VII. Differences in au.

A. 71-STO basis[11]

Δ	q_{elec}	q_{nuc}	shell contributions to q_{elec}		
			1st shell	2nd shell	3rd shell
1	.02392	-.00183	.00000	.00161	.02230
2	.02344	-.00180	.00000	.00159	.02187
3	.02293	-.00176	.00000	.00153	.02189
4	.02251	-.00174	.00000	.00153	.02099

B. GW+9 basis (Chapter III)

Δ	q_{elec}	q_{nuc}	shell contributions to q_{elec}		
			1st shell	2nd shell	3rd shell
1	.02244	-.00186	.00000	.00062	.02183
2	.02175	-.00183	.00000	.00056	.02119
3	.02104	-.00180	.00000	.00053	.02051
4	.02036	-.00176	.00000	.00049	.01987
5	.01965	-.00174	.00000	.00045	.01921
6	.01893	-.00171	.00000	.00036	.01855

the R-dependence of q well even for relatively small changes in internuclear distance, since the GW+9 basis was chosen (Chapter III) to concentrate charge at 2.4087 au from the Cl nucleus.

Poor behavior for q_2 seems to be an intrinsic failing of OCE bases. As HCl is dissociated by increasing the internuclear distance to infinity, the exact wavefunction changes from that for HCl to that for the separated neutral Cl and H atoms. The OCE-SCF and TCE-SCF calculations, however, yield a Cl^- ion and a bare proton at infinite separation[33]. Thus q_{elec} from the exact wavefunction tends, as R approaches infinity, to q_{elec} of the Cl atom (≈5.6 au[35]), while the OCE-SCF and TCE-SCF q_{elec} tend to q_{elec} of the Cl^- ion (=0 because of spherical symmetry). Thus the true q_{elec} keeps increasing as R is increased, while the MO calculated values at some point begin a decrease to zero. Therefore, the OCE-SCF and TCE-SCF q_i must for some i be lower than the corresponding exact q_i in order that the exact $q(\xi)$ be, for some values of ξ, greater than the SCF $q(\xi)$ in (3). Thus one expects that a set of OCE-SCF or TCE-SCF calculations could give accurately only the first several q_i, after which one (or several) q_i significantly lower than the corresponding experimental quantity would follow. For OCE-SCF calculations of HCl it appears that q_1 is the last q_i that is given accurately, since q_2 even in the extensive 71-STO set is 100% too low.[42] For a series of TCE-SCF calculations[33], Huo[36,37] reports q_0=3.569 au, q_1=5.31 au,

q_2=-5.50 au. Comparison with Table III shows that this q_2 agrees well with experiment; a TCE-SCF basis, then, is significantly better than OCE-SCF basis for R-dependent effects, as one expects since the TCE-SCF wavefunction retains more charge near the proton as R changes. Higher q_i from the TCE-SCF calculations cannot be compared, since Kaiser's experimental values are calculated only through q_2.

In conclusion, OCE-SCF calculations reproduce the R-dependence of the EFG for HCl rather poorly, and lead to inaccurate vibrationally averaged properties. For vibrational modes of polyatomic molecules which do not involve R-changes (such as the symmetric bending of NH_3[3,38]), however, OCE-SCF wavefunctions have been reported to give accurate vibrational averages.

REFERENCES

1. S. Green, J. Chem. Phys. 58, 4327 (1973).
2. H.H. Michels, J. Chem. Phys. 56, 665 (1972).
3. R. Moccia and L. Randaccio, J. Chem. Phys. 45, 4303 (1966).
4. K.K. Docken and J. Hinze, J. Chem. Phys. 57, 1369 (1972).
5. M. Yoshimine, A.D. McLean, and B. Liu, J. Chem. Phys. 58, 4412 (1973).
6. J.L. Dunham, Phys. Rev. 41, 721 (1932).
7. D. ter Haar, Phys. Rev. 70, 222 (1946).
8. M. Born and R. Oppenheimer, Ann. der Physik 84, 457 (1927).
9. P.R. Bunker, J. Mol. Spec. 45, 151 (1973).
10. J.K.G. Watson, J. Mol. Spec. 45, 99 (1973).
11. R. Moccia, Theor. Chim. Acta 8, 8 (1967).
12. A. Ralston, First Course in Numerical Analysis, McGraw-Hill, N.Y., 1965. Chapter 6.
13. C.A. Coulson and I. Fischer, Phil. Mag. 40, 386 (1949).
14. R. McWeeny and B.T. Sutcliffe, Methods of Molecular Quantum Mechanics, Academic, London, 1969. p. 121.
15. Subroutine CURVFT, McGill University Computing Centre.
16. P.R. Bunker, J. Mol. Spec. 39, 90 (1971).
17. E.W. Kaiser, J. Chem. Phys. 53, 1686 (1970).

18. G. Herzberg, Molecular Spectra and Molecular Structure: I. Spectra of Diatomic Molecules, Van Nostrand, N.Y., 2nd edition, 1950.

19. R. Rydberg, Zeits. fur Physik 73, 376 (1931).

20. O. Klein, Zeits. fur Physik 76, 226 (1932).

21. A.L.G. Rees, Proc. Phys. Soc. A59, 998 (1947).

22. R.N. Zare, J. Chem. Phys. 40, 1934 (1964).

23. J.W. Cooley, Math. Comput. 15, 363 (1961).

24. D.H. Rank, D.P. Eastman, B.S. Rao, and T.A. Wiggins, J. Opt. Soc. Am. 52, 1 (1962).

25. D.H. Rank, B.S. Rao, and T.A. Wiggins, J. Mol. Spec. 17, 122 (1965).

26. N.F. Ramsey, Molecular Beams, Oxford, 1956. p. 59.

27. C. Schlier, Fortschritte der Physik 9, 455 (1961).

28. L.H. Jones and E.S. Robinson, J. Chem. Phys. 24, 1246 (1956).

29. H.J. Zeiger and D.I. Bolef, Phys. Rev. 85, 788 (1952).

30. K. Kuchitsu, Bull. Chem. Soc. Japan 40, 498 (1967).

31. G.F. Koster, Phys. Rev. 86, 148 (1952).

32. E.R. Cohen and J.W.M. DuMond, Rev. Mod. Phys. 37, 537 (1965).

33. P.E. Cade and W.M. Huo, J. Chem. Phys. 47, 649 (1967).

34. A.D. McLean and M. Yoshimine, J. Chem. Phys. 47, 3256 (1967).

35. V. Jaccarino and J.G. King, Phys. Rev. 83, 471 (1951).

36. W.M. Huo, reported as a private communication to E.W. Kaiser in ref. 17.

37. P.E. Cade, J. Chem. Phys. 47, 2390 (1967).

38. P. Grigolini and R. Moccia, J. Chem. Phys. 57, 1369 (1972).

39. C.A. Burrus, W. Gordy, B. Benjamin, and R. Livingston, Phys. Rev. 97, 1661 (1955).

40. C.L. Beckel and R. Engelke, J. Chem. Phys. 49, 5199 (1968).

41. G. Simons, R.G. Parr, and J.M. Finlan, J. Chem. Phys. 59, 3229 (1973).

42. If, however, one is willing to expend the computer time necessary to adjust the OCE basis for each R (which is especially easy for the GW+9 basis), q_2 might be considerably improved.

CHAPTER VII: EFG of the 1σ MO

It was observed in Chapter III that the first and second electron shells of Cl^-, which in a first approximation remain spherically symmetric in the HCl molecule, account for about 15% of the molecular q_{elec} from the OCE-SCF wavefunction in the GW+9 basis. Table I shows that this agrees well with the two-center calculations of McLean and Yoshimine[1] and Cade and Huo[2]. The q's of the second shell also agree well. The first shell (1σ MO), however, warrants closer investigation for three reasons: (a) there is a large relative difference between the 1σ MO q of the OCE-SCF and those of the TCE-SCF wavefunctions, though the absolute difference is small, and the two TCE-SCF calculations do not agree well; (b) all basis adjustment in the GW+N basis series of Chapter III, section 4, involved orbitals which emphasized the region near the proton, with no additions of orbitals concentrated close to the Cl nucleus; (c) the Cl nucleus is not spherical and can distort the inner shells from spherical symmetry[4], but this interaction was not included in the Hamiltonian in the OCE-SCF calculations of this work (Chapter II) nor in the TCE-SCF calculations[1,2]. Point (c) will be examined first.

1. The Sternheimer effect

The distortion of inner shells by the quadrupolar nucleus and the distortion of spherically symmetric shells by

TABLE I: Analysis by electron shells of HCl q_{elec} from the McLean-Yoshimine and Cade-Huo two-center and GW+9 one-center bases. All calculations at r_e=2.4087 au. All quantities in atomic units.

shell	McL-Yosh[a]	C-H[b]	GW+9[c]
1	-.00214	-.00013	-.00005
2	.45270	.52143	.53881
3	2.96126	3.01163	2.95542
total q_{elec}	3.41182	3.53293	3.49418
% from shells 1+2	13%	15%	15%

experimental value of q_{elec}[29]: 3.4908 au.

[a]Calculated in this laboratory from wavefunction of ref. 3.

[b]Calculated in this laboratory from wavefunction of ref. 2.

[c]Basis defined Chapter III, section 4.

external electric fields were first studied by Sternheimer[4,5,6]; the phenomenon of an EFG induced in a nominally spherical shell is usually referred to as the Sternheimer effect[7]. It has been pointed out[8,9] that confusion exists in the literature on this effect; for this reason a simple description will be given here. The HCl molecule provides a convenient example. Consider the molecule as a Cl^- ion perturbed by a proton. As a first approximation the electron shells of Cl^- do not distort in the presence of the proton (this is more nearly true if the proton is farther away than the equilibrium distance; alternately, the proton could be replaced by a positive ion in a crystal lattice); in this assumption the EFG at the Cl nucleus is just that due to the proton, or, assuming the equilibrium internuclear distance of HCl, $(3\cos^2\theta-1)/r^3=2/(2.4087)^3=.14311$ au. However, from Chapter III, Table VIII, the electrons (in the GW+9 OCE-SCF wavefunction) produce an EFG of 3.49418 au, so that the total EFG at the nucleus is .14311+3.49418=3.63729 au. Thus the calculated EFG allowing for electronic distortion is of the same sign but larger than that in the assumption of spherical electron shells; this is an example of antishielding of the nucleus by the electron shells, since the induced gradient is of the same sign as the gradient of the perturbing field[5]. In some cases the perturbing field induces a gradient of opposite sign in the closed shells, giving rise to a shielding of the nucleus[10].

So far the distortion of the shells by direct inter-

action with the quadrupolar nucleus has been ignored. This distortion is small, as will be seen later in this chapter. However, this distortion may be used to calculate the energy of interaction between the EFG induced by the external field (in the above example the field due to the proton) and the quadrupolar nucleus. This fact has probably caused much of the confusion about the Sternheimer effect. It was first shown by Sternheimer and Foley[11], using methods specific to the nuclear quadrupole-external field problem; Lucken[7] has given a more general demonstration, presented here considerably modified.

Consider two perturbations of the (hermitian) Hamiltonian H_0,

$$\begin{aligned} H' &= H_0 + H_1 \\ H'' &= H_0 + H_2, \end{aligned} \tag{1}$$

with perturbing Hamiltonians H_1 and H_2. Let ψ_0, ψ_1, and ψ_2 be such that

$$H_0\psi_0 = E_0\psi_0 \tag{2}$$

$$(H_0-E_0)\psi_1 = -(H_1-E_1)\psi_0 \tag{3}$$

$$(H_0-E_0)\psi_2 = -(H_2-E_2)\psi_0. \tag{4}$$

ψ_1 and ψ_2 are the first order corrections in normal Rayleigh-

Schrodinger perturbation theory[12] to ψ_0 for the perturbed Hamiltonians H_0+H_1 and H_0+H_2 respectively. ψ_1 and ψ_2 are taken to be orthogonal to ψ_0 to preserve normalization to first-order of the perturbed wavefunction[13]; multiplying (3) and (4) on the left by ψ_0 and integrating gives $E_1=\langle\psi_0|H_1|\psi_0\rangle$ and $E_2=\langle\psi_0|H_2|\psi_0\rangle$. Multiplying (3) by ψ_2 and (4) by ψ_1 on the left and integrating gives

$$\langle\psi_2|H_0|\psi_1\rangle - E_0\langle\psi_2|\psi_1\rangle = -\langle\psi_2|H_1|\psi_0\rangle \tag{5}$$

$$\langle\psi_1|H_0|\psi_2\rangle - E_0\langle\psi_1|\psi_2\rangle = -\langle\psi_1|H_2|\psi_0\rangle, \tag{6}$$

which yield directly

$$\langle\psi_1|H_2|\psi_0\rangle = \langle\psi_2|H_1|\psi_0\rangle, \tag{7}$$

(7) is known as Dalgarno's Interchange Theorem[12], introduced by Dalgarno and Stewart[14]. Note that (7) follows directly from (3) and (4) and the orthogonality of ψ_1 and ψ_2 to ψ_0; it is not dependent on the form of H_1 or H_2.

In nuclear quadrupole interactions, the difference in energy of two states with different nuclear m_I (spin angular momentum) numbers (Chapter I) is of interest. The perturbed Hamiltonian for the system is

$$H^m = H_0 + H_e + H_Q^m, \tag{8}$$

where H_0 is the Hamiltonian of the spherically symmetric system, H_e is the Hamiltonian for the external field, and H_Q^m is the Hamiltonian for the interaction of the quadrupolar nucleus in the state $m_I=m$ with the EFG. In the example above of the HCl molecule, H_0 is the Hamiltonian for the Cl^- ion and H_e is $\sum_i Z_i/r_{i\alpha}$, where i ranges over all charged particles in the system, Z_i is the charge of the ith particle, and $r_{i\alpha}$ is the distance between the ith particle and the proton. The form of H_Q^m for this case will be given later. Because H_e is in this case rather large, HCl can not accurately be treated by first-order perturbation theory. ψ_e and ψ_Q^m are defined by

$$(H_0-E_0)\psi_e = -(H_e-E_e)\psi_0 \tag{9}$$

$$(H_0-E_0)\psi_Q^m = -(H_Q^m-E_Q^m)\psi_0, \tag{10}$$

analogously to (3) and (4). E_e and E_Q^m correspond to E_1 and E_2. From (7),

$$\langle\psi_e|H_Q^m|\psi_0\rangle = \langle\psi_Q^m|H_e|\psi_0\rangle. \tag{11}$$

(9) and (10) give

$$(H_0-E_0)(\psi_e+\psi_Q^m) = -(H_e+H_Q^m-E_e-E_Q^m)\psi_0,$$

so that $\psi_0+\psi_e+\psi_Q^m$ is the first-order wavefunction of the perturbed system. ψ_Q^m will be assumed negligible compared to ψ_e; this will be investigated later in the chapter. Thus the wavefunction

for the system with Hamiltonian (8) will be taken to be $\psi_0+\psi_e$, which is independent of m. Evaluating the difference $\Delta E^{m-m'}$ between the energies of the states with $m_I=m$ and $m_I=m'$,

$$\Delta E^{m-m'}=\langle\psi_0+\psi_e|H_Q^m|\psi_0+\psi_e\rangle-\langle\psi_0+\psi_e|H_Q^{m'}|\psi_0+\psi_e\rangle$$

$$=\langle\psi_0|H_Q^m|\psi_0\rangle-\langle\psi_0|H_Q^{m'}|\psi_0\rangle+2[\langle\psi_e|H_Q^m|\psi_0\rangle-\langle\psi_e|H_Q^{m'}|\psi_0\rangle]$$

$$+\langle\psi_e|H_Q^m|\psi_e\rangle-\langle\psi_e|H_Q^{m'}|\psi_e\rangle. \qquad (12)$$

$\Delta E^{m-m'}$ in (12) is correct to 3rd order (since wavefunction corrections through nth order give energy corrections through 2n+1 order[15]); if $\Delta E^{m-m'}$ is required only to 2nd order (neglecting, for example, $\langle\psi_e|H_Q^m|\psi_e\rangle$), this becomes

$$\Delta E^{m-m'}=\langle\psi_0|H_Q^m|\psi_0\rangle-\langle\psi_0|H_Q^{m'}|\psi_0\rangle$$

$$+2[\langle\psi_e|H_Q^m|\psi_0\rangle-\langle\psi_e|H_Q^{m'}|\psi_0\rangle]. \qquad (13)$$

Using (11) for H_Q^m and $H_Q^{m'}$, and the fact that $\langle\psi_0|H_Q^m|\psi_0\rangle=0$ for a spherically symmetric ψ_0 (equations (29) and (30) below),

$$\Delta E^{m-m'}=2[\langle\psi_Q^m|H_e|\psi_0\rangle-\langle\psi_Q^{m'}|H_e|\psi_0\rangle] \qquad (14)$$

Thus the energy difference can be calculated to second order without calculating ψ_e (assuming that ψ_Q^m and $\psi_Q^{m'}$ can be calculated) even though the electronic wavefunction for both states is assumed to be $\psi_0+\psi_e$. Thus ψ_Q^m can be used to calculate

nuclear quadrupole transition energies due to the EFG, even though ψ_Q^m may not be an important correction to ψ_0. This is a consequence of the interchange theorem (7); the utility of (14) is that if one is interested, for example, in the nuclear quadrupole-EFG interaction of a Cl^- ion perturbed by external charges in several different arrangements, one need only calculate ψ_Q^m and $\psi_Q^{m'}$ and evaluate $\langle\psi_Q^m|H_e|\psi_0\rangle$ and $\langle\psi_Q^{m'}|H_e|\psi_0\rangle$ for the different H_e; if (13) were used directly a new ψ_e would have to be calculated for each arrangement of external charges. Thus Sternheimer[4,5,6] calculated the distortion ψ_Q^m due to the nonsphericity of the nucleus even though the physical effect being considered was the distortion by the external field. This fact has probably been the cause of the confusion in the literature on the effect, although it was explained by Sternheimer and Foley[11] (in considerably different terms) and further clarified by Abragam[8].

For an SCF calculation, (14) is of little use, because an SCF calculation yields $\psi_0+\psi_e$ without an explicit perturbation treatment, and $\Delta E^{m-m'}$ can be evaluated directly from (12). Also, because ψ_Q^m is small compared to ψ_0 and ψ_e (section 2), it is not given accurately by including H_Q^m in the Hamiltonian of the system; Sternheimer[4,5,6] calculates ψ_Q^m by a power-series solution of (10) using a modified Thomas-Fermi Hamiltonian[16] as H_0; except for inaccuracies due to this choice of H_0, ψ_Q^m is given fairly accurately despite its small size relative to ψ_0. On the other hand perturbation treatments of the coupled Hartree-

Fock equations quickly become unwieldy as basis size is increased[17]. Thus although (14) is appropriate for Sternheimer's calculations it is of no practical use for OCE-SCF calculations.

Thus to study the Sternheimer effect by MO calculations, one studies the deviation from spherical symmetry of the inner electron shells as calculated from a normal SCF wavefunction. Initially, however, it is necessary to verify the assumption that underlies the above argument: that H_Q^m is a small perturbation and produces a negligible change in the wavefunction.

2. Inclusion of the nuclear quadrupole interaction in the SCF Hamiltonian

In Chapter I the total interaction energy of an external charge distribution with a non-spherical nucleus was developed as a multipole expansion[18,19]; the only two non-zero terms for the Cl nucleus (both ^{35}Cl and ^{37}Cl isotopes) with $m_I=m$ were

$$E^{(0)} + E^{(2)} = Z\int\rho(\bar{r}_e)/r_e d\tau_e + \frac{1}{6}\sum_{i=1}^{3}\sum_{j=1}^{3} Q_{ij}^{(m)}\int\rho(\bar{r}_e)\left[\frac{\partial}{\partial x_{e_i}}\frac{\partial}{\partial x_{e_j}}\frac{1}{r_e}\right]d\tau_e, \qquad (15)$$

where $\rho(\bar{r}_e)$ is the charge density due to all charged particles except the quadrupolar nucleus in the volume element $d\tau_e$ centered at $\bar{r}_e$; $\bar{r}_e$ is measured in a spherical system centered at the nuclear center of mass[18]. Z is the atomic number of the

quadrupolar nucleus. Electron density within a small sphere centered at the nuclear center of mass and enclosing the nucleus is excluded in the integrations (hence the subscript e for external); the density within this sphere adds only a constant amount to the energy independent of the nuclear spin quantum number m_I[20]. The cartesian coordinates x_{e_i} are numbered so that $x_{e_1}=x_e, x_{e_2}=y_e, x_{e_3}=z_e$, with z the axis of quantization of the nuclear angular momentum (in the HCl molecule in the absence of external magnetic fields this coincides with the principal axis of the EFG, so this choice of z is consistent with that of Chapter III). Note that the operator by which $\rho(\bar{r}_e)$ is weighted in the integration in the second term of (15) is the $\hat{q}_{x_i x_j}$ of the introduction to Chapter III. The first term of (15) is already included in the nuclear attraction integrals of the OCE-SCF calculations (Appendix I, section 2). Thus modifying an SCF calculation to include the effects of the quadrupole moment of the Cl nucleus involves simply adding the second term of (15) to the nuclear attraction integrals with the quadrupolar nucleus.

$Q_{ij}^{(m)}$ in (15) is defined as[20]

$$Q_{ij}^{(m)} = Ze\langle m|Q_{ij}|m\rangle = \int \rho^{(m)}(\bar{r}_n)[3x_{n_i}x_{n_j} - \delta_{ij}r_n^2]d\tau_n, \qquad (16)$$

where $\rho^{(m)}(\bar{r}_n)$ is the nuclear charge density for the state $|m\rangle$ (with $m_I=m$) in the volume element $d\tau_n$ centered at $\bar{r}_n$. The proton charge is e. The allowed values for m_I are I, I-1, ..., -I,

where I is the nuclear spin. A more formal but compact notation is

$$Q_{ij}^{(m)} = Ze\langle m|Q_{ij}|m\rangle = Ze\langle m|3x_{n_i}x_{n_j} - \delta_{ij}r_n^2|m\rangle. \qquad (17)$$

Attention can be confined to Q_{ij} tensors diagonal in m_I such as (17) only if the EFG is cylindrically symmetric, i.e. if

$$\int\rho(\bar{r}_e)\left[\frac{\partial^2}{\partial x_e^2}\frac{1}{r_e}\right]d\tau_e = \int\rho(\bar{r}_e)\left[\frac{\partial^2}{\partial y_e^2}\frac{1}{r_e}\right]d\tau_e$$

in (15). If this is not true, the interaction between the nuclear quadrupole moment and the EFG has non-zero matrix elements between states with different m_I[21]; m_I is then no longer a good quantum number for the system and (15) does not apply; the treatment is then more complicated[21]. However HCl is cylindrically symmetric, so attention can be restricted to Q_{ij} tensors diagonal in m_I.

It is a familiar result of group theory (a corollary to the Wigner-Eckart theorem[19,22,23]) that all those symmetric, traceless tensors are proportional which are constructed in a similar manner from vectors whose components satisfy the same commutation relations with respect to the operators for the Cartesian components of the angular momentum satisfied by the components of the angular momentum themselves. The x, y, and z components of an ordinary Cartesian vector commute with the components of the angular momentum in the same way that the angular momentum components themselves do[24]; thus the above

result can be applied to (17).

It is convenient to express $Q_{ij}^{(m)}$ as a constant times a tensor constructed from the components of the nuclear spin vector $\bar{I}$,

$$Q_{ij}^{(m)} = ZeC\langle m|3\frac{I_iI_j + I_jI_i}{2} - \delta_{ij}\bar{I}\cdot\bar{I}|m\rangle, \tag{18}$$

because simple rules exist for determining $I_i|m\rangle$. Note that $3x_{n_i}n_j$ in (17) became $\frac{3}{2}(I_iI_j + I_jI_i)$ because while x_ix_j is symmetric in i and j, I_iI_j is not since I_i and I_j do not commute. The rules for determining $I_i|m\rangle$ are[18]

$$\begin{aligned} &I_z|m\rangle = m|m\rangle \\ &I_\pm \equiv I_x \pm iI_y \\ &I_\pm|m\rangle = [(I\mp m)(I\pm m+1)]^{\frac{1}{2}}|m\pm 1\rangle \\ &\bar{I}\cdot\bar{I}|m\rangle = I(I+1)|m\rangle. \end{aligned} \tag{19}$$

Using (19) and the orthonormality of the $|m\rangle$, it follows that

$$\begin{aligned} &Q_{ij}^{(m)} = 0 \quad \text{if } i\neq j \\ &Q_{11}^{(m)} = Q_{22}^{(m)} = ZeC[\tfrac{1}{2}I(I+1) - \tfrac{3}{2}m^2] \\ &Q_{33}^{(m)} = ZeC[3m^2 - I(I+1)]. \end{aligned} \tag{20}$$

The nuclear quadrupole moment Q is defined by[20]

$$Q = \frac{1}{e} Q_{33}^{(I)} = Z\langle I | 3z_n^2 - r_n^2 | I\rangle; \tag{21}$$

$m_I = I$ is the nuclear state with maximum spin projection on the axis of quantization. Then by (20),

$$eQ = Q_{33}^{(I)} = ZeC\,[3I^2 - I^2 - I] = ZeC[I(2I-1)],$$

so

$$ZeC = eQ/I(2I-1)$$

and the final formulas for the $Q_{ij}^{(m)}$ are

$$\begin{aligned} Q_{ij}^{(m)} &= 0, \quad i \neq j \\ Q_{11}^{(m)} &= Q_{22}^{(m)} = (eQ/I(2I-1))\,[\tfrac{1}{2}I(I+1) - \tfrac{3}{2}m^2] \\ Q_{33}^{(m)} &= (eQ/I(2I-1))\,[3m^2 - I(I+1)]. \end{aligned} \tag{22}$$

For ^{35}Cl and ^{37}Cl, $I = \frac{3}{2}$; thus for the Cl nucleus in HCl (22) becomes

$$\begin{aligned} Q_{ij}^{(m)} &= 0, \quad i \neq j \\ Q_{11}^{(\pm\frac{1}{2})} &= Q_{22}^{(\pm\frac{1}{2})} = eQ/2 \\ Q_{11}^{(\pm\frac{3}{2})} &= Q_{22}^{(\pm\frac{3}{2})} = -eQ/2 \\ Q_{33}^{(\pm\frac{3}{2})} &= eQ \\ Q_{33}^{(\pm\frac{1}{2})} &= -eQ. \end{aligned} \tag{23}$$

Then, taking

$$q_{ij} = \int \rho(\bar{r}_e)\left[\frac{\partial}{\partial x_{e_i}}\frac{\partial}{\partial x_{e_j}}\frac{1}{r_e}\right]d\tau_e, \tag{24}$$

as in Chapter III, (15) becomes

$$E^{(0)}+E^{(2)} = Z\int \rho(\bar{r}_e)/r_e\,d\tau_e+\frac{1}{6}[(eQ/2)q_{xx}+(eQ/2)q_{yy}-eQq_{zz}],$$

$$\text{for } m=\pm\tfrac{1}{2} \tag{25}$$

$$E^{(0)}+E^{(2)} = Z\int \rho(\bar{r}_e)/r_e\,d\tau_e+\frac{1}{6}[-(eQ/2)q_{xx}-(eQ/2)q_{yy}+eQq_{zz}],$$

$$\text{for } m=\pm\tfrac{3}{2} \tag{26}$$

Using $q_{xx}=q_{yy}=-\frac{1}{2}q_{zz}$ (Chapter III, section 1),

$$E^{(0)}+E^{(2)} = Z\int \rho(\bar{r}_e)/r_e\,d\tau_e - \tfrac{1}{2}eQq_{zz},\ m=\pm\tfrac{1}{2} \tag{27}$$

$$E^{(0)}+E^{(2)} = Z\int \rho(\bar{r}_e)/r_e\,d\tau_e + \tfrac{1}{2}eQq_{zz},\ m=\pm\tfrac{3}{2} \tag{28}$$

The operator which yields q_{zz} upon integration over the charge density in (24) is the $\hat{q}$ of Chapter III, sections 1 and 2. Then the operators which correspond to the energy correction terms $E^{(2)}$ in (27) and (28) are

$$H_Q^{(\pm\frac{1}{2})} = -\tfrac{1}{2}eQ\hat{q} \tag{29}$$

$$H_Q^{(\pm\frac{3}{2})} = \tfrac{1}{2}eQ\hat{q} \tag{30}$$

Thus to correct the nuclear attraction integral with the Cl nucleus for the interaction between the nuclear quadrupole and the electron distribution, it suffices to add the term $-\frac{1}{2}eQ\langle\phi_i|\hat{q}|\phi_j\rangle$ or $+\frac{1}{2}eQ\langle\phi_i|\hat{q}|\phi_j\rangle$ to the term $Z\langle\phi_i|\frac{1}{r}|\phi_j\rangle$ in evaluating the nuclear attraction integral between basis orbitals ϕ_i and ϕ_j. We use Koster's[25] value for $Q(^{35}Cl)$ (Chapter I), $-.0782\times10^{-24}$ $cm^2 = -2.793\times10^{-9}$ au (for Q, 1 au = 1 $bohr^2$).

Several comments on the OCE-SCF calculation of HCl including (29) or (30) in the Hamiltonian can be made before performing the calculation. $H_Q^{(m)}$ can be regarded as a perturbing Hamiltonian,

$$H = H_0 + H_Q^{(m)}, \tag{31}$$

with H_0 now the normal SCF Hamiltonian (note the difference between this definition of H_0 and that of (8), where H_0 referred to a spherically symmetric system). ψ_0 and $\psi_Q^{(m)}$ are defined analogously to (2) and (3); the first-order energy correction is[13]

$$E_Q^{(m)} = \langle\psi_0|H_Q^m|\psi_0\rangle = \pm\tfrac{1}{2}eQ\langle\psi_0|\hat{q}|\psi_0\rangle = \pm\tfrac{1}{2}eQq, \tag{32}$$

with ψ_0 the normal OCE-SCF wavefunction. The electronic part of q is tabulated in Chapter III, Table VIII. From this table, q_{elec} for the OCE-SCF calculation of HCl in the GW+9 basis is 3.49418 au; adding the contribution from the proton at R_e=2.4087 au, the total q at the Cl nucleus in this basis is 3.63729 au.

Then, since e=1 in au,

$$E_Q^{(\pm\frac{1}{2})} = -\tfrac{1}{2}(2.793\text{x}10^{-9})(3.63729) = 2.540\text{x}10^{-9} \text{ au} \qquad (33)$$

$$E_Q^{(\pm\frac{3}{2})} = \tfrac{1}{2}(-2.793\text{x}10^{-9})(3.63729) = -2.540\text{x}10^{-9} \text{ au.} \qquad (34)$$

The total energy of the molecule in this calculation is -460.06893838015 au, so the total energy for (33) and (34) is, to first-order,

$$E_{total}^{(\pm\frac{1}{2})} = -460.06893838016 + .00000000254$$
$$= -460.06893837762 \text{ au} \qquad (35)$$

$$E_{total}^{(\pm\frac{3}{2})} = -460.06893838016 + .00000000254$$
$$= -460.06893838270 \text{ au} \qquad (36)$$

Note that the first-order corrections (33) and (34) are very small relative to the total energy. The total energy is carried to 14 significant figures here because, although energy convergence was carried in the iterative process only to 12 significant figures, the highest occupied MO eigenvalue was in this case still changing in excess of its convergence criterion when the energy had converged to 12 figures; when the eigenvalue had converged to 6 figures, the electronic energy had ceased to change in the 14th figure. One expects the second order change in energy to be smaller than (33) and

(34) by a factor of about Q (in au), and thus out of the range of significance of the calculation. Since the first-order wavefunction correction first appears in calculation of the second order energy correction, it appears that calculation of $\psi_Q^{(m)}$ is outside the sensitivity of the OCE-SCF calculation. Thus one expects, upon adding the terms (29) and (30) to the OCE-SCF Hamiltonian, to see no change in the MO coefficients within the range of significance (6 decimal places) and energy changes given by (33) and (34). These calculations were carried out for the GW+9 basis; exactly the expected result was obtained. The MO q values and the total q_{elec} were also unchanged to five decimal places from their values in Chapter III, Table VIII.

However it is possible that the smallness of the change induced in the HCl wavefunction in the GW+9 basis is due to the lack of orbitals in this basis suitable for describing polarization of the 1σ MO. Since the $H_Q^{(m)}$ operators (29) and (30) contain $\hat{q}$ as a factor, the matrix elements $\langle\phi_i|H_Q^{(m)}|\phi_j\rangle$ between basis orbitals are non-zero only if $\langle\phi_i|\hat{q}|\phi_j\rangle$ is non-zero; this is true only for the ℓ_i-ℓ_j pairs of Chapter III, equation (12). In particular, if ϕ_i is an s-orbital, $\langle\phi_i|H_Q^{(m)}|\phi_j\rangle$ is non-zero only if ϕ_j is a d-orbital. Since 1σ MO in the unperturbed wavefunction is composed almost entirely of s-orbitals (Chapter II, Table VI), one does not expect a significant change in the wavefunction to be induced by $H_Q^{(m)}$ unless the basis contains a d-orbital with r_{max} close

to the nucleus (<.1 au, cf. Chapter V, Table IV). The GW basis does not contain such a d-orbital; Chapter III, Table VI shows that the non-s-orbital of lowest r_{max} in this basis has r_{max}=.097 au, and this is a p- rather than d-orbital. To investigate the effect of adding a d-orbital of low r_{max}, OCE-SCF calculations of HCl were done with the Hamiltonian corrections (29) and (30) included for a 22-orbital basis consisting of the GW basis plus a 2pσ and a 3dσ orbital with r_{max}=.025 au (details of this choice are given in the next section). Again the energies were exactly those given by the analogs of (35) and (36). The MO coefficients were unchanged to six decimal places. The EFG, however, was changed within the range of significance by inclusion of the nuclear quadrupole interaction. For this basis without the nuclear quadrupole interaction, q_{elec} is 1.00552 au; with $H_Q^{(\pm\frac{1}{2})}$ included q_{elec}= 1.00486 au; for $H_Q^{(\pm\frac{3}{2})}$, q_{elec}=1.00619 au. Since q_{elec} is estimated to have four significant decimal places (Chapter III), this represents a change of ±7 in the last significant place, which appears too large to be an artifact of the convergence criteria. Note that these q_{elec} are far from the H-F and GW+9 values; the smaller basis was used to reduce the computation time for basis set experimentation and is badly suited to describe the 4σ and 5σ MO's. Here, however, only the 1σ MO is of interest, and the smaller basis is as well suited to describe this MO as would be the 31-orbital basis formed by adding the 2pσ and 3dσ orbitals with r_{max}=.025 au to the GW+9 basis. The

calculations including the nuclear quadrupole interaction in both the GW+9 and 22-orbital bases are summarized in Table II. To our knowledge this is the first report of an SCF calculation directly including $H_Q^{(m)}$ in the Hamiltonian. The appearance of this effect is probably due to the fact that several (≈5) iterations beyond 12-figure energy convergence are needed to attain 6-figure eigenvalue convergence; an effect too small to be resolved by the energy convergence may be resolved by the eigenvalue convergence.

In addition the induced q_{elec} agrees roughly with an order-of-magnitude estimate by first-order perturbation theory. The coefficient C_{3d} of the 3dσ AO with r_{max}=.025 in the perturbed 1σ MO (i.e. the 1σ MO with H_Q^m included in the Hamiltonian) is, by first-order theory, $\langle\phi_{1s}|H_Q^m|\phi_{3d}\rangle/(E_{1s}-E_{3d})$, since the 1s AO of the GW basis is approximately the unperturbed 1σ MO. The methods of Chapter III give $\langle\phi_{1s}|\hat{q}|\phi_{3d}\rangle \approx 5\times10^3$; then $\langle\phi_{1s}|H_Q^m|\phi_{3d}\rangle \approx 4\times10^{-6}$, with all values in au. In the unperturbed OCE-SCF wavefunction, one of the unoccupied MO's is almost exactly the 3dσ AO with r_{max}=.025 au; the difference of the eigenvalue of this MO and the 1σ MO is $\approx 7\times10^2$ au. Thus $C_{3d} \approx \pm 5\times10^{-9}$. Then the contribution of the 1s-3d interaction to the q of this MO is $\approx -4C_{1s}C_{3d}\langle\phi_{1s}|\hat{q}|\phi_{3d}\rangle$, with the negative sign from the electronic charge and the factor of 4 from the orbital occupancy (2) and the fact that the interaction is off-diagonal and appears twice in the summation for the MO q. Thus the induced change in q should be

TABLE II: Effect of including ^{35}Cl quadrupole interaction in Hamiltonian upon calculated q_{elec} in HCl in two OCE bases. All calculations at r_e=2.4087 au. All values in atomic units.

	GW+9[a]		
	contributions to q_{elec}		
shell	NQ[b]	$m=\pm\frac{1}{2}$	$m=\pm\frac{3}{2}$
1	-.00005	-.00005	-.00005
2	.53881	.53881	.53882
3	2.95542	2.95542	2.95542
total q_{elec}	3.49418	3.49418	3.49419
q_{nuc}	.14311	.14311	.14311
total q	3.63729	3.63729	3.63730

continued

TABLE II: (cont'd.)

GW+9 (cont'd.)

elec. energy	-467.12668737338	-467.12668737094	-467.12668737582
nuc. point-charge rep.	7.05774899322	7.05774899322	7.05774899322
nuc. quad. interact. with proton field[c]	- - - -	.00000000010	-.00000000010
total energy	-460.06893838016	-460.06893837762	-460.06893838270

1st order energy correction, $m=\pm\frac{1}{2}$: $.25 \times 2.793 \times 10^{-9} \times 3.63729 = 2.540 \times 10^{-9}$

1st order energy correction, $m=\pm\frac{3}{2}$: $-.25 \times 2.793 \times 10^{-9} \times 3.63729 = -2.540 \times 10^{-9}$

total energy to 1st order, $m=\pm\frac{1}{2}$: $-460.06893838016 + .00000000254 = -460.06893837762$

total energy to 1st order, $m=\pm\frac{3}{2}$: $-460.06893838016 - .00000000254 = -460.06893838270$

continued

TABLE II: (cont'd.)

	22-orbital basis[d]		
	contributions to q_{elec}		
shell	NQ[b]	$m=\pm\frac{1}{2}$	$m=\pm\frac{3}{2}$
1	-.01715	-.01776	-.01654
2	-.36216	-.36221	-.36211
3	1.38483	1.38482	1.38483
total q_{elec}	1.00552	1.00486	1.00619
q_{nuc}	.14311	.14311	.14311
total q	1.14863	1.14797	1.14930

continued

TABLE II: (cont'd.)

	22-orbital basis[d] (cont'd.)		
elec. energy	-467.00009206644	-467.00009206574	-467.00009206714
nuc. point-charge rep.	7.05774899322	7.05774899322	7.05774899322
nuc. quad. interact. with proton field[c]	- - - -	.00000000010	-.00000000010
total energy	-459.94234307322	-459.94234307242	-459.94234307402

1st order energy correction, $m=\pm\frac{1}{2}$: $.25 \times 2.793 \times 10^{-9} \times 1.14863 = .8020 \times 10^{-9}$

1st order energy correction, $m=\pm\frac{3}{2}$: $-.25 \times 2.793 \times 10^{-9} \times 1.14863 = -.8020 \times 10^{-9}$

total energy to 1st order, $m=\pm\frac{1}{2}$: $-459.94234307322 + .00000000080 = -459.94234307242$

total energy to 1st order, $m=\pm\frac{3}{2}$: $-459.94234307322 - .00000000080 = -459.94234307402$

[a]Basis defined Chapter III, section 4.

[b]Nuclear quadrupole interaction neglected (normal H-F Hamiltonian).

[c]$\pm\frac{1}{2}eQq_{nuc}$, with $Q=-2.793 \times 10^{-9}$ au and $q_{nuc}=.14311$ au.

[d]GW basis of Chapter III, Table VI with $2p\sigma$ and $3d\sigma$ orbitals added with $r_{max}=.025$ au.

$\approx \pm 4\times1\times5\times10^{-9}\times5\times10^{3} \approx \pm1\times10^{-4}$ au. The observed induced change was $\approx \pm 7\times10^{-4}$; since the above estimate is very rough the agreement is reasonable.

Note that the 22-orbital basis gives a negative contribution to q_{elec} from the 2nd electron shell (2σ, 3σ, and 1π MO's) in contradiction to all calculations in Table I; this is because the σ-basis was increased without a corresponding π-basis increase to preserve the balance between the 3σ and 1π MO's. A calculation in a 26-orbital basis including $2p\pi$ and $3d\pi$ orbitals with r_{max}=.025 was done to verify this (without $H_Q^{(m)}$ included); the 2nd shell in this case contributed .34039 au to q_{elec}, in good agreement with the comparable (GW) basis in Chapter III, Table XI. The 1σ MO q was unchanged. The 22-orbital calculations are analysed in terms of orbital pair contributions in Table III; note that essentially all the q of the 1σ MO is due to s-d pairs, and the changes with m_I are concentrated in this pair type.

Before accepting the above changes in q_{elec} as being effects of the nuclear quadrupole interaction rather than artifacts of the convergence criteria it is important to verify that these changes are of the sign expected for this interaction. Since the quadrupole moment of Cl (for both ^{35}Cl and ^{37}Cl) is negative[25], the nucleus is flattened along the spin axis ("like a Gouda cheese"[26]), with charge more concentrated in the plane perpendicular to the spin axis than along it. Since the spin number $I=\frac{3}{2}$ for both isotopes, the nuclear angular momentum has

TABLE III: Orbital pair type analysis of total q_{elec} and q of the 1σ MO for OCE-SCF calculations of HCl in 22-orbital basis[a] including nuclear quadrupole interaction. All quantities in atomic units.

	contribution to q_{elec} from 1σ MO		
pair type	NQ[b]	$m=\pm\frac{1}{2}$	$m=\pm\frac{3}{2}$
s-d	-.01715	-.01776	-.01654
p-p	.00000	.00000	.00000
d-d	.00000	.00000	.00000
total 1σ q	-.01715	-.01776	-.01654

	total q_{elec}		
pair type	NQ[b]	$m=\pm\frac{1}{2}$	$m=\pm\frac{3}{2}$
s-d	-.05714	-.05780	-.05648
p-p	1.08206	1.08206	1.08206
d-d	-.01940	-.01940	-.01940
total q_{elec}	1.00552	1.00486	1.00619

[a]GW basis of Chapter III, Table VI, with 2pσ and 3dσ orbitals added with r_{max}=.025 au.

[b]Nuclear quadrupole interaction neglected (normal H-F Hamiltonian).

the magnitude $\sqrt{\frac{3}{2}(\frac{3}{2}+1)}\,\hbar = (\sqrt{15}/2)\hbar$; the projection upon the axis of spin quantization is $\pm\frac{3}{2}\hbar$ for $m_I = \pm\frac{3}{2}$ and $\pm\frac{1}{2}\hbar$ for $m_I = \pm\frac{1}{2}$. A simple trigonometric calculation shows that the $m_I = \pm\frac{3}{2}$ case corresponds classically to the spin axis inclined at an angle of about 39°14' to the spin quantization axis; the $m_I = \pm\frac{1}{2}$ case corresponds to an inclination of about 75°32' to the quantization axis. The spin vector precesses about the quantization axis so that cylindrical symmetry about this axis is preserved[18] (Figure 1). The result is that for $m_I = \pm\frac{1}{2}$ there is a relative increase of positive charge along the spin quantization axis (in HCl the principal EFG axis) and a relative depletion of positive charge in the plane perpendicular to this axis; for $m_I = \pm\frac{3}{2}$ the opposite is true. In a classical electrostatic view, the $m_I = \pm\frac{1}{2}$ case would tend to cause a relative increase in electron density along the z-axis and a depletion along the x- and y-axes; the opposite holds for $m_I = \pm\frac{3}{2}$. The field of the proton produces a relative depletion of charge close to the nucleus on the z-axis and an increase along the x- and y-axes (Chapter V); thus the $m_I = \pm\frac{3}{2}$ nuclear orientation should reinforce the polarization by the proton and increase the absolute value of q_{elec} over the value calculated without the nuclear quadrupole interaction, while the $m_I = \pm\frac{1}{2}$ orientation should give a q_{elec} decreased in absolute value. This is in fact what was observed above (Table II), which supports the hypothesis that the changes observed in q_{elec} are indeed due to polarization by the quadrupolar nucleus.

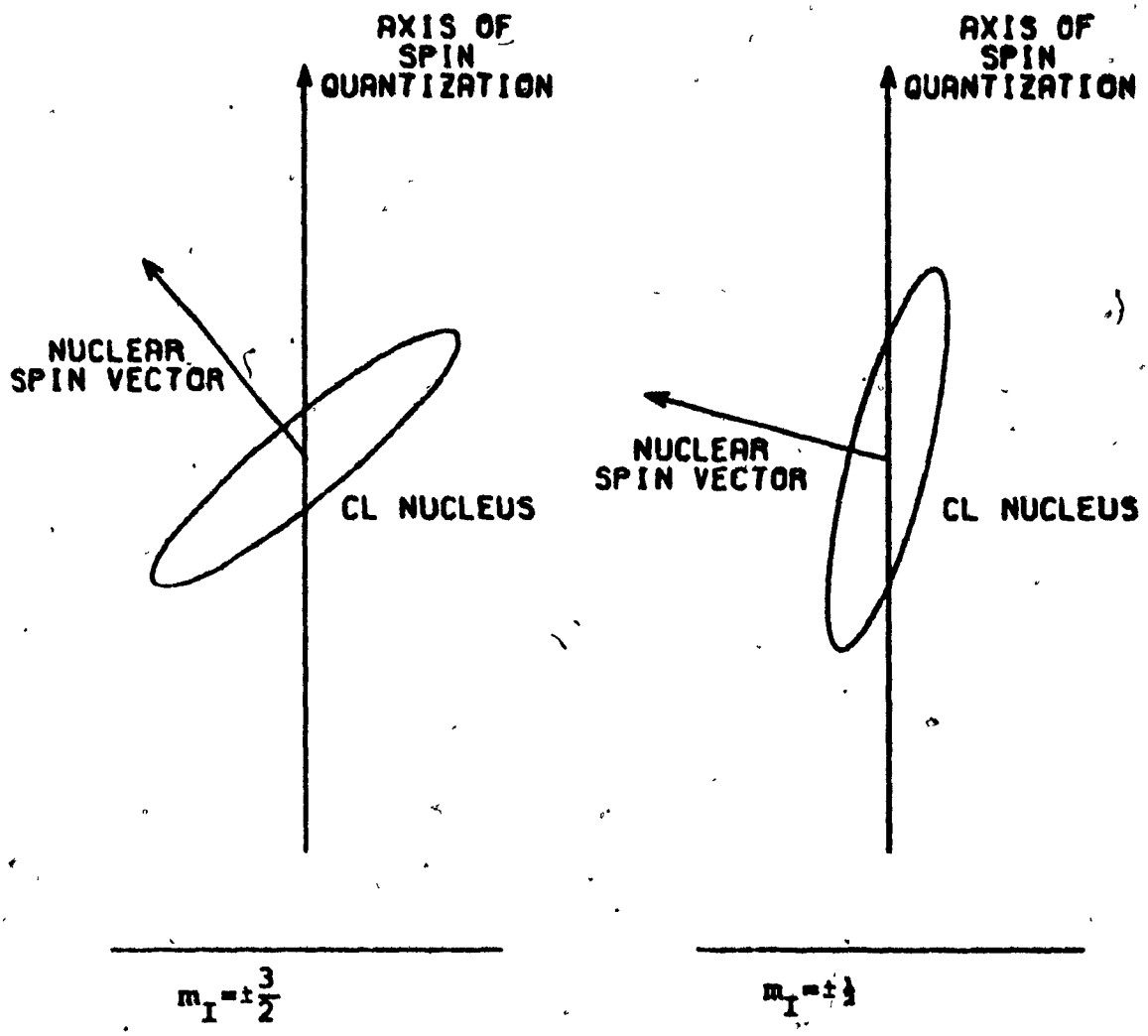

Figure 1. Possible orientations of the Cl nucleus ($I=\frac{3}{2}$). The nuclear spin vector precesses about the axis of spin quantization.

Since the calculated change in q induced by the nuclear quadrupole interaction is about .0007 au, and the total q is about 3.6 au, the relative change is about .02%. However because of the limited basis experimentation and the smallness of the perturbation this should be taken only as an order-of-magnitude estimate; the actual relative change probably lies somewhere in the range .01% - .1%. Grigolini and Moccia[27] have performed a complicated perturbation calculation of the EFG induced by the quadrupole moment of ^{14}N in NH_3; they were forced to make several approximations of unknown accuracy. They estimated a change in q due to the polarization by the nucleus of about .1%. This agrees roughly with our calculation for HCl. It should be made clear here that we do not propose direct inclusion of $H_Q^{(m)}$ in the SCF Hamiltonian as a method for accurate calculation of the induced changes in q; a serious calculation of this effect, such as that of Grigolini and Moccia, would have to employ a perturbation treatment. It is noteworthy, however, that a change in q_{elec} within the range of significance of the calculation is induced by direct inclusion of $H_Q^{(m)}$ if suitable basis orbitals are included.

3. Polarization of the 1σ MO by the proton

All bases in the GW+N series gave contributions to q_{elec} from the 1σ MO of about -.00005 au (Chapter III, Table VIII). The two near H-F TCE-SCF wavefunctions for HCl disagree

rather greatly on the q for this MO, the McLean-Yoshimine[1] wavefunction giving -.00214 au, the Cade-Huo[2] giving -.00013 au. None of these bases contain orbitals with $\ell > 0$ with $r_{max} < .1$ au, which, in view of Chapter V, Table IV, would be necessary to describe accurately a non-spherical 1σ MO. Thus a natural hypothesis for explaining the disagreement among the three calculations on the q of the 1σ MO is that all the calculations underestimate the absolute value of this quantity, a more flexible basis for low r being necessary to approach the H-F value.

In order to test this hypothesis a series of calculations was made with augmented bases. Orbitals were added to the 20-orbital GW basis[28] rather than the GW+9 basis in order to reduce the computation time, with the understanding that the 4σ and 5σ MO's in these bases would be unreliable. In view of the heavy contributions of p-orbitals to the 3σ, 4σ, and 5σ MO's, it would seem by analogy that a p-orbital with low r_{max} should be added to the GW basis. However, as in Chapter III, equation (12), an s-p orbital pair makes no contribution to q_{elec}; changes in q_{elec} would be expected to be due mainly to s-d pairs. Thus for study of q of the 1σ MO it is important to add a d-orbital of low r_{max}. Two trial OCE-SCF calculations were done in 21-orbital bases, one adding only a $2p\sigma$ orbital with r_{max}=.05 au to the GW basis (Chapter III, Table VI), the other adding only a $3d\sigma$ orbital with the same r_{max}. The $2p\sigma$ orbital caused a much larger lowering of

the energy than did the 3dσ orbital, but the 3dσ caused a much larger change in q of the 1σ MO; for subsequent calculations both a 2pσ and a 3dσ orbital of the same r_{max} were added to the GW basis, making a 22-orbital basis.

Three r_{max} values were tried: .05 au, .025 au, and .01 au. The lowest energy was calculated for .025, and the highest for r_{max}=.01 au. The energies and electron shell q's for these calculations and the unaugmented GW basis are given in Table IV. Note that the 2nd shell q changes greatly with r_{max}; as mentioned in section 2 this is because addition of the two σ orbitals creates an unbalance between the σ and π MO's of the 2nd shell. The r_{max}=.025 au basis was chosen for the $H_Q^{(m)}$ calculations of section 2 because it gives the lowest energy of the three; however it is not entirely clear that this is a good criterion since the 2pσ and 3dσ orbitals of low r_{max} do participate slightly in the MO's of the 2nd and 3rd shells and it is possible that the energy is more sensitive to the participation in these MO's than in the 1σ MO; thus the minimum of energy with respect to r_{max} may not be an indicator of suitability for describing the 1σ MO. However since the p basis orbitals for the 2nd shell in the GW, McLean-Yoshimine, and Cade-Huo bases all have r_{max}= .1 au, and since the minimum of energy with r_{max} in Table IV lies somewhere between .025 and .05 au, we will assume that this minimum indicates basis suitability for the first shell, with the understanding that more extensive orbital additions could prove this wrong. The orbital

TABLE IV: Electron shell analysis of q_{elec}, and energies, for HCl in 22-orbital bases, GW+2pσ+3dσ, r_{max}=.01, .025, .05 au. All calculations at r_e=2.4087 au. All quantities in atomic units.

shell	.01 au	.025 au	.05 au	GW basis
1	-.00155	-.01715	-.03496	-.00002
2	.05693	-.36216	.00248	.36271
3	1.39231	1.38483	1.40475	1.40430
q_{elec}	1.44768	1.00552	1.37227	1.76700
E_{elec}	-466.999944	-467.000092	-466.999985	-466.999903
E_{tot}	-459.942195	-459.942343	-459.942236	-459.942154

pair partitioning of the contributions to q_{elec} and to the q of the 1σ MO for these wavefunctions is given in Table V; note that the largest absolute changes with r_{max} are in the p-p pairs and in shells other than the first, whose net q are due mainly to the σ-π basis imbalance. The largest relative changes are for the s-d pairs. As in Table III, essentially all the 1σ MO q is due to s-d pairs.

Since the energy minimum with respect to r_{max} lies somewhere between r_{max}=.025 au and r_{max}=.05 au, it is expected that the 1σ MO q at the minimum energy r_{max} is between the values for these two bases, or somewhere between .01 au and .04 au. The 1σ MO should have about the same q in a more extensive basis including the same 2pσ and 3dσ orbital pair. Since the total molecular q for the GW+9 basis is about 3.6 au, addition of orbitals suitable for describing the distortion of the 1σ MO by the field of the proton causes a relative change in q of between .01/3.6 and .04/3.6, of the order of 1%. Note that this is roughly ten times as large as the relative change produced by the inclusion of the nuclear quadrupole interaction in the SCF Hamiltonian in section 2.

The implication for TCE-SCF calculations of HCl is clear: if suitable p- and d-orbitals of low r_{max} were added to the basis, the 1σ MO would have a q of between -.01 and -.04 au. This would induce in the total q_{elec} a change .1 to .5 the size of the difference between the q_{elec} of the McLean-Yoshimine and Cade-Huo wavefunctions; however it would change both in the

TABLE V: Orbital pair type analysis of q_{elec} for HCl OCE-SCF wavefunctions in 22-orbital bases, GW+2pσ+3dσ, r_{max}=.01, .025, .05 au. All quantities in atomic units. Calculations at r_e=2.4087 au.

	total q_{elec}			
pair type	.01 au	.025 au	.05 au	GW basis
s-d	-.03711	-.05714	-.08663	-.03514
p-p	1.50419	1.08206	1.47832	1.82154
d-d	-.01940	-.01940	-.01942	-.01940
total q_{elec}	1.44768	1.00552	1.37227	1.76700

	1σ MO q			
pair type	.01 au	.025 au	.05 au	GW basis
s-d	-.00155	-.01715	-.03496	-.00001
p-p	.00000	.00000	-.00001	.00000
d-d	.00000	.00000	.00000	.00000
total	-.00155	-.01715	-.03496	-.00002

same direction and thus not explain the difference between the two which (Table I) is clearly due to the third shell (4σ, 5σ, and 2π MO's). Thus the change in q induced by adding orbitals to describe the distortion of the 1σ MO is important, since it accounts for about 1% of the total q, but cannot remove the uncertainty of about 6% in the H-F limit for q_{elec} in HCl from existing TCE-SCF calculations (Chapter IV, section 2). Inclusion of the nuclear quadrupole interaction with the electron distribution in the SCF Hamiltonian would not result in an important change in q_{elec}.

REFERENCES

1. A.D. McLean and M. Yoshimine, J. Chem. Phys. 47, 3256 (1967).
2. P.E. Cade and W.M. Huo, J. Chem. Phys. 47, 649 (1967).
3. A.D. McLean and M. Yoshimine, Tables of Linear Molecule Wave Functions, Supplement to IBM Journal of Research and Development, 1967.
4. R.M. Sternheimer, Phys. Rev. 80, 102 (1950).
5. R.M. Sternheimer, Phys. Rev. 84, 244 (1951).
6. Sternheimer has published many papers on this effect, the major ones being those cited above and below and: Phys. Rev. 86, 316 (1952), Phys. Rev. 96, 951 (1954), Phys. Rev. 105, 158 (1957), Phys. Rev. 146, 140 (1966), Phys. Rev. 159, 266 (1967), Phys. Rev. 164, 10 (1967), Phys. Rev. A 6, 1702 (1972); R.M. Sternheimer and R.F. Peierls, Phys. Rev. A 3, 837 (1971), Phys. Rev. A 4, 1722 (1971).
7. E.A.C. Lucken, Nuclear Quadrupole Coupling Constants, Academic, N.Y., 1969. Chapter 5.
8. A. Abragam, Principles of Nuclear Magnetism, Oxford, 1961. p. 168.
9. a. S.L. Kahalas and R.K. Nesbet, J. Chem. Phys. 39, 529 (1963).

   b. C. Schwartz, Phys. Rev. 105, 173 (1957).
10. R.M. Sternheimer, Phys. Rev. 95, 736 (1954).

11. R.M. Sternheimer and H.M. Foley, Phys. Rev. 92, 1460 (1953).

12. J.O. Hirschfelder, W.B. Brown, and S.T. Epstein, Adv. Quant. Chem. 1, 255 (1964).

13. H. Eyring, J. Walter, and G.E. Kimball, Quantum Chemistry, Wiley, N.Y., 1944. p. 94.

14. A. Dalgarno and A.L. Stewart, Proc. Roy. Soc. A247, 245 (1958).

15. A. Dalgarno and A.L. Stewart, Proc. Roy. Soc. A238, 269 (1956).

16. J.C. Slater, Quantum Theory of Atomic Structure, v. 1, McGraw-Hill, N.Y., 1960. Appendix 17.

17. R.M. Stevens, R.M. Pitzer, and W.N. Lipscomb, J. Chem. Phys. 38, 550 (1963).

18. M.H. Cohen and F. Reif, Solid State Physics 5, 321 (1957).

19. J.D. Jackson, Classical Electrodynamics, Wiley, N.Y., 1962. p. 100.

20. N.F. Ramsey, Nuclear Moments, Wiley, N.Y.,1953. Chapter 2.

21. Reference 7, Chapter 3.

22. E.P. Wigner, Group Theory and its Application to the Quantum Mechanics of Atomic Spectra, Academic, N.Y., 1959. p. 245.

23. C. Eckart, Revs. Mod. Phys. 2, 305 (1930), esp. pp. 352-354.

24. P.M. Brink and G.R. Satchler, Angular Momentum, 2nd ed., Oxford, 1968. p. 9.

25. G.F. Koster, Phys. Rev. 86, 148 (1952).

26. E. Schemp and P.J. Bray, in Physical Chemistry: an Advanced Treatise, v. IV, H. Eyring, D. Henderson, and W. Jost. ed., Academic, N.Y., 1970. pp. 521-632, esp. p. 527.

27. P. Grigolini and R. Moccia, J. Chem. Phys. 57, 1369 (1972).

28. T.L. Gilbert and A.C. Wahl, J. Chem. Phys. 55, 5247 (1971).

29. E.W. Kaiser, J. Chem. Phys. 53, 1686 (1970).

APPENDIX I: Integral evaluation

Two very different classes of integrals were needed for this work: the one-center integrals for the OCE-SCF calculations (Chapter II) and the two-center EFG integrals (Chapter IV). The only point in common between the two types is that they are both over STO's. The two are treated in separate sections, after an introductory section defining the basis functions. Discussion is minimal in the interest of brevity.

1. Definitions

a) Associated Legendre polynomial[1]:

$$P_\ell^{|m|}(\cos\theta) = (-1)^\ell \frac{\sin^{|m|}(\theta)}{2^\ell \ell!} \frac{d^{\ell+|m|}}{d(\cos\theta)^{\ell+|m|}} \sin^{2\ell}(\theta) \qquad (1)$$

b) Normalized associated Legendre polynomial[1]:

$$\Theta_\ell^{|m|}(\cos\theta) = \left(\frac{2\ell+1}{2}\frac{(\ell-|m|)!}{(\ell+|m|)!}\right)^{\frac{1}{2}} P_\ell^{|m|}(\cos\theta) \qquad (2)$$

c) Normalized real spherical harmonic[2]:

$$S_{\ell 0}(\theta,\phi) = \frac{1}{\sqrt{2\pi}}\,\Theta_\ell^0(\cos\theta)$$

$$S_{\ell|m|}(\theta,\phi) = \frac{1}{\sqrt{\pi}}\,\Theta_\ell^{|m|}(\cos\theta)\cos|m|\phi \qquad (3)$$

$$S_{\ell-|m|}(\theta,\phi) = \frac{1}{\sqrt{\pi}}\,\Theta_\ell^{|m|}(\cos\theta)\sin|m|\phi$$

In all cases $|m| \leq \ell, \ell \geq 0$.

d) Normalized complex spherical harmonic[1]:

$$Y_{\ell m}(\theta,\phi) = \frac{1}{\sqrt{2\pi}}\,\Theta_{\ell}^{|m|}(\cos\theta)\,\exp\,(im\phi), \qquad (4)$$

$$|m| \leq \ell,\ \ell \geq 0.$$

e) Normalized real spherical harmonics in terms of normalized complex spherical harmonics:

$$S_{\ell m}(\theta,\phi) = \frac{i^{\left(\frac{\mathrm{sgn}(m)-1}{2}\right)}}{\sqrt{2}}\left(Y_{\ell m}(\theta,\phi) + \mathrm{sgn}(m)\,Y_{\ell -m}(\theta,\phi)\right),\ \text{for } m \neq 0$$

$$= Y_{\ell 0}(\theta,\phi),\ m=0, \qquad (5)$$

with $\mathrm{sgn}(m)=1$ if $m>0$ and -1 if $m<0$.

f) Normalized real Slater-type orbital (STO)[2,3]:

$$\phi(n,\ell,m,\zeta,r,\theta,\phi) = \left(\frac{(2\zeta)^{2n+1}}{(2n)!}\right)^{\frac{1}{2}} r^{n-1}\exp(-\zeta r)\,S_{\ell m}(\theta,\phi)$$

$$\equiv N\, r^{n-1}\exp(-\zeta r)\,S_{\ell m}(\theta,\phi), \qquad (6)$$

$n \geq 1, 0 \leq \ell \leq n-1, -\ell \leq m \leq \ell$, all integers, $\zeta > 0$. N is the radial normalization constant.

2. One-center integrals

A) Types of integrals

(i) Basic molecular integrals

a) Electron repulsion:

$$[ij|k\ell] \equiv \int d\tau_1 d\tau_2 \phi_i^*(1)\phi_k^*(2) r_{12}^{-1}\phi_j(1)\phi_\ell(2);$$

i,j etc. label orbitals; 1,2 label electrons.

b) Nuclear attraction with non-central nucleus:

$$\langle \phi_i(1) | \frac{1}{r_{1a}} | \phi_j(1) \rangle,$$

with r_{1a} the distance between electron 1 and off-center nucleus a. In the Fock matrix this must be multiplied by $-Z_a$.

c) Overlap:

$$\langle \phi_i(1) | \phi_j(1) \rangle,$$

d) Nuclear attraction with central nucleus:

$$\langle \phi_i(1) | \frac{1}{r_1} | \phi_j(1) \rangle,$$

r_1 the radial coordinate of electron 1 in the spherical system on the central nucleus. In the Fock matrix this is multiplied by -Z.

e) Kinetic energy:

$$\langle \phi_i(1) | -\tfrac{1}{2}\nabla^2 | \phi_j(1) \rangle,$$

with $\nabla^2 = \frac{\partial^2}{\partial x^2} + \frac{\partial^2}{\partial y^2} + \frac{\partial^2}{\partial z^2}$.

(ii) Auxiliary integrals

a) Integral over product of three real normalized spherical harmonics:

$$\left[\begin{smallmatrix}\ell\ell' L\\ mm' M\end{smallmatrix}\right] = \int_0^{\pi}\sin\theta d\theta \int_0^{2\pi} d\phi S_{\ell m}(\theta,\phi) S_{\ell' m'}(\theta,\phi) S_{LM}(\theta,\phi). \qquad (7)$$

The square bracket notation is not standard for this quantity but is used here for convenience.

b) Radial integral, Type I:

$$\int_0^{\infty} r^k \exp(-ar) dr = k!/a^{k+1}, \qquad (8)$$

integer $k \geqslant 0$, real $a > 0$. This is related to the usual Γ-function[4].

c) The A-function[5,6]:

$$A_k(a) = (-1)^k \left(\frac{d}{da}\right)^k \frac{\exp(-a)}{a}, \qquad (9)$$

$k \geqslant 0$ integral, real $a \neq 0$.

d) Radial integral, Type II:

$$\int_0^1 r^k \exp(-ar) dr, \qquad (10)$$

$k \geqslant 0$ integral, real $a > 0$.

e) Double radial integral:

$$\int_0^\infty dr_1 r_1^{k_1} \exp(-a_1 r_1) \int_{r_1}^\infty dr_2 r_2^{k_2} \exp(-a_2 r_2), \qquad (11)$$

integers $k_1, k_2 \geq 0$, real $a_1, a_2 > 0$.

B) Evaluation of auxiliary integrals

(1) Integral over product of three real normalised spherical harmonics:

a) Formulas

Formulas have been published for the integral over three complex spherical harmonics[7,8]:

$$(\ell\ell' L|mm' M) = \int_0^\pi \sin\theta d\theta \int_0^{2\pi} d\phi Y_{\ell m}(\theta,\phi) Y_{\ell' m'}(\theta,\phi) Y_{LM}(\theta,\phi)$$

$$= \frac{1}{\sqrt{2\pi}} \frac{(-1)^{g-\ell-|m'|}(2g-2\ell)!g!}{(g-\ell)!(g-\ell')!(g-L)!(2g+1)!} \cdot$$

$$\cdot \left(\frac{(2\ell+1)(2\ell'+1)(2L+1)(L-|m|-|m'|)!(\ell+|m|)!(\ell'+|m'|)!(\ell'-|m'|)!}{2(L+|m|+|m'|)!(\ell-|m|)!}\right)^{\frac{1}{2}} \cdot$$

$$\cdot \sum_t (-1)^t \frac{(L+|m|+|m'|+t)!(\ell+\ell'-|m|-|m'|-t)!}{(L-|m|-|m'|-t)!(\ell-\ell'+|m|+|m'|+t)!(\ell'-|m'|-t)!t!} \qquad (12)$$

for $m+m'+M=0$ and $|m|+|m'|=M$; $2g=\ell+\ell'+L$, g an integer; $|\ell-\ell'| \leq L \leq \ell+\ell'$; integer t ranging through all values (≥ 0) that do not lead to negative arguments of factorials. The integral is zero unless the above conditions are met. Assume that m, m', M are such that the absolute value of the sum of

any two equals the absolute value of the third (the integral is zero otherwise), and that $\ell+\ell'+L$ is even with $|\ell-\ell'|\leq L\leq \ell+\ell'$. Then it follows from (5) that:

$$
\begin{aligned}
\begin{bmatrix}\ell\ell' L\\ mm' M\end{bmatrix} &= \frac{1}{\sqrt{2}}(\ell\ell' L,-mm' M), && \text{if } m,m' M > 0\\
&= -\frac{1}{\sqrt{2}}(\ell\ell' L,mm' M), && \text{if one of } m,m',M > 0 \text{ and the other}\\
& && \text{two } <0 \text{ and } m+m'+M=0\\
&= \frac{1}{\sqrt{2}}(\ell\ell' L,-mm' M), && \text{if one of } m,m',M > 0 \text{ and the other}\\
& && \text{two } <0 \text{ and } -m+m'+M=0\\
&= (\ell\ell' L,|m|,-|m'|,0), && \text{if one of } m,m',M=0; \text{ must have}\\
& && |m|=|m'|.\\
&= (\ell\ell' L,000), && \text{if } m,m',M=0\\
&= 0, && \text{in all other cases.} \qquad (13)
\end{aligned}
$$

In all of the above a permutation of the ℓ-m pairs may be necessary so that $|m|+|m'|=M$.

b) Documentation

No tables exist for the $\begin{bmatrix}\ell\ell' L\\ mm' M\end{bmatrix}$ directly, but the $(\ell\ell' L,mm' M)$ are simply related to the 3j-symbols[9]. Table I compares values of $(\ell\ell' L,mm' M)$ for a range of index values

TABLE I: Integrals over three complex spherical harmonics, equation (12); comparison between subroutine DGAUNT and tables of Rotenberg et al[9].

ℓ	ℓ'	L	m	m'	M	DGAUNT and table[a]
0	0	0	0	0	0	.28209479177388
1	0	1	0	0	0	.28209479177388
1	0	1	1	0	-1	.28209479177388
1	1	2	1	0	-1	.21850968611842
1	1	2	1	-1	0	-.12615662610101
2	2	2	0	0	0	.18022375157287
2	3	5	1	-1	0	-.16943317729359
2	8	8	0	-1	1	.15271591580648
2	8	8	-1	-1	2	$.68037933497716\times10^{-1}$
3	3	6	1	0	-1	.22177545476550
4	6	8	-1	-1	2	.13277080895316
6	8	8	0	0	0	.10742199291837
6	8	8	0	-1	1	$.76090578317175\times10^{-1}$
6	8	8	-1	0	1	$.41022451154285\times10^{-1}$
6	8	8	-1	-1	2	.10054386748407
6	8	8	2	-1	-1	.11007478726157
7	7	8	-1	-1	2	.10687376255394
8	8	8	0	0	0	.10032076135028
8	8	8	0	-1	1	$.50160380675141\times10^{-1}$
8	8	8	1	1	-2	.10174382195135

continued

TABLE 1: (cont'd.)

[a]Values were converted from the power-of-primes notation of ref. 9 to decimal representation in double precision (16 significant figures) on the IBM 360 and printed to 14 significant figures. In all cases the output of DGAUNT was identical to this length.

computed by the author's routine for (12) (subroutine DGAUNT) with values calculated from the 3j-symbol table of Rotenberg et al[9]. These tables are in a power-of-primes notation so the only limit to the number of figures accuracy the tables yield is that imposed by the computer used to convert from the power-of-primes notation to decimal notation. In Table I the value calculated by DGAUNT and from the tables is given to 14 significant figures. Only $|m|$ values ≤ 2 are tabulated since only these arose in calculations with the basis sets used in this thesis; other $|m|$ values were tested against the tables and agreed similarly. Some $[{}^{\ell\ell' L}_{mm' M}]$ were calculated by hand to insure the accuracy of (13). DGAUNT is accurate to at least 14 significant figures; $[{}^{\ell\ell' L}_{mm' M}]$ (subroutine RETRIP) should have similar accuracy.

(ii) Radial integral, type I:

No discussion necessary since this integral is equal to a simple quotient.

(iii) The A function:

The recursion formula for the A-function is[6,10]

$$A_k(a) = A_0(a) + \frac{k}{a} A_{k-1}(a), \tag{14}$$

with

$$A_0(a) = \exp(-a)/2.$$

If $a > 0$ all terms in the recursion process are positive; if

$a < 0$ they are all negative. Either way no cancellation errors can arise in the application of (14)[11]. Values from our routine for this function (subroutine A) were compared with those of Miller et al.[12]; they are not tabulated here since this is not a numerically difficult function. Agreement was to 14 significant figures, the number tabulated by Miller et al.

(iv) Radial integral, Type II

a) Formulas

This integral can be expressed

$$\int_0^1 r^k \exp(-ar)dr = \int_0^\infty r^k \exp(-ar)dr - \int_1^\infty r^k \exp(-ar)dr;$$

from (9) it can be verified that for $a > 0$ the second integral is $A_k(a)$; then

$$\int_0^1 r^k \exp(-ar)dr = k!/a^{k+1} - A_k(a). \qquad (15)$$

However another expression for $A_k(a)$ is[13]

$$A_k(a) = \frac{k!\exp(-a)}{a^{k+1}} \sum_{n=0}^{k} \frac{a^n}{n!}; \qquad (16)$$

the finite sum is the first n+1 terms of the series for exp(a). If a is small and k large the sum will nearly converge to exp(a), which would give $A_k(a) \approx k!/a^{k+1}$ and a large cancellation error would result from direct application of (15). To avoid this (15) may be written

$$\int_0^1 r^k \exp(-ar)\,dr = \frac{k!\exp(-a)}{a^{k+1}} \sum_{n=0}^{\infty} \frac{a^n}{n!} - \frac{k!\exp(-a)}{a^{k+1}} \sum_{n=0}^{k} \frac{a^n}{n!}$$

$$= \frac{k!\exp(-a)}{a^{k+1}} \sum_{n=k+1}^{\infty} \frac{a^n}{n!}, \qquad (17)$$

with the sum truncated when the terms fall below the range of significance of the calculation. (17) is most accurate for small a and large n, since for these conditions the summation converges in the fewest terms. More precisely, (15) should be numerically accurate if

$$k!/a^{k+1} - A_k(a) > \frac{1}{10}\, k!/a^{k+1}, \qquad (18)$$

since then not more than one of the 16 significant figures in the machine representation is lost through cancellation. In our routine for this function (subroutine ATTSER) (15) was used if (18) held; if not, (17) was used.

b) Documentation

These integrals are related to Pearson's incomplete Γ-function[14,15] by

$$I(a,n) = \frac{1}{n!}\, a^{n+1} (n+1)^{\frac{n+1}{2}}\, F(n, a(n+1)^{\frac{1}{2}}),$$

with

$$F(n,a) = \int_0^1 r^n \exp(-ar)\,dr$$

and $I(a,n)$ Pearson's incomplete Γ-function. In Table II values of $I(a,n)$ calculated using our routine ATTSER for $F(n,a)$ are compared with the 11-significant figure values tabulated by Harter[16]. We estimate our integrals to have at least 14-significant figures. The tabulated values represent cases of both (15) and (17).

(v) Double radial integral

By the change of variable $t=r_2/r_1$ the integral (11) becomes:

$$\int_0^\infty dr_1 r_1^{k_1} \exp(-a_1 r_1) \int_{r_1}^\infty dr_2 r_2^{k_2} \exp(-a_2 r_2)$$

$$= \int_0^\infty dr_1 r_1^{k_1+k_2+1} \exp(-a_1 r_1) \int_1^\infty dt\, t^{k_2} \exp(-a_2 r_1 t)$$

$$= \int_0^\infty dr_1 r_1^{k_1+k_2+1} \exp(-a_1 r_1) A_{k_2}(a_2 r_1).$$

Thus the double radial integral is a case of[17]

$$S(n,m,a_1,a_2) = \int_0^\infty dr\, r^m \exp(-a_1 r) A_n(a_2 r),$$

with real $a_1, a_2 > 0$ and integral n,m such that $m-n > 0$. By (14),

$$S(n,m,a_1,a_2) = S(0,m,a_1,a_2) + \frac{n}{a_2} S(n-1,m-1,a_1,a_2). \qquad (19)$$

TABLE II: Pearson's incomplete Γ-function[15] as calculated using ATTSER (see text) and as tabulated[16].

n	a	$b=a(n+1)^{\frac{1}{2}}$	$F(n,b)^c$	$\frac{b^{n+1}}{n!}F(n,b)^d$	$I(a,n)^e$
3	.1	.2	.21315090284309	$.56840240758157\times10^{-4}$	$.56840\times10^{-4}$
3	.5	1.	.11392894125692	$.18988156876154\times10^{-1}$	$.18988157\times10^{-1}$
3	2.5	5.	$.70557512131453\times10^{-2}$	.73497408476264	.734974085
3	3.	6.	$.39296116538118\times10^{-2}$	.84879611722335	.848796117
7	1.1	3.1	$.83185234575701\times10^{-2}$	$.14491626706789\times10^{-1}$	$.14491627\times10^{-1}$
7	1.6	4.5	$.25411796383013\times10^{-2}$	$.88700208272376\times10^{-1}$	$.88700208\times10^{-1}$
7	5.	14.1	$.30579137016009\times10^{-5}$	.97076625447646	.970766254
7	6.	17.0	$.72853583127830\times10^{-6}$	.99446689628512	.994466896
12	1.7	6.1	$.28852005006006\times10^{-3}$	$.10382616256444\times10^{-1}$	$.10382616\times10^{-1}$
12	2.3	8.3	$.43100477241618\times10^{-4}$	$.78929394864303\times10^{-1}$	$.78929395\times10^{-1}$
12	5.	18.0	$.20503347579341\times10^{-7}$	.90934703762468	.909347038
12	6.	21.6	$.20692146274928\times10^{-8}$	.98189855458457	.981898555

continued

TABLE II: (cont'd.)

n	a	$b=a(n+1)^{\frac{1}{2}}$	$F(n,b)^c$	$\frac{b^{n+1}}{n!}F(n,b)^d$	$I(a,n)^e$
18	2.6	11.3	$.13690605967092\times10^{-5}$	$.23053372691187\times10^{-1}$	$.23053373\times10^{-1}$
18	3.1	13.5	$.19370419884404\times10^{-6}$	$.92220910664212\times10^{-1}$	$.92220911\times10^{-1}$
18	7.5	32.7	$.10724637600399\times10^{-12}$	.99624193577030	.996241936
18	8.	34.9	$.31543964080308\times10^{-13}$	.99872109593925	.998721096
24	2.5	12.5	$.27950855396868\times10^{-6}$	$.11924488482317\times10^{-2}$	$.1192449\times10^{-2}$
24	3.5	17.5	$.27699542772992\times10^{-8}$	$.53176303853513\times10^{-1}$	$.53176304\times10^{-1}$
24	8.	40.	$.54859862841959\times10^{-16}$	.99551734343443	.995517343
24	8.5	42.5	$.12087675490235\times10^{-16}$	.99852828928160	.998528289

[c]Directly from ATTSER.

[d]Calculated in IBM 360 double precision from previous column.

[e]Reference 16.

with

$$S(0,m,a_1,a_2) = \frac{1}{a_2}\,\frac{(m-1)!}{(a_1+a_2)^m}\ ;$$

as in (14) there are no cancellation difficúlties. Then $S(n,m,a_1,a_2)$ can be calculated by the process (in a brief notation):

$$\begin{aligned}
&(0,m-n+1) + (0,m-n) \rightarrow (1,m-n+1)\\
&(0,m-n+2) + (1,m-n+1) \rightarrow (2,m-n+2)\\
&\qquad\qquad \cdots\\
&(0,m) + (n-1,m-1) \rightarrow (n,m).
\end{aligned}$$

No tables are available for direct comparison, but no numerical difficulties arise in the evaluation of this integral. We estimate that our routine for the $S(n,m,a_1,a_2)$ functions (subroutine ESS) is accurate to at least 14 significant figures.

C) Evaluation of molecular integrals.

(i) Electron repulsion

a) Formulas

The inverse interelectronic distance $1/r_{12}$ can be expanded[18]:

$$\frac{1}{r_{12}} = 4\pi \sum_{\ell=0}^{\infty} \frac{1}{2\ell+1}\,\frac{r_<^{\ell}}{r_>^{\ell+1}} \sum_{m=-\ell}^{\ell} S_{\ell m}(\theta_1,\phi_1)S(\theta_2,\phi_2), \qquad (20)$$

where $(r_<,r_>)$ denotes the (lesser, greater) of r_1,r_2. The

expansion in the reference is in terms of complex spherical harmonics; the change to real spherical harmonics is straightforward. Then the electron repulsion integral becomes:

$$\int_0^\infty r_1^2 dr_1 \int_0^\infty r_2^2 dr_2 \int_0^\pi \sin\theta_1 d\theta_1 \int_0^\pi \sin\theta_2 d\theta_2 \int_0^{2\pi} d\phi_1 \int_0^{2\pi} d\phi_2 \phi_i$$

$$(n_i, \ell_i, m_i, \zeta_i, r_1, \theta_1, \phi_1) \cdot$$

$$\cdot \phi_j(n_j, \ell_j, m_j, \zeta_j, r_1, \theta_1, \phi_1) \cdot \phi_k(n_k, \ell_k, m_k, \zeta_k, r_2, \theta_2, \phi_2) \cdot$$

$$\cdot \phi_\ell(n_\ell, \ell_\ell, m_\ell, \zeta_\ell, r_2, \theta_2, \phi_2) \cdot \frac{1}{r_{12}} \cdot$$

$$= 4\pi N_i N_j N_k N_\ell \sum_{\ell=0}^{\infty} \frac{1}{2\ell+1} \left[\int_0^\infty dr_1 \int_0^\infty dr_2 \; r_1^{n_i+n_j} r_2^{n_k+n_\ell} \right.$$

$$\frac{r_<^\ell}{r_>^{\ell+1}} \exp(-(\zeta_i+\zeta_j) r_1) \cdot$$

$$\left. \cdot \exp(-(\zeta_k+\zeta_\ell) r_2) \right] \sum_{m=-\ell}^{\ell} \left[\int_0^\pi \sin\theta_1 d\theta_1 \int_0^{2\pi} d\phi_1 \quad S_{\ell_i m_i}(\theta_1, \phi_1) \cdot \right.$$

$$\left. \cdot S_{\ell_j m_j}(\theta_1, \phi_1) S_{\ell m}(\theta_1, \phi_1) \right] \left[\int_0^\pi \sin\theta_2 d\theta_2 \int_0^{2\pi} d\phi_2 \quad S_{\ell_k m_k}(\theta_2, \phi_2) \cdot \right.$$

$$\left. \cdot S_{\ell_\ell m_\ell}(\theta_2, \phi_2) S_{\ell m}(\theta_2, \phi_2) \right] \tag{21}$$

The N_i are radial normalization constants. The angular integrals are those of (7). The last possible non-zero ℓ term is for $\ell = \min(\ell_i+\ell_j, \ell_k+\ell_\ell)$. Because of the occurrence of $(r_<, r_>)$ the radial integral must be done as a sum over two regions of space, $r_1 < r_2$ and $r_2 < r_1$. For $r_1 < r_2$ the radial integral is

$$\int_0^\infty dr_1 r_1^{n_i+n_j+\ell} \exp(-\zeta_i+\zeta_j)r_1) \int^\infty r_1 dr_2 r_2^{n_k+n_\ell-\ell-1} \exp(-(\zeta_k+\zeta_\ell)r_2); \tag{22}$$

which is auxiliary integral (11) if $n_k+n_\ell-\ell-1 > 0$. For a non-zero angular term $\ell < \ell_k+\ell_\ell < n_k-1+n_\ell-1=n_k+n_\ell-2$, so $n_k+n_\ell-\ell-1 > 0$. The $r_2 < r_1$ case is similar.

b) Documentation

Since the auxiliary integral (7) was shown to be accurate to at least 14 significant figures and the auxiliary integral (11) should be of the same accuracy, we estimate that the electron repulsion integrals are accurate to 13 or 14 figures. This cannot be verified directly since there are no values published to this length. Roney et al.[19] have given the value of two electron repulsion integrals to 11 figures:

$$\langle\phi(2,1,1,1.2,\bar{r}_1)\phi(2,1,1,1.2,\bar{r}_1)|\frac{1}{r_{12}}|\phi(2,1,1,1.2,\bar{r}_2)\phi(2,1,1,1.2,\bar{r}_2)\rangle$$

$$= .46968750000,$$

$$\langle\phi(2,1,1,1.2,\bar{r}_1)\phi(2,1,1,1.2,\bar{r}_1)|\frac{1}{r_{12}}|\phi(2,1,1,1.8,\bar{r}_2)\phi(2,1,1,1.8,\bar{r}_2)\rangle$$

$$= .54925056000.$$

The same integrals were calculated with our routine (subroutine REP1C) and the same numbers were obtained, with the final zeros continuing to the 14th figure. Since the two integrals are

exact decimal numbers, with the zeros continuing to an arbitrary number of places, on these integrals REPIC is accurate to at least 14 figures; if the final zeros are discounted the agreement with the values of Roney et al. [illegible] to 8 figures. No other integrals in the literature were found reported to this number of places. Pople and Beveridge[20] have published to five decimal places the electron repulsion integrals necessary for a minimal basis calculation of HF; the one-center integrals among these are compared with REPIC in Table III. Scherr[21] has published to five decimal places some one-center electron repulsion integrals for N_2; these are also compared with REPIC in Table III. The n, ℓ, and m values available for comparison are unfortunately quite restricted; for high n and ℓ values, which are important in the OCE-SCF calculations, there are no published values available. The strongest documentation for the electron repulsion integrals is the documentation (Table I) of the angular integrals (7), since this is the only part of the integral calculation complicated enough to be liable to error.

(ii) Nuclear attraction integral with non-central nucleus

a) Formulas

Expanding $1/r_{1\alpha}$, the integral of section 2A(i)b becomes

$$4\pi N_i N_j \sum_{\ell=0}^{\infty} \frac{1}{2\ell+1} \left[\int_0^\infty dr\, r^{n_i+n_j} \exp(-(\zeta_i+\zeta_j)r) \frac{r_<^\ell}{r_>^{\ell+1}}\right] \cdot$$

$$\cdot \sum_{m=-\ell}^{\ell} S_{\ell m}(\theta_\alpha,\phi_\alpha) \int_0^\pi \sin\theta d\theta \int_0^{2\pi} d\phi\, S_{\ell_i m_i}(\theta,\phi) S_{\ell_j m_j}(\theta,\phi) S_{\ell m}(\theta,\phi), \qquad (23)$$

TABLE III: Comparison of one-center electron repulsion integral routine REP1C with published values. Integral $[ij|k\ell]$. Values in atomic units of energy.

Pople and Beveridge[a]:

ϕ_i	ϕ_j	ϕ_k	ϕ_ℓ	REP1C	Literature[a]
1	1	1	1	$.54375000000000 \times 10^{+1}$	5.43750
2	1	1	1	.79102719780241	.79103
2	1	2	1	.14632821330504	.14633
2	2	1	1	$.12907460654510 \times 10^{1}$	1.29075
2	2	2	1	.29564280233143	.29564
2	2	2	2	.94453125000000	.94453
3	1	3	1	$.31039317973797 \times 10^{-1}$	.03104
3	2	3	1	$.46826786945545 \times 10^{-1}$	.04683
3	2	3	2	.20876736111111	.20877
3	3	1	1	$.12907460654510 \times 10^{1}$	1.29075
3	3	2	1	.29564280233143	.29564
3	3	2	2	.94453125000000	.94453
3	3	3	3	$.10176562500000 \times 10^{1}$	1.01766
4	3	4	3	$.54843750000000 \times 10^{-1}$	.05484
4	4	3	3	.90796875000000	.90797
5	5	5	5	.62500000000000	.62500

continued

TABLE III: (cont'd.)

Scherr[b]

ϕ_i	ϕ_j	ϕ_k	ϕ_ℓ	REPlC	Literature[b]
1	1	1	1	$.41875000000000 \times 10^{1}$	4.18750
2	2	1	1	.96858094469273	.96858
2	1	2	1	$.21843462898945 \times 10^{-1}$	.02184
2	2	2	2	.76324218750000	.76324
3	3	1	1	.96858094469273	.96858
3	1	3	1	$.21843462898945 \times 10^{-1}$	.02184
3	3	2	2	.68097656250000	.68098
3	2	3	2	$.41132812500000 \times 10^{-1}$	.04113
3	3	3	3	.76324218750000	.76324

[a]Ref. 20. The orbitals are:

	n	ℓ	m	ζ	type
ϕ_1	1	0	0	8.7	1s
ϕ_2	2	0	0	2.6	2s
ϕ_3	2	1	0	2.6	2pσ
ϕ_4	2	1	1	2.6	2pπ
ϕ_5	1	0	0	1.0	1s

[b]Ref. 21. The orbitals are:

	n	ℓ	m	ζ	type
ϕ_1	1	0	0	6.7	1s
ϕ_2	2	1	0	1.95	2pσ
ϕ_3	2	1	1	1.95	2pπ

with $\theta_\alpha, \phi_\alpha$ the angular coordinates of the off-center nucleus, r_α its radial coordinate, and $(r_<, r_>)$ the (lesser, greater) of r_α, r. The angular integral is again auxiliary function (7). $S_{\ell m}(\theta_\alpha, \phi_\alpha)$ was evaluated as in (3); the only possibly complicated part of this evaluation is the associated Legendre polynomial (1); however in all calculations reported in this thesis $\theta_\alpha = 0$, in which case $P_\ell^{|m|}(\cos\theta_\alpha) = 1$ if $m = 0$ and zero otherwise[22]. Our off-center nuclear attraction integral routine (subroutine XNUK2) was designed to be applicable to any choice of coordinates, so a routine to evaluate $P_\ell^{|m|}(\cos\theta)$ for any value of θ was coded from an algorithm published by Herndon[23] and tested against tables[22]; agreement was obtained to as many figures (8) as the table listed. However this is not important for the calculations reported in the thesis. The radial integral in (23) is done as the sum over two regions, $r < r_\alpha$ and $r_\alpha < r$. For $r < r_\alpha$ the radial integral is

$$\frac{1}{r_\alpha^{\ell+1}} \int_0^{r_\alpha} dr\, r^{n_i+n_j+\ell} \exp(-(\zeta_i+\zeta_j)r)$$

$$= r_\alpha^{n_i+n_j} \int_0^1 dt\, t^{n_i+n_j+\ell} \exp(-(\zeta_i+\zeta_j)r_\alpha t),$$

which is a constant times auxiliary integral (10). For $r_\alpha < r$ the integral is

$$r_\alpha^{\ell} \int_{r_\alpha}^{\infty} dr\, r^{n_i+n_j-\ell-1} \exp(-(\zeta_i+\zeta_j)r)$$

$$= r_\alpha^{n_i+n_j} \int_1^{\infty} dt\, t^{n_i+n_j-\ell-1} \exp(-\zeta_i+\zeta_j)r_\alpha t),$$

which is a constant times the A-function (9).

b) Documentation

For these integrals comparison values in the literature are even scarcer than for the electron repulsion integrals; Scherr[21] has published several to six decimal places. These are compared with XNUK2 in Table IV. The best documentation of this routine is the documentation of DGAUNT and ATTSER, Tables I and II. We estimate XNUK2 to be accurate to at least 14 figures.

(iii) Overlap integrals

These integrals reduce to

$$\langle\phi_i|\phi_j\rangle = N_i N_j \int_0^\infty dr\, r^{n_i+n_j} \exp(-(\zeta_i+\zeta_j)r)\cdot$$

$$\cdot \int_0^\pi \sin\theta d\theta \int_0^{2\pi} d\phi\; S_{\ell_i m_i}(\theta,\phi) S_{\ell_j m_j}(\theta,\phi)\cdot$$

The angular integral is the product of Kronecker deltas $\delta_{\ell_i \ell_j}\delta_{m_i m_j}$ by orthonormality of the spherical harmonics; the radial integral is auxiliary integral (8). No numerical difficulties arise.

(iv) Nuclear attraction integral with central nucleus

This integral is the overlap integral with n_i+n_j reduced by one; since $n_i+n_j \geqslant 2$, the exponent of r is positive and and no new auxiliary functions are needed.

(v) Kinetic energy integral

In spherical coordinates ∇^2 is[24]

$$\nabla^2 = \frac{1}{r^2}\frac{\partial}{\partial r}(r^2\frac{\partial}{\partial r}) + \frac{1}{r^2}[\frac{1}{\sin\theta}\frac{\partial}{\partial\theta}(\sin\theta\frac{\partial}{\partial\theta}) + \frac{1}{\sin^2\theta}\frac{\partial^2}{\partial\phi^2}];$$

TABLE IV: Nuclear attraction integral with off-center nucleus. Comparison of XNUK2 with values published by Scherr[a] of integral $\langle\phi_i|\frac{1}{r_{1\alpha}}|\phi_j\rangle$; R=2.0675 au. Values in atomic units of energy.

ϕ_i	ϕ_j	XNUK2	Literature[a]
1	1	.48367613344782	.483676
1	2	$.14235438511833 \times 10^{-1}$	.014235
2	2	.55084208211614	.550842
3	3	.43977910248707	.439779

[a]Ref. 21. The orbitals are:

	n	ℓ	m	ζ	type
ϕ_1	1	0	0	6.7	1s
ϕ_2	2	1	0	1.95	2pσ
ϕ_3	2	1	1	1.95	2pπ

using[25]

$$\left[\frac{1}{\sin\theta}\frac{\partial}{\partial\theta}\left(\sin\theta\frac{\partial}{\partial\theta}\right) + \frac{1}{\sin^2\theta}\frac{\partial^2}{\partial\phi^2}\right]S_{\ell m}(\theta,\phi) = -\ell(\ell+1)S_{\ell m}(\theta,\phi)$$

it follows that[2]

$$\nabla^2(\phi(n,\ell,m,\zeta,\bar{r})) = \zeta^2\left[\phi(n,\ell,m,\zeta,\bar{r}) - \left(\frac{2n}{2n-1}\right)^{\frac{1}{2}}\phi(n-1,\ell,m,\zeta,\bar{r})\right.$$

$$\left. + \frac{4(n+\ell)(n-\ell-1)}{(2n(2n-1)(2n-2)(2n-3))^{\frac{1}{2}}}\phi(n-2,\ell,m,\zeta,\bar{r})\right];$$

then $-\frac{1}{2}\langle\phi_i|\nabla^2|\phi_j\rangle$ can be expressed in terms of overlap integrals. If $n=1$ only $\ell=0$ is allowed, and the coefficient of $\phi(-1,\ell,m,\zeta,\bar{r})$ is zero; the coefficient of $\phi(0,\ell,m,\zeta,\bar{r})$ is non-zero, but this causes no problem since the overlap of an $n=0$ STO with another STO can be calculated by the same formula as for the overlap between STO's with $n>0$. No comparison values are tabulated because again there are no numerical difficulties, although our kinetic energy integral routine (subroutine SKINNY) was checked against values given by Scherr[21].

D) Program listing

In the next several pages the flowchart, subroutine calling diagram, subroutine descriptions, and FORTRAN listing of the program used to calculate and store on tape the electron repulsion integrals (program WINZ) are given. The one-electron integral routines are listed with the program WUNIT in Appendix II.

Flowchart for program WINE

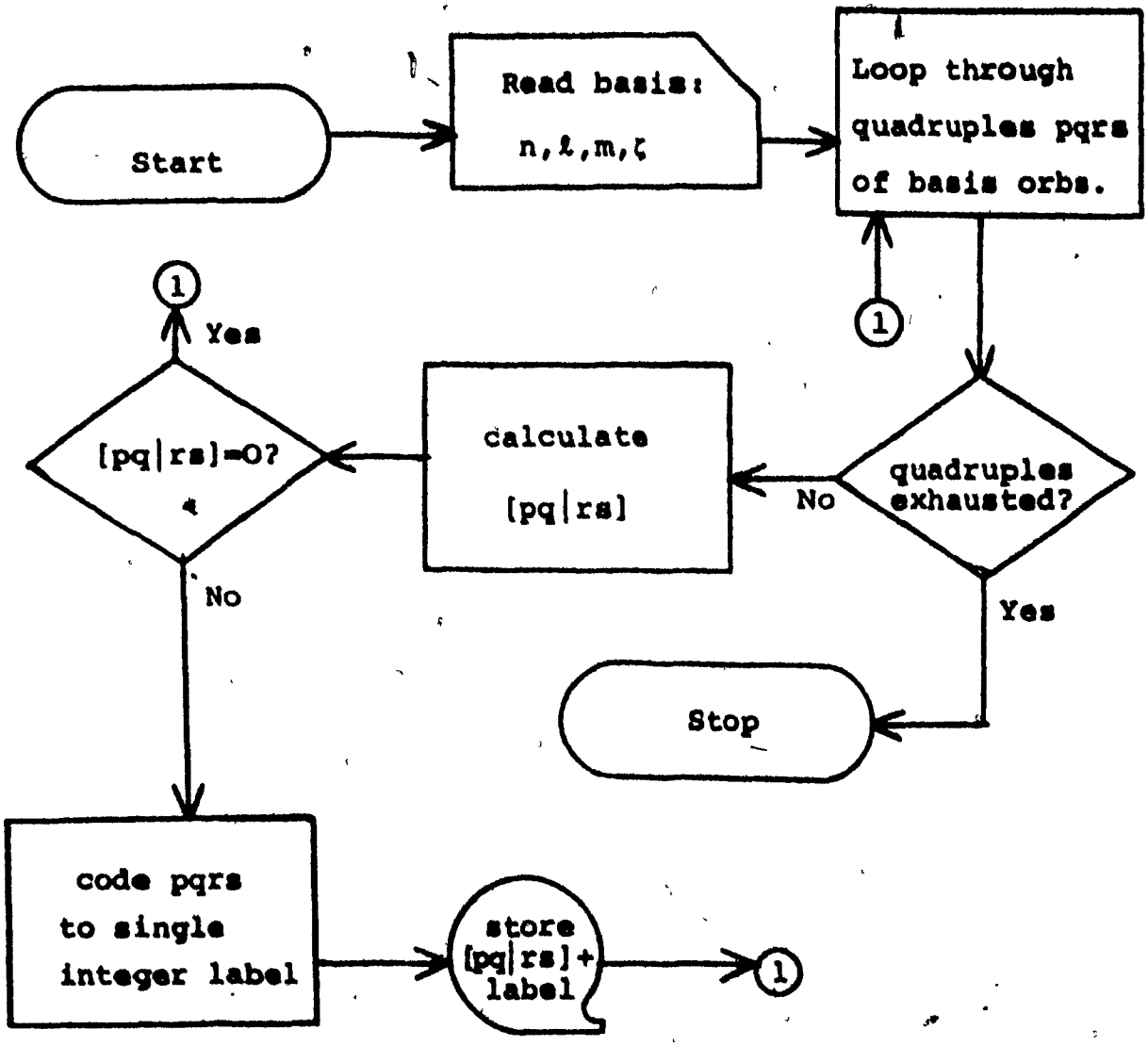

Subroutine calling diagram for program WINZ, calculation and storage of one-center electron repulsion integrals between STO's. Double arrows indicate transfer of control, single arrows indicate mathematical function call. Dashed arrow indicates reference to an array.

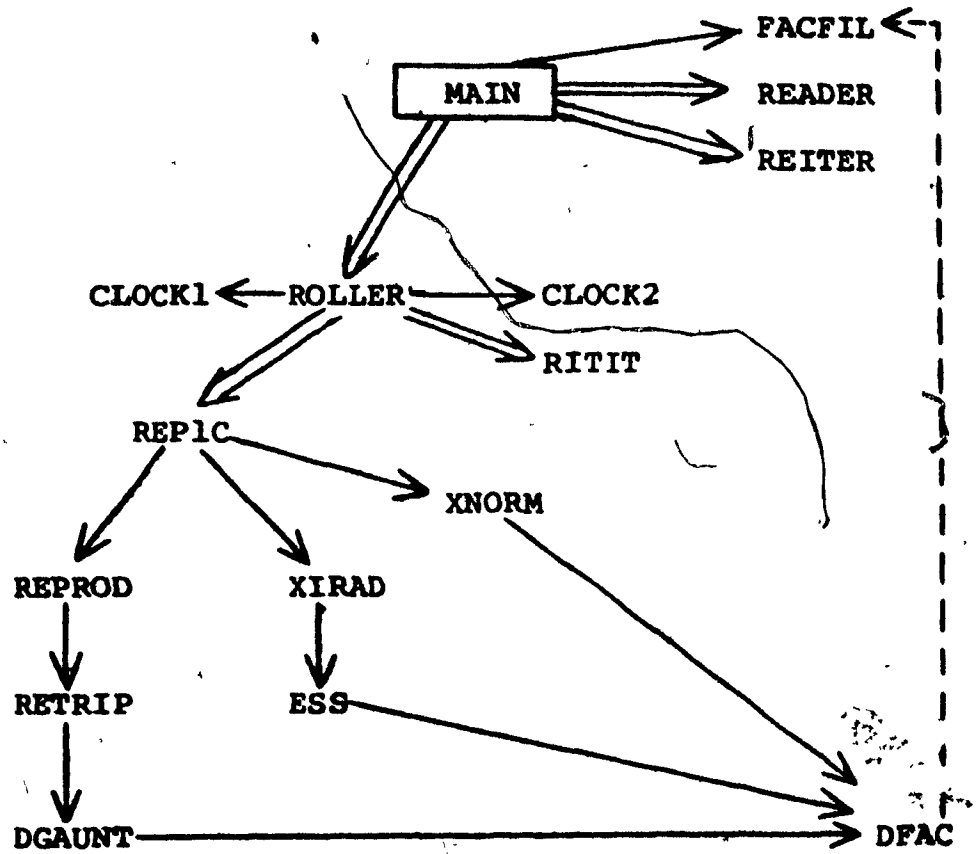

Subroutine descriptions, program WINZ

MAIN - initiates and directs calculation.

FACFIL - fills array with double precision factorials of integers for access by DFAC.

READER - reads in all input data.

REITER - prints out input data.

ROLLER - loops through all distinct electron repulsion integrals, calls routines for their calculation, calculates an integer label for each integral, and directs writing of integral and label on tape.

RITIT - does actual writing of integral and label on tape.

REP1C - does actual computation of electron repulsion integrals. Essentially a coding of (21).

REPROD - calculates the product of two triple integrals over real normalized spherical harmonics.

RETRIP - calculates the triple integral over real normalized spherical harmonics.

DGAUNT - calculates triple integral over complex normalized spherical harmonics.

XIRAD - calculates the radial integral in (21).

ESS - calculates the auxiliary integral (11).

XNORM - calculates the radial normalization constant for an STO.

DFAC - returns double precision factorial of an integer.

CLOCK1, CLOCK2 - timing routines devised by McGill University Computing Centre.

PROGRAM WINZ

```
C       MAIN PROGRAM
C
        IMPLICIT REAL*8(A-H,O-Z)
        COMMON/ORBS/NOR(100),LOR(100),MOR(100),ZOR(100),N,NINT,N2,N3
        COMMON/FAC/F1(51)
        COMMON/INZ/LABEL(1000),XER(1000)
        CALL FACFIL
        CALL READER
        CALL REITER
        CALL ROLLER
        STOP
        END
C
C
C
        REAL FUNCTION REP1C*8(N1A,L1A,M1A,Z1A,N1B,L1B,M1B,Z1B,N2A,L2A,M2A,
       |Z2A,N2B,L2B,M2B,Z2B)
C       CALCULATES A SINGLE CENTER, TWO ELECTRON INTEGRAL WITH
C       1/R12 AS THE OPERATOR AND NORMALIZED NON-ORTHOGONAL SLATER
C       FUNCTIONS AS THE ORBITALS. N1A,L1A,M1A, AND Z1A ARE RESPECTIVELY
C       THE PRINCIPAL QUANTUM NO., THE ORBITAL ANG MOM QUANTUM NUMBER,
C       THE AZIMUTHAL QUANT NO.% AND THE ORBITAL EXPONENT OF THE FIRST
C       ORBITAL (A) WHOSE ARGUMENT IS THE COORDINATES OF ELECTRON 1
C       (DENOTED BY THE 1 IN L1A).
        IMPLICIT REAL*8(A-H,O-Z)
        SUM=0.D0
        XCON=0.D0
        IC1=L1A+L1B+L2A+L2B
        IF(MOD(IC1,2).NE.0) GO TO 4
        IC1=M1A+M1B+M2A+M2B
        IF(MOD(IC1,2).NE.0) GO TO 4
        IC1=1
        IF(M1A.LT.0)  IC1=-IC1
        IF(M1B.LT.0)  IC1=-IC1
        IC2=1
        IF(M2A.LT.0)  IC2=-IC2
        IF(M2B.LT.0)  IC2=-IC2
        IF(IC1.NE.IC2) GO TO 4
        PI=3.1415926535897930D0
        II1=IABS(L1A-L1B)
        II2=IABS(L2A-L2B)
        KLOW=MAX0(II1,II2)+1
        KUP=MIN0(L1A+L1B,L2A+L2B)+1
        IF(KLOW.GT.KUP) GO TO 4
        IM1=IABS(M1A)+IABS(M1B)
        IM2=IABS(IABS(M1A)-IABS(M1B))
        II1=IABS(M2A)+IABS(M2B)
        II2=IABS(IABS(M2A)-IABS(M2B))
        MINAM=MAX0(IM2,II2)
        MAXAM=MIN0(IM1,II1)
        IF((MINAM.EQ.0).AND.(IC1.LT.0)) MINAM=2
        IF(KLOW-1.LT.MINAM) KLOW=KLOW+2*((MINAM-KLOW+2)/2)
        IF(KLOW.GT.KUP) GO TO 4
        IF(MINAM.GT.MAXAM) GO TO 4
        IF((IM1.EQ.II1).OR.(IM1.EQ.II2)) GO TO 5
        IF((IM2.EQ.II1).OR.(IM2.EQ.II2)) GO TO 5
        GO TO 4
      5 DO 1 I=KLOW,KUP,2
```

```
      XINNER=0.D0
      MM=MINAM
    2 IF(MM.GT.I-1) GO TO 3
      M=MM*IC1
      XINNER=XINNER+REPROD(L1A,L1B,M1A,M1B,L2A,L2B,M2A,M2B,I-1,N)
      IF(MM.EQ.MAXAM) GO TO 3
      MM=MAXAM
      GO TO 2
    3 CONTINUE
      IF(XINNER.EQ.0.D0) GO TO 1
      XX1=1.D0/DFLOAT(2*(I-1)+1)
      XX1=XX1*XIRAD(N1A+N1B,N2A+N2B,Z1A+Z1B,Z2A+Z2B,I-1)
      SUM=SUM+XX1*XINNER
    1 CONTINUE
      IF(SUM.EQ.0.D0) GO TO 4
      XCON=PI*XNORM(N1A,Z1A)*XNORM(N1B,Z1B)*XNORM(N2A,Z2A)*XNORM(N2B,Z2B
     )*4.D0
    4 REPIC=XCON*SUM
      RETURN
      END
C
C
C
      REAL FUNCTION DGAUNT*8(L1,L2,L,M1,M2,M)
C     CALCULATES INT(Y(L1,M1)*Y(L2,M2)*Y(L,M))
C     MUST HAVE M1+M2+M=0 FOR THE INTEGRAL TO BE NON-ZERO
      IMPLICIT REAL*8 (A-H,O-Z)
      IF((L.GT.(L1+L2)).OR.(L.LT.IABS(L1-L2))) GO TO 1
      IF((M1+M2+M).NE.0) GO TO 1
C     XXC=1/SQRT(2*PI)
      XXC=.39894228040143270D0
      III=(L1+L2+L)/2
      III=III+III
      IF(III.NE.(L1+L2+L)) GO TO 1
      LL1=L1
      LL2=L2
      LL=L
      MM1=IABS(M1)
      MM2=IABS(M2)
      MM=IABS(M)
      ICHK=0
      IF(M1.GE.0) ICHK=ICHK+1
      IF(M2.GE.0) ICHK=ICHK+1
      IF(M.GE.0) ICHK=ICHK+1
      GO TO (3,4,5),ICHK
    3 IF(M.GE.0) GO TO 5
      IF(M1.GE.0) GO TO 12
      MM=M2
      MM2=IABS(M)
      LL=L2
      LL2=L
      GO TO 5
   12 MM=M1
      MM1=IABS(M)
      LL=L1
      LL1=L
      GO TO 5
    4 IF(M.LT.0) GO TO 5
```

```
      IF(M1.LT.0) GO TO 10
      MM=IABS(M2)
      MM2=M
      LL=L2
      LL2=L
      GO TO 5
   10 MM=IABS(M1)
      MM1=M
      LL=L1
      LL1=L
    5 IG=(LL1+LL2+LL)/2
      SIGN=1.D0
      IF(MOD(IG-LL1-MM2,2).NE.0) SIGN=-1.D0
      XTOP=SIGN*DFAC(2*(IG-LL2))*DFAC(IG)
      XBOT=DFAC(IG-LL1)*DFAC(IG-LL2)*DFAC(IG-LL)*DFAC(2*IG+1)
      XRAT=DFLOAT((2*LL1+1)*(2*LL2+1)*(2*LL+1))*
     |DFAC(LL1+MM1)*DFAC(LL-MM1-MM2)*DFAC(LL2+MM2)*DFAC(LL2-MM2)/
     |(DFAC(LL1-MM1)*DFAC(LL+MM1+MM2)*2.D0)
      XFAC=DSQRT(XRAT)
      XFAC=XXC*XTOP*XFAC/XBOT
      XSUM=0.D0
      SIGN=1.D0
      IIT=0
      II1=LL2-MM2
      II2=LL-MM1-MM2
      II3=LL1-MM1+II1
      II4=LL1+MM1-II1
      II5=LL+MM1+MM2
    6 IF((II1.LT.0).OR.(II2.LT.0).OR.(II3.LT.0)) GO TO 7
      IF(II4.LT.0) GO TO 8
      DSUM=SIGN*DFAC(II5)*DFAC(II3)/(DFAC(II2)*DFAC(II4)*DFAC(II1)*
     |DFAC(IIT))
      XSUM=XSUM+DSUM
    8 IIT=IIT+1
      II1=II1-1
      II2=II2-1
      II3=II3-1
      II4=II4+1
      II5=II5+1
      SIGN=-SIGN
      GO TO 6
    7 DGAUNT=XFAC*XSUM
      RETURN
    1 WRITE(6,2)
    2 FORMAT(' ','GAUNT COEFF INDEX ERROR')
      STOP
      END
C
C
C
      SUBROUTINE FACFIL
      IMPLICIT REAL*8(A-H,O-Z)
      COMMON/FAC/F1(51)
C     FILLS UP VECTOR ARRAY WITH FACTORIALS. PRELIMINARY TO USE OF DFAC.
C     F(N) CONTAINS FACTORIAL (N-1)
      F1(1)=1.D0
      X=1.D0
      DO 1 I=1,50
```

```
      III=I+1
      X=X*I
      F1(III)=X
    1 CONTINUE
      RETURN
      END
C
C
C
      REAL FUNCTION DFAC*8(J)
      IMPLICIT REAL*8(A-H,O-Z)
      COMMON/FAC/F1(51)
C     RETURNS FACTORIAL J. ARRAY F1 MUST BE FILLED BEFORE ROUTINE
C     CAN BE USED.
      IF((J.GT.50).OR.(J.LT.0)) GO TO 25
      JJ1=J+1
      DFAC=F1(JJ1)
      RETURN
   25 WRITE(6,26)
   26 FORMAT('0     DFAC CALLING ERROR')
      XX1=(1.0-50)**5
      STOP
      END
C
C
C
      SUBROUTINE ROLLER
C     THIS ROUTINE LOOPS THROUGH THE NECESSARY INDICES FOR TWO-ELECTRON
C     INTEGRALS AND STORES THE NON-ZERO INTEGRALS WITH AN INTEGER
C     INDICATING THE ORBITAL INDICES ON OUTPUT UNIT 10 (TAPE OR DISK).
      IMPLICIT REAL*8(A-H,O-Z)
      COMMON/ORBS/NOR(100),LOR(100),MOR(100),ZOR(100),N,NINT,N2,N3
      COMMON/INZ/LABEL(1000),XER(1000)
      EQUIVALENCE (MABEL(1),LABEL(1))
      DIMENSION MABEL(3000)
      CALL CLOCK1
      NINT=0
      ILAB=0
      DO 1 I=1,N
      III=I+1
      IM1=I-1
      DO 1 J=I,N
      JM1=J-1
      DO 5 L=J,N
      XX1=REP1C(NOR(I),LOR(I),MOR(I),ZOR(I),NOR(J),LOR(J),MOR(J),ZOR(J),
     |NOR(I),LOR(I),MOR(I),ZOR(I),NOR(L),LOR(L),MOR(L),ZOR(L))
      IF(XX1.EQ.0.D0) GO TO 5
      NINT=NINT+1
      ILAB=ILAB+1
    4 LABEL(ILAB)=IM1*N3+JM1*N2+IM1*N+L-1
      XER(ILAB)=XX1
      IF(ILAB.EQ.1000) CALL RITIT(ILAB)
    5 CONTINUE
      DO 1 K=III,N
      KM1=K-1
      DO 1 L=K,N
      XX1=REP1C(NOR(I),LOR(I),MOR(I),ZOR(I),NOR(J),LOR(J),MOR(J),ZOR(J),
     |NOR(K),LOR(K),MOR(K),ZOR(K),NOR(L),LOR(L),MOR(L),ZOR(L))
```

```
      IF(XX1.EQ.0.D0) GO TO 1
      NINT=NINT+1
      ILAB=ILAB+1
      LABEL(ILAB)=IM1*N3+JM1*N2+KM1*N+L-1
      XER(ILAB)=XX1
      IF(ILAB.EQ.1000) CALL RITIT(ILAB)
    1 CONTINUE
      IF(ILAB.NE.0) CALL RITIT(ILAB)
    3 END FILE 10
      CALL CLOCK2(NN2)
      NCHK=N*(N+1)
      NCHK=NCHK*(NCHK+2)/8
      XX1=DFLOAT(NINT)/DFLOAT(NCHK)
      WRITE(6,25) NCHK,NINT,XX1
   25 FORMAT('0',3X,'POSSIBLE R12 INTS',1X,I10,5X,'NUMBER NON-ZERO',1X,I
     |10,10X,'FRACTION NON-ZERO',1X,F5.2)
      XX1=DFLOAT(NN2)/60.D0
      WRITE(6,26) XX1
   26 FORMAT('0',3X,'R12 INTEGRAL CALCULATING TIME',1X,F7.2,1X,'SECONDS'
     |)
      RETURN
      END
C
C
C
      SUBROUTINE RITIT(N)
C     DOES THE ACTUAL UNFORMATTED WRITING OF INTEGRAL AND LABEL ON TAPE
      IMPLICIT REAL*8(A-H,O-Z)
      COMMON/INZ/LABEL(1000),XER(1000)
      EQUIVALENCE(MABEL(1),LABEL(1))
      DIMENSION MABEL(3000)
      IF(N.EQ.1000) GO TO 1
      IF(N.GT.1000) GO TO 2
      WRITE(10) (LABEL(KK),KK=1,N),(XER(KK),KK=1,N)
      RETURN
    1 WRITE(10) MABEL
      N=0
      RETURN
    2 WRITE(6,3) N
    3 FORMAT('0RITIT CALL ERROR',1X,I10)
      STOP
      END
C
C
C
      REAL FUNCTION XNORM*8(N,ZETA)
C     RETURNS THE NORMALIZATION CONSTANT OF A SLATER ORBITAL
C     WITH PRINCIPAL QUANTUM NUMBER N AND EXPONENT ZETA
      IMPLICIT REAL*8(A-H,O-Z)
      IF(N.LT.0) GO TO 25
      III=N+N
      TOP=(ZETA+ZETA)**(III+1)
      BOT=DFAC(III)
      XNORM=DSQRT(TOP/BOT)
      RETURN
   25 WRITE(6,26)
   26 FORMAT('0      XNORM CALLING ERROR')
      STOP
```

```
      END
C
C
C
      REAL FUNCTION RFPROD*8(LA1,LA2,MA1,MA2,LB1,LB2,MB1,MB2,L,M)
C     RETURNS THE PRODUCT S(LA1,LA2,L,MA1,MA2,M)*S(LB1,LB2,L,MB1,MB2,M)
C     WHERE THE S FUNCTIONS ARE INTEGRALS OVER 3 NORMALIZED REAL
C     SPHERICAL HARMONICS.
      IMPLICIT REAL*8(A-H,O-Z)
      ICHK=1
      IF(MA1.LT.0) ICHK=-ICHK
      IF(MA2.LT.0) ICHK=-ICHK
      IF(M.LT.0) ICHK=-ICHK
      IF(ICHK.LT.0) GO TO 25
      IF(MB1.LT.0) ICHK=-ICHK
      IF(MB2.LT.0) ICHK=-ICHK
      IF(M.LT.0) ICHK=-ICHK
      IF(ICHK.LT.0) GO TO 25
      III=LA1+LA2+L
      II2=III/2
      II3=III-II2-II2
      IF(II2.NE.0) GO TO 25
      III=LB1+LB2+L
      II2=III/2
      II3=III-II2-II2
      IF(II2.NE.0) GO TO 25
      IF((L.GT.(LA1+LA2)).OR.(L.GT.(LB1+LB2))) GO TO 25
      IF((L.LT.IABS(LA1-LA2)).OR.(L.LT.IABS(LB1-LB2))) GO TO 25
      IF((IABS(M).NE.IABS(MA1+MA2)).AND.(IABS(M).NE.IABS(MA1-MA2))) GO T
     |O 25
      IF((IABS(M).NE.IABS(MB1+MB2)).AND.(IABS(M).NE.IABS(MB1-MB2))) GO T
     |O 25
      IF((IABS(MA1).GT.LA1).OR.(IABS(MA2).GT.LA2).OR.(IABS(M).GT.L)) GO
     |TO 25
      IF((IABS(MB1).GT.LB1).OR.(IABS(MB2).GT.LB2)) GO TO 25
      RFPROD=RFTRIP(LA1,LA2,L,MA1,MA2,M)*RFTRIP(LB1,LB2,L,MB1,MB2,M)
      RETURN
   25 RFPROD=0.D0
      RETURN
      END
C
C
C
      REAL FUNCTION CSS*8(INDEX,INTGER,EXPNT,AARG)
C     RETURNS INT(0 TO INF)(X**INTGER*EXP(-EXPNT)*A(SUB INDEX)(AARG))DX
C     WHERE A IS THE FAMILIAR A FUNCTION
      IMPLICIT REAL*8 (A-H,O-Z)
      IF(INTGER.LE.INDEX) GO TO 25
      IF(INDEX.LT.0) GO TO 25
      XXM=1.D0/AARG
      XXS=EXPNT*AARG
      II2=INTGER-INDEX
      IFC=II2-1
      XS1=1.D0/(XXS**II2)
      XX1=XXM*DFAC(IFC)*XS1
      IF(INDEX.EQ.0) GO TO 5
      XXF=0.D0
      DO 1 I=1,INDEX
```

```
      IFC=IFC+1
      XS1=XS1/XXS
      XXF=XXF+XXM
      XX2=XXM*DFAC(IFC)*XS1
      XX1=XX2+XXF*XX1
    1 CONTINUE
    5 ESS=XX1
      RETURN
   25 WRITE(6,26)
   26 FORMAT(' ESS CALLING ERROR')
      STOP
      END
C
C
C
      REAL FUNCTION XIRAD*8(N1,N2,A,B,K)
C     RETURNS INT(R1**N1*EXP(-A)*(RMIN**K/RMAX**(K+1))*R2**N2*EXP(-B))
C     DR1DR2
      IMPLICIT REAL*8(A-H,O-Z)
      III=N1+N2
      INDEX1=N1-K-1
      INDEX2=N2-K-1
      XIRAD=ESS(INDEX2,III,A,B)+ESS(INDEX1,III,B,A)
      RETURN
      END
C
C
C
      SUBROUTINE READER
C     READS THE INPUT DATA
      IMPLICIT REAL*8(A-H,O-Z)
      COMMON/ORBS/NOR(100),LOR(100),MOR(100),ZOR(100),N,NINT,N2,N3
C     READ IN TITLE CARD.
      READ(5,20)
   20 FORMAT('                                                        ')
      WRITE(6,20)
      I=1
    1 READ(5,3,END=50) NOR(I),LOR(I),MOR(I),ZOR(I)
    3 FORMAT(2X,3I2,F10.6)
      I=I+1
      GO TO 1
   50 N=I-1
C     CALCULATE POWERS OF BASIS SET SIZE FOR ROLLER
      N2=N*N
      N3=N2*N
      RETURN
      END
C
C
C
      REAL FUNCTION RETRIP*8(L1,L2,L,M1,M2,M)
C     RETURNS INT(S(L1,M1)*S(L2,M2)*S(L,M)), WHERE S DENOTES REAL NOR-
C     MALIZED SPHERICAL HARMONIC
      IMPLICIT REAL*8(A-H,O-Z)
      IZERO=1
      IF(M1.EQ.0) IZERO=IZERO+1
      IF(M2.EQ.0) IZERO=IZERO+1
      IF(M.EQ.0) IZERO=IZERO+1
```

```
      GO TO (6,9,25,5),IZERO
   25 RETRIP=0.D0
      RETURN
    5 RETRIP=DGAUNT(L1,L2,L,0,0,0)
      RETURN
    9 MM1=IABS(M1)
      MM2=-IABS(M2)
      MM3=-IABS(M)
      IF((MM1+MM2).LT.0) MM3=-MM3
      RETRIP=DGAUNT(L1,L2,L,MM1,MM2,MM3)
      RETURN
    6 INEG=0
      IF(M1.LT.0) INEG=INEG+1
      IF(M2.LT.0) INEG=INEG+1
      IF(INEG.GT.0) GO TO 10
      SIGN=1.D0
   11 LL1=L1
      LL2=L2
      MM1=IABS(M1)
      MM2=-IABS(M2)
      MM3=-IABS(M)
      IF(MM1.GE.MM2) GO TO 7
      MSAVE=MM1
      MM1=MM2
      MM2=MSAVE
      MSAVE=LL1
      LL1=LL2
      LL2=MSAVE
    7 IF(IABS(M).EQ.(MM1-MM2)) MM2=-MM2
C     XCON=1/SQRT(2)
      XCON=.7071067811865475D0
      RETRIP=SIGN*XCON*DGAUNT(LL1,LL2,L,MM1,MM2,MM3)
      RETURN
   10 SIGN=1.D0
      IF((M1+M2+M).EQ.0) SIGN=-SIGN
      GO TO 11
   26 WRITE(6,27)
   27 FORMAT('  RETRIP CALLING ERROR')
      STOP
      END
C
C
C
      SUBROUTINE REITER
C     PRINTS OUT INPUT DATA
      IMPLICIT REAL*8(A-H,O-Z)
      COMMON/ORBS/NOR(100),LOR(100),MOR(100),ZOR(100),N,NINT,N2,N3
      WRITE(6,7)
    7 FORMAT('0',2X,'BASIS SET INFORMATION')
      WRITE(6,8)
    8 FORMAT('0',5X,'ORBITAL',10X,'N',5X,'L',5X,'M',7X,'EXPONENT')
      DO 9 I=1,N
    9 WRITE(6,10) I,NOR(I),LOR(I),MOR(I),ZOR(I)
   10 FORMAT(' ',8X,I2,11X,I2,4X,I2,4X,I2,3X,F12.6)
      RETURN
      END
```

3. Two-center EFG integrals

A) Coordinate system

The EFG is to be evaluated at center a; center b lies at distance R from a on the +z-axis; the spherical system on b has a +z-axis which coincides with that of the system on a and x,y axes obtained from those on a by translation. If a point has coordinates r_a, θ_a, ϕ_a in the system on a and r_b, θ_b, ϕ_b in the system on b, then its coordinates μ, ν, ϕ in an elliptical coordinate system are[24]

$$\begin{aligned} \mu &= (r_a + r_b)/R \\ \nu &= (r_a - r_b)/R \\ \phi &= \phi_a = \phi_b \\ d\tau &= \frac{R^3}{8}(\mu^2 - \nu^2)\, d\mu\, d\nu\, d\phi . \end{aligned} \tag{24}$$

It follows that

$$\begin{aligned} r_a &= \tfrac{1}{2}R(\mu+\nu) \\ r_b &= \tfrac{1}{2}R(\mu-\nu) \\ \cos\theta_a &= \frac{1+\mu\nu}{\mu+\nu} \\ \cos\theta_b &= \frac{1-\mu\nu}{\nu-\mu} . \end{aligned} \tag{25}$$

B) Definition of the integrals

The integrals to be evaluated are:

$$\text{Type AB: } \langle\phi_i(\bar{r}_a)|\frac{3\cos^2\theta_a-1}{r_a^3}|\phi_j(\bar{r}_b)\rangle + \frac{4\pi}{3}\phi_i(0,0,0)\phi_j(R,\pi,0)$$

$$\text{Type BB: } \langle\phi_i(\bar{r}_b)|\frac{3\cos^2\theta_a-1}{r_a^3}|\phi_j(\bar{r}_b)\rangle + \frac{4\pi}{3}\phi_i(R,\pi,0)\phi_j(R,\pi,0),$$

where the added term makes the EFG tensor traceless (Chapter III). For convenience it is dropped in what follows. From the definition of STO's ϕ_i and ϕ_j (6) these become:

$$\text{Type AB: } N_iN_j\int d\tau\, r_a^{n_i-1} r_b^{n_j-1} \exp(-\zeta_i r_a)\exp(-\zeta_j r_b)\left(\frac{3\cos^2\theta_a-1}{r_a^3}\right)\cdot$$

$$\cdot\, S_{\ell_i m_i}(\theta_a,\phi)S_{\ell_j m_j}(\theta_b,\phi)$$

$$\text{Type BB: } N_iN_j\int d\tau\, r_b^{n_i+n_j-2} \exp(-(\zeta_i+\zeta_j)r_b)\left(\frac{3\cos^2\theta_a-1}{r_a^3}\right)\cdot$$

$$\cdot\, S_{\ell_i m_i}(\theta_b,\phi)S_{\ell_j m_j}(\theta_b,\phi)\cdot$$

C) Evaluation

Note that, by the orthonormality of the spherical harmonics, both integrals are zero unless $m_i = m_j$, in which case integration over ϕ gives a factor of one. In what follows we take $m_i = m_j = m$ and assume the integration over ϕ already

performed, we indicate the volume element with ϕ integrated out $d\tau'$. The non-ϕ-dependent part of the spherical harmonic is the normalized associated Legendre polynomial $\Theta_\ell^{|m|}(\cos\theta)$ of (2). The integrals become

$$\text{Type AB: } N_i N_j \int d\tau' \; r_a^{n_i-1} r_b^{n_j-1} \exp(-\zeta_i r_a)\exp(\zeta_j r_b)\left(\frac{3\cos^2\theta_a-1}{r_a^3}\right)\cdot$$

$$\cdot\,\Theta_{\ell_i}^{|m_i|}(\cos\theta_a)\Theta_{\ell_j}^{|m_j|}(\cos\theta_b) \tag{26}$$

$$\text{Type BB: } N_i N_j \int d\tau' \; r_b^{n_i+n_j-2} \exp(-(\zeta_i+\zeta_j) r_b)\left(\frac{3\cos^2\theta_a-1}{r_a^3}\right)$$

$$\cdot\,\Theta_{\ell_i}^{|m_i|}(\cos\theta_b)\Theta_{\ell_j}^{|m_j|}(\cos\theta_b)\;. \tag{27}$$

The radial terms can be expressed in terms of μ,ν by direct application of (24), as can $3\cos^2\theta_a-1$. The problem which remains is expansion of the products $\Theta_{\ell_i}^{|m_i|}(\cos\theta_a)\Theta_{\ell_j}^{|m_j|}(\cos\theta_b)$ and $\Theta_{\ell_i}^{|m_i|}(\cos\theta_b)\Theta_{\ell_j}^{|m_j|}(\cos\theta_b)$. It might appear practical to expand the product $(3\cos^2\theta_a-1)\Theta_{\ell_i}^{|m_i|}(\cos\theta_a)$ as a sum over associated Legendre polynomials in $\cos\theta_a$ but this is not done because of certain convergence problems with integrals which arise[26]. Also it might appear practical to expand $\Theta_{\ell_i}^{|m_i|}(\cos\theta_b)\Theta_{\ell_j}^{|m_j|}(\cos\theta_b)$ as

a sum of associated Legendre polynomials in $\cos\theta_b$, but it proved simpler to expand the product directly in terms of μ,ν.

Guseinov[27] has given an expansion of $\Theta_{\ell_i}^{|m_i|}(\cos\theta_a)\Theta_{\ell_j}^{|m_j|}(\cos\theta_b)$ in terms of μ,ν; his coordinate system is slightly different from ours, since he took the +z-axis on b to coincide with the -z-axis on a. The formulas we give here are adjusted from those of Guseinov's paper to be consistent with the coordinate system defined in section A. Starting from the explicit form of the unnormalized associated Legendre polynomial[28]

$$P_\ell^{|m|}(x) = \frac{(1-x^2)^{\frac{|m|}{2}}}{2^\ell} \sum_{p=0}^{[\frac{\ell-|m|}{2}]} (-1)^p \frac{x^{\ell-2p-|m|}(2\ell-2p)!}{p!(\ell-p)!(\ell-2p-m)!},$$

Guseinov derived (adjusted to our coordinates):

$$\Theta_{\ell_i}^m(\cos\theta_a)\Theta_{\ell_j}^m(\cos\theta_b) =$$

$$\sum_{\alpha=-m}^{\ell_i} \sum_{\beta=m}^{\ell_j} \sum_{q=0}^{\alpha+\beta} g_{\alpha\beta}^q(\ell_i,\ell_j,m) \frac{(\mu\nu)^q}{(\mu+\nu)^\alpha(\mu-\nu)^\beta}$$

with $m \geq 0$ (no restriction since only $|m|$ enters above) and

$$g_{\alpha\beta}^q(\ell_i,\ell_j,m) = 0 \text{ unless } \ell_i \pm \alpha \text{ and } \ell_j \pm \beta \text{ both even}$$

$$g_{\alpha\beta}^q(\ell_i,\ell_j,m) = g_{\alpha\beta}^0 F_q(\alpha+m,\beta-m)$$

with F defined implicitly by the series

$$(\mu+\nu)^N \ (\mu-\nu)^M = \sum_{i=0}^{N+M} F_i(N,M)\,\mu^{N+M-i} \cdot \nu^i$$

and

$$g^0_{\alpha\beta}(\ell_i,\ell_j,m) = \frac{1}{2^{\ell_i+\ell_j+1}} \left[\frac{(2\ell_i+1)(2\ell_j+1)(\ell_i-m)!(\ell_j-m)!}{(\ell_i+m)!(\ell_j+m)!}\right]^{\frac{1}{2}} \cdot$$

$$\cdot\ (-1)^{\left(\frac{(\ell_i-\alpha)}{2}+\frac{(\ell_j-\beta)}{2}+\ell_j\right)} \cdot \frac{(\ell_j+\beta)!}{\left(\frac{(\ell_j-\beta)}{2}\right)!\left(\frac{(\ell_j+\beta)}{2}\right)!(\beta-m)!} \cdot$$

$$\cdot \sum_{k=0}^{m} (-1)^k \frac{(\ell_i+\alpha+2m-2k)!\binom{m}{k}}{(\frac{1}{2}(\ell_i-\alpha)-m+k)!(\frac{1}{2}(\ell_i+\alpha)+m-k)!(\alpha+m-2k)!} \qquad (28)$$

Guseinov did not treat the $\Theta^{|m|}_{\ell_i}(\cos\theta_b)\Theta^{|m|}_{\ell_j}(\cos\theta_b)$ case; using similar techniques we were able to derive, for $m \geq 0$,

$$\Theta^m_{\ell_i}(\cos\theta_b)\Theta^m_{\ell_j}(\cos\theta_b = \sum_{\gamma=0}^{\ell_i+\ell_j} \sum_{q=0}^{\gamma} H^q_\gamma(\ell_i,\ell_j,m)\,\frac{(\mu\nu)^q}{(\mu-\nu)^\gamma}$$

$$H^q_\gamma(\ell_i,\ell_j,m) = 0 \text{ unless } \ell_i+\ell_j-\gamma \text{ even}$$

$$H^q_\gamma(\ell_i,\ell_j,m) = \sum_{i=m}^{\ell_j} h^q_{\gamma-i,i}(\ell_i,\ell_j,m),$$

with

$h^q_{\alpha\beta}(\ell_i,\ell_j,m) = 0$ unless $\ell_i-\alpha, \ell_j-\beta$ both even

$$h^q_{\alpha\beta}(\ell_i,\ell_j,m) = \frac{1}{2^{\ell_i+\ell_j+1}} \binom{\alpha+\beta}{q} (-1)^{\left(\frac{\ell_i-\alpha}{2}\right) + \left(\frac{\ell_j-\beta}{2}\right) - m + \ell_i + \ell_j + q} \cdot$$

$$\cdot \sum_{k=0}^{m} (-1)^k \frac{(\ell_i+\alpha+2m-2k)! \quad \binom{m}{k}}{\left(\frac{\ell_i+\alpha+2m-2k}{2}\right)! \left(\frac{\ell_i-\alpha-2m+2k}{2}\right)! (\alpha+2m-2k)!} \tag{29}$$

The remaining angular and radial factors are

$$3\cos^2\theta_a - 1 = \frac{3\left(\frac{1+\mu\nu}{\mu+\nu}\right)^2 - 1}{\frac{1}{8}R^3(\mu+\nu)^3} ;$$

$$r_a^{\,n_i-1} r_b^{\,n_j-1} = \frac{1}{2^{n_i+n_j-2}} R^{n_i+n_j-2} (\mu+\nu)^{n_i-1} (\mu-\nu)^{n_j-1} ,$$

$$\exp(-\zeta_i r_a - \zeta_j r_b) = \exp(-a\mu)\exp(-b\nu),$$

with

$$a = \tfrac{1}{2}R(\zeta_i+\zeta_j)$$

$$b = \tfrac{1}{2}R(\zeta_i-\zeta_j).$$

Defining

$$K = \frac{1}{2^{n_i+n_j-2}} R^{n_i+n_j-2} N_i N_j ,$$

(26) and (27) become

$$\text{Type AB: } K\int_{-1}^{1} d\nu \int_{1}^{\infty} d\mu\, (\mu+\nu)^{n_i} (\mu-\nu)^{n_j} \exp(-a\mu)\exp(-b\nu) \frac{3\left(\frac{1+\mu\nu}{\mu+\nu}\right)^2 - 1}{(\mu+\nu)^3} \cdot$$

$$\cdot \sum_{\alpha=-m}^{\ell_i} \sum_{\beta=m}^{\ell_j} \sum_{q=0}^{\alpha+\beta} g^q_{\alpha\beta}(\ell_i, \ell_j, m) \frac{(\mu\nu)^q}{(\mu+\nu)^\alpha (\mu-\nu)^\beta} \tag{30}$$

$$\text{Type BB: } K\int_{-1}^{1} d\nu \int_{1}^{\infty} d\mu\, (\mu-\nu)^{n_i+n_j-1} \exp(-a\mu)\exp(a\nu) \frac{3\left(\frac{1+\mu\nu}{\mu+\nu}\right)^2 - 1}{(\mu+\nu)^2} \cdot$$

$$\cdot \sum_{\gamma=0}^{\ell_i+\ell_j} \sum_{q=0}^{\gamma} H^q_\gamma(\ell_i, \ell_j, m) \frac{(\mu\nu)^q}{(\mu-\nu)^\gamma} , \tag{31}$$

with the volume factor $\frac{1}{8}R^3(\mu+\nu)(\mu-\nu)$ included. (30) and (31) cannot be integrated directly because powers of $(\mu+\nu)$ greater than one appear in the denominators of some terms; at the point $\mu=1$, $\nu=-1$, $\mu+\nu$ vanishes and gives an undefined integral unless the terms can be arranged so that a suitably vanishing numerator appears for each occurrence of $\mu+\nu$ to a power greater than one in the denominator. Kolker and Karplus[26] showed how to make this arrangement; their method applied to (30) and (31) gives

$$\text{Type AB: } K \sum_{\alpha=-m}^{\ell_i} \sum_{\beta=m}^{\ell_j} \sum_{q=0}^{\alpha+\beta} g^q_{\alpha\beta}(\ell_i,\ell_j,m) \sum_{k=0}^{q+n_j-\beta-1} d_k(q,\beta,n_j) \cdot$$

$$\cdot \int_{-1}^{1} d\nu\, \nu^{2q+n_j-\beta-1-k} \exp(-b\nu) \int_1^\infty d\mu \frac{p(\mu,\nu)\exp(-a\mu)}{(\mu+\nu)^{5-n_i+\alpha-k}} \tag{32}$$

$$\text{Type BB: } K \sum_{\gamma=0}^{\ell_i+\ell_j} \sum_{q=0}^{\gamma} H^q_\gamma(\ell_i,\ell_j,m) \sum_{k=0}^{q+n_i+n_j-2-\gamma} d_k(q,1+\gamma-n_i,n_j) \cdot$$

$$\cdot \int_{-1}^{1} d\nu\, \nu^{2q+n_i+n_j-2-\gamma} \exp(a\nu) \int_1^\infty d\mu \frac{p(\mu,\nu)\exp(-a\mu)}{(\mu+\nu)^{4-k}}\ ; \tag{33}$$

with $d_k(n_1,n_2,n_3)$ defined implicitly by

$$\mu^{n_1}(\mu-\nu)^{n_3-n_2-1} \equiv (\mu+\nu-\nu)^{n_1}(\mu+\nu-2\nu)^{n_3-n_2-1}$$

$$= \sum_{k=0}^{n_1+n_3-n_2-1} d_k(n_1,n_2,n_3)\nu^{n_1+n_3-n_2-k-1}(\mu+\nu)^k \tag{34}$$

and

$$p(\mu,\nu) = -6\nu(1-\nu^2)^2 - 3(1-\nu^2)(1-5\nu^2)(\mu+\nu) + 4\nu(2-3\nu^2)(\mu+\nu)^2$$

$$+ (3\nu^2-1)(\mu+\nu)^3.$$

Thus evaluation of the EFG integrals reduces to evaluation of the $g^q_{\alpha\beta}$, H^q_γ, d_k, and integrals of the form

$$D(n_1,a,n_2,b) = \int_{-1}^{1} d\nu\ \nu^{n_2} \exp(-b\nu) \int_1^{\infty} d\mu \frac{p(\mu,\nu)\exp(-a\mu)}{(\mu+\nu)^{n_1}} . \qquad (35)$$

For Type AB, $n_1 = 5-n_i+\alpha-k$; the ranges of k and α and the restriction $\ell_i \leq n_i-1$ give $5-n_i+\alpha-k \leq 4$; similarly $n_2 = 2q+n_j-\beta-k-1 \geq 0$; for Type BB, $n_1 = 4-k \leq 4$, $n_2 = 2q+n_i+n_j-\gamma-2 \geq 0$. The parameter a is always positive; b may be positive, negative, or zero. The D integrals (35) can be evaluated in terms of the auxiliary integrals[26]

$$E(n,m,a,b) = \int_{-1}^{1} d\nu\ \nu^n (1-\nu^2)^m \exp(-b\nu) \int_1^{\infty} d\mu \frac{\exp(-a\mu)}{(\mu+\nu)^{m+1}} , \qquad (36)$$

the A-function (9), and

$$B_n(b) = \int_{-1}^{1} d\nu\ \nu^n \exp(-b\nu) . \qquad (37)$$

The A-function was discussed in the one-center integral section; the B-function must be evaluated carefully because of potential cancellation errors[11]. We used a routine for the B-function published by Pople and Beveridge[29] slightly modified to be accurate to at least 14 figures; it was checked against the tables of Miller et al.[12]. The E-functions of (36) can be expressed (by repeated integration by parts) in terms of

$$E(n,0,a,b) = \int_{-1}^{1} d\nu\ \nu^n \exp(-b\nu) \int_1^{\infty} d\mu \frac{\exp(-a\mu)}{(\mu+\nu)} . \qquad (38)$$

Ruedenberg, Roothaan, and Jaunzemis[30] have given formulas for

this integral (their notation is considerably different):

$$E(n,0,a,b) = (-1)^n \left(\frac{\partial}{\partial b}\right)^n E(0,0,a,b) \tag{39}$$

$$E(0,0,a,b) = A_0(a-b)[Ei(-2b) - \ln|2b| + \ln(2a)]$$
$$+ A_0(b-a)E_i(-2a), \tag{40}$$

where Ei is the exponential integral,

$$Ei(x) = \int_{-\infty}^{x} \frac{e^t}{t}\,dt, \quad x < 0$$

$$= \lim_{\varepsilon \to 0} \left[\int_{-\infty}^{-\varepsilon} \frac{e^t}{t}\,dt + \int_{\varepsilon}^{x} \frac{e^t}{t}\,dt\right], \quad x > 0. \tag{41}$$

A routine to calculate Ei(x) to double precision on the IBM 360 has been published[31] and documented[32]; it was used in this work. It was checked against tabulated values[4]. Evaluation of (39) involves, by (40), differentiation of the A-functions, which can be done by (9), and evaluation of

$$\left(\frac{\partial}{\partial b}\right)^k [Ei(-2b) - \ln|2b| + \ln(2a)] \equiv \left(\frac{\partial}{\partial b}\right)^k F,$$

for k=0 to n. By (41), for k > 0,

$$\left(\frac{\partial}{\partial b}\right)^k F = \left(\frac{d}{db}\right)^{k-1} \left(\frac{\exp(-2b)-1}{b}\right) = (-2)^k \int_0^1 dx\, x^{k-1} \exp(-2bx).$$

The integral is that of (10); its accurate evaluation was

discussed earlier.

This completes discussion of the evaluation of the two-center EFG integrals. The final formulas are

$$\text{Type AB: } K \sum_{\alpha=-m}^{\ell_i} \sum_{\beta=m}^{\ell_j} \sum_{q=0}^{\alpha+\beta} g^q_{\alpha\beta}(\ell_i,\ell_j,m) \sum_{k=0}^{q+n_j-\beta-1} d_k(q,\beta,n_j) \cdot$$

$$\cdot\, D(5-n_i+\alpha-k,a,2q+n_j-\beta-k-1,b) \tag{42}$$

$$\text{Type BB: } K \sum_{\gamma=0}^{\ell_i+\ell_j} \sum_{q=0}^{\gamma} H^q_\gamma(\ell_i,\ell_j,m) \sum_{k=0}^{q+n_i+n_j-\gamma-2} d_k(q,1+\gamma-n_i,n_j) \cdot$$

$$\cdot\, D(4-k,a,2q+n_i+n_j-\gamma-2,-a), \tag{43}$$

with D as defined in (35). We have not presented full details, as the details of expressing the D functions in terms of the E functions and of expressing (36) in terms of (38) are tedious and require much space. The details can be deduced from the FORTRAN listing in a later section.

D) Documentation

Most of the auxiliary functions for the two-center EFG integrals are not common functions and are not available in tables, with the exception of $B_n(x)$ and $Ei(x)$, whose documentation has already been mentioned. The $g^q_{\alpha\beta}(\ell_i,\ell_j,m)$ were

tested against Guseinov's tabulations[27]; with allowances made for sign changes induced by the different choice of coordinate system agreement was to at least 14 places. There is a very accurate source for values of two-center EFG integrals: Flygare et al.[33] evaluated a number of integrals for the Foster and Boys[34] basis for formaldehyde by two different methods: Gaussian transform[35,36], and Barnett-Coulson expansion[37] about a single center. They verified that the two agreed to six decimal places and published the numbers to this accuracy. Both the above methods are different from ours; thus this tabulation provides a good test of our routines. In Table V our EFG integrals are given to 9 places for comparison to the 6-place integrals of Flygare et al. Note that in every case agreement is to the full 6 places. An earlier tabulation of some two-center EFG integrals for CO by Scrocco[38] is compared with our routines in Table VI; Scrocco's values were published to five decimal places. Agreement is to the full five places in most cases, but for the Type BB integrals there is one disagreement in the fourth decimal place and two in the fifth. Since these integrals are similar to those calculated by Flygare et al. (the orbital exponents are identical, with the C-O distance changing slightly), we conclude that Scrocco's program was inaccurate for these integrals, which is possible since the calculations were done at a time (1960) when no other programs were available for comparison. Unfortunately neither the Flygare nor Scrocco test basis contains a d-orbital; however Kahalas and Nesbet[39]

TABLE V: Comparison of our two-center EFG integral routines with values published by Flygare et al.[a] for H_2CO. All values in atomic units.

1. Type AB: $\langle\phi_i(a)|q(a)|\phi_j(b)\rangle$ (subroutine EFGAB)

ϕ_i	ϕ_j	EFGAB	Literature[a]
1	5	.000232264	.000232
1	6	.035274869	.035275
1	7	-.067265099	-.067265
2	5	.008151706	.008152
2	6	.056658030	.056658
2	7	-.090492184	-.090492
3	5	.013739810	.013740
3	6	.200200955	.200201
3	7	-.320260870	-.320261
4	8	-.034336699	-.034337

2. Type BB: $\langle\phi_i(b)|q(a)|\phi_j(b)\rangle$ (subroutine EFGBB)

ϕ_i	ϕ_j	EFGBB	Literature[a]
5	5	.164379056	.164379
5	6	.036232517	.036233
5	7	-.014887167	-.014887
6	6	.112154723	.112155

continued

TABLE V: (cont'd.)

ϕ_i	ϕ_j	EFGBB	Literature[a]
6	7	-.091607059	-.091607
7	7	.188215035	.188215
8	8	.074124568	.074125

[a]Ref. 33. The orbitals are:

	n	ℓ	m	ζ	type
ϕ_1	1	0	0	7.7	1sO
ϕ_2	2	0	0	2.275	2sO
ϕ_3	2	1	0	2.275	2pσO
ϕ_4	2	1	1	2.275	2pπO
ϕ_5	1	0	0	5.7	1sC
ϕ_6	2	0	0	1.625	2sC
ϕ_7	2	1	0	1.625	2pσC
ϕ_8	2	1	1	1.625	2pπC

Internuclear distance: 2.3 au.

TABLE VI: Comparison of our routines for two-center EFG integrals with values published by Scrocco[a]. All values in atomic units. For the CO molecule.

1. Type AB: $\langle\phi_i(a)|q(a)|\phi_j(b)\rangle$ (subroutine EFGAB)

ϕ_i	ϕ_j	EFGAB	Literature[a]
1	5	.000604470	.00060
1	6	.040680656	.04068
1	7	-.079154320	-.07915
2	5	.013770853	.01377
2	6	.061979853	.06198
2	7	-.097297731	-.09730
3	5	.023171450	.02317
3	6	.228650410	.22865
3	7	-.360345326	-.36035
4	8	-.045435643	-.04544

2. Type BB: $\langle\phi_i(b)|q(a)|\phi_j(b)\rangle$ (subroutine EFGBB)

ϕ_i	ϕ_j	EFGBB	Literature[a]
5	5	.206380358	.20580
5	6	.045471759	.04548
5	7	-.020132626	-.02011

continued

TABLE VI: (cont'd.)

ϕ_i	ϕ_j	EFGBB	Literature[a]
6	6	.124502104	.12450
6	7	-.100387862	-.10039
7	7	.210769799	.21077
8	8	.081368257	.08137

[a]Ref. 38. The orbitals are:

	n	ℓ	m	ζ	type
ϕ_1	1	0	0	7.7	1sO
ϕ_2	2	0	0	2.275	2sO
ϕ_3	2	1	0	2.275	2pσO
ϕ_4	2	1	1	2.275	2pπO
ϕ_5	1	0	0	5.7	1sC
ϕ_6	2	0	0	1.625	2sC
ϕ_7	2	1	0	1.625	2pσC
ϕ_8	2	1	1	1.625	2pπC

Internuclear distance: 2.132 au.

published a wavefunction and the calculated q_{elec} at the Li nucleus for LiH in a basis containing a 3d-orbital centered on Li. The published value of Kahalas and Nesbet for q_{elec} at 3.02 au internuclear distance in this basis is -.105976018 au, while the value calculated using our EFG integrals and their 8-place MO coefficients is -.105975920 au; the disagreement is 1 in the seventh place, which is within the expected error range for 8-place coefficients. Since integrals for higher n and ℓ values involve the same formulas as those for s,p, and d orbitals, with differences only in indices and parameters, we estimate that EFGAB and EFGBB are accurate to at least 7 significant figures.

E) Program listings

The flowchart, subroutine calling diagram, subroutine descriptions, and FORTRAN listing of the program TOOCE, which calculates all EFG integrals, both one- and two-center, necessary for a diatomic molecule in a two-center basis of STO's, appear in the following pages.

Flowchart for program TOOCE

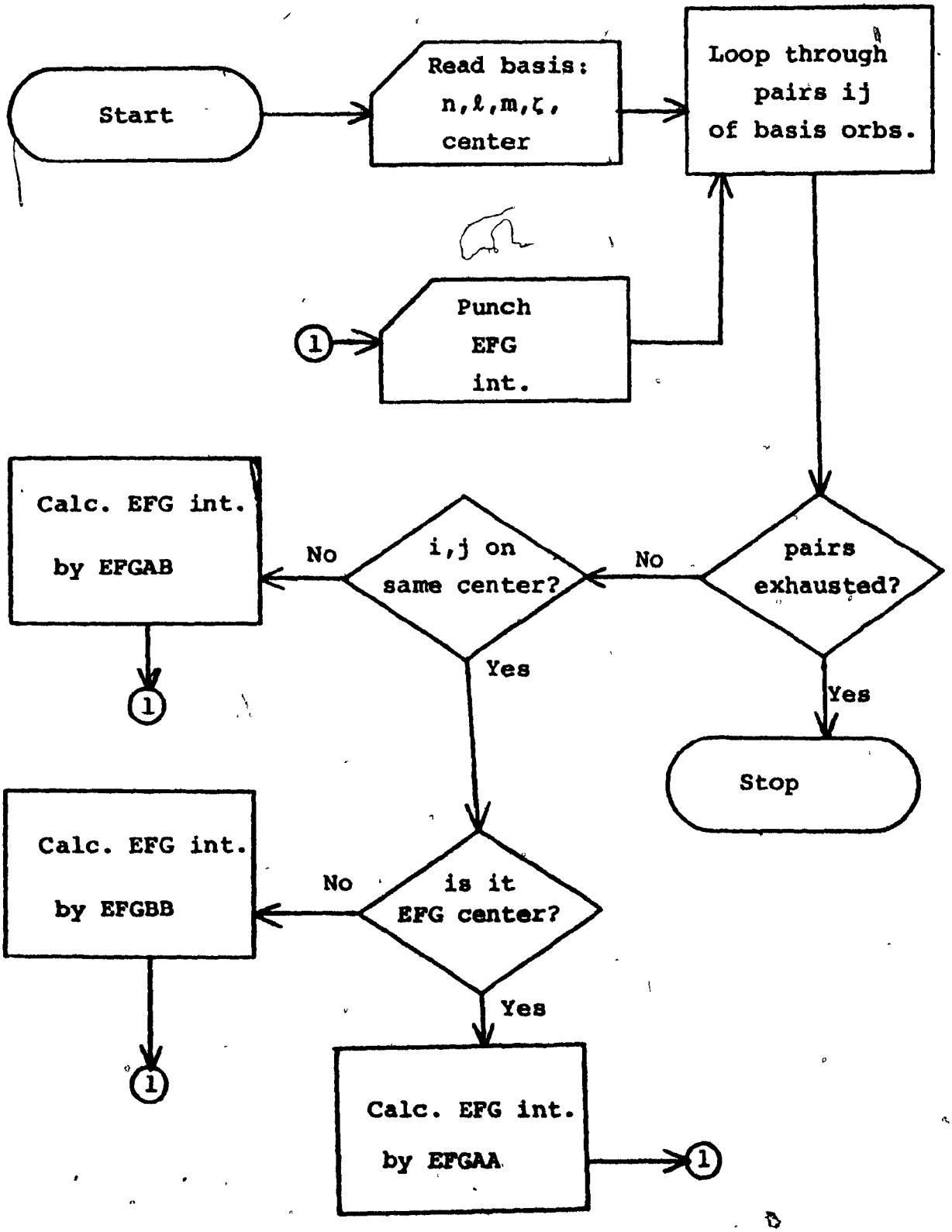

Subroutine calling diagram for program TOOCE, calculation of EFG integrals for diatomic molecule in two-center basis of STO's. Double arrows indicate transfer of control; single arrows indicate mathematical function calls. Dashed arrow indicates reference to an array.

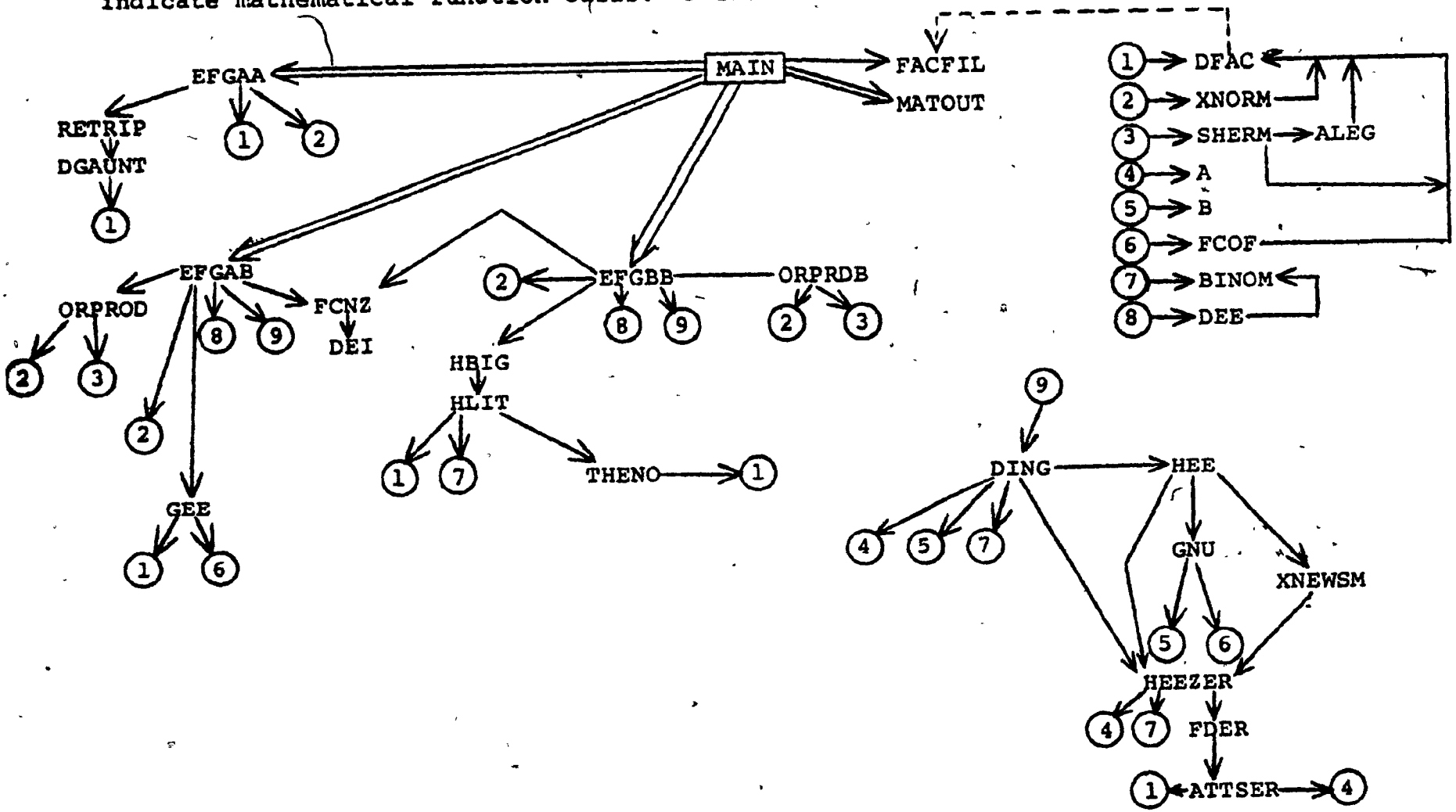

Subroutine descriptions, program TOOCE.

MAIN - reads input data, prints out input data, directs calculation.

FACFIL - fills an array with double precision factorials of integers for access by DFAC.

MATOUT - prints nxn array.

EFGAA - one-center EFG integrals.

RETRIP - integral over three real normalized spherical harmonics.

DGAUNT - integral over three complex normalized spherical harmonics.

EFGAB - calculates Type AB EFG integral.

FCNZ - calculates two quantities needed for evaluation of (38).

DEI - exponential integral routine of Paciorek[31].

ORPROD - the product of the values of $\phi_i(a)$ and $\phi_j(b)$ at center a.

GEE - the Guseinov expansion coefficient (28).

EFGBB - Type BB two-center EFG integral.

ORPRDB - product of values of $\phi_i(b)$ and $\phi_j(b)$ at center a.

HBIG - the H coefficients defined above (29).

HLIT - the h coefficients of (29).

THENO - normalization constant for associated Legendre polynomial.

DFAC - returns double precision factorial of an integer from array filled by FACFIL.

XNORM - radial normalization constant for an STO.

SHERM - evaluates real normalized spherical harmonic at a point (θ,ϕ)

ALEG - evaluates associated Legendre polynomial at a point $-1 < x < 1$, coded from algorithm by Herndon[23].

A - the A-function (9).

B - the B-function (37).

FCOF - the coefficients defined implicitly above (28).

BINOM - binomial coefficient.

DEE - the d coefficients defined implicitly in (34).

DING - the D integrals of (35).

HEE - the E functions (36).

HEEZER - the E-functions with second index = 0, (38).

GNU - function which arises in expressing HEE in terms of HEEZER.

XNEWSM - function which arises in expressing HEE in terms of HEEZER.

FDER - the iterated differentiation (below (41)) in evaluation of HEEZER.

ATTSER - auxiliary function (10).

PROGRAM TOOCF

```
C
C     MAIN PROGRAM
C
      IMPLICIT REAL*8(A-H,O-Z)
      COMMON/FAC/F1(51)
      DIMENSION N(100),L(100),M(100),Z(100),NC(100),EFG(100,100)
      CALL FACFIL
      I=1
C     READ INTERNUCLEAR DISTANCE, AU
      READ(5,3) R
    2 FORMAT(F10.5)
C     READ IN BASIS INFO--CENTER,QUANTUM NUMBERS, EXPONENT
    1 READ(5,2,END=50) NC(I),N(I),L(I),M(I),Z(I)
      FORMAT(4I2,F10.5)
      I=I+1
      GO TO 1
   50 NO=I-1
C     PRINT BASIS INFO AND INTERNUCLEAR DISTANCE
      WRITE(6,11)
   11 FORMAT('0    BASIS SET'/' ',2X,'CENTER',5X,'N',2X,'L',2X,'M',5X,'EX
     1PONENT'/' ')
      DO 12 I=1,NO
    1 WRITE(6,13) NC(I),N(I),L(I),M(I),Z(I)
   13 FORMAT(' ',4X,I ,6X,I2,2I3,5X,F8.5)
      WRITE(6,14) R
   14 FORMAT('0'/' ',2X,'INTERNUCLEAR DISTANCE, AU',2X,F10.6)
C     DETERMINE IF TYPE AA, AB, OR BB AND DIRECT TO PROPER ROUTINE
      DO 4 I=1,NO
      DO 4 J=I,NO
      III=NC(I)+NC(J)-1
      GO TO (5,6,7),III
      EFG(I,J)=EFGAA(N(I),L(I),M(I),Z(I),N(J),L(J),M(J),Z(J))
      GO TO 4
    6 II=I
      IF(NC(I).NE.1) II=J
      I2=I+J-II
      EFG(I,J)=EFGAB(N(II),L(II),M(II),Z(II),N(I2),L(I2),M(I2),Z(I2),R)
      GO TO 4
    7 EFG(I,J)=EFGBB(N(I),L(I),M(I),Z(I),N(J),L(J),M(J),Z(J),R)
    4 CONTINUE
C     PRINT CALCULATED EFG MATRIX
      WRITE(6,8)
    8 FORMAT('0    EFG MATRIX')
      CALL MATOUT(EFG,Z,NC,100,NO,1)
      DO 9 I=1,NO
    9 WRITE(7,10) ((I,J,EFG(I,J)),J=I,NO)
   10 FORMAT(3(2I2,D21.14))
      STOP
      END
C
C
C
      REAL FUNCTION A*B(N,X)
      IMPLICIT REAL*8(A-H,O-Z)
C     RETURNS THE N-TH ORDER A-FCN EVALUATED AT X.
C     I.E. (-D/DX)**N(EXP(-X)/X).
      IF(X.EQ.0.D0) GO TO 25
      IF(N.LT.0) GO TO 25
```

PROGRAM TOOCE

```
    1 FK1=3.D0*HEEZER(INU+2  ,AX,BX,F,G)-HEEZER(INU    ,AX,BX,F,G)
      FK2=AX*(12.D0*HEEZER(INU+3  ,AX,BX,F,G)-8.D0*HEEZER(INU+1,AX,BX,F,
     |G)+7.5D0*HEE(1,INU+2  ,AX,BX,F,G)-1.5D0*HEE(1,INU    ,AX,BX,F,G)
     |+2.D0*HEE(2,INU+1,AX,BX,F,G))
      FK3=(DEXP(-AX)/2.D0)*(13.D0*B(INU+2  ,BX)-6.D0*B(INU+1,BX)-3.D0*B(
     |INU    ,BX))
      DING=FK1+FK2-FK3
      GO TO 10
    2 FK1=(DEXP(-AX)/AX)*(3.D0*B(INU+2,BX)-B(INU    ,BX))
      FK2=-12.D0*HEEZER(INU+3  ,AX,BX,F,G)
     |+9.D0*HEEZER(INU+1  ,AX,BX,F,G)+3.D0*HEE(1,INU    ,AX,BX,F,G)
     |-15.D0*HEE(1,INU+2,AX,BX,F,G)-6.D0*HEE(2,INU+1  ,AX,BX,F,G)
      DING=FK1+FK2
      GO TO 10
    3 XX1=A(1,AX)
      XX2=A(0,AX)
      FK1=3.D0*HEEZER(INU,AX,BX,F,G)-18.D0*HEEZER(INU+2,AX,BX,F,G)
     |+15.D0*HEEZER(INU+4,AX,BX,F,G)
      FK2=6.D0*HEE(1,INU+3,AX,BX,F,G)-6.D0*HEE(1,INU+1,AX,BX,F,G)
      FK3=-XX1*B(INU,BX)+7.D0*XX2*B(INU+1,BX)
      FK4=3.D0*XX1*B(INU+2,BX)-9.D0*XX2*B(INU+3,BX)
      DING=FK1+FK2+FK3+FK4
      GO TO 10
    4 XX0=A(0,AX)
      XX1=A(1,AX)
      XX2=A(2,AX)
      FK1=6.D0*(-HEEZER(INU+1,AX,BX,F,G)+2.D0*HEEZER(INU+3,AX,BX,F,G)
     |-HEEZER(INU+5,AX,BX,F,G))
      FK2=B(INU,BX)*(3.D0*XX0-XX2)
      FK3=B(INU+1,BX)*6.D0*XX1
      FK4=B(INU+2,BX)*(-11.D0*XX0+3.D0*XX2)
      FK5=-B(INU+3,BX)*XX1*6.D0
      FK6=B(INU+4,BX)*XX0*6.D0
      DING=FK1+FK2+FK3+FK4+FK5+FK6
   10 CONTINUE
      WRITE(6,100)  INU,IMPN,K,AX,BX,F,G,DING
  100 FORMAT('    DING',2X,3I7,2X,4D15.5,3X,D21.14)
      RETURN
      END
C
C
C
      REAL FUNCTION B*8(N,X)
C     RETURNS THE FAMILIAR B-FCN--INTEGRAL(NU=-1 TO 1) NU**N*EXP(-X*NU)
C     MODIFIED VERSION OF POPLE AND BEVERIDGE ROUTINE
      IMPLICIT REAL*8(A-H,O-Z)
      ABSX=DABS(X)
      IF(ABSX.GT.3.D0) GO TO 120
      IF(ABSX.GT.2.D0) GO TO 70
      IF(ABSX.GT.1.D0) GO TO 50
      IF(ABSX.GT..500) GO TO 80
      IF(ABSX.GT..0000001D0) GO TO 110
      GO TO 170
  110 LAST=12
      GO TO 140
   80 IF(N.LE.5) GO TO 120
      LAST=18
      GO TO 140
```

```
 90 IF(N.LE.7) GO TO 120
    LAST=19
    GO TO 140
 90 IF(N.LE.10) GO TO 120
    LAST=23
    GO TO 140
120 EXPX=DEXP(X)
    EXPMX=1.D0/EXPX
    TERM=(EXPX-EXPMX)/X
    IF(N.EQ.0) GO TO 100
    FAC=1.D0
    DO 130 I=1,N
    FAC=-FAC
130 TERM=(DFLOAT(I)*TERM+FAC*EXPX-EXPMX)/X
    GO TO 100
140 TERM=0.D0
    FAC=1.D0
    FACM=1.D0
    FACN=2.D0
    IF(MOD(N,2).NE.0) FACN=0.D0
    DO 150 M=1,LAST
    I=M-1
    TERM=TERM+(FAC*FACM*FACN)/(DFAC(I)*DFLOAT(I+N+1))
    FAC=-FAC
    FACM=FACM*X
    FACN=2.D0-FACN
150 CONTINUE
    GO TO 100
170 TERM=0.D0
    IF(MOD(N,2).EQ.0) TERM=2.D0/DFLOAT(N+1)
100 H=TERM
    RETURN
    END


C
C
C
      REAL FUNCTION HEP*8(M,N,AX,BX,F,G)
C     AUXILIARY FCN FOR FIELD GRADIENT INTEGRALS--
C     INTEGRAL (NU=-1 TO 1) NU**N*(1-NU**2)**M*EXP(-BX*NU)*INTEGRAL
C     (MU=1 TO INF)EXP(-AX*MU)/(MU + NU)**(M+1)
      IMPLICIT REAL*8(A-H,O-Z)
      IF(M.EQ.0) GO TO 20
      IF((M.LT.0).OR.(N.LT.0)) GO TO 25
      SUM=0.D0
      K=0
      ITOP=M-1
      FAC=DFLOAT(M)
      SN=1.D0
      AY=1.D0
    1 SUM=SUM+GNU(M,N,K,BX)*SN*AY/FAC
      K=K+1
      IF(K.LQ.M) GO TO 2
      FAC=FAC*DFLOAT(M-K)
      SN=-SN
      AY=AY*AX
      GO TO 1
    2 SUM=SUM*DEXP(-AX)
      TERM=AY*AX*XNEWSM(M,N,AX,BX,F,G)/FAC
```

```
      IF(MOD(M,2).NE.0) TERM=-TERM
      SUM=SUM+TERM
      HEF=SUM
      RETURN
   20 HEF=HEFZER(N,AX,BX,F,G)
      RETURN
   25 WRITE(6,26)  M,N
   26 FORMAT('0     HEF CALLING ERROR',3X,2I10)
      HEF=0.D0
      XX1=1.D72**2
      RETURN
      END
C
C
C
      REAL FUNCTION HEFZER*8(N,AX,BX,F,G)
C     AUXILIARY FCN FOR FIELD GRADIENT INTEGRALS--
C     INTEGRAL(NU=-1 TO 1) NU**N*EXP(-BX*NU)*INTEGRAL(MU=1 TO INF)
C     EXP(-AX*MU)/(MU + NU)
      IMPLICIT REAL*8(A-H,O-Z)
      SUM=0.D0
      ITOP=N+1
      FAC=1.D0
      IF(MOD(N,2).NE.0) FAC=-1.D0
      XX1=AX-BX
      DO 1 II=1,ITOP
      I=II-1
      XX2=A(I,XX1)
    1 SUM=SUM+BINOM(N,I)*XX2*FDER(N-I,F,BX)
    1 CONTINUE
      XX2=A(N,XX1)
      SUM=FAC*SUM*XX2*G
      HEFZER=SUM
      RETURN
      END
C
C
C
      REAL FUNCTION GNU*8(M,N,K,BX)
C     AUXILIARY FCN FOR FIELD GRADIENT INTEGRALS--
C     INTEGRAL(NU=-1 TO 1) NU**N*(1-NU)**M*(1+NU)**K*EXP(-BX*NU)
      IMPLICIT REAL*8(A-H,O-Z)
      SUM=0.D0
      KQ=0
      KTOP=M+K
    1 SUM=SUM+FCOM(KQ,K,M)*H(KQ+N,BX)
      KQ=KQ+1
      IF(KQ.LE.KTOP) GO TO 1
      GNU=SUM
      RETURN
      END
C
C
C
      REAL FUNCTION XNEWSM*8(M,N,A,B,F,G)
C     AUXILIARY FCN FOR FIELD GRADIENT INTEGRALS--
C     INTEGRAL(NU=-1 TO 1) NU**N*(1-NU**2)**M*EXP(-BX*NU)*
C     INTEGRAL(MU=1 TO INF) EXP(-AX*MU)/(MU + NU)
```

```
      IMPLICIT REAL*8(A-H,O-Z)
      SUM=0.D0
      FAC=1.D0
      ICOF=1
      IND=N
      ITOP=M+1
      DO 1 I=1,ITOP
      K=I-1
      SUM=SUM+FAC*DFLOAT(ICOF)*HFEZER(IND,A,B,F,G)
      FAC=-FAC
      ICOF=(M-K)*ICOF/I
      IND=IND+2
    1 CONTINUE
      XNEWSM=SUM
      RETURN
      END
C
C
C
      REAL FUNCTION XNORM*8(N,ZETA)
C     RETURNS THE RADIAL NORMALIZATION CONST OF A SLATER ORBITAL WITH
C     PRINCIPAL QUANTUM NUMBER N AND EXPONENT ZETA.
      IMPLICIT REAL*8(A-H,O-Z)
      IF(N.LT.0) GO TO 25
      III=N+N
      TOP=(ZETA+ZETA)**(III+1)
      BOT=DFAC(III)
      XNORM=DSQRT(TOP/BOT)
      RETURN
   25 WRITE(6,26)
   26 FORMAT('0    XNORM CALLING ERROR')
      XNORM=0.D0
      RETURN
      END
C
C
C
      REAL FUNCTION SHERM*8(L,M,COSTHT,CFI,SFI)
C     RETURNS THE VALUE OF THE REAL NORMALIZED SPHERICAL HARMONIC
C     S(L,M) EVALUATED AT THE POINT (THETA,FI).
C     COSTHT IS COSINE THETA. CFI AND SFI ARE SINE AND COSINE OF FI.
      IMPLICIT REAL*8(A-H,O-Z)
      M1=IABS(M)
      IF(M.EQ.0) GO TO 1
      CH=CFI
      SH=SFI
      IF(M1.EQ.1) GO TO 3
      DO 2 I=2,M1
      CHS=CH*CFI-SH*SFI
      SH=SH*CFI+CH*SFI
      CH=CHS
    2 CONTINUE
    3 XANG=CH
      IF(M.LT.0) XANG=SH
    4 PI=3.1415926535897930D0
      XFIN=1.D0/DSQRT(PI)
      IF(M.EQ.0) XFIN=XFIN/DSQRT(2.D0)
      XTHIN=DFLOAT(2*L+1)*DFAC(L-M1)/(2.D0*DFAC(L+M1))
```

```
      XTHIN=DSQRT(XTHIN)
      SHERM=ALEG(L,M1,COSTHT)*XTHIN*XFIN*XANG
      RETURN
    1 XANG=1.D0
      GO TO 4
      END
C
C
C
      REAL FUNCTION ALEG*8(L,M,X)
C     RETURNS THE VALUE OF THE ASSOCIATED LEGENDRE POLYNOMIAL P(L,M)
C     EVALUATED AT X=COS(A) FOR SOME ANGLE A. CODED FROM ALGORITHM BY
C     HERNDON, COMM OF THE ACM, APRIL, 1961.
      IMPLICIT REAL*8(A-H,O-Z)
      M1=IABS(M)
      IF(DABS(X).GT.1.D0) GO TO 26
      IF((X.EQ.1.D0).AND.(M1.NE.0)) GO TO 25
      IF(L.LT.M1) GO TO 25
      IF(L.EQ.0) GO TO 10
      IF(X.EQ.0.D0) GO TO 8
      XX1=1.D0
      IF(L.EQ.M1) GO TO 1
      XX1=X**(L-M1)
    1 XX2=-1.D0/(X*X)
      GO TO 2
    8 II1=(L-M1)/2
      IF(2*II1.NE.(L-M1)) GO TO 25
      XX4=DFAC(L+M1)/(DFAC(II1)*DFAC(M1+II1))
      IF(MOD(II1,2).NE.0) XX4=-XX4
      GO TO 3
    2 II1=0
      XX4=0.D0
    4 IF(2*II1.GT.(L-M1)) GO TO 3
      XX4=XX4+DFAC(2*(L-II1))*XX1/(DFAC(II1)*DFAC(L-II1)*DFAC(L-2*II1-M1
     ))
      XX1=XX1*XX2
      II1=II1+1
      GO TO 4
    3 XX4=XX4/DFLOAT(2**L)
      XX1=DSQRT(1.D0-X*X)
      IF(M1.EQ.0) GO TO 6
      XX1=XX1**M1
    7 XX4=XX4*XX1
    5 ALEG=XX4
      RETURN
    6 XX1=1.D0
      GO TO 7
   25 ALEG=0.D0
      RETURN
   10 ALEG=1.D0
      RETURN
   26 WRITE(6,27)
   27 FORMAT('0     ALEG CALLING ERROR')
      GO TO 25
      END
C
C
C
```

```
      REAL FUNCTION DEE*8(IB,IQ,IK,N2)
C     RETURNS THE COEFFICIENT OF THE IK-TH POWER OF (MU + NU) IN
C     THE EXPANSION OF MU**IQ*(MU - NU)**(N2-IB-1)
      IMPLICIT REAL*8(A-H,O-Z)
      ISAVE=N2-IB-1
      III=ISAVE+IQ-IK
      FAC=1.D0
      IF(MOD(III,2).NE.0) FAC=-1.D0
      IPTOP=ISAVE+1
      XXM=1.D0
      IF(ISAVE.NE.0) XXM=2.D0**ISAVE
      SUM=0.D0
      DO 1 I=1,IPTOP
      IP=I-1
      XX1=BINOM(ISAVE,IP)*BINOM(IQ,IK-IP)
      SUM=SUM+XX1*XXM
      XXM=XXM/2.D0
    1 CONTINUE
      DEE=FAC*SUM
      RETURN
      END
C
C
C
      REAL FUNCTIONEFGAB*8(N1,L1,M1,Z1,N2,L2,M2,Z2,R)
C     RETURNS THE QZZ FIELD GRADIENT INTEGRAL BETWEEN TWO SLATER ORBITAL
C     TYPE ORBITALS--THE FIRST CENTERED ON THE EFG CENTER AND THE SECOND
C     ON A CENTER +R ATOMIC UNITS ALONG THE Z AXIS.
      IMPLICIT REAL*8(A-H,O-Z)
      IF(M1.NE.M2) GO TO 25
      MM=IABS(M1)
      MM1=-MM
      IF(MOD(L1-MM,2).NE.0) MM1=MM1+1
      MM2=MM
      IF(MOD(L2-MM,2).NE.0) MM2=MM2+1
      SUM=0.D0
      SUM1=0.D0
      PI=3.14159265358979300
      XCON=4.D0/3.D0
      XCON=XCON*PI
      AX=.5D0*R*(Z1+Z2)
      BX=.5D0*R*(Z1-Z2)
      CALL FCNZ(F,G,Z1,Z2,R)
      IATOP=L1
      IBTOP=L2
      IA=MM1
    1 IB=MM2
    2 IQTOP=IA+IB
      IQ=0
    5 FAC=GEF(IA,IB,IQ,L1,L2,MM)
      IF(FAC.EQ.0.D0) GO TO 4
      SUM1=0.D0
      IK=0
      KTOP=IQ+N2-IB-1
      INU=KTOP+IQ
      IMPN=5-N1+IA
    3 SUM1=SUM1+DEE(IB,IQ,IK,N2)*DING(INU,IMPN,IK,AX,BX,F,G)
      IF(IK.EQ.KTOP) GO TO 4
```

```
      IK=IK+1
      INU=INU-1
      IMPN=IMPN-1
      GO TO 3
    4 SUM=SUM+FAC*SUM1
      IF(IQ.EQ.IQTOP) GO TO 6
      IQ=IQ+1
      GO TO 5
    6 IF(IB.EQ.IBTOP) GO TO 7
      IB=IB+2
      GO TO 2
    7 IF(IA.EQ.IATOP) GO TO 8
      IA=IA+2
      GO TO 1
    8 SUM=SUM*XNORM(N1,Z1)*XNORM(N2,Z2)
      II1=N1+N2-2
      IF(II1.EQ.0) GO TO 9
      SUM=SUM*(R/2.D0)**II1
    9 SUM=SUM+XCON*CRPROD(N1,L1,M1,Z1,N2,L2,M2,Z2,R)
      EFGAB=SUM
      RETURN
   25 EFGAB=0.D0
      RETURN
      END
C
C
C
      REAL FUNCTION FDER*8(N,F,BX)
C     AUXILIARY FUNCTION FOR EFG INZ--
C     (D/DBX)**N(F(BX)), WHERE THE FCN F IS DEFINED IN ROUTINE FCNZ.
      IMPLICIT REAL*8(A-H,O-Z)
      IF(N.LT.0) GO TO 25
      IF(N.EQ.0) GO TO 10
      IF(BX.EQ.0.D0) GO TO 3
      XX2=BX+BX
      FDER=(-2.D0)**N*ATTSER(N-1,XX2)
      RETURN
    3 FDER=(-2.D0)**N/DFLOAT(N)
      IF(MOD(N,2).EQ.0) FDER=-FDER
      RETURN
   10 FDER=F
      RETURN
   25 WRITE(6,26) N
   26 FORMAT('0 FDER CALL ERROR',1X,I10)
      STOP
      END
C
C
C
      REAL FUNCTION ATTSER*8(N,X)
      IMPLICIT REAL*8(A-H,O-Z)
C     RETURNS INT(0 TO 1) R**N*EXP(-X*R) DR
      XAE=X**(N+1)
      XX1=DFAC(N)/XAE
      XX2=A(N,X)
      XX3=XX1-XX2
      XCH=XX3/XX1
C     CHECK FOR CANCELLATION ERROR
```

```
      IF(XCH.LT..100) GO TO 1
C     ACCEPT SUBTRACTION IF NO CANCELLATION ERROR
      ATTSER=XX3
      RETURN
C     SERIES CALC IF CANCELLATION ERROR
    1 XCON=XX1*DEXP(-X)
      SUM=XAF/DFAC(N+1)
      K=N+2
      TERM=XAF*X/DFAC(K)
      SUM=SUM+TERM
    2 XCHK=DABS(TERM/SUM)
C     CHECK FOR CONV OF SERIES
      IF(XCHK.LT..5D-16) GO TO 3
      K=K+1
      TERM=TERM*(X/DFLOAT(K))
      SUM=SUM+TERM
      GO TO 2
    3 ATTSER=XCON*SUM
      RETURN
      END
C
C
C
      SUBROUTINE FCNZ(F,G,Z1,Z2,R)
C     RETURNS THE FCNS F AND G, WHEREG=EI(-(Z1+Z2)*R) AND
C     F=EI((Z2-Z1)*R)-LOG(ABS(Z2-Z1*R)+LOG((Z1+Z2)*R). IF Z1=Z2, F=GAMMA
C     +LOG((Z1+Z2)*R)
      IMPLICIT REAL*8(A-H,O-Z)
      GARG=-(Z1+Z2)*R
      G=DEI(GARG)
      FARG1=(Z2-Z1)*R
      FARG2=DABS(FARG1)
      FARG3=-GARG
      F=0.D0
      IF(FARG1.EQ.0.D0) GO TO 2
      F=DEI(FARG1)+DLOG(FARG3/FARG2)
      RETURN
    2 F=.57721566490153290D0+DLOG(FARG3)
      RETURN
      END
C
C
C
      REAL FUNCTION DEI*8(X1)
C     AN EXPONENTIAL INTEGRAL ROUTINE
C     BY K. PACIOREK
C     FOR X GREATER THAN 0, THE EXPONENTIAL INTEGRAL, EI, IS DEFINED BY
C     EI(X)=INTEGRAL(EXP(T)/T DT), FROM T = -INFINITY TO T=X.
C     THE INTEGRAL IS TAKEN AS THE CAUCHY PRINCIPAL VALUE.
C     FOR X LESS THAN ZERO, EI(X)=-EI(-X), WHERE
C     EI(Z)=INTEGRAL(EXP(-T)/T DT) FROM T=Z TO T=INFINITY.
      DOUBLE PRECISION DEI,X1,X,X0,XMX0,Y,R,DENM,FRAC,W,A,B,C,D,E,
     |F,P0,P1,P2,P3,P4,Q0,Q1,Q2,Q3,Q4,PX,QX,T,SUMP,SUMQ
      DIMENSION P1(9),Q1(9),P2(9),Q2(8),P3(10),Q3(9),PX(10),QX(10),
     |P4(10),Q4(9),P0(6),Q0(6)
      DIMENSION A(6),B(6),C(8),D(8),E(8),F(8)
      DATA P0/1.D0,2.23069937666899751D0,1.70277059606809295D0,
     |5.10499279623219400D-1,4.89089253789279154D-2,
```

PROGRAM TOOCE

```
|3.6546222413236842 9D-4/
 DATA Q0/1.D0,2.7306993766689975 1D0,2.7347869510692583 6D0,
|1.2176596296015153 2D0,2.2881793399052641 2D-1,
|1.3111415119497770 6D-2/
 DATA P1/5.9956994689237001 0D9,-2.5038999488635136 2D8,
|7.0592160959005674 7D8,-3.3689956420159190 1D6,
|8.9468329164375831 3D6,7.3714779018465744 3D4,2.8544688181364701 5D4,
|4.1262666724891193 9D2,1.1063954724163958 0D1/
 DATA Q1/2.5592649760761635 0D9,-2.7967335112298459 1D9,
|8.0282778294695650 7D8,-1.4498071439302389 3D8,1.7715830801079988 4D7
|,-1.4057545720255921 8D6,8.5377100018074097 D4,-3.0252368223822741 0
|D3,5.1257812 5D1/
 DATA P2/9.9895766651655170 4D-1,5.7311670574450801 8D0,
|4.1410242256285662 2D0,5.8865824075328111 1D0,-1.9413296751443070 2D1
|,7.3947220920445722 1D0,2.3273023389039141 D1,-3.6778311347831145 8D
|1,-2.4694098344836126 5D0/
 DATA Q2/1.1462525324901619 1D0,-1.9914960023123516 4D2,
|3.4136521292437553 9D2,5.2316558873455861 4D1,3.1727948925436932 8D2,
|-8.3876708418964070 7D0,9.6540521742928030 3D2,2.6398300731802459 3D0
|/
 DATA P3/9.9999331061605687 4D-1,-1.8450862323912786 7D0,
|2.6525758184527998 2D1,2.4954877304020594 4D1,
|-3.3236125793439622 8D1,-9.1348356999987425 5D-1,
|-2.1057407925480404 5D1,-1.0006419133992848 3D1,
|-1.8600921217264375 8D1,-1.6477211724634631 4D0/
 DATA Q3/1.0015338520453427 0D0,-1.0935561953910912 4D1,
|1.9910044708177424 7D2,1.1928324239686010 1D3,
|4.2941317833728840 D1,2.5388193156307080 3D2,
|5.9943323256674073 6D1,6.4038004053524155 D1,
|9.7324035992172903 D1/
 DATA P4/1.0000000000300486 D0,-3.0000000032099126 6D0,
|-3.0000664041313100 2D0,-7.0681097783502935 9D0,
|-1.5285662436929637 D1,-7.6314770162025363 1D0,
|-2.7379852862430538 9D1,-1.8194966492986890 6D1,
|-2.2312767077763241 0D2,1.7533880126546597 2D2/
 DATA Q4/1.9999999999904810 4D0,-2.9999989404032496 0D0,
|-7.9924359577633974 1D0,-1.2018776354715474 3D1,
|7.0483184718042467 6D1,1.1717922050208645 5D2,
|1.3779039023574799 D2,3.9727710910041451 8D0,
|3.9784597716741472 1D4/
 DATA A/-5.7721566490153286 3D-1,7.5416431366301662 0D-1,
|1.2384232927373234 D-1,2.4068135568397741 3D-2,
|1.3209430920960937 1D-3,6.5773939975326450 1D-5/
 DATA B/1.D0,4.2589919381158982 2D-1,7.9779471841022822 D-2,
|8.3208476098771677 D-3,4.8642713839301641 6D-4,
|1.3065519582284887 8D-5/
 DATA C/8.6774595483844374 4D-8,9.9999551930139030 2D-1,
|1.1348310555494584 4D1,4.5593064425338982 3D1,
|6.9327945129100302 3D1,4.2520203476884077 9D1,8.9367180880384393 9D0,
|4.0137766494066472 0D-1/
 DATA D/1.D0,1.2848193537915665 0D1,5.6443356956180319 9D1,
|1.3964318376991388 3D2,8.9731109712528980 2D1,3.1497184917044075 0D1,
|3.7355900037621222 4 3D0,9.0880456918886921 9D-2/
 DATA E/-9.9999999999973414 D-1,-3.4406199500668489 5D1,
|-4.2753267120198853 9D2,-2.3960194324749054 0D3,
|-5.1688521005547635 1D3,-6.5760969874802117 9D3,
|-2.1060773714263328 9D3,-1.4899084997294816 9D1/
 DATA F/1.D0,3.6406199500645980 4D1,4.9434507020990364 5D2,
```

PROGRAM TOOCE

```
     |3.190272374895433040D3,1.033707530858409770D4,
     |1.632414535577835030D4,1.114977528710966200D4,
     |2.378138991021602210D3/
      DATA X0/.372507410781366634D0/
      X=X1
    1 IF(X.LE.0.D0) GO TO 100
      IF(X.GE.12.D0) GO TO 60
      IF(X.GE.6.D0) GO TO 40
C     X IN (0,6)
      T=X+X
      T=T/3.D0-2.D0
      PX(10)=0.D0
      QX(10)=0.D0
      PX(9)=P1(9)
      QX(9)=Q1(9)
C     THE RATIONAL FUNCTION IS EXPRESSED AS A RATIO OF FINITE SUMS OF
C     SHIFTED CHEBYSHEV POLYNOMIALS AND IS EVALUATED BY NOTING THAT
C     T*(X)=T(2X-1) AND USING THE CLENSHAW-RICE ALGORITHM FOUND IN
C     REFERENCE 4.
      DO 10 L=2,8
      I=10-L
      PX(I)=T*PX(I+1)-PX(I+2)+P1(I)
   10 QX(I)=T*QX(I+1)-QX(I+2)+Q1(I)
      R=(.5D0*T*PX(2)-PX(3)+P1(1))/(.5D0*T*QX(2)-QX(3)+Q1(1))
C     (X-X0)=(X-X1)-X2, WHERE X1=409576229586./2**40 AND
C     X2=-.767177250199394 0D-12.
      XMX0=(X-409576229586.D0/1099511627776.D0)-.767177250199394 0D-12
      IF(DABS(XMX0).LT..037D0) GO TO 15
      DEI=DLOG(X/X0)+XMX0*R
      RETURN
C     A RATIONAL APPROXIMATION TO LOG(X/X0)=LOG(1+Y), WHERE Y=(X-X0)/X0
C     AND DABS(Y) IS LESS THAN .1, THAT IS FOR DABS(X-X0) LESS THAN .037
   15 Y=XMX0/X0
      SUMP=((((P0(6)*Y+P0(5))*Y+P0(4))*Y+P0(3))*Y+P0(2))*Y+P0(1)
      SUMQ=((((Q0(6)*Y+Q0(5))*Y+Q0(4))*Y+Q0(3))*Y+Q0(2))*Y+Q0(1)
      DEI=(SUMP/(SUMQ*X0)+R)*XMX0
      RETURN
C     X IN (6,12)
   40 DENM=P2(9)+X
      FRAC=Q2(8)/DENM
C     THE RATIONAL FUNCTION IS EXPRESSED AS A J-FRACTION.
      DO 25 J=2,8
      I=9-J
      DENM=P2(I+1)+X+FRAC
   25 FRAC=Q2(I)/DENM
      DEI=DEXP(X)*((P2(1)+FRAC)/X)
      RETURN
   60 IF(X.GE.24.D0) GO TO 80
C     X IN (12,24)
      DENM=P3(10)+X
      FRAC=Q3(9)/DENM
C     THE RATIONAL FUNCTION IS EXPRESSED AS A J-FRACTION.
      DO 26 J=2,9
      I=10-J
      DENM=P3(I+1)+X+FRAC
   26 FRAC=Q3(I)/DENM
      DEI=DEXP(X)*((P3(1)+FRAC)/X)
      RETURN
```

```
C       X GREATER THAN 24.
   80   IF(X.LE.174.673D0) GO TO 90
C       IF X IS GREATER THAN 174.673 DEI IS SET TO HIGHEST NUMBER ON S/36
        DEI=7.2D75
        RETURN
   90   Y=1.D0/X
        DENM=P4(10)+X
        FRAC=Q4(9)/DENM
C       THE RATIONAL FUNCTION IS EXPRESSED AS A J-FRACTION.
        DO 20 J=2,9
        I=10-J
        DENM=P4(I+1)+X+FRAC
   20   FRAC=Q4(I)/DENM
        DEI=DEXP(X)*(Y+Y*Y*(P4(1)+FRAC))
        RETURN
  100   IF(X.NE.0.D0)  GO TO 101
C       IF X=0 DEI IS SET TO MOST NEGATIVE NUMBER OF S/360
        DEI=-7.[redacted]5
        WRITE(6,500)
  500   FORMAT('0   DEI CALLED WITH A ZERO ARGUMENT, RESULT SET TO -INFINI
       |TY')
        RETURN
  101   Y=-X
  110   W=1.D0/Y
        IF(Y.GT.4.D0) GO TO 300
        IF(Y.GT.1.D0) GO TO 200
C       X IN (-1,0)
        DEI=DLOG(Y)-(((((A(6)*Y+A(5))*Y+A(4))*Y+A(3))*Y+A(2))*Y+A(1))/
       |((((((B(6)*Y+B(5))*Y+B(4))*Y+B(3))*Y+B(2))*Y+B(1))
        RETURN
C       X IN (-4,-1)
  200   DEI=-DEXP(-Y)*(((((((((C(8)*W+C(7))*W+C(6))*W+C(5))*W+C(4))*W+C(3))
       |*W+C(2))*W+C(1))/(((((((D(8)*W+D(7))*W+D(6))*W+D(5))*W+D(4))*W+
       |D(3))*W+D(2))*W+D(1)))
        RETURN
C       X LESS THAN -4
  300   DEI=-DEXP(-Y)*(W*(1.D0+W*(((((((E(8)*W+E(7))*W+E(6))*W+E(5))*W+
       |E(4))*W+E(3))*W+E(2))*W+E(1))/(((((((F(8)*W+F(7))*W+F(6))*W+F(5))
       |*W+F(4))*W+F(3))*W+F(2))*W+F(1))))
        RETURN
        END
C
C
C
        REAL FUNCTION GCE*8(I,J,K,L1,L2,M)
        IMPLICIT REAL*8(A-H,O-Z)
C       CALCULATES THE G COEFFICIENTS IN GUSEINOV'S EXPANSION OF PRODUCT
C       OF TWO ASSOC LEGENDRE POLYNOMIALS ON DIFFERENT CENTERS IN
C       ELLIPSOIDAL COORDINATES.
        IF(MOD(I+L1,2).NE.0) GO TO 10
        IF(MOD(J+L2,2).NE.0) GO TO 10
        XX1=2.D0**(L1+L2+1)
        XF1=DFLOAT((2*L1+1)*(2*L2+1))
        XF2=DFAC(L1-M)*DFAC(L2-M)/(DFAC(L1+M)*DFAC(L2+M))
        XF1=DSQRT(XF1*XF2)
        XF2=DFAC(L2+J)/(DFAC((L2-J)/2)*DFAC((L2+J)/2)*DFAC(J-M))
        III=(L1-I)/2+(L2-J)/2+L2
        IF(MOD(III,2).NE.0) XF2=-XF2
```

```
      SUM=0.D0
      KS=-2
      XSN=-1.D0
    1 IF(KS.EQ.M+M) GO TO 2
      KS=KS+2
      XSN=-XSN
      III=L1+I+M+M-KS
      II2=(L1-I)/2-M+KS/2
      II3=II2+I+M+M-KS
      II4=I+M-KS
      IF(II2.LT.0) GO TO 1
      IF((III.LT.0).OR.(II3.LT.0).OR.(II4.LT.0)) GO TO 2
      TERM=XSN*DFAC(III)*FCOF(KS,M,M)/(DFAC(II2)*DFAC(II3)*DFAC(II4))
      SUM=SUM+TERM
      GO TO 1
    2 XX1=XF1*XF2*SUM/XX1
      IF(K.EQ.0) GO TO 3
      XX1=XX1*FCOF(K,I+M,J-M)
    3 GCF=XX1
      RETURN
   10 GCF=0.D0
      RETURN
      END
C
C
C
      REAL FUNCTION DRPROD*8(N1,L1,M1,Z1,N2,L2,M2,Z2,R)
C     RETURNS THE PRODUCT OF TWO STO'S EVALUATED AT THE CENTER OF THE
C     FIRST, WHERE THE SECOND IS +R ALONG THE Z AXIS.
      IMPLICIT REAL*8(A-H,O-Z)
      PROD=0.D0
      IF(N1.NE.1) GO TO 1
      XX1=XNORM(1,Z1)*XNORM(N2,Z2)
      PROD=SHERM(0,0,1.D0,1.D0,0.D0)*SHERM(L2,M2,-1.D0,1.D0,0.D0)*R**(N2
     1-1)
      PROD=PROD*DEXP(-Z2*R)*XX1
    1 DRPROD=PROD
      RETURN
      END
C
C
C
      REAL FUNCTION FCGDR*8(N1,L1,M1,Z1,N2,L2,M2,Z2,R)
C     RETURNS THE Q2Z FIELD GRADIENT INTEGRAL BETWEEN TWO STO'S WHEN
C     THE FCG CENTER IS R ATOMIC UNITS ALONG Z-AXIS FROM THE COMMON
C     EXPANSION CENTER OF THE TWO ORBS.
      IMPLICIT REAL*8(A-H,O-Z)
      SUM=0.D0
      IF(M1.NE.M2) GO TO 1
      CALL FCN2(F,G,0.D0,Z1+Z2,R)
      III=N1+N2-2
      AX=.5D0*R*(Z1+Z2)
      DX=-AX
      PI=3.14159265358979D0
      XCON=4.D0*PI/3.D0
      XFAC=XNORM(N1,Z1)*XNORM(N2,Z2)
      IF(N1+N2.NE.2) XFAC=XFAC*(R/2.D0)**III
      I=0
```

```
      ITOP=L1+L2
      IF(MOD(ITOP,2).NE.0) I=1
    2 JTOP=I
      J=0
    4 XJFAC=HBIG(I,J,L1,L2,M1)
      IF(XJFAC.EQ.0.D0) GO TO 5
      SUM1=0.D0
      IPTOP=J+III-1
      IP=0
      IN1=J+IPTOP
      IMPN=4
    3 SUM1=SUM1+DCF(I+I-N1,J,IP,N2)*DING(IN1,IMPN,IP,AX,BX,F,G)
      IP=IP+1
      IN1=IN1-1
      IMPN=IMPN-1
      IF(IP.LE.IPTOP) GO TO 3
      SUM=SUM+XJFAC*SUM1
    5 J=J+1
      IF(J.LE.JTOP) GO TO 4
      I=I+2
      IF(I.LE.ITOP) GO TO 2
      SUM=XFAC*SUM+XCON*ORPRDB(N1,L1,M1,Z1,N2,L2,M2,Z2,R)
    1 FEGBD=SUM
      RETURN
      END
C
C
C
      REAL FUNCTION ORPRDB*8(N1,L1,M1,Z1,N2,L2,M2,Z2,R)
C     RETURNS THE PRODUCT OF TWO STO'S EVALUATED AT POINT +R AUS ALONG
C     THE Z AXIS FROM THE COMMON CENTER OF THE CRDS.
      IMPLICIT REAL*8(A-H,O-Z)
      XX1=1.D0
      IF(N1+N2.NE.2) XX1=R**(N1+N2-2)
      XX1=XX1*XNORM(N1,Z1)*XNORM(N2,Z2)
      XXE=DEXP(-(Z1+Z2)*R)
      XXA=SHERM(L1,M1,-1.D0,1.D0,0.D0)*SHERM(L2,M2,-1.D0,1.D0,0.D0)
      ORPRDB=XX1*XXE*XXA
      RETURN
      END
      REAL FUNCTION THENO*8(L,M)
C     RETURNS THE NORMALIZATION CONSTANT OF THE L,M
C     ASSOC LEGENDRE POLYNOMIAL.
      IMPLICIT REAL*8(A-H,O-Z)
      XX1=.5D0*(2.D0*DFLOAT(L)+1.D0)
      MM=IABS(M)
      XX2=DFAC(L-MM)/DFAC(L+MM)
      THENO=DSQRT(XX1*XX2)
      RETURN
      END
C
C
C
      REAL FUNCTION BINOM*8(N,M)
C     RETURNS THE BINOMIAL COEFF(N|M)
      IMPLICIT REAL*8(A-H,O-Z)
      IA=0
      IF((M.LT.0).OR.(M.GT.N)) GO TO 2
```

```
      IA=1
      IB=M
      IF(IB+IB.GT.N) IB=N-IB
      IF(IB.EQ.0) GO TO 2
      I=0
    1 IA=(N-I)*IA/(I+1)
      I=I+1
      IF(I.LT.M) GO TO 1
    2 BINOM=DFLOAT(IA)
      RETURN
      END
C
C
C
      SUBROUTINE FACFIL
      IMPLICIT REAL*8(A-H,O-Z)
      COMMON/FAC/F1(51)
C     FILLS UP VECTOR ARRAY WITH FACTORIALS. PRELIMINARY TO USE OF DFAC.
C     F(N) CONTAINS FACTORIAL (N-1)
      F1(1)=1.D0
      X=1.D0
      DO 1 I=1,50
      III=I+1
      X=X*I
      F1(III)=X
    1 CONTINUE
      RETURN
      END
C
C
C
      REAL FUNCTION DFAC*8(J)
      IMPLICIT REAL*8(A-H,O-Z)
      COMMON/FAC/F1(51)
C     RETURNS FACTORIAL J. ARRAY F1 MUST BE FILLED BEFORE THIS ROUTINE
C     CAN BE USED.
      IF((J.GT.50).OR.(J.LT.0)) GO TO 25
      JJ1=J+1
      DFAC=F1(JJ1)
      RETURN
   25 WRITE(6,26) J
   26 FORMAT('0',10X,'DFAC CALLING ERROR',3X,I10)
      XX1=(1.D-50)**3
      DFAC=1.D0
      RETURN
      END
C
C
C
      REAL FUNCTION FCOF*8(MM,NN1,NN2)
      IMPLICIT REAL*8(A-H,O-Z)
C     CALCULATES COEFFICIENTS IN THE EXPANSION OF (X+Y)**N1*(X-Y)**N2
C     IN POWERS OF X AND Y.
      IF((MM.LT.0).OR.(MM.GT.NN1+NN2)) GO TO 10
      IF(MM.EQ.0) GO TO 11
      IF(MM.EQ.NN1+NN2) GO TO 13
      IF(NN1.EQ.NN2) GO TO 12
      IF(NN1.LT.NN2) GO TO 3
```

```
      N1=NN1
      N2=NN2
      XF1=1.D0
      GO TO 4
    3 N1=NN2
      N2=NN1
      XF1=1.D0
      IF(MOD(MM,2).NE.0) XF1=-1.D0
    4 IF(MM+MM.GT.N1+N2) GO TO 5
      M=MM
      GO TO 6
    5 M=N1+N2-MM
      IF(MOD(N2,2).NE.0) XF1=-XF1
    6 XF1=XF1*DFAC(N1)*DFAC(N2)
      SUM=0.D0
      KS=-1
      XSN=-1.D0
    1 IF(KS.EQ.N2) GO TO 2
      KS=KS+1
      XSN=-XSN
      III=M-KS
      II2=N2-KS
      II3=N1-M+KS
      IF(II3.LT.0) GO TO 1
      IF((III.LT.0).OR.(II2.LT.0)) GO TO 2
      TERM=XSN/(DFAC(KS)*DFAC(III)*DFAC(II2)*DFAC(II3))
      SUM=SUM+TERM
      GO TO 1
    2 FCOF=XF1*SUM
      RETURN
   10 FCOF=0.D0
      RETURN
   11 FCOF=1.D0
      RETURN
   12 IF(MOD(MM,2).NE.0) GO TO 10
      III=MM/2
      FCOF=DFAC(NN1)/(DFAC(III)*DFAC(NN1-III))
      IF(MOD(III,2).EQ.1) FCOF=-FCOF
      RETURN
   13 FCOF=1.D0
      IF(MOD(NN2,2).NE.0) FCOF=-1.D0
      RETURN
      END
C
C
C
      REAL FUNCTION HLIT*8(IA,IB,IQ,L1,L2,M)
C     GIVES SOME COEFFS IN EXPANSION OF PRODUCT OF TWO NORMALIZED ASSOC
C     LEGENDRE POLYNOMIALS ON THE SAME CENTER IN POWERS OF MU*NU AND
C     (MU-NU)
      IMPLICIT REAL*8(A-H,O-Z)
      FAC=1.D0
      IF(MOD(IQ,2).NE.0) FAC=-FAC
      FAC=FAC*BINOM(IA+IB,IQ)
      III=L1-IA
      II2=L2-IB
      IF(MOD(III,2).NE.0) GO TO 25
      IF(MOD(II2,2).NE.0) GO TO 25
```

```
      II1=III/2
      II2=II2/2
      II3=III+II2-M+L1+L2
      CONST=1.D0
      IF(MOD(II3,2).NE.0) CONST=-1.D0
      CONST=CONST*DFAC(L2+IB)/(DFAC(II2)*DFAC(II2+IB)*DFAC(IB-M))
      XNO=THENO(L1,M)*THENO(L2,M)
      CONST=CONST*FAC*XNO
      CONST=CONST/(2.D0**(L1+L2))
      SUM1=0.D0
      K=0
      FAC=1.D0
      KTOP=M+M
      III=IA+KTOP
      II2=L1+III
      II3=II2/2
      II4=II3-III
    1 IF(II4.LT.0) GO TO 2
      IF((III.LT.0).OR.(II2.LT.0).OR.(II3.LT.0)) GO TO 4
      XKFAC=FAC*FCOF(K,M,M)*DFAC(II2)/(DFAC(II3)*DFAC(II4)*DFAC(III))
      SUM1=SUM1+XKFAC
    2 K=K+2
      IF(K.GT.KTOP) GO TO 4
      III=III-2
      II2=II2-2
      II3=II3-1
      II4=II4+1
      FAC=-FAC
      GO TO 1
    4 HLIT=CONST*SUM1
      RETURN
   25 HLIT=0.D0
      RETURN
      END
C
C
C
      REAL FUNCTION HBIG*8(IGAM,IQ,L1,L2,M)
C     GIVES THE COEFF OF (NU*MU)**IQ/(MU-NU)**IGAM IN EXPANSION OF PROD
C     OF TWO NORMALIZED ASSOC LEGENDRE POLYNOMIALS ON SAME CENTER (B).
      IMPLICIT REAL*8(A-H,O-Z)
      SUM=0.D0
      III=L1+L2-IGAM
      IF(MOD(III,2).NE.0) GO TO 2
      MM=IABS(M)
      IBOT=MM+1
      ITOP=L2+1
      DO 1 III=IBOT,ITOP
      I=III-1
      II=IGAM-I
      SUM=SUM+HLIT(II,I,IQ,L1,L2,MM)
    1 CONTINUE
    2 HBIG=SUM
      RETURN
      END
C
C
C
```

```
      REAL FUNCTION DGAUNT*8(L1,L2,L,M1,M2,M)
C     CALCULATES INT(Y(L1,M1)*Y(L2,M2)*Y(L,M))
C     MUST HAVE M1+M2+M=0 FOR THE INTEGRAL TO BE NON-ZERO
      IMPLICIT REAL*8(A-H,O-Z)
      IF((L1.LT.0).OR.(L2.LT.0).OR.(L.LT.0)) GO TO 1
      IF((L.GT.(L1+L2)).OR.(L.LT.IABS(L1-L2))) GO TO 1
      IF((M1+M2+M).NE.0) GO TO 1
C     XXC=1/SQRT(2*PI)
      XXC=.39894228040143270D0
      III=(L1+L2+L)/2
      III=III+III
      IF(III.NE.(L1+L2+L)) GO TO 1
      LL1=L1
      LL2=L2
      LL=L
      MM1=IABS(M1)
      MM2=IABS(M2)
      MM=IABS(M)
      ICHK=0
      IF(M1.GE.0) ICHK=ICHK+1
      IF(M2.GE.0) ICHK=ICHK+1
      IF(M.GE.0) ICHK=ICHK+1
      GO TO (3,4,5),ICHK
    3 IF(M.GE.0) GO TO 5
      IF(M1.GE.0) GO TO 12
      MM=M2
      MM2=IABS(M)
      LL=L2
      LL2=L
      GO TO 5
   12 MM=M1
      MM1=IABS(M)
      LL=L1
      LL1=L
      GO TO 5
    4 IF(M.LT.0) GO TO 5
      IF(M1.LT.0) GO TO 10
      MM=IABS(M2)
      MM2=M
      LL=L2
      LL2=L
      GO TO 5
   10 MM=IABS(M1)
      MM1=M
      LL=L1
      LL1=L
    5 IG=(LL1+LL2+LL)/2
      SIGN=1.D0
      IF(MOD(IG-LL1-MM2,2).NE.0) SIGN=-1.D0
      XTOP=SIGN*DFAC(2*(IG-LL2))*DFAC(IG)
      XBOT=DFAC(IG-LL1)*DFAC(IG-LL2)*DFAC(IG-LL)*DFAC(2*IG+1)
      XRAT=DFLOAT((2*LL1+1)*(2*LL2+1)*(2*LL+1))*
     |DFAC(LL1+MM1)*DFAC(LL-MM1-MM2)*DFAC(LL2+MM2)*DFAC(LL2-MM2)/
     |(DFAC(LL1-MM1)*DFAC(LL+MM1+MM2)*2.D0)
      XFAC=DSQRT(XRAT)
      XFAC=XXC*XTOP*XFAC/XBOT
    9 XSUM=0.D0
      SIGN=1.D0
```

```
      IIT=0
      II1=LL2-MM2
      II2=LL-MM1-MM2
      II3=LL1-MM1+III
      II4=LL1+MM1-III
      II5=LL+MM1+MM2
    6 IF((III.LT.0).OR.(II2.LT.0).OR.(II3.LT.0)) GO TO 7
      IF(II4.LT.0) GO TO 8
      PSUM=SIGN*DFAC(II5)*DFAC(II3)/(DFAC(II1)*DFAC(IIT)*DFAC(II2)*
     |DFAC(II4))
      XSUM=XSUM+PSUM
    8 IIT=IIT+1
      II1=II1-1
      II2=II2-1
      II3=II3-1
      II4=II4+1
      II5=II5+1
      SIGN=-SIGN
      GO TO 6
    7 DGAUNT=XFAC*XSUM
      RETURN
    1 WRITE(6,2)
    2 FORMAT(' ','GAUNT COEFF INDEX ERROR')
      DGAUNT=0.D0
      RETURN
      END
C
C
C
      REAL FUNCTION RETRIP*8(L1,L2,L,M1,M2,M)
C     RETURNS INT(S(L1,M1)*S(L2,M2)*S(L,M)), WHERE S DENOTES REAL NOR-
C     MALIZED SPHERICAL HARMONIC
      IMPLICIT REAL*8(A-H,O-Z)
      IF((L1.LT.0).OR.(L2.LT.0).OR.(L.LT.0)) GO TO 26
      IF((L.GT.(L1+L2)).OR.(L.LT.IABS(L1-L2))) GO TO 25
      ICHK=1
      IF(M1.LT.0) ICHK=-ICHK
      IF(M2.LT.0) ICHK=-ICHK
      IF(M.LT.0) ICHK=-ICHK
      IF(ICHK.LT.0) GO TO 25
      III=L1+L2+L
      II2=2*(III/2)-III
      IF(II2.NE.0) GO TO 25
      IF((IABS(M).NE.IABS(M1+M2)).AND.(IABS(M).NE.IABS(M1-M2))) GO TO 25
      IZERO=0
      IF(M1.EQ.0) IZERO=IZERO+1
      IF(M2.EQ.0) IZERO=IZERO+1
      IF(M.EQ.0) IZERO=IZERO+1
      IGO=IZERO+1
      GO TO (6,9,25,5),IGO
   25 RETRIP=0.D0
      RETURN
    5 MM1=0
      MM2=0
      MM3=0
    8 RETRIP=DGAUNT(L1,L2,L,MM1,MM2,MM3)
      RETURN
    9 MM1=IABS(M1)
```

```
      MM2=-IABS(M2)
      MM3=-IABS(M)
      IF((MM1+MM2).LT.0) MM3=-MM3
      GO TO 8
    6 INEG=0
      IF(M1.LT.0) INEG=INEG+1
      IF(M2.LT.0) INEG=INEG+1
      IF(INEG.GT.0) GO TO 10
      SIGN=1.D0
   11 LL1=L1
      LL2=L2
      MM1=IABS(M1)
      MM2=IABS(M2)
      MM3=-IABS(M)
      IF(MM1.GE.MM2) GO TO 7
      MSAVE=MM1
      MM1=MM2
      MM2=MSAVE
      MSAVE=LL1
      LL1=LL2
      LL2=MSAVE
    7 IF(IABS(M).EQ.(MM1-MM2)) MM2=-MM2
C     XCON=1/SQRT2
      XCON=.7071067841865475D0
      RETRIP=SIGN*XCON*DGAUNT(LL1,LL2,L,MM1,MM2,MM3)
      RETURN
   10 SIGN=1.D0
      IF((M1+M2+M).EQ.0) SIGN=-SIGN
      GO TO 11
   26 WRITE(6,27)
   27 FORMAT('  RETRIP CALLING ERROR')
      RETRIP=0.D0
      RETURN
      END
C
C
C
      REAL FUNCTION EFGAA*8(N1,L1,M1,Z1,N2,L2,M2,Z2)
      IMPLICIT REAL*8(A-H,O-Z)
      IF(M1.NE.M2) GO TO 25
      IF(N1+N2.EQ.2) GO TO 25
      IF((L1.EQ.0).AND.(L2.EQ.0)) GO TO 25
      XX1=XNORM(N1,Z1)*XNORM(N2,Z2)
C     XXC=4*SQRT(PI/5)
      XXC=3.1706618308480 9D0
      XXA=RETRIP(L1,L2,2,M1,M2,0)
      XXR=DFAC(N1+N2-3)/(Z1+Z2)**(N1+N2-2)
      EFGAA=XX1*XXC*XXA*XXR
      RETURN
   25 EFGAA=0.D0
      RETURN
      END
C
C
C
      SUBROUTINE MATOUT(A,D,ID,K1,N,IM)
C     PRINTS OUT NXN SQUARE MATRIX WITH ROWS AND COLUMNS NUMBERED.
C
```

PROGRAM TODCE

```
C     IF MATRIX IS SYMMETRIC AND STORED IN DIAG AND TOP HALF ONLY,
C     IM=1, IF MATRIX IS STORED IN WHOLE ARRAY, IM=0.
C
C     IF MATRIX IS IMPLICITLY ORDERED VIA ARRAY ID, IM=-1 AND
C     EIGENVALUE ARRAY D IS PRINTED OUT UNDER THE COLUMNS
      IMPLICIT REAL*8(A-H,O-Z)
      DIMENSION A(K1,1),D(K1),ID(K1)
      IP=0
      K=6
      II1=MOD(N-1,6)
      II2=MOD(N-1,7)
      IF(II2.GT.II1) GO TO 1
    2 II2=MOD(N-1,8)
      IF(II2.GT.II1) K=8
      GO TO 3
    1 K=7
      II1=II2
      GO TO 2
    3 LLOW=K*IP+1
      LUP=K*(IP+1)
      IF(LUP.GT.N) LUP=N
      WRITE(6,4) (I,I=LLOW,LUP)
    4 FORMAT('0',10X,I2,8(10X,I2))
      DO 5 I=1,N
      IF(IM.EQ.1) GO TO 6
      IF(IM.LT.0) GO TO 10
      WRITE(6,7) I,(A(I,J),J=LLOW,LUP)
    7 FORMAT(' ',1X,I2,1X,8F12.6)
      GO TO 5
   10 WRITE(6,7) I,(A(I,ID(J)),J=LLOW,LUP)
      GO TO 5
    6 IF((LLOW.LT.I).AND.(LUP.LE.I)) GO TO 8
      IF((LLOW.LT.I).AND.(LUP.GT.I)) GO TO 9
      WRITE(6,7) I,(A(I,J),J=LLOW,LUP)
      GO TO 5
    8 WRITE(6,7) I,(A(J,I),J=LLOW,LUP)
      GO TO 5
    9 IIJ=I+1
      WRITE(6,7) I,(A(J,I),J=LLOW,I),(A(I,J),J=IIJ,LUP)
    5 CONTINUE
      IF(IM.LT.0) GO TO 11
   13 IF(LUP.EQ.N) RETURN
      IP=IP+1
      GO TO 3
   11 WRITE(6,12) (D(ID(J)),J=LLOW,LUP)
   12 FORMAT('0',2X,'E',1X,8F12.6)
      GO TO 13
      END
```

REFERENCES

1. H. Eyring, J. Walter, and G.E. Kimball, Quantum Chemistry, Wiley, N.Y., 1944. p. 58.
2. C.C.J. Roothaan, J. Chem. Phys. 19, 1445 (1951).
3. J.C. Slater, Phys. Rev. 36, 57 (1930).
4. M. Abramowitz and I.A. Stegun, Handbook of Mathematical Functions, U.S. Govt. Printing Office, Washington 1964. p. 255.
5. R.S. Mulliken, C.A. Rieke, D. Orloff, and H. Orloff, J. Chem. Phys. 17, 1248 (1949).
6. K. Ruedenberg, J. Chem. Phys. 19, 1459 (1951).
7. E.U. Condon and G.H. Shortley, The Theory of Atomic Spectra, Cambridge, 1963. p. 176.
8. J.A. Gaunt, Phil. Trans. Roy. Soc. 228A, 151 (1929).
9. M. Rotenberg, R. Bivins, N. Metropolis, and J.K. Wooten, The 3-j and 6-j Symbols, Technology Press, Cambridge, Mass., 1959.
10. C. Zener and V. Guillemin, Jr., Phys. Rev. 34, 999 (1929).
11. W.H. De Jeu, Chem. Phys. Lett. 5, 109 (1970).
12. J. Miller, J.M. Gerhauser, and F.A. Matsen, Quantum Chemistry Integrals and Tables, University of Texas Press, Austin, 1959.
13. Ref. 1, p. 389.
14. Ref. 4, p. 262.
15. K. Pearson, Tables of the Incomplete Γ-Function, Cambridge, 1951 (2nd reissue).

16. H.L. Harter, New Tables of the Incomplete Gamma-Function Ratio and of Percentage Points of the Chi-Square and Beta Distributions, U.S. Govt. Printing Office, Washington, 1963.

17. F.E. Harris and H.H. Michels, Adv. Chem. Phys. 13, 205 (1967).

18. Ref. 1, p. 369.

19. B.D. Roney, T.M. Spotswood, M.L. Heffernan, and B.H. James, certification for Integral Evaluation Routines Package, program QCPE 131, Quantum Chemistry Program Exchange, Bloomington, Indiana. (1968).

20. J.A. Pople and D.L. Beveridge, Approximate Molecular Orbital Theory, McGraw-Hill, N.Y., 1970. p. 48.

21. C.W. Scherr, J. Chem. Phys. 23, 569 (1955).

22. A.N. Lowan and Mathematical Tables Project, Tables of Associated Legendre Functions, Columbia University Press, N.Y., 1945.

23. J.R. Herndon, Comm. ACM 4, 178 (1961); R. George, Comm. ACM 6, 446 (1963) (erratum); S.M. Cobb; Comm. ACM 12, 635 (1969) (erratum).

24. Ref. 1, p. 367.

25. Ref. 1, p. 44.

26. H.J. Kolker and M. Karplus, J. Chem. Phys. 36, 960 (1962).

27. I.I. Guseinov, J. Phys. B 3, 1399 (1970).

28. E. Jahnke and F. Emde, Tables of Functions, Teubner, Berlin, 1938. p. 176.

29. Ref. 20, p. 175.

30. K. Ruedenberg, C.C.J. Roothaan, and W. Jaunzemis, J. Chem. Phys. 24, 201 (1956).

31. K.A. Paciorek, Comm. ACM 13, 446 (1970).

32. E.W. Ng, Comm. ACM 13, 448 (1970).

33. W.H. Flygare, J.M. Pochan, G.I. Kerley, T. Caves, M. Karplus, S. Aung, R.M. Pitzer, and S.I. Chan, J. Chem. Phys. 45, 2793 (1966).

34. J.M. Foster and S.F. Boys, Revs. Mod. Phys. 32, 303 (1960).

35. I. Shavitt, Meth. Comp. Phys. 2, 1 (1963).

36. C.W. Kern and M. Karplus, J. Chem. Phys. 42, 1062 (1965).

37. M.P. Barnett and C.A. Coulson, Phil. Trans. Roy. Soc. A243, 221 (1951).

38. E. Scrocco, Adv. Chem. Phys. 5, 319 (1963).

39. S.L. Kahalas and R.K. Nesbet, J. Chem. Phys. 39, 529 (1963).

APPENDIX II: Program for OCE-SCF Calculations

This program, which calculates a molecular wavefunction once the electron repulsion integrals have been stored on tape by program WINE, uses standard techniques for the iterative solution of the Hartree-Fock-Roothaan equations[1]; no discussion beyond that of Chapter II will be given except documentation, the subroutine flowchart, subroutine descriptions, and the program listing (program WUNIT).

Documentation

This program was used to repeat the calculation of the Cl^- ion by Clementi[2]; the energy and coefficient matrix agreed with Clementi's to as many places as published (5 decimal places in the coefficients, 8 significant figures in the energy). This calculation uses all the routines that a molecular calculation uses except XNUK2, the off-center nuclear attraction integral routine. This routine was documented in Appendix I; however attempts to reproduce early OCE-SCF molecular calculations by Moccia[3] always resulted in small differences in the energy and coefficients. As discussed in Chapter II, our attempt to repeat Moccia's 71-orbital OCE-SCF calculation of HCl[4] gave differences in the energy of about 1 in the second decimal place and differences in some of the coefficients of the 5σ MO of about 5 in the second decimal place. The q_{elec}'s differed by about .2 au. Moccia has informed us[5]

that his electron repulsion integrals were stored on tape only to six significant figures, while ours were stored to 16 figures; it is necessary to decide whether these differences in the electron repulsion integrals are sufficient to explain the difference in the two OCE-SCF calculations of HCl. A test calculation was made at r_e=2.4087 au using our OCE-SCF program and rounding the electron repulsion integrals to six significant figures[6]. The results (q_{elec}, energy, and MO coefficients) are presented in Table I; they are to be compared with Chapter II, Table VI and Chapter III, Table I. The energy differs by about 4 in the second place, and some of the coefficients in the 5σ MO differ by about 5 in the second place. This is of the same order as the differences between our repeat of Moccia's r=2.424 calculation and his published values. We emphasize that one would not expect to reproduce Moccia's results exactly by truncating the integrals (even had we done the truncated calculation at the 2.424 au internuclear separation for which Moccia published MO coefficients; we instead used 2.4087 au, at which distance Moccia indirectly reported q_{elec} but not the coefficients) since the truncation in storing his integrals would not have been to exactly six decimal figures but to a machine-dependent binary word-length. The q_{elec} for our truncated-integral 71-orbital calculation was 3.48 au (compared to an experimental value of 3.49 au[7]), while the calculation with the full 16-figure integrals gave (Chapter III, Table I) 3.73 au. Moccia did not report q_{elec} as such at r=2.4087 au but did report that his total

TABLE I: OCE-SCF calculation of HCl at R_e=2.4087 au with electron repulsion integrals rounded to 6 significant figures. Basis orbital numbering is that of Chapter II, Table II.

E_{elec} = -467.07666 au E_{tot} = -460.01892 au

q_{elec} = 3.47564 au q_{tot} = 3.61876 au

	MO coefficients				
basis orb.	1σ	2σ	3σ	4σ	5σ
1	-.091852	-.001574	.000049	-.030092	.010257
2	-1.078612	.203946	-.000957	.304322	-.100444
3	.223407	.223503	-.000354	-.295388	.105751
4	-.118629	-.115058	-.000549	.635446	-.218463
5	.064271	-.935896	.005156	-1.257639	.408454
6	-.015242	-.120495	-.001434	.607985	-.209897
7	.002768	.007865	-.000576	1.055450	-.251976
8	.001530	.004994	.000039	-.013356	-.019853
9	-.000701	-.002272	.000002	-.009895	.024805
10	-.002558	-.008125	.000157	-.242082	.162983
11	-.000196	-.000418	-.316325	-.010854	-.051664
12	.000208	-.001931	-.631672	-.017811	-.192122
13	-.000102	-.000672	-.118417	-.006225	.075296
14	.000034	-.000257	.022566	.140715	.706652
15	.000034	.000179	.020728	-.045261	.197018
16	-.000010	-.000053	-.005382	.019026	.006622

continued

TABLE I: (cont'd.)

	σ MO coefficients (cont'd.)				
basis orb.	1σ	2σ	3σ	4σ	5σ
17	-.000038	-.000146	-.026486	.071501	.057733
18	-.004596	.004222	-.002692	-.073840	.085065
19	.008322	-.009960	.003927	.165583	.046533
20	-.003861	.004570	-.001827	-.100791	.006450
21	-.000998	.001248	-.000465	.089004	.126427
22	.000000	.000130	.001629	-.039544	-.033850
23	.000006	-.000273	.006445	.032274	-.007022
24	-.000003	-.000099	-.007299	.067682	.125197
25	.000003	.000004	-.000086	-.003681	-.022608
26	-.000002	-.000078	-.000070	.039206	.086212
27	-.000001	.000059	.000002	-.025546	-.038231
28	.000002	-.000121	-.000096	.047625	.078741
29	-.000001	.000083	.000062	-.036910	-.059451
30	.000002	-.000126	-.000122	.051752	.085645
31	.000000	-.000026	-.000039	.010829	.019050
Eigen-value (au)	-104.833549	-10.561675	-8.028613	-1.108937	-.610706

	π MO coefficients	
basis orb.	1π	2π
32	-.307652	-.073177
33	-.643798	-.190421

continued

TABLE I: (cont'd.)

basis orb.	π MO coefficients (cont'd.) 1π	2π
34	-.125394	-.003256
35	.062879	.763899
36	-.085475	.193455
37	.104054	.174536
38	-.049692	-.013732
39	-.013990	.100427
40	.046662	-.236762
41	-.030768	.166758
42	-.005338	.039293
43	.015545	-.102340
44	-.001016	.015623
45	-.014412	.079909
46	.000045	.000779
47	-.000111	.009364
48	-.000014	.000266
49	-.000026	.007086
50	-.000023	.003948
51	-.000014	.002252
Eigenvalue (au)	-8.020966	-.465214

q combined with the eQq value of 67.3 MHz for ^{35}Cl in DCl determined by Cowan and Gordy[8] gave $Q(^{35}Cl) = .0782 \times 10^{-24}$ cm^2, which agrees to 3 figures with the value given by Ramsey[9]. One can deduce from this that Moccia's q_{elec} was 3.52 au. Thus the six-place integral truncation in our program produces a q_{elec} differing by .04 au from that reported by Moccia, although that calculated with the untruncated integrals differs from Moccia's value by about .2 au. This confirms that the integral storage differences indeed suffice to explain the differences between our calculation and that of Moccia.

The flowchart, subroutine calling diagram, subroutine descriptions, and FORTRAN listing of WUNIT appear in the following pages.

Flowchart for program WUNIT.

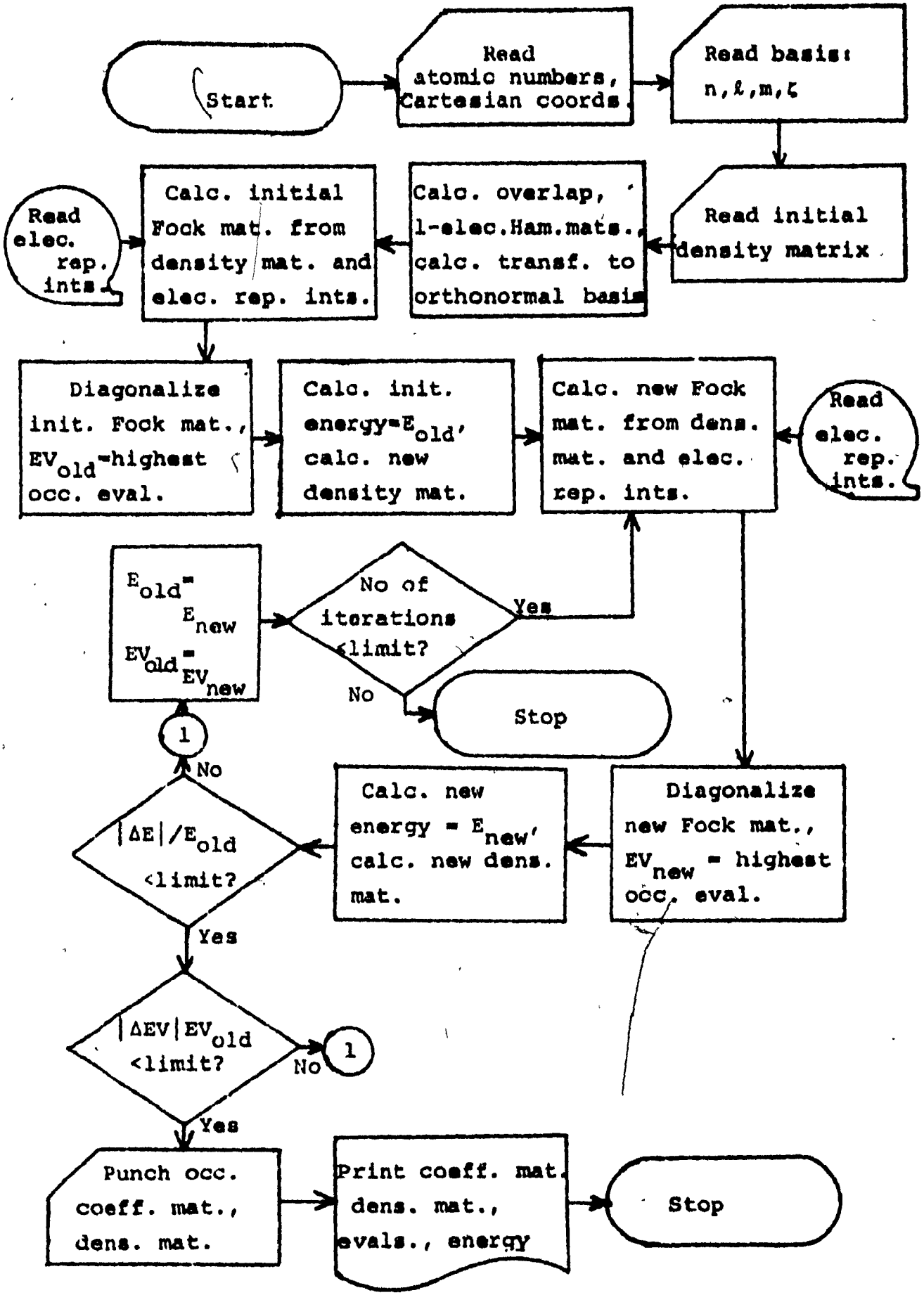

Subroutine calling diagram for program WUNIT, which performs molecular OCE-SCF calculation once electron repulsion integrals have been stored on tape by WINZ. Double arrows indicate transfer of control; single arrows indicate mathematical function calls. Dashed arrow indicates reference to an array.

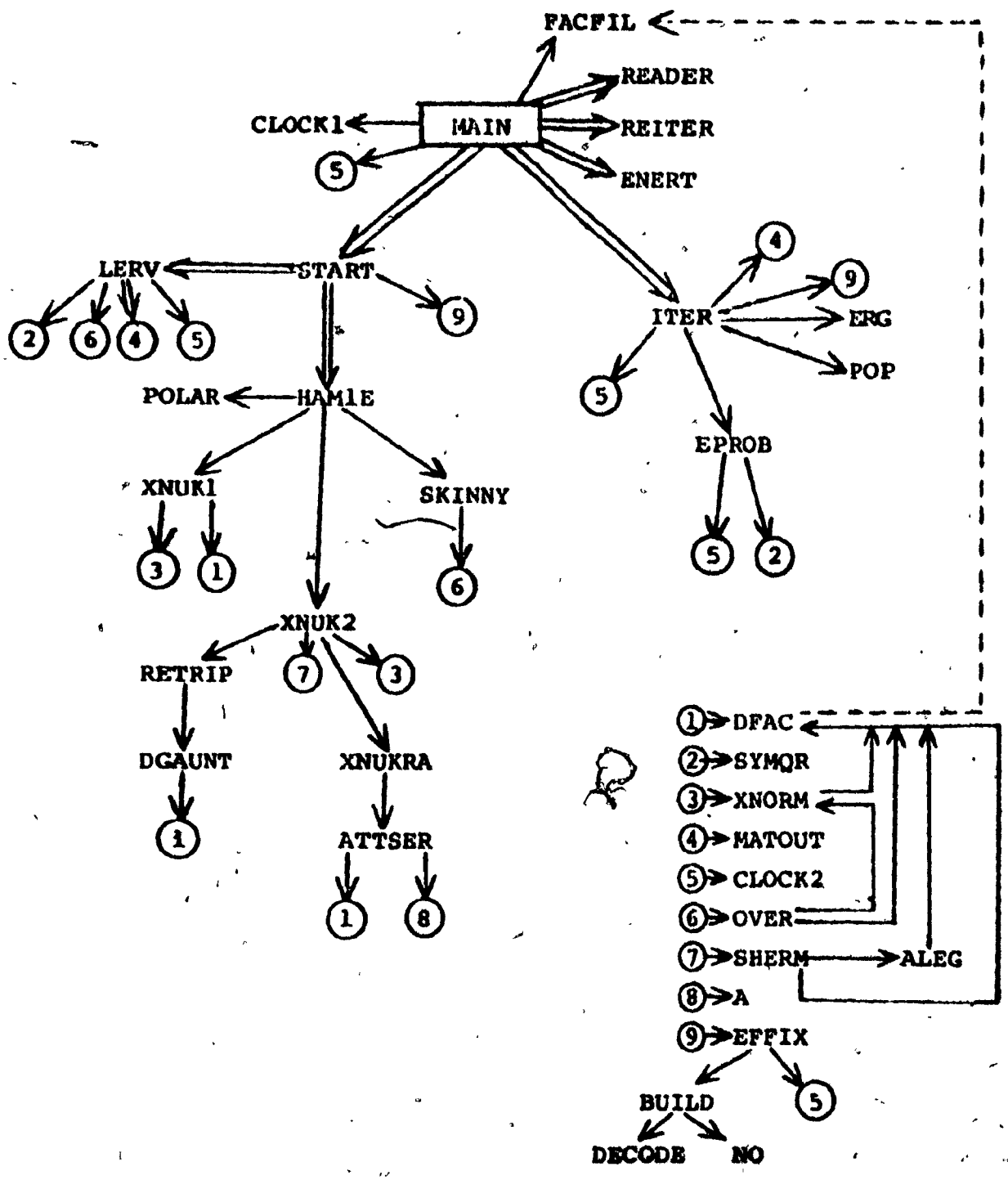

Subroutine descriptions for WUNIT.

MAIN - begins timing, directs reading and printing of input data, directs calculation, prints out total program time.

READER - reads input data and an initial guess of density matrix.

REITER - prints out input data.

DGAUNT - integral over three complex normalized spherical harmonics, Appendix I, equation (12).

FACFIL - fills array with double precision factorials of integers for later access by DFAC.

DFAC - returns double precision factorial of integer from array filled by FACFIL.

XNORM - radial normalization constant of STO, Appendix I, equation (6).

RETRIP - integral over three real normalized spherical harmonics, Appendix I, equation (7).

MATOUT - prints an nxn matrix.

POP - constructs density matrix for closed shell system given coefficient matrix.

LERV - constructs transformation matrix between STO basis and orthonormal OAO basis (Chapter II).

NO - determines how many distinct integers appear in the quadruple I,J,K,L; used in interpreting integral labels.

DECODE - determines the four basis orbital numbers represented by the single integral labeling integer.

SYMQR - Householder - QR routine for diagonalization of a symmetric matrix; routine published by Stewart[10].

ENERT - calculates and prints total molecular energy given the electronic energy.

XNUKRA - radial integral for off-center nuclear attraction integral. Appendix I, equation (23).

ATTSER - auxiliary integral of Appendix I, equation (10).

OVER - 1-center overlap integral for STO's.

SKINNY - kinetic energy integral between STO's on same center.

XNUK1 - nuclear attraction integral with central nucleus.

XNUK2 - nuclear attraction with off-center nucleus.

BUILD - interprets the labeling integers for electron repulsion integrals and adds the appropriate amounts to elements of the Fock matrix - builds the Fock matrix given the repulsion integrals and density matrix.

ERG - calculates electronic energy from density matrix and one-electron parts of Fock matrix.

EFFIX - reads electron repulsion integrals and labels from tape - directs construction of Fock matrix by BUILD.

EPROB - solves eigenvalue problem in non-orthonormal basis by transforming to OAO basis (Chapter II). Arranges eigenvalues and vectors in order of increasing energy.

ITER - directs iterative part of calculation, checks convergence, prints and punches out results.

START - directs the preliminaries to the iterative part of calculation.

SHERM - evaluates real normalised spherical harmonic at point θ,ϕ.

ALEG - evaluates associated Legendre polynomial (Appendix I, equation (1)), coded from algorithm by Herndon, Appendix I, reference 23.

POLAR - returns spherical polar coordinates of a point given the Cartesian coordinates.

A - the A-function, Appendix I, equation (9).

HAMIE - calculates and stores the one-electron part of the Fock matrix.

CLOCK1, CLOCK2 - timing routines devised by McGill University Computing Centre.

PROGRAM WUNIT

```
C
C     MAIN PROGRAM
C
      IMPLICIT REAL*8(A-H,O-Z)
      COMMON/ORBS/NOR(72),LOR(72),MOR(72),ZOR(72),N,NINT,N2,N3,N4
      COMMON/SCF/P(72,72),F(72,72),V(72,72),H(72),CD(72),D(72),E(72),ID(
     |72)
      COMMON/FAC/F1(51)
      COMMON/INZ/LABEL(1000),XFP(1000)
C     DIRECTS SCF CALCULATION -- MAIN PROGRAM.
      CALL CLOCK1
      CALL FACFIL
      CALL READER
      CALL REITER
      CALL START(E1)
      CALL ITER(N,E1)
      CALL ENERT(E1)
      CALL CLOCK2(NT2)
      XX1=DFLOAT(NT2)/60.D0
      WRITE(6,1) XX1
    1 FORMAT('0TOTAL PROGRAM TIME',2X,F8.2,1X,'SECONDS')
      STOP
      END
C
C
C
      SUBROUTINE READER
      IMPLICIT REAL*8(A-H,O-Z)
      COMMON/ORBS/NOR(72),LOR(72),MOR(72),ZOR(72),N,NINT,N2,N3,N4
      COMMON/STORE/X(20),Y(20),Z(20),NATOM(20),NAT,NOCC
      COMMON/SCF/P(72,72),F(72,72),V(72,72),H(72),CD(72),D(72),E(72),ID(
     |72)
C     READ IN TITLE CARD.
      READ(5,20,END=50)
   20 FORMAT('                                                          ')
      WRITE(6,20)
C     READ IN NUMBER OF ATOMS AND NO. OF ORBS IN BASIS SET.
      READ(5,1) NAT,N
    1 FORMAT(2I2)
C     READ IN NUMBER OF NON-ZERO ELEC REP INTEGRALS--OUTPUT FROM WINZ
      READ(5,4) NINT
    4 FORMAT(I6)
C     READ IN CARTESIAN COORDS AND ATOMIC NOS-EXPANSION CENTER MUST BE
C     AT ORIGIN.
      READ(5,2) ((X(I),Y(I),Z(I),NATOM(I)),I=1,NAT)
    2 FORMAT(3F15.5,5X,I2)
C     READ IN BASIS SET INFO.
      READ(5,3) ((NOR(I),LOR(I),MOR(I),ZOR(I)),I=1,N)
    3 FORMAT(2X,3I2,F10.6)
C     READ IN INPUT DENSITY MATRIX
      DO 5 I=1,N
    5 READ(5,6) (P(I,J),J=I,N)
    6 FORMAT(3(4X,D21.14))
      RETURN
   50 STOP
      END
C
C
```

```
C
      SUBROUTINE REITER
C     PRINTS OUT INPUT DATA AND GUESSED DENSITY MATRIX.
      IMPLICIT REAL*8(A-H,O-Z)
      COMMON/ORBS/NOR(72),LOR(72),MOR(72),ZOR(72),N,NINT,N2,N3,NA
      COMMON/STUFF/X(20),Y(20),Z(20),NATOM(20),NAT,NOCC
      COMMON/SCF/P(72,72),F(72,72),V(72,72),H(72),CD(72),D(72),E(72),ID(
     |72)
      WRITE(6,5)
    5 FORMAT('0',2X,'ATOMIC NUMBERS AND CARTESIAN COORDINATES - ATOMIC U
     |NITS')
      WRITE(6,2)
    2 FORMAT('0',5X,'ATOM',4X,'ATOMIC NUMBER',10X,'X',20X,'Y',20X,'Z')
      DO 6 I=1,NAT
    6 WRITE(6,4) I,NATOM(I),X(I),Y(I),Z(I)
    4 FORMAT(' ',5X,I3,9X,I2,11X,F12.6,9X,F12.6,9X,F12.6)
      WRITE(6,7)
    7 FORMAT('0',2X,'BASIS SET INFORMATION')
      WRITE(6,8)
    8 FORMAT('0',5X,'ORBITAL',10X,'N',5X,'L',5X,'M',7X,'EXPONENT')
      DO 9 I=1,N
    9 WRITE(6,10) I,NOR(I),LOR(I),MOR(I),ZOR(I)
   10 FORMAT(' ',5X,I2,11X,I2,4X,I2,4X,I2,4X,F12.6)
      WRITE(6,11) NINT
   11 FORMAT('0',2X,'NUMBER OF NON-ZERO R12 INTS',2X,I7)
      WRITE(6,12)
   12 FORMAT('0',2X,'INPUT DENSITY MATRIX')
      CALL MATOUT(P,0,10,72,N,1)
      RETURN
      END
C
C
C
      REAL FUNCTION DGAUNT*8(L1,L2,L,M1,M2,M)
C     CALCULATES INT(Y(L1,M1)*Y(L2,M2)*Y(L,M)).
C     MUST HAVE M1+M2+M=0 FOR THE INTEGRAL TO BE NON-ZERO
      IMPLICIT REAL*8(A-H,O-Z)
      IF((L1.LT.0).OR.(L2.LT.0).OR.(L.LT.0)) GO TO 1
      IF((L.GT.(L1+L2)).OR.(L.LT.IABS(L1-L2))) GO TO 1
      IF((M1+M2+M).NE.0) GO TO 1
C     XXC=1/SQRT(2*PI)
      XXC=.39894228040143270D0
      III=(L1+L2+L)/2
      III=III+III
      IF(III.NE.(L1+L2+L)) GO TO 1
      LL1=L1
      LL2=L2
      LL=L
      MM1=IABS(M1)
      MM2=IABS(M2)
      MM=IABS(M)
      ICHK=0
      IF(M1.GE.0) ICHK=ICHK+1
      IF(M2.GE.0) ICHK=ICHK+1
      IF(M.GE.0) ICHK=ICHK+1
      GO TO (3,4,5),ICHK
    3 IF(M.GE.0) GO TO 5
      IF(M1.GE.0) GO TO 12
```

```
      MM=M2
      MM2=IABS(M)
      LL=L2
      LL2=L
      GO TO 5
   12 MM=M1
      MM1=IABS(M)
      LL=L1
      LL1=L
      GO TO 5
    4 IF(M.LT.0) GO TO 5
      IF(M1.LT.0) GO TO 10
      MM=IABS(M2)
      MM2=M
      LL=L2
      LL2=L
      GO TO 5
   10 MM=IABS(M1)
      MM1=M
      LL=L1
      LL1=L
    5 IG=(LL1+LL2+LL)/2
      SIGN=1.D0
      IF(MOD(IG-LL1-MM2,2).NE.0) SIGN=-1.D0
      XTOP=SIGN*DFAC(2*(IG-LL2))*DFAC(IG)
      XBOT=DFAC(IG-LL1)*DFAC(IG-LL2)*DFAC(IG-LL)*DFAC(2*IG+1)
      XRAT=DFLOAT(2*LL1+1)*(2*LL2+1)*(2*LL+1))*
     |DFAC(LL1+MM1)*DFAC(LL-MM1-MM2)*DFAC(LL2+MM2)*DFAC(LL2-MM2)/
     |(DFAC(LL1-MM1)*DFAC(LL+MM1+MM2)*2.D0)
      XFAC=DSQRT(XRAT)
      XFAC=XXC*XTOP*XFAC/XBOT
      XSUM=0.D0
      SIGN=1.D0
      IIT=0
      III=LL2-MM2
      II2=LL-MM1-MM2
      II3=LL1-MM1+III
      II4=LL1+MM1-III
      II5=LL+MM1+MM2
    6 IF(((III.LT.0).OR.(II2.LT.0).OR.(II3.LT.0)) GO TO 7
      IF(II4.LT.0) GO TO 8
      PSUM=SIGN*DFAC(II5)*DFAC(III)/(DFAC(IIT)*DFAC(II2)*
     |DFAC(II4))
      XSUM=XSUM+PSUM
    8 IIT=IIT+1
      III=III-1
      II2=II2-1
      II3=II3-1
      II4=II4+1
      II5=II5+1
      SIGN=-SIGN
      GO TO 6
    7 DGAUN1=XFAC*XSUM
      RETURN
    1 WRITE(6,2)
    2 FORMAT(' ','GAUNT COEFF INDEX ERROR')
      DGAUNT=0.D0
      RETURN
```

```
      END
C
C
C
      SUBROUTINE FACFIL
      IMPLICIT REAL*8(A-H,O-Z)
      COMMON/FAC/F1(51)
C     FILLS UP VECTOR ARRAY WITH FACTORIALS, PRELIMINARY TO USE OF DFAC.
C     F(N) CONTAINS FACTORIAL (N-1)
      F1(1)=1.D0
      X=1.D0
      DO 1 I=1,50
      III=I+1
      X=X*I
      F1(III)=X
    1 CONTINUE
      RETURN
      END
C
C
C
      REAL FUNCTION DFAC*8(J)
      IMPLICIT REAL*8(A-H,O-Z)
      COMMON/FAC/F1(51)
C     RETURNS FACTORIAL J. ARRAY F MUST BE FILLED BEFORE THIS ROUTINE
C     CAN BE USED.
      IF((J.GT.50).OR.(J.LT.0)) GO TO 25
      JJ1=J+1
      DFAC=F1(JJ1)
      RETURN
   25 WRITE(6,26)
   26 FORMAT('0     DFAC CALLING ERROR')
      XX1=(1.D-50)**5
      DFAC=1.D0
      RETURN
      END
C
C
C
      REAL FUNCTION XNORM*8(N,ZETA)
C     RETURNS THE NORMALIZATION CONSTANT OF A SLATER ORBITAL
C     WITH PRINCIPAL QUANTUM NUMBER N AND EXPONENT ZETA
      IMPLICIT REAL*8(A-H,O-Z)
      IF(N.LT.0) GO TO 25
      III=N+N
      TOP=(ZETA+ZETA)**(III+1)
      BOT=DFAC(III)
      XNORM=DSQRT(TOP/BOT)
      RETURN
   25 WRITE(6,26)
   26 FORMAT('0      XNORM CALLING ERROR')
      XNORM=0.D0
      RETURN
      END
C
C
C
      REAL FUNCTION RETRIP*8(L1,L2,L,M1,M2,M)
```

PROGRAM WUNIT

```
C       RETURNS INT(S(L1,M1)*S(L2,M2)*S(L,M)), WHERE S DENOTES REAL NOR-
C       MALIZED SPHERICAL HARMONIC
        IMPLICIT REAL*8(A-H,O-Z)
        IF((L1.LT.0).OR.(L2.LT.0).OR.(L.LT.0)) GO TO 26
        IF((L.GT.(L1+L2)).OR.(L.LT.IABS(L1-L2))) GO TO 25
        ICHK=1
        IF(M1.LT.0) ICHK=-ICHK
        IF(M2.LT.0) ICHK=-ICHK
        IF(M.LT.0) ICHK=-ICHK
        IF(ICHK.LT.0) GO TO 25
        III=L1+L2+L
        II2=2*(III/2)-III
        IF(II2.NE.0) GO TO 25
        IF((IABS(M).NE.IABS(M1+M2)).AND.(IABS(M).NE.IABS(M1-M2))) GO TO 25
        IZERO=0
        IF(M1.EQ.0) IZERO=IZERO+1
        IF(M2.EQ.0) IZERO=IZERO+1
        IF(M.EQ.0) IZERO=IZERO+1
        IGO=IZERO+1
        GO TO (7,9,25,5),IGO
   25   RETRIP=0.D0
        RETURN
    5   MM1=0
        MM2=0
        MM3=0
    8   RETRIP=DGAUNT(L1,L2,L,MM1,MM2,MM3)
        RETURN
    9   MM1=IABS(M1)
        MM2=-IABS(M2)
        MM3=-IABS(M)
        IF((MM1+MM2).LT.0) MM3=-MM3
        GO TO 8
    6   INEG=0
        IF(M1.LT.0) INEG=INEG+1
        IF(M2.LT.0) INEG=INEG+1
        IF(INEG.GT.0) GO TO 10
        SIGN=1.D0
   11   LL1=L1
        LL2=L2
        MM1=IABS(M1)
        MM2=IABS(M2)
        MM3=-IABS(M)
        IF(MM1.GE.MM2) GO TO 7
        MSAVE=MM1
        MM1=MM2
        MM2=MSAVE
        MSAVE=LL1
        LL1=LL2
        LL2=MSAVE
    7   IF(IABS(M).EQ.(MM1-MM2)) MM2=-MM2
C       XCON=1/SQRT2
        XCON=.707106781186547 5D0
        RETRIP=SIGN*XCON*DGAUNT(LL1,LL2,L,MM1,MM2,MM3)
        RETURN
   10   SIGN=1.D0
        IF((M1+M2+M).EQ.0) SIGN=-SIGN
        GO TO 11
   26   WRITE(6,27)
```

```
   27 FORMAT(' RETRIP CALLING ERROR')
      RETRIP=0.D0
      RETURN
      END
C
C
C
      SUBROUTINE MATOUT(A,D,ID,K1,N,IM)
C     PRINTS OUT NXN SQUARE MATRIX WITH ROWS AND COLUMNS NUMBERED.
C
C     IF MATRIX IS SYMMETRIC AND STORED IN DIAG AND TOP HALF ONLY,
C     IM=1. IF MATRIX IS STORED IN WHOLE ARRAY, IM=0.
C
C     IF MATRIX IS IMPLICITLY ORDERED VIA ARRAY ID, IM=-1 AND
C     EIGENVALUE ARRAY D'S PRINTED OUT UNDER THE COLUMNS
      IMPLICIT REAL*8(A-H,O-Z)
      DIMENSION A(K1,1),D(K1),ID(K1)
      IP=0
      K=6
      III=MOD(N-1,6)
      II2=MOD(N-1,7)
      IF(II2.GT.III) GO TO 1
    2 II2=MOD(N-1,8)
      IF(II2.GT.III) K=8
      GO TO 3
    1 K=7
      III=II2
      GO TO 2
    3 LLOW=K*IP+1
      LUP=K*(IP+1)
      IF(LUP.GT.N) LUP=N
      WRITE(6,4) (I,I=LLOW,LUP)
    4 FORMAT('0',10X,I2,8(10X,I2))
      DO 5 I=1,N
      IF(IM.EQ.1) GO TO 6
      IF(IM.LT.0) GO TO 10
      WRITE(6,7) I,(A(I,J),J=LLOW,LUP)
    7 FORMAT(' ',1X,I2,1X,8F12.6)
      GO TO 5
   10 WRITE(6,7) I,(A(I,ID(J)),J=LLOW,LUP)
      GO TO 5
    6 IF((LLOW.LT.I).AND.(LUP.LE.I)) GO TO 8
      IF((LLOW.LT.I).AND.(LUP.GT.I)) GO TO 9
      WRITE(6,7) I,(A(I,J),J=LLOW,LUP)
      GO TO 5
    8 WRITE(6,7) I,(A(J,I),J=LLOW,LUP)
      GO TO 5
    9 IIJ=I+1
      WRITE(6,7) I,(A(J,I),J=LLOW,I),(A(I,J),J=IIJ,LUP)
    5 CONTINUE
      IF(IM.LT.0) GO TO 11
   13 IF(LUP.EQ.N) RETURN
      IP=IP+1
      GO TO 3
   11 WRITE(6,12) (D(ID(J)),J=LLOW,LUP)
   12 FORMAT('0',2X,'E',1X,8F12.6)
      GO TO 13
      END
```

```
C
C
C
      SUBROUTINE POP(N)
      IMPLICIT REAL*8(A-H,O-Z)
      COMMON/SCF/P(72,72),F(72,72),V(72,72),H(72),CD(72),D(72),E(72),ID(
     |72)
      COMMON/STOFF/X(20),Y(20),Z(20),NATOM(20),NAT,NOCC
C     RETURNS POPULATION-BOND ORDER MATRIX IN TOP AND DIAG OF P.
C     WORKS ONLY FOR CLOSED SHELL SYSTEMS.
C     NEW FOCK MATRIX MUST BE CONSTRUCTED BEFORE THIS ROUTINE IS CALLED.
C
C     CALCULATE P.
      DO 2 I=1,N
      DO 2 J=I,N
      P(I,J)=0.D0
      DO 2 K=1,NOCC
      K1=ID(K)
    2 P(I,J)=P(I,J)+2.D0*F(I,K1)*F(J,K1)
      RETURN
      END
C
C
C
      SUBROUTINE LERV
C     CALCULATES THE SYMMETRIC TRANSFORMATION MATRIX BETWEEN NON-
C     ORTHOG. SET AND THE LOWDIN ORTH SET AND STORS IN TOP OF V.
      IMPLICIT REAL*8(A-H,O-Z)
      COMMON/SCF/P(72,72),F(72,72),V(72,72),H(72),CD(72),D(72),E(72),ID(
     |72)
      COMMON/ORBS/NOR(72),LOR(72),MOR(72),ZOR(72),N,NINT,N2,N3,N4
      NN1=N-1
C     GET OVERLAP MATRIX INTO TOP OF F.
      DO 1 I=1,NN1
      III=I+1
      DO 2 J=III,N
    2 F(I,J)=OVER(NOR(I),LOR(I),MOR(I),ZOR(I),NOR(J),LOR(J),MOR(J),ZOR(J
     |))
    1 F(I,I)=1.D0
      F(N,N)=1.D0
      WRITE(6,5)
    5 FORMAT('0',2X,'OVERLAP MATRIX')
      CALL MATOUT(F,D,ID,72,N,1)
      CALL CLOCK2(NT1)
      CALL SYMOR(F,D,E,0.D0,N,72,1.D-14,.TRUE.,.TRUE.,.FALSE.,NERR)
      IF(NERR.NE.0) GO TO 6
      CALL CLOCK2(NT2)
      XX1=DFLOAT(NT2-NT1)/60.D0
      WRITE(6,8) XX1
    8 FORMAT('0',10X,'LERV DIAG TIME',2X,F5.2,1X,'SECONDS')
C     PUT UD(-1/2)U(T) INTO V.
      DO 3 I=1,N
    3 D(I)=1.D0/DSQRT(D(I))
      DO 4 I=1,N
      DO 4 J=I,N
      V(I,J)=0.D0
      DO 4 K=1,N
    4 V(I,J)=V(I,J)+F(I,K)*D(K)*F(J,K)
```

```
      RETURN
    6 WRITE(6,7)
    7 FORMAT('0     LPRV DIAG ERROR')
      STOP
      END
C
C
C
      INTEGER FUNCTION NO*4(I,J,K,L)
C     DETERMINES HOW MANY DISTINCT ORBITALS REPRESENTED BY THE NUMBERS
C     I,J,K,L .
      NO=4
      IF(I.EQ.J) GO TO 1
      IF(I.EQ.K) GO TO 1
      IF(I.EQ.L) GO TO 1
    2 IF(J.EQ.K) GO TO 3
      IF(J.EQ.L) GO TO 3
    4 IF(K.EQ.L) GO TO 5
      GO TO 6
    1 NO=NO-1
      GO TO 2
    3 NO=NO-1
      GO TO 4
    5 NO=NO-1
    6 RETURN
      END
C
C
C
      SUBROUTINE DECODE(ICODE,I,J,K,L)
      IMPLICIT REAL*8(A-H,O-Z)
      COMMON/ORBS/NOR(72),LOR(72),MOR(72),ZOR(72),N,NINT,N2,N3,N4
C     CONVERTS THE SINGLE INTEGER INTEGRAL LABEL BACK TO THE FOUR
C     ORBITAL INDICES I,J,K,L.
      IF(ICODE.GT.(N4-1)) GO TO 25
      III=ICODE/N3
      NREM=ICODE-N3*III
      JJ1=NREM/N2
      NREM=NREM-N2*JJ1
      KK1=NREM/N
      LL1=NREM-KK1*N
      I=III+1
      J=JJ1+1
      K=KK1+1
      L=LL1+1
      RETURN
   25 WRITE(6,11)
   11 FORMAT(' DECODE CALLING ERROR')
      I=1
      J=1
      K=1
      L=1
      RETURN
      END
C
C
C
      SUBROUTINE SYMOR(A,D,F,KO,N,NA,EPS,ABSCNV,VEC,TND,FAIL)
```

PROGRAM WUNIT

```
C
C     ALGORITHM BY G. W. STEWART, COMM. OF THE ACM, 13,369(1970) WITH
C     CORRECTIONS PUBLISHED IN COMM. OF THE ACM 13,750(1970).
C
C     EXPLANATION OF THE PARAMETERS IN THE CALLING SEQUENCE.
C
C     A       MATRIX TO BE DIAGONALIZED IF NOT INITIALLY TRIDIAG. ROUTINE
C             USES DIAG AND UPPER HALF OF A. IF EIGENVECTORS WANTED THEY
C             GO INTO A; OTHERWISE BOTTOM HALF OF A UNTOUCHED.
C
C     D       VECTOR ARRAY. IF MATRIX INITIALLY TRIDIAG, D CONTAINS ITS
C             DIAG. ON RETURN D CONTAINS EIGENVALUES.
C
C     E       VECTOR. IF MATRIX INITIALLY TRIDIAG, CONTAINS THE OFF-DIAG
C             ELEMENTS. E(I) RETURNS NO. OF ITERATIONS FOR EVALUE D(I).
C
C     KO      REAL VARIABLE CONTAINING INITIAL ORIGIN SHIFT. CAN BE 0.D0.
C     N       THE ORDER OF THE MATRIX BEING DIAGONALIZED.
C     NA      DIMENSION OF THE ARRAY A.
C     EPS     CONVERGENCE TOLERANCE.
C
C     ABSCNV  LOGICAL=.TRUE. FOR ABSOLUTE, .FALSE. FOR RELATIVE CONV.
C     VEC     LOGICAL VARIABLE, .TRUE. IF EIGENVECTORS WANTED.
C     TRD     LOGICAL= .TRUE. IF MATRIX TRIDIAG AND STORED IN D AND E.
C
C     FAIL    INTEGER ERROR SIGNAL. EIGENVALUES OF INDEX GT FAIL ARE OK.
C
      INTEGER
     |N,NM1,NM2,NA,FAIL,I,II,J,L,L1,LL,LL1,NI,NU,NUM1,SINCOS,RETURN
      DOUBLE PRECISION
     |A(NA,1),D(1),E(1),K0,K1,K2,K,EPS,S2,CON,NINE,TEST,CO,CC,
     |CD,C,S,TEMP,P,PP,0.0D0,NORM,P,TITTER,SUM,SUM1,MAX
      LOGICAL
     |ABSCNV,VEC,TRD,SHFT
      TITTER=50.D0
      FAIL=0
      NM1=N-1
      NM2=N-2
      NINE=0.D0
      ASSIGN 500 TO SINCOS
C
C     MAKE SURE N POSITIVE
C
      IF(N.GT.0) GO TO 1
      FAIL=-1
      RETURN
C
C     SPECIAL SECTION FOR MATRIX ORDER 1.
C
    1 IF(N.GT.1) GO TO 5
      IF(.NOT.TRD) D(1)=A(1,1)
      IF(VEC) A(1,1)=1.D0
      FAIL=0
      RETURN
C
C     IF MATRIX TRIDIAG, SKIP HOUSEHOLDER SECTION
C
    5 IF(TRD) GO TO 100
```

```
      IF(N.EQ.2) GO TO 80
C
C     HOUSEHOLDER SECTION
C
      DO 70 L=1,NM2
      LI=L+1
      D(L)=A(L,L)
      MAX=0.00
      DO 10 I=LI,N
   10 MAX=DMAX1(MAX,DABS(A(L,I)))
      IF(MAX.NE.0.00) GO TO 11
      F(L)=0.00
      A(L,L)=1.00
      GO TO 70
   11 SUM=0.00
      DO 17 I=LI,N
      A(L,I)=A(L,I)/MAX
   17 SUM=SUM+A(L,I)**2
      S2=SUM
      S2=DSQRT(S2)
      IF(A(L,LI).LT.0.00) S2=-S2
      F(L)=-S2*MAX
      A(L,LI)=A(L,LI)+S2
      A(L,L)=S2*A(L,LI)
      SUM1=0.00
      DO 50 I=LI,N
      SUM=0.00
      DO 20 J=LI,I
   20 SUM=SUM+A(J,I)*A(L,J)
      IF(I.EQ.N) GO TO 40
      II=I+1
      DO 30 J=II,N
   30 SUM=SUM+A(I,J)*A(L,J)
   40 F(I)=SUM/A(L,L)
   50 SUM1=SUM1+A(L,I)*F(I)
      CON=.500*SUM1/A(L,L)
      DO 60 I=LI,N
      F(I)=F(I)-CON*A(L,I)
      DO 60 J=LI,I
   60 A(J,I)=A(J,I)-A(L,I)*F(J)-A(L,J)*F(I)
   70 CONTINUE
   80 D(NM1)=A(NM1,NM1)
      D(N)=A(N,N)
      F(NM1)=A(NM1,N)
C
C     IF EIGENVECTORS REQUIRED, INITIALIZE A.
C
  100 IF(.NOT.VEC) GO TO 180
C
C     IF MATRIX WAS TRIDIAG, SET A EQUAL TO IDENTITY MATRIX.
C
      IF(.NOT.TRD.AND. N.NE.2) GO TO 130
      DO 120 I=1,N
      DO 110 J=1,N
  110 A(I,J)=0.00
  120 A(I,I)=1.00
      GO TO 180
C
```

```
C     IF MATRIX WASN'T TRIDIAG. MULTIPLY OUT TRANSFORMATIONS FROM
C     HOUSEHOLDER SECTION.
C
  170 A(N,N)=1.D0
      A(NM1,NM1)=1.D0
      A(NM1,N)=0.D0
      A(N,NM1)=0.D0
      DO 170 I=1,NM2
      LL=NM2-I+1
      LL1=LL+1
      DO 140 I=LL1,N
      SUM=0.D0
      DO 135 J=LL1,N
  135 SUM=SUM+A(LL,J)*A(J,I)
  140 A(I,LL)=SUM/A(LL,LL)
      DO 150 I=LL1,N
      DO 150 J=LL1,N
  150 A(I,J)=A(I,J)-A(LL,I)*A(J,LL)
      DO 160 I=LL1,N
      A(I,LL)=0.D0
  160 A(LL,I)=0.D0
  170 A(LL,LL)=1.D0
C
C     IF USING ABSOLUTE CONV CRITERION, COMPUTE  THE INFINITY NORM
C     OF THE MATRIX  (I.E., IF ABSCNV=.TRUE.)
C
  180 IF(.NOT.ABSCNV) GO TO 200
      NINF=DMAX1(DABS(D(1))+DABS(E(1)),DABS(D(N))+DABS(E(NM1)))
      IF(N.EQ.2) GO TO 200
      DO 190 I=2,NM1
  190 NINF=DMAX1(NINF,DABS(D(I))+DABS(E(I))+DABS(E(I-1)))
C
C     START THE QR ITERATION
C
  200 NU=N
      NUM1=N-1
      SHFT=.FALSE.
      KI=KO
      TEST=NINF*EPS
      E(N)=0.D0
C
C     CHECK FOR CONVERGENCE AND LOCATE THE SUBMATRIX IN WHICH THE
C     QR STEP IS TO BE PERFORMED.
C
  210 DO 220 NNL=1,NUM1
      NL=NUM1-NNL+1
      IF(.NOT.ABSCNV)TEST=EPS*DMIN1(DABS(D(NL)),DABS(D(NL+1)))
      IF(DABS(E(NL)).LE.TEST) GO TO 230
  220 CONTINUE
      GO TO 240
  230 E(NL)=0.D0
      NL=NL+1
      IF(NL.EQ.NU) GO TO 240
      IF(NUM1.EQ.1) RETURN
      NU=NUM1
      NUM1=NU-1
      GO TO 210
  240 E(NU)=E(NU)+1.D0
```

```
      IF(E(NU).LE.TITTEN) GO TO 250
      FAIL=NU
      RETURN
C
C     CALCULATE THE SHIFT.
C
  250 CB=(D(NUM1)-D(NU))/2.00
      MAX=DMAX1(DABS(CB),DABS(E(NUM1)))
      CB=CB/MAX
      CC=(E(NUM1)/MAX)**2
      CD=DSQRT(CB**2+CC)
      IF(CB.NE.0.00) CD=DSIGN(CD,CB)
      K2=D(NU)-MAX*CC/(CB+CD)
      IF(SHFT) GO TO 270
      IF(DABS(K2-K1).LT. .500*DABS(K2)) GO TO 260
      K1=K2
      K=K0
      GO TO 300
  260 SHFT=.TRUE.
  270 K=K2
C
C     PERFORM ONE QR STEP WITH SHIFT K ON ROWS AND COLUMNS NL THRU NU
C
  300 P=D(NL)-K
      Q=E(NL)
      ASSIGN 310 TO RETURN
      GO TO SINCOS.(500)
  310 DO 380 I=NL,NUM1
C
C     IF REQUIRED, ROTATE THE EIGENVECTORS.
C
      IF(.NOT.VEC) GO TO 330
      DO 320 J=1,N
      TEMP=C*A(J,I)+S*A(J,I+1)
      A(J,I+1)=-S*A(J,I)+C*A(J,I+1)
  320 A(J,I)=TEMP
C
C     PERFORM SIMILARITY TRANSFORMATION AND CALCULATE NEXT ROTATION.
C
  330 D(I)=C*D(I)+S*E(I)
      TEMP=C*E(I)+S*D(I+1)
      D(I+1)=-S*E(I)+C*D(I+1)
      E(I)=-S*K
      D(I)=C*D(I)+S*TEMP
      IF(I.EQ.NUM1) GO TO 380
      IF(DABS(S).GT.DABS(C)) GO TO 350
      R=S/C
      D(I+1)=-S*E(I)+C*D(I+1)
      P=D(I+1)-K
      Q=C*E(I+1)
      ASSIGN 340 TO RETURN
      GO TO SINCOS.(500)
  340 E(I)=R*NORM
      E(I+1)=Q
      GO TO 380
  350 P=C*E(I)+S*D(I+1)
      Q=S*E(I+1)
      D(I+1)=C*P/S+K
```

```
      E(I+1)=C*E(I+1)
      ASSIGN 100 TO RETURN
      GO TO SINCOS,(500)
  160 E(I)=NORM
  100 CONTINUE
      TEMP=C*E(NUM1)+S*D(NU)
      D(NU)=-S*E(NUM1)+C*D(NU)
      E(NUM1)=TEMP
      GO TO 210
C
C     INTERNAL PROCEDURE TO CALCULATE THE ROTATION CORRESPONDING
C     TO THE VECTOR (P,Q).
C
  500 PP=DABS(P)
      QQ=DABS(Q)
      IF(QQ.GT.PP) GO TO 510
      NORM=PP*DSQRT(1.D0+(QQ/PP)**2)
      GO TO 520
  510 IF(QQ.EQ.0.D0) GO TO 530
      NORM=QQ*DSQRT(1.D0+(PP/QQ)**2)
  520 C=P/NORM
      S=Q/NORM
      GO TO RETURN,(110,140,160)
  530 C=1.D0
      S=0.D0
      NORM=0.D0
      GO TO RETURN,(110,140,160)
      END
C
C
C
      SUBROUTINE ENERT(E1)
C     CALCULATES TOTAL ENERGY OF MOLECULE AND PRINTS IT OUT-ELECTRONIC
C     ENERGY MUST BE SUPPLIED AS E1.
      IMPLICIT REAL*8(A-H,O-Z)
      COMMON/STUFF/X(20),Y(20),Z(20),NATOM(20),NAT,NOCC
      SUM=0.D0
      NTOP=NAT-1
      DO 1 I=1,NTOP
      III=I+1
      DO 1 J=III,NAT
      RIJ=DSQRT((X(I)-X(J))**2+(Y(I)-Y(J))**2+(Z(I)-Z(J))**2)
    1 SUM=SUM+DFLOAT(NATOM(I))*DFLOAT(NATOM(J))/RIJ
      E1=E1+SUM
      WRITE(6,2) E1
    2 FORMAT('0',2X,'TOTAL ENERGY OF MOLECULE',2X,F12.6,1X,'AU')
      RETURN
      END
C
C
C
      REAL FUNCTION XNUKRA*8(NA,ZA,NB,ZB,R,L)
C     RADIAL INTEGRAL THAT ARISES IN THE TWO-CENTER NUCLEAR ATTRACTION
C     INTEGRAL.. L IS AN INDEX THAT ARISES FROM SPHERICAL HARMONIC
C     EXPANSION OF THE ELECTRON-OTHER NUCLEAR DISTANCE.
      IMPLICIT REAL*8(A-H,O-Z)
      IF(R.EQ.0.D0) GO TO 25
      ZSUM=ZA+ZB
```

```
      AARG=ZSUM*R
      IND1=NA+NB+L
      IND2=NA+NB-L-1
      IF(IND2.LT.0) GO TO 25
      XX1=ATTSER(IND1,AARG)+A(IND2,AARG)
      XNUKRA=XX1*R**(NA+NB)
      RETURN
   25 WRITE(6,11)
   11 FORMAT(' XNUKRA CALLING ERROR')
      XNUKRA=0.D0
      RETURN
      END
C
C
C
      REAL FUNCTION ATTSER*8(N,X)
      IMPLICIT REAL*8(A-H,O-Z)
C     RETURNS INT(0 TO 1) R**N*EXP(-X*R) DR
      XAF=X**(N+1)
      XX1=DFAC(N)/XAF
      XX2=A(N,X)
      XX3=XX1-XX2
      XCH=XX3/XX1
C     CHECK FOR CANCELLATION ERROR
      IF(XCH.LT..1D0) GO TO 1
C     ACCEPT SUBTRACTION IF NO CANCELLATION ERROR
      ATTSER=XX3
      RETURN
C     SERIES CALC IF CANCELLATION ERROR
    1 XCON=XX1*DEXP(-X)
      SUM=XAF/DFAC(N+1)
      K=N+2
      TERM=XAF*X/DFAC(K)
      SUM=SUM+TERM
    2 XCHK=DABS(TERM/SUM)
C     CHECK FOR CONV OF SERIES
      IF(XCHK.LT..5D-16) GO TO 3
      K=K+1
      TERM=TERM*(X/DFLOAT(K))
      SUM=SUM+TERM
      GO TO 2
    3 ATTSER=XCON*SUM
      RETURN
      END
C
C
C
      REAL FUNCTION OVER*8(NA,LA,MA,ZA,NB,LB,MB,ZB)
C     RETURNS THE OVERLAP INTEGRAL  ((NA,LA,MA)|(NB,LB,MB)) BETWEEN TWO
C     SLATER ORBITALS ON THE SAME CENTER WITH EXPONENTS ZA AND ZB.
      IMPLICIT REAL*8(A-H,O-Z)
      IF((NA.LT.0).OR.(NB.LT.0)) GO TO 25
      IF((LA.NE.LB).OR.(MA.NE.MB)) GO TO 10
      IF((NA.EQ.NB).AND.(ZA.EQ.ZB)) GO TO 12
      ZSUM=ZA+ZB
      IF(ZSUM.EQ.0.D0) GO TO 25
      NSUM=NA+NB
      XX1=DFAC(NSUM)/ZSUM**(NSUM+1)
```

```
      XX1=XX1*XNORM(NA,ZA)*XNORM(NB,ZB)
    1 OVER=XX1
      RETURN
   10 XX1=0.D0
      GO TO 1
   25 WRITE(6,11)
   11 FORMAT(' OVER CALLING ERROR')
      XX1=0.D0
      GO TO 1
   12 XX1=1.D0
      GO TO 1
      END
C
C
C
      REAL FUNCTION SKINNY*8(NA,LA,MA,ZA,NB,LB,MB,ZB)
C     RETURNS THE KINETIC ENERGY INTEGRAL ((NA,LA,MA)|OP|(NB,LB,MB))
C     WHERE (NA,LA,MA) AND (NB,LB,MB) ARE SLATER ORBITALS ON THE SAME
C     CENTER WITH EXPONENTS ZA AND ZB, AND OP = -1/2 DELSQUARED.
      IMPLICIT REAL*8(A-H,O-Z)
      IF((LA.NE.LB).OR.(MA.NE.MB)) GO TO 10
      IF((NA.LT.1).OR.(NB.LT.1)) GO TO 25
      XX1=DFLOAT(NB)
      XX2=DFLOAT(LB)
      XFAC1=2.D0*DSQRT((XX1+XX1)/(XX1+XX1-1.D0))
      IF(NB.EQ.1) GO TO 3
      XFAC2=4.D0*(XX1+XX2)*(XX1-XX2-1.D0)/DSQRT((XX1+XX1)*(XX1+XX1-1.D0)
     |*(XX1+XX1-2.D0)*(XX1+XX1-3.D0))
    4 XSUM=OVER(NA,LA,MA,ZA,NB,LB,MB,ZB)-XFAC1*OVER(NA,LA,MA,ZA,NB-1,LB,
     |MB,ZB)
      IF(XFAC2.EQ.0.D0) GO TO 2
      XSUM=XSUM+XFAC2*OVER(NA,LA,MA,ZA,NB-2,LB,MB,ZB)
    2 XSUM=-(ZB*ZB)*XSUM/2.D0
    1 SKINNY=XSUM
      RETURN
   10 XSUM=0.D0
      GO TO 1
    3 XFAC2=0.D0
      GO TO 4
   25 WRITE(6,11)
   11 FORMAT(' SKINNY CALLING ERROR')
      XSUM=0.D0
      GO TO 1
      END
C
C
C
      REAL FUNCTION XNUK1*8(NA,LA,MA,ZA,NB,LB,MB,ZB,NATOM)
C     THIS ROUTINE RETURNS THE ONE-CENTER NUCLEAR ATTRACTION INTEGRAL
C     BETWEEN TWO SLATER ORBITALS. NA, NB ARE THE PRINCIPAL Q NOS, LA, L
C     AZIMUTHAL, MA,MB THE MAGNETIC, AND ZA, ZB THE EXPONENTS. NATOM IS
C     THE ATOMIC NUMBER OF THE EXPANSION CENTER.
      IMPLICIT REAL*8(A-H,O-Z)
      IF((LA.NE.LB).OR.(MA.NE.MB)) GO TO 25
      NSUM=NA+NB
      ZSUM=ZA+ZB
      XX1=DFAC(NSUM-1)/ZSUM**(NSUM)
      XNUK1=XX1*DFLOAT(NATOM)*XNORM(NA,ZA)*XNORM(NB,ZB)*(-1.D0)
```

```
      RETURN
   25 XNUK1=0.D0
      RETURN
      END
C
C
C
      REAL FUNCTION XNUK2*8(NA,LA,MA,ZA,NB,LB,MB,ZB,NATOM,R,COSTHT,CFI,
     |SFI)
C     TWO-CENTER NUCLEAR ATTRACTION INTEGRAL - TWO SLATER ORBITALS CENTE
C     ON ONE CENTER WITH A NUCLEUS AT R,THETA,FI OF ATOMIC NUMBER NATOM.
C     COSTHT IS THE COSINE OF THETA AND CFI AND SFI AND THE COSINE AND
C     SINE OF FI.
      IMPLICIT REAL*8(A-H,O-Z)
      IF(R.EQ.0.D0) GO TO 25
      PI=3.14159265358979300
      XCON=0.D0
      LLOW=IABS(LA-LB)+1
      LUP=LA+LB+1
      MINAM=IABS(IABS(MA)-IABS(MB))
      MAXAM=IABS(MA)+IABS(MB)
      IC1=1
      IF(MA.LT.0) IC1=-IC1
      IF(MB.LT.0) IC1=-IC1
      SUM=0.D0
      IF((MINAM.EQ.0).AND.(IC1.LT.0)) MINAM=2
      IF(MINAM.GT.MAXAM) GO TO 4
      DO 1 L1=LLOW,LUP,2
      L=L1-1
      IF(L.LT.MINAM) GO TO 1
      XINNER=0.D0
      MM=MINAM
    2 IF(MM.GT.L) GO TO 3
      M=IC1*MM
      XINNER=XINNER+SHERM(L,M,COSTHT,CFI,SFI)*RETRIP(LA,LB,L,MA,MB,M)
      IF(MM.EQ.MAXAM) GO TO 3
      MM=MAXAM
      GO TO 2
    3 IF(XINNER.EQ.0.D0) GO TO 1
      XFAC=(PI/DFLOAT(2*L+1))*XNUKRA(NA,ZA,NB,ZB,R,L)
      SUM=SUM+XFAC*XINNER
    1 CONTINUE
      IF(SUM.EQ.0.D0) GO TO 4
      XCON=DFLOAT(NATOM)*XNORM(NA,ZA)*XNORM(NB,ZB)*(-1.D0)
    4 XNUK2=SUM*XCON*4.D0
      RETURN
   25 WRITE(6,11)
   11 FORMAT(' XNUK2 CALLING ERROR')
      XNUK2=0.D0
      RETURN
      END
C
C
C
      SUBROUTINE BUILD(NTAKE)
C     THIS ROUTINE ADDS THE RIGHT AMOUNTS TO ELEMENTS OF THE FOCK MATRIX
C     UPPER RIGHT HALF, GIVEN THE FOUR-ORBITAL INDICES I,J,K,L AND THE
C     REPULSION INTEGRAL VALUE XXI.
```

PROGRAM WUNIT

```
      IMPLICIT REAL*8(A-H,O-Z)
      COMMON/SCF/P(72,72),F(72,72),V(72,72),H(72),CD(72),D(72),E(72),ID(
     1 72)
      COMMON/INZ/LABEL(1000),XER(1000)
      COMMON/ORBS/NOR(72),LOR(72),MOR(72),ZOR(72),N,NINT,N2,N3,N4
      DO 1 II=1,NTAKE
      CALL DECODE(LABEL(II),I,J,K,L)
      XX1=XER(II)
      IF((I.GT.J).OR.(K.GT.L)) GO TO 25
      IF(I.GT.K) GO TO 25
      IF((I.EQ.K).AND.(J.GT.L)) GO TO 25
      III=NO(I,J,K,L)
      GO TO (10,11,12,13),III
   10 F(I,I)=F(I,I)+P(I,I)*XX1*.5D0
      GO TO 1
   11 IF(I.NE.J) GO TO 15
      IF(K.EQ.L) GO TO 16
      F(I,I)=F(I,I)+P(I,L)*XX1
      F(I,L)=F(I,L)+P(I,I)*XX1*.5D0
      GO TO 1
   17 F(J,J)=F(J,J)+P(I,J)*XX1
      F(I,J)=F(I,J)+P(J,J)*XX1*.5D0
      GO TO 1
   16 F(I,I)=F(I,I)+P(K,K)*XX1
      F(K,K)=F(K,K)+P(I,I)*XX1
      F(I,K)=F(I,K)-P(I,K)*XX1*.5D0
      GO TO 1
   15 IF(K.EQ.L) GO TO 17
      AAA=.5D0*XX1
      F(I,I)=F(I,I)-P(J,J)*AAA
      F(J,J)=F(J,J)-P(I,I)*AAA
      AAA=AAA+AAA+AAA
      F(I,J)=F(I,J)+P(I,J)*AAA
      GO TO 1
   12 IF((I.EQ.J).OR.(K.EQ.L)) GO TO 18
      IF(I.EQ.K) GO TO 19
      M=K+L-J
      F(J,J)=F(J,J)-P(I,M)*XX1
      AAA=.5D0*XX1
      F(I,M)=F(I,M)-P(J,J)*AAA
      AAA=AAA+AAA+AAA
      MM=MAX0(J,M)
      MI=J+M-MM
      F(I,J)=F(I,J)+P(MI,MM)*AAA
      F(MI,MM)=F(MI,MM)+P(I,J)*AAA
      GO TO 1
   19 F(I,I)=F(I,I)-P(J,L)*XX1
      AAA=.5D0*XX1
      F(J,L)=F(J,L)-P(I,I)*AAA
      AAA=AAA+AAA+AAA
      F(I,J)=F(I,J)+P(I,L)*AAA
      F(I,L)=F(I,L)+P(I,J)*AAA
      GO TO 1
   18 IF(I.EQ.J) GO TO 20
      F(I,J)=F(I,J)+P(K,K)*XX1
      AAA=.5D0*XX1
      MM=MAX0(J,K)
      MI=J+K-MM
```

```
      F(I,K)=F(I,K)-P(MI,MM)*AAA
      F(MI,MM)=F(MI,MM)-P(I,K)*AAA
      AAA=XX1+XX1
      F(K,K)=F(K,K)+P(I,J)*AAA
      GO TO 1
   20 AAA=.5D0*XX1
      F(K,L)=F(K,L)+P(I,I)*XX1
      F(I,K)=F(I,K)-P(I,L)*AAA
      F(I,L)=F(I,L)-P(I,K)*AAA
      AAA=XX1+XX1
      F(I,I)=F(I,I)+P(K,L)*AAA
      GO TO 1
   13 AAA=XX1+XX1
      F(I,J)=F(I,J)+P(K,L)*AAA
      F(K,L)=F(K,L)+P(I,J)*AAA
      AAA=.5D0*XX1
      MM=MAX0(J,L)
      MI=J+L-MM
      F(I,K)=F(I,K)-P(MI,MM)*AAA
      F(MI,MM)=F(MI,MM)-P(I,K)*AAA
      MM=MAX0(J,K)
      MI=J+K-MM
      F(I,L)=F(I,L)-P(MI,MM)*AAA
      F(MI,MM)=F(MI,MM)-P(I,L)*AAA
    1 CONTINUE
      RETURN
   25 WRITE(6,26)
   26 FORMAT('0      BUILD CALLING ERROR')
      STOP
      END
C
C
C
      REAL FUNCTION ERG*8(N)
C     RETURNS ELECTRONIC ENERGY ONCE POPULATION MATRIX HAS BEEN FORMED.
      IMPLICIT REAL*8(A-H,O-Z)
      COMMON/SCF/P(72,72),F(72,72),V(72,72),H(72),CD(72),D(72),E(72),ID(
     |72)
      NN1=N-1
      SUM=0.D0
      DO 1 I=1,NN1
      II1=I+1
      DO 2 J=II1,N
    2 SUM=SUM+P(I,J)*(V(J,I)+F(I,J))
    1 SUM=SUM+P(I,I)*(H(I)+F(I,I))/2.D0
      SUM=SUM+P(N,N)*(H(N)+F(N,N))/2.D0
      ERG=SUM
      RETURN
      END
C
C
C
      SUBROUTINE EFFIX
C     CONSTRUCTS NEW FOCK MATRIX ONCE NEW POP MATRIX HAS BEEN FORMED.
      IMPLICIT REAL*8(A-H,O-Z)
      COMMON/SCF/P(72,72),F(72,72),V(72,72),H(72),CD(72),D(72),E(72),ID(
     |72)
      COMMON/INZ/LABEL(1000),XER(1000)
```

```
      COMMON/ORBS/NUR(72),LOR(72),MOR(72),ZOR(72),N,NINT,N2,N3,N4
      DIMENSION MABEL(3000)
      EQUIVALENCE (MABEL(1),LABEL(1))
C     FIRST PUT TOP OF COEFF MATRIX IN BOTTOM OF P, DIAG OF COEFF IN CO,
C     AND PUT 1-ELEC HAM ELEMENTS IN TOP AND DIAG OF F.
      CALL CLOCK2(NT1)
      NN1=N-1
      DO 1 I=1,NN1
      III=I+1
      DO 2 J=III,N
      P(J,I)=F(I,J)
    2 F(I,J)=V(J,I)
      CO(I)=F(I,I)
    1 F(I,I)=H(I)
      CO(N)=F(N,N)
      F(N,N)=H(N)
C     PUT 2-ELEC PART OF FOCK MATRIX IN TOP AND DIAG OF F.
      REWIND 10
      IK=NINT/1000
      IREM=NINT-1000*IK
      DO 3 I=1,IK
      READ(10) MABEL
      CALL BUILD(1000)
    3 CONTINUE
      READ(10) (LABEL(KK),KK=1,IREM),(XER(KK),KK=1,IREM)
      CALL BUILD(IREM)
      IIN=1000*IK+IREM
      WRITE(6,4) IIN
    4 FORMAT(' ',10X,'NUMBER OF R12 INTS READ',2X,I7)
      CALL CLOCK2(NT2)
      XX1=DFLOAT(NT2-NT1)/60.D0
      WRITE(6,5) XX1
    5 FORMAT(' ',10X,'FFFIX TIME',2X,F7.2,1X,'SECONDS')
      RETURN
      END
C
C
C
      SUBROUTINE EIGEN(N)
C     SOLVES EIGENVALUE PROBLEM WITH NON-UNIT METRIC.
C     ALSO ORDERS EIGENVALUES AND VECTORS IN ORDER OF INCREASING ENERGY.
      IMPLICIT REAL*8(A-H,O-Z)
      COMMON/SCF/P(72,72),F(72,72),V(72,72),H(72),CO(72),O(72),E(72),ID(
     1 72)
      CALL CLOCK2(NX1)
C     FIRST FORM FV IN P.
      NN1=N-1
      DO 1 I=1,N
      DO 1 J=1,N
      P(I,J)=0.D0
      I1=MIND(I,J)
      I2=I+J-I1
      DO 13 K=1,I1
   13 P(I,J)=P(I,J)+F(K,I)*V(K,J)
      IF(I.EQ.J) GO TO 16
      IK1=I1+1
      IF(I1.NE.I) GO TO 17
      DO 14 K=IK1,I2
```

```
   14 P(I,J)=P(I,J)+F(I,K)*V(K,J)
      GO TO 16
   17 DO 18 K=IK1,I2
   18 P(I,J)=P(I,J)+F(K,I)*V(J,K)
   16 IF(I2.EQ.N) GO TO 1
      IK1=I2+1
      DO 15 K=IK1,N
   15 P(I,J)=P(I,J)+F(I,K)*V(J,K)
    1 CONTINUE
C     FORM VFV AND STORE IN TOP AND DIAG OF F.
      DO 2 I=1,NN1
      IK1=I+1
      DO 2 J=I,N
      F(I,J)=0.D0
      DO 10 K=1,I
   10 F(I,J)=F(I,J)+V(K,I)*P(K,J)
      DO 2 K=IK1,N
    2 F(I,J)=F(I,J)+V(I,K)*P(K,J)
      F(N,N)=0.D0
      DO 11 K=1,N
   11 F(N,N)=F(N,N)+V(K,N)*P(K,N)
C     DIAGONALIZE TOP HALF OF F.
      CALL CLOCK2(NT1)
      CALL SYMQR(F,D,F,0.D0,N,72,1.D-14,.TRUE.,.TRUE.,.FALSE.,NERR)
      IF(NERR.NE.0) GO TO 25
      CALL CLOCK2(NT2)
      XX1=DFLOAT(NT2-NT1)/60.D0
      WRITE(6,8) XX1
    8 FORMAT(' ',10X,'EPROB DIAG TIME',2X,F5.2,1X,'SECONDS')
C     MULTIPLY F BY V COLUMN BY COLUMN AND STORE NON-ORTHOG COEFF MATRIX
C     IN F.
      DO 3 J=1,N
      DO 4 I=1,NN1
      E(I)=0.D0
      IK1=I+1
      DO 5 K=1,I
    5 E(I)=E(I)+V(K,I)*F(K,J)
      DO 4 K=IK1,N
    4 E(I)=E(I)+V(I,K)*F(K,J)
      E(N)=0.D0
      DO 12 K=1,N
   12 E(N)=E(N)+V(K,N)*F(K,J)
      DO 3 I=1,N
    3 F(I,J)=E(I)
C     PUT EVALUES IMPLICITLY IN ASCENDING ORDER WITH VECTOR ID.
      DO 6 I=1,NN1
      III=I+1
      DO 6 J=III,N
      IF(D(ID(I)).GT.D(ID(J))) GO TO 7
      GO TO 6
    7 IS=ID(I)
      ID(I)=ID(J)
      ID(J)=IS
    6 CONTINUE
      CALL CLOCK2(NX2)
      XX1=DFLOAT(NX2-NX1)/60.D0
      WRITE(6,9) XX1
    9 FORMAT(' ',10X,'TOTAL EPROB TIME',2X,F5.2,1X,'SECONDS')
```

```
      RETURN
   25 WRITE(6,26) NERR
   26 FORMAT('0ERROR DIAG ERROR--NERR=',1X,I1)
      STOP
      END
C
C
C
      SUBROUTINE ITER(N,E1)
C     GOVERNS ITERATIVE PART OF SCF CALCULATION.
C     LIMIT ON NUMBER OF ITERATIONS = 20. PRINTS OUT ELECTRONIC ENERGY,
C     DENSITY MATRIX, AND COEFF MATRIX IF CONVERGES -- ENERGY AND
C     DENSITY MATRIX ONLY IF DOESN'T
      IMPLICIT REAL*8(A-H,O-Z)
      COMMON/SCF/P(72,72),F(72,72),V(72,72),H(72),CD(72),D(72),E(72),ID(
     |72)
      COMMON/STUFF/X(20),Y(20),Z(20),NATOM(20),NAT,NOCC
      CALL CLOCK2(NT1)
      IT=1
    1 CALL EPROB(N)
      CALL POP(N)
      CALL EFFIX
      E2=ERG(N)
      D2=DCID(NOCC))
      WRITE(6,13) IT,E2,D2
   13 FORMAT(' ',10X,'ELECTRONIC ENERGY AT ITERATION',1X,I2,5X,D21.14,5X
     |,'HIGHEST EVALUE',2X,D21.14)
C     TEST ENERGY AND HIGHEST EIGENVALUE FOR CONVERGENCE.
      CHK=DABS((E1-E2)/E2)
      CHK1=DABS(D2-D1)
      E1=E2
      D1=D2
      IF(CHK.LT..5D-12) GO TO 19
   18 IT=IT+1
C     TERMINATE IF CALCULATION HAS NOT CONVERGED IN 20 ITERATIONS
      IF(IT.GT.20) GO TO 1
      GO TO 1
   19 IF(CHK1.LT..5D-6) GO TO 2
      GO TO 18
    2 WRITE(6,4) IT
C     TERMINATION SEQUENCE IF CALCULATION HAS CONVERGED
    4 FORMAT('0',10X,'NUMBER OF ITERATIONS TO CONVERGE',1X,I3)
      WRITE(6,5) E1
    5 FORMAT('0',10X,'ELECTRONIC ENERGY',2X,D21.14,1X,'AU')
      WRITE(6,9)
    9 FORMAT('0',2X,'DENSITY MATRIX')
      CALL MATOUT(P,D,ID,72,N,1)
C     PUNCH OUT DENSITY MATRIX ON CARDS
      DO 14 I=1,N
   14 WRITE(7,16) ((I,J,P(I,J)),J=I,N)
   16 FORMAT(3(2I2,D21.14))
      WRITE(6,10)
   10 FORMAT('0',2X,'COEFFICIENT MATRIX')
C     PUT COEFF MATRIX BACK IN F FOR PRINTING
      NN1=N-1
      DO 15 I=1,NN1
      III=I+1
      DO 12 J=III,N
```

```
   12 F(I,J)=P(J,I)
   15 F(I,I)=CD(I)
      F(N,N)=CD(N)
      CALL MATOUT(F,D,ID,72,N,-1)
C     PUNCH OUT FINAL COEFFICIENT MATRIX
      DO 17 I=1,N
   17 WRITE(7,16) ((I,J,F(I,ID(J))),J=1,NOCC)
      CALL CLOCK2(NT2)
      XX1=DFLOAT(NT2-NT1)/60.D0
      WRITE(6,11) XX1
   11 FORMAT('0        ITER TIME',2X,F7.2,2X,'SECONDS')
      RETURN
    3 WRITE(6,6)
C     TERMINATION SECTION IF CALCULATION HAS NOT CONVERGED
    6 FORMAT('0',10X,'WENT 20 ITERATIONS WITHOUT CONVERGING')
      WRITE(6,7) E1
    7 FORMAT('0',10X,'ELECTRONIC ENERGY AT EXIT',2X,D17.9,1X,'AU')
      WRITE(6,8)
    8 FORMAT('0',2X,'DENSITY MATRIX AT EXIT')
      CALL MATOUT(P,D,ID,72,N,1)
C     PUNCH DENSITY MATRIX
      DO 20 I=1,N
   20 WRITE(7,16) ((I,J,P(I,J)),J=1,N)
      CALL CLOCK2(NT2)
      XX1=DFLOAT(NT2-NT1)/60.D0
      WRITE(6,11) XX1
      RETURN
      END
C
C
C
      SUBROUTINE START(E1)
      IMPLICIT REAL*8(A-H,O-Z)
      COMMON/SCF/D(72,72),F(72,72),V(72,72),H(72),CD(72),O(72),E(72),ID(
     1 72)
      COMMON/STUFF/X(20),Y(20),Z(20),NATOM(20),NAT,NOCC
      COMMON/ IRRS/NOR(72),LOR(72),MOR(72),ZOR(72),N,NINT,N2,N3,N4
C     CALCULATE TRANS MATRIX TO ORTHOGONAL SET, CALCULATE 2-ELEC
C     INTEGRALS, CALCULATE 1-ELECTRON HAMILTONIAN INTEGRALS.
      CALL LERV
      CALL HAMIF
C     CALCULATE NUMBER OF (DOUBLY) OCCUPIED MOLECULAR ORBS.
      NELEC=0
      DO 10 I=1,NAT
   10 NELEC=NELEC+NATOM(I)
      NOCC=NELEC/2
      IF((2*NOCC-NELEC).NE.0) GO TO 25
C     CALCULATE POWERS OF THE BASIS SET SIZE FOR DECODE.
      N2=N*N
      N3=N2*N
      N4=N3*N
C     INITIALIZE ID ORDERING VECTOR.
      DO 7 I=1,N
    7 ID(I)=I
      E1=0.D0
      CALL EFFIX
      RETURN
   25 WRITE(6,26)
```

```
26 FORMAT('0        START CALLING ERROR')
   STOP
   END
C
C
C
      REAL FUNCTION SHERM*8(L,M,COSTHT,CFI,SFI)
C     RETURNS THE VALUE OF THE REAL NORMALIZED SPHERICAL HARMONIC
C     S(L,M) (VALUATED AT THE POINT (THETA,FI)
C     COSTHT IS COSINE THETA, CFI AND SFI ARE SINE AND COSINE OF FI.
      IMPLICIT REAL*8(A-H,O-Z)
      MI=IABS(M)
      IF(M.EQ.0) GO TO 1
      CH=CFI
      SH=SFI
      IF(MI.EQ.1) GO TO 1
      DO 2 I=2,MI
      CHS=CH*CFI-SH*SFI
      SH=SH*CFI+CH*SFI
      CH=CHS
    2 CONTINUE
    1 XANG=CH
      IF(M.LT.0) XANG=SH
    4 PI=3.141592653589793D0
      XFIN=1.D0/DSQRT(PI)
      IF(M.EQ.0) XFIN=XFIN/DSQRT(2.D0)
      XTHIN=DFLOAT(2*L+1)*DFAC(L-MI)/(2.D0*DFAC(L+MI))
      XTHIN=DSQRT(XTHIN)
      SHERM=ALEG(L,MI,COSTHT)*XTHIN*XFIN*XANG
      RETURN
    1 XANG=1.D0
      GO TO 4
      END
C
C
C
      REAL FUNCTION ALEG*8(L,M,X)
C     RETURNS THE VALUE OF THE ASSOCIATED LEGENDRE POLYNOMIAL P(L,M)
C     EVALUATED AT X=COS(A) FOR SOME ANGLE A, CODED FROM ALGORITHM BY
C     HERNDON, COMMUNICATIONS OF THE ACM, APRIL, 1961.
      IMPLICIT REAL*8(A-H,O-Z)
      MI=IABS(M)
      IF(DABS(X).GT.1.D0) GO TO 26
      IF((X.EQ.1.D0).AND.(MI.NE.0)) GO TO 25
      IF(L.LT.MI) GO TO 25
      IF(L.EQ.0) GO TO 10
      IF(X.EQ.0.D0) GO TO 8
      XX1=1.D0
      IF(L.EQ.MI) GO TO 1
      XX1=X**(L-MI)
    1 XX2=-1.D0/(X*X)
      GO TO 2
    8 III=(L-MI)/2
      IF(2*III.NE.(L-MI)) GO TO 25
      XX4=DFAC(L+MI)/(DFAC(III)*DFAC(MI+III))
      IF(MOD(III,2).NE.0) XX4=-XX4
      GO TO 3
    2 III=0
```

```
      XX4=0.D0
    4 IF(2*III.GT.(L-MI)) GO TO 3
      XX4=XX4+DFAC(2*(L-III))*XX1/(DFAC(III)*DFAC(L-III)*DFAC(L-2*III-MI
     ))
      XX1=XX1*XX2
      III=III+1
      GO TO 4
    3 XX4=XX4/DFLOAT(2**L)
      XX1=DSQRT(1.D0-X*X)
      IF(MI.EQ.0) GO TO 6
      XX1=XX1**MI
    7 XX4=XX4*XX1
    5 ALEG=XX4
      RETURN
    6 XX1=1.D0
      GO TO 7
   25 ALEG=0.D0
      RETURN
   10 ALEG=1.D0
      RETURN
   26 WRITE(6,27)
   27 FORMAT('0     ALEG CALLING ERROR')
      GO TO 25
      END
C
C
C
      SUBROUTINE POLAR(X,Y,Z,R,COSTHT,CFI,SFI)
C     POLAR COORD ROUTINE. RETURNS R, COSINE THETA (COSTHT), AND THE
C     SINE (SFI) AND COSINE (CFI) OF PHI, GIVEN THE CARTESIAN COORDS
C     X,Y,Z.
      IMPLICIT REAL*8(A-H,O-Z)
      R=DSQRT(X*X+Y*Y+Z*Z)
      IF(R.EQ.0.D0) GO TO 25
      COSTHT=Z/R
      IF(X.EQ.0.D0) GO TO 26
      IF(Y.EQ.0.D0) GO TO 27
      RP=DSQRT(X*X+Y*Y)
      CFI=X/RP
      SFI=Y/RP
      RETURN
   25 COSTHT=1.D0
   27 CFI=1.D0
      SFI=0.D0
      IF(X.LT.0.D0) CFI=-1.D0
      RETURN
   26 CFI=0.D0
      SFI=1.D0
      IF(Y.LT.0.D0) SFI=-1.D0
      RETURN
      END
C
C
C
      REAL FUNCTION A*8(N,X)
C     RETURNS THE VALUE OF THE N-TH ORDER A FUNCTION EVALUATED AT X.
C     THE N-TH ORDER A FUNCTION IS INT(1 TO INF) (T**N*EXP(-TX)) DT
      IMPLICIT REAL*8(A-H,O-Z)
```

```
      IF(X.EQ.0.D0) GO TO 25
      IF(N.LT.0) GO TO 25
      XX1=DEXP(-X)/X
      XX2=XX1
      IF(N.EQ.0) GO TO 10
      DO 1 I=1,N
      XX2=XX1+(DFLOAT(I)/X)*XX2
    1 CONTINUE
   10 A=XX2
      RETURN
   25 WRITE(6,11)
   11 FORMAT(' A CALLING ERROR')
      A=0.D0
      RETURN
      END
C
C
C
      SUBROUTINE HAMIF
C     CALCULATES 1-ELEC HAM MATRIX, STORES OFF-DIAG IN BOTTOM OF V,
C     DIAG IN VECTOR H.
      IMPLICIT REAL*8(A-H,O-Z)
      COMMON/STUFF/X(20),Y(20),Z(20),NATOM(20),NAT,NOCC
      COMMON/ORBS/NOR(72),LOR(72),MOR(72),ZOR(72),N,NINT,N2,N3,N4
      COMMON/SCF/P(72,72),F(72,72),V(72,72),H(72),CO(72),D(72),E(72),ID(
     |72)
      CALL CLOCK2(NT1)
      DO 1 I=1,N
      DO 1 J=I,N
      SUM=0.D0
      DO 2 K=1,NAT
      CALL POLAR(X(K),Y(K),Z(K),R,COSTHT,CFI,SFI)
      IF(R.EQ.0.D0) GO TO 3
      XX1=XNUK2(NOR(I),LOR(I),MOR(I),ZOR(I),NOR(J),LOR(J),MOR(J),ZOR(J),
     |NATOM(K),R,COSTHT,CFI,SFI)
      SUM=SUM+XX1
      GO TO 2
    3 XX1=XNUK1(NOR(I),LOR(I),MOR(I),ZOR(I),NOR(J),LOR(J),MOR(J),ZOR(J),
     |NATOM(K))
      SUM=SUM+XX1
    2 CONTINUE
      SUM=SUM+SKINNY(NOR(I),LOR(I),MOR(I),ZOR(I),NOR(J),LOR(J),MOR(J),ZO
     |R(J))
      IF(I.EQ.J) GO TO 4
      V(J,I)=SUM
      GO TO 1
    4 H(I)=SUM
    1 CONTINUE
      CALL CLOCK2(NT2)
      XX1=DFLOAT(NT2-NT1)/60.D0
      WRITE(6,5) XX1
    5 FORMAT('0',3X,'1-ELEC HAM INT CALCULATING TIME',1X,F5.2,1X,'SECOND
     |S')
      RETURN
      END
```

REFERENCES

1. J.A. Pople and D.L. Beveridge, Approximate Molecular Orbital Theory, McGraw-Hill, N.Y., 1970. Chapter 2.
2. E. Clementi, Tables of Atomic Functions, supplement to IBM Journal of Research and Development 9, 2 (1965).
3. R. Moccia, J. Chem. Phys. 37, 910 (1962), 40, 2164, 2176, 2186 (1964).
4. R. Moccia, Theor. Chim. Acta 8, 8 (1967).
5. R. Moccia, private communication, January, 1973.
6. This calculation was performed at the suggestion of Dr. J.M. Sichel.
7. E.W. Kaiser, J. Chem. Phys. 53, 1686 (1970).
8. M. Cowan and W. Gordy, Phys. Rev. 111, 209 (1958).
9. N.F. Ramsey, Molecular Beams, Oxford, 1956. p. 173.
10. G.W. Stewart, Comm. ACM 13, 369 (1970).

CLAIMS TO ORIGINAL RESEARCH

1. The 71-orbital OCE-SCF calculation of HCl reported by Moccia (Reference 5, Chapter II) has been repeated with electron repulsion integrals stored to greater precision; for some properties the results are considerably altered (Chapter II).
2. A series of OCE bases for HCl has been constructed by adding STO's to a basis proposed by Gilbert and Wahl (Reference 27, Chapter II); in the largest basis of this series (29-orbitals), the total energy (-460.068938 au) at the equilibrium internuclear distance was below that in the 71-orbital basis (-460.052595 au) (Chapters II and III).
3. Calculations of Cl^- ion wavefunctions in several OCE bases showed that the poor quality of the EFG in the 71-orbital basis was due to poor basis choice for the 2nd electron shell (Chapter III).
4. EFG's have been calculated for the OCE-SCF wavefunctions in the basis series of claim 2 above; for the 29-orbital basis the calculated electronic EFG was 3.4942 au compared with an experimental value of 3.4908 au (Kaiser, Reference 7, Chapter I) (Chapter III).
5. The formula of Guseinov (Reference 14, Chapter II) for the expansion in elliptical coordinates of the product of two associated Legendre polynomials on different centers has

been used to construct a computer routine for the evaluation of two-center integrals over STO's of the EFG operator (Chapter IV and Appendix I).

6. The electronic EFG in the 29-orbital basis has been analysed to determine the spatial origin of the EFG; about 96% of the EFG was found to originate within .3 au of the Cl nucleus, and about 85% of this was due to the third (outer) electron shell (Chapter V).

7. The 1st and 2nd derivatives of the EFG with respect to internuclear distance have been calculated in the 29- and 71-orbital bases by polynomial fitting and compared with experiment (Kaiser, Reference 7, Chapter I). The 71-orbital basis was in good agreement for the 1st derivative but in error by 100% for the 2nd. The 29-orbital basis was in error by 15% for the 1st and 200% for the 2nd (Chapter VI).

8. An OCE-SCF calculation of HCl has been performed including in the Hamiltonian the interaction of the nuclear quadrupole moment with the electrons. Small effects were observable in a basis sufficiently flexible near the Cl nucleus (Chapter VII).

9. A 22-orbital OCE basis has been constructed to investigate polarization of the 1st shell (1σ MO) electrons by the aspherical distribution of the proton and outer electrons. The 1σ MO was found to contribute about 1% of the experimental electronic EFG (Chapter VII).